Zeitschrift: IABSE reports = Rapports AIPC = IVBH Berichte
Band: 56 (1987)

Rubrik: Session 2. Monitoring instrumentation and systems

SESSION 2

Monitoring Instrumentation and Systems

Instruments et systèmes de surveillance

Überwachungsmessgeräte und Systeme

Leere Seite
Blank page
Page vide

Automated Instrumentation at some U.S.B.R. Dams

Mesures automatiques dans des barrages américains (U.S.B.R.)

Automatische Ueberwachung von amerikanischen (U.S.B.R.) Staudämmen

Dewayne L. MISTEREK
Chief, Structural Behavior Branch
Bureau of Reclamation
Denver, CO, USA

Dewayne Misterek, born 1934, received his civil engineering bachelor of science degree from South Dakota School of Mines and Technology and his master of science degree from the University of Colorado. He has spent almost his entire career working for the Bureau of Reclamation, specializing in field instrumentation of dams and other structures and in the area of rock mechanics.

Dr. Charles L. BARTHOLOMEW
Professor and Chairman
Department of Civil Engineering
Widener University
Chester, PA, USA

Charles Bartholomew, born 1936, received a civil engineering bachelor of science degree from the University of Kansas and master and doctoral degrees in civil engineering from the University of Illinois. He has been in professional consulting practice in geotechnical engineering for 19 years and during the past 7 years as Associate Professor of Civil Engineering at Bradley University in Peoria, Illinois and at the University of Colorado. He has, for the past 2 years, worked on special projects for the Bureau or Reclamation involving instrumentation of embankment and concrete dams.

SUMMARY

In 1979, the Bureau of Reclamation began a program to automate the acquisition, storage, transmission, and evaluation of instrumentation data from selected major dams. This paper presents the status of that program and the philosophy used to develop the program and to select which dams to be included.

RESUME

En 1979 le Bureau of Reclamation a commencé un programme pour automatiser l'acquisition, l'accumulation, la trasmission et l'évaluation des donnés tirés de quelques grands barrages. L'article presente le programme et la philosophie employée pour le developper ainsi que pour le choix des barrages.

ZUSAMMENFASSUNG

1979 hat der Bureau of Reclamation ein Programm angefangen um die Erwerbung die Sammlung, die Fernsehsendung und die Einschätzung, deren Daten, die aus großen Dämme ausgewählt werden, zu automatisieren. Dieser Artikel beschreibt das Programm und wie es entwickelt wird und wie die Dämme ausgewählt werden.

1. INTRODUCTION

The primary and most important purpose of monitoring a dam with various instruments is to provide necessary information for assessing the performance of the dam for control purposes, for any indications of adverse conditions, and for continuing evaluation of the structural safety of the dam during construction, reservoir filling, and service operations (USCOLD 1986).

Most instrumentation devices can now be read with automated equipment. Over the past 2 decades, electronic technology has developed the necessary computer equipment, mini-pressure transducers, data logger equipment, and radio and satellite transmittal devices to provide the accuracy, dependability, and economically affordable systems desired.

The advantages of the automation of observations are quite clear. Although the design, installation, use, and maintenance of any automatic or partially automatic system require a thoroughly developed technology basis, the implementation of automation is much to be desired. Automation will prove inevitable whenever the automatic equipment can perform the operations required at greater speed, lower cost, and with less errors than the human operator. (ICOLD 1982)

There is, however, a valid concern that automating instrumentation at a dam may lead to over reliance on the measured results and the consequent neglect or elimination of human judgment either at the site or in the office. Human onsite observations might be minimized or evem eliminated. Adopting this philosophy could lead to a false sense of security and may represent a threat to the safety of a dam. These factors need to be recognized and avoided.

In general, advantages of automating the data collection and processing of structural behavior instrumentation at a dam include:

- Decreases labor required to measure, reduce, and portray data
- Decreases elapsed time between measurement and interpretation of data
- Provides automatic warning if limiting values for readings are exceeded
- Allows more frequent readings without significant increased cost
- Automatically transmits data to another location for evaluation
- Decreases errors in data collection and reduction
- Enables continuous long-term collection of data at the required intervals
- Enables direct entry of data into a computer data base
- Enables readings to be taken at times when equipment is not accessible due to high water or severe weather conditions

In addition to the previously discussed possible minimization of human observations, automation is also somewhat limited in regard to the following:

- Displacement measurements by geodetic methods
- Measurements of the thickness of ice in the reservoir
- The appearance or extent of new cracks in concrete or embankment dams
- The appearance of new seepage leaks

2. USBR AUTOMATION PROGRAM

The U.S. Bureau of Reclamation has long recognized the importance of instrumentation in the design, construction, and operaiton of dams under its jurisdiction. During the last 10 years, an increased emphasis has been placed on the timely use of instrumentation data for surveillance and analysis of USBR dams. Early instrumentation systems relied on manual input of hand-recorded data which was transmitted by mail, but recent emphasis has been given to automation of many of these devices with electronic transmission of data. The dam monitoring automation program encompasses a wide range of areas, from landslide surveillance to embankment and concrete dam instrumentation throughout the Western United States.

Although a few devices on USBR dams have been partially automated for a number of years, the first major or "full" automation was accomplished at Monticello Dam in California in 1981. Later, Flaming Gorge, Morrow Point, Crystal, Glen Canyon (all part of the Colorado River Storage Project) and Yellowtail Dams were automated. Figure 1 illustrates this data gathering system for the series of dams on the Colorado River. Now, automation systems are being installed at Calamus, Ridgway, and Navajo embankment Dams. It is anticipated that additional dams will be automated in the future.

The development of the USBR automation program required both the setting of goals and the flexibility to make changes during the development process. It was quickly recognized that a diverse set of needs existed involving the integration of many technical and organizational facets within the USBR. Engineers in the design office require timely presentation of structural behavior data in the form of plots, charts, printouts, etc. in order to ascertain whether the structures meet design criteria. Regional and project office personnel need this information to fulfill their operation and maintenance responsibilites. In addition, personnel at the dams need the data displays of selected instruments for inspection purposes.

To meet these diverse requirements, systems have been designed which provide for the distribution of sensor data within a dam. Data monitors are strategically located throughout a dam and linked to a master station which gathers the information for transmission outside the dam.

2.1 Types of Instruments Automated

With the use of modern electronics, virtually any type of instrument can be automated. For example, a recent article in (USCOLD 1984) the development of an automated plumbline monitor with no moving parts is described. Figure 2 shows the device while Figure 3 illustrates a comparison of automated versus manual readings. The agreement between the two methods is considered to be excellent.

The types of instruments in concrete dams which are presently automated include:

- Reservoir level
- Plumblines
- Stess meters
- Strain meters

- Uplift pressure devices
- Temperature
- Foundation deformation meters
- Seepage flow devices

Instruments either presently automated or soon to be automated in embankment dams include:

- Seepage flow devices
- Vibrating-wire piezometers
- Observation wells
- Reservoir level
- Pneumatic piezometers
- Extensometers
- Pneumatic settlement sensors
- Total pressure cells
- Measurement points

2.2 USBR Criteria for Dam Automation Selection

USBR experience thus far with automation has resulted in a realization of the advantages of automation listed earlier. It is, therefore, anticipated that the automation of readings will continue to increase.

The criteria normally used in the determination of whether to automate or not include:

- Cost benefit criteria. - The systems should be able to pay for themselves in labor savings and other benefits over a reasonable life expectancy of the equipment. Dams containing a large amount of insrumentation can potentially save a much greater amount of labor.
- Accuracy. - It has been shown that accuracy, precision, and reproduceability of results are much improved with automated devices.
- Safety. - It may be desirable at some dams, which have a high risk potential, to install an automatic alarm system together with very frequent scanning of certain instrument readings.
- Accessibility. - Some locations at certain dams may not be accessible during high reservoir level periods and some entire dams may not be readily accessible during severe winter seasons.

Any of these criteria may justify the automation of a system.

3. RESULTS

It is believed that all of the installations to date have been very successful and excellent data are flowing from these dams.

A number of lessons have been learned from the installations thus far. Those include:

- One of the major expense items for the projects was cabling. Cable lengths to provide power to each sensor and carry the analog signal back to the digitizer for recording should be kept to a minimum. From this experience, a system of smaller distributed monitors was envisioned.
- A readout device located near the sensor installation would decrease the time and effort required to install and check out the sensor.
- Each data point should be accompanied by identification information describing its function and location.
- Data from specifically developed microprocessor based instrumentation, such as the plumbline monitor, can be collected at the dam monitor through a digital interface. These data can then be labeled with time information from the system clock and transmitted in the same block of data containing other sensor scans.
- Each data set needs to be identified with location, time, and project designators.
- Each measured electrical signal should be converted into engineering values and units at the time it is scanned.
- The data should be accessible upon demand by an operator, and the system should be programmable at places both inside and outside the dam.
- Security must be provided against unauthorized or accidental intrusion into the system.
- Provisions should be made to test the memory and communications of each monitor.
- User programming of each parameter should be in a question and answer dialog (menu-driven).
- Alarm functions should be provided to alert personnel at the dam and at several other locations of possible structural problems in the dam.
- The cabinet depth should not exceed 1 foot to allow for passage in a 5-foot-wide gallery.
- Field data acquisition equipment should have onboard, battery-backed memory in case of exterior power loss.
- The system should be of modular design so that new instruments and types of data may be added.
- The system should have built in data verification so that obviously incorrect or duplicate data are identified immediately upon entry into the system.
- The system should provide for mathematical reduction of data from all instruments included.
- The system should provide for direct and automatic data entry from data acquisition hardware.
- The software should have the ability to interface with all types of data collection and communications system.
- The system should provide for outside telephone access so that data may be reviewed and additional data added.
- The system should be capable of supporting a wide range of printers and plotters.

4. CONCLUSIONS

The USBR's experience with automation this far has been very encouraging from the standpoints of accuracy, precision, repeatability, and in terms of durability of the equipment. It is envisioned that additional installations will continue to be made in the future.

5. REFERENCES

1. USCOLD (U.S. Committee on Large Dams) CARPENTER, L. R. AND MISTEREK, D. L. "Automatic Monitoring of Structural Behavior Instruments for Reclamation Concrete Dams," January 1984.
2. USCOLD "General Considerations Applicable to Performance Monitoring of Dams," December 1986.
3. ICOLD (International Commission on Large Dams) "Automated Observation for the Safety Control of Dams," Bulletin 41, 1982.
4. BARTHOLOMEW, C. L. and MURRAY, B. C., "Automated Instrumentation at USBR Embankment Dams," unpublished 1986.
5. CARPENTER, L., HUTCHCROFT, T., AND HERZ, N. "Automatic Plumbline Monitoring System" Water Power and Dam Construction, June 1987.
6. HUTCHCROFT, T. and HERZ, N. "Optical Monitoring System Measures Dam Movement," Laser Focus/Electro-Optics, April 1987.

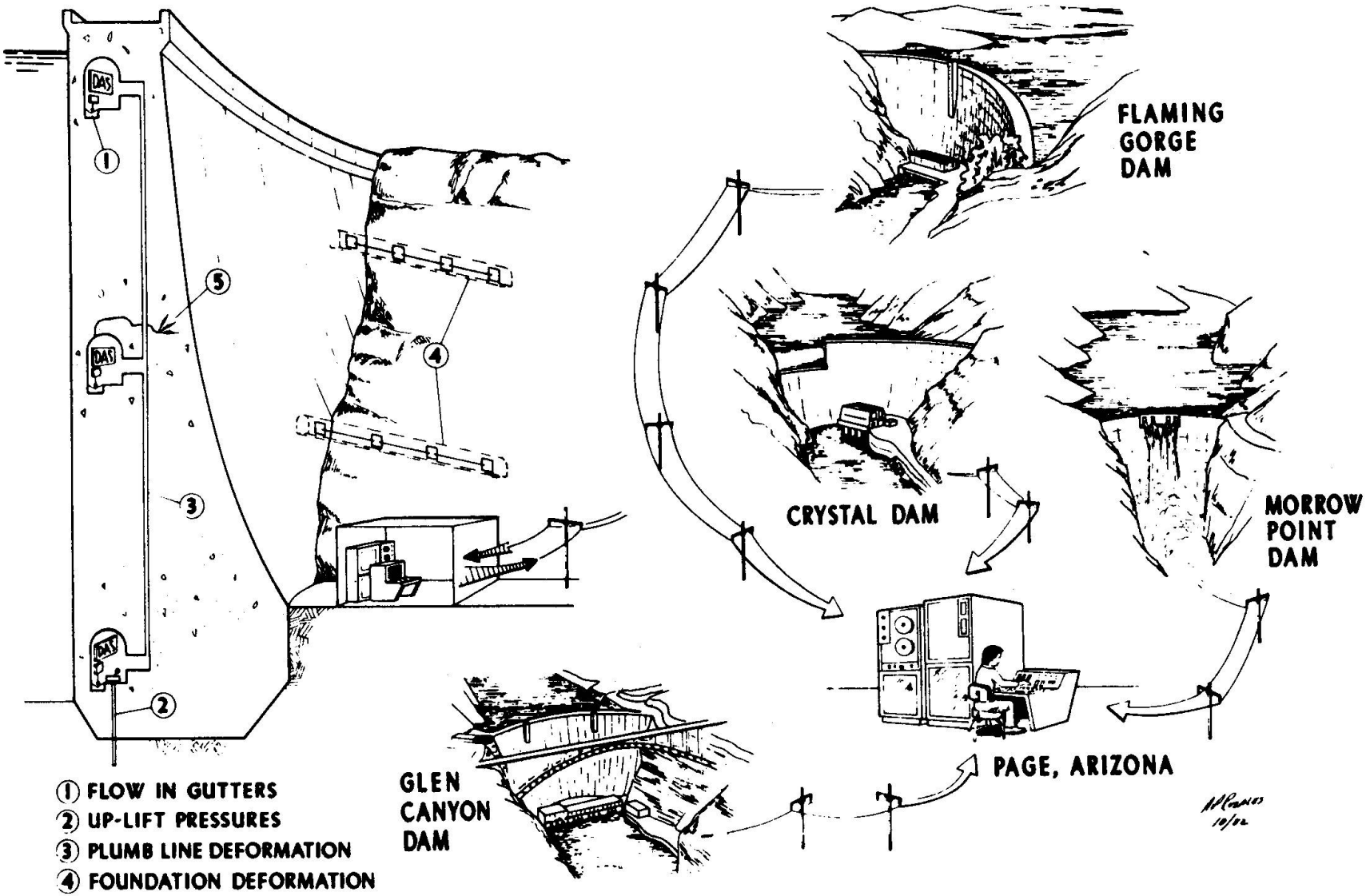

Fig. 1 Schematic drawing of integrated dam monitoring system

Fig. 2 Plumbline monitoring system prior to installation

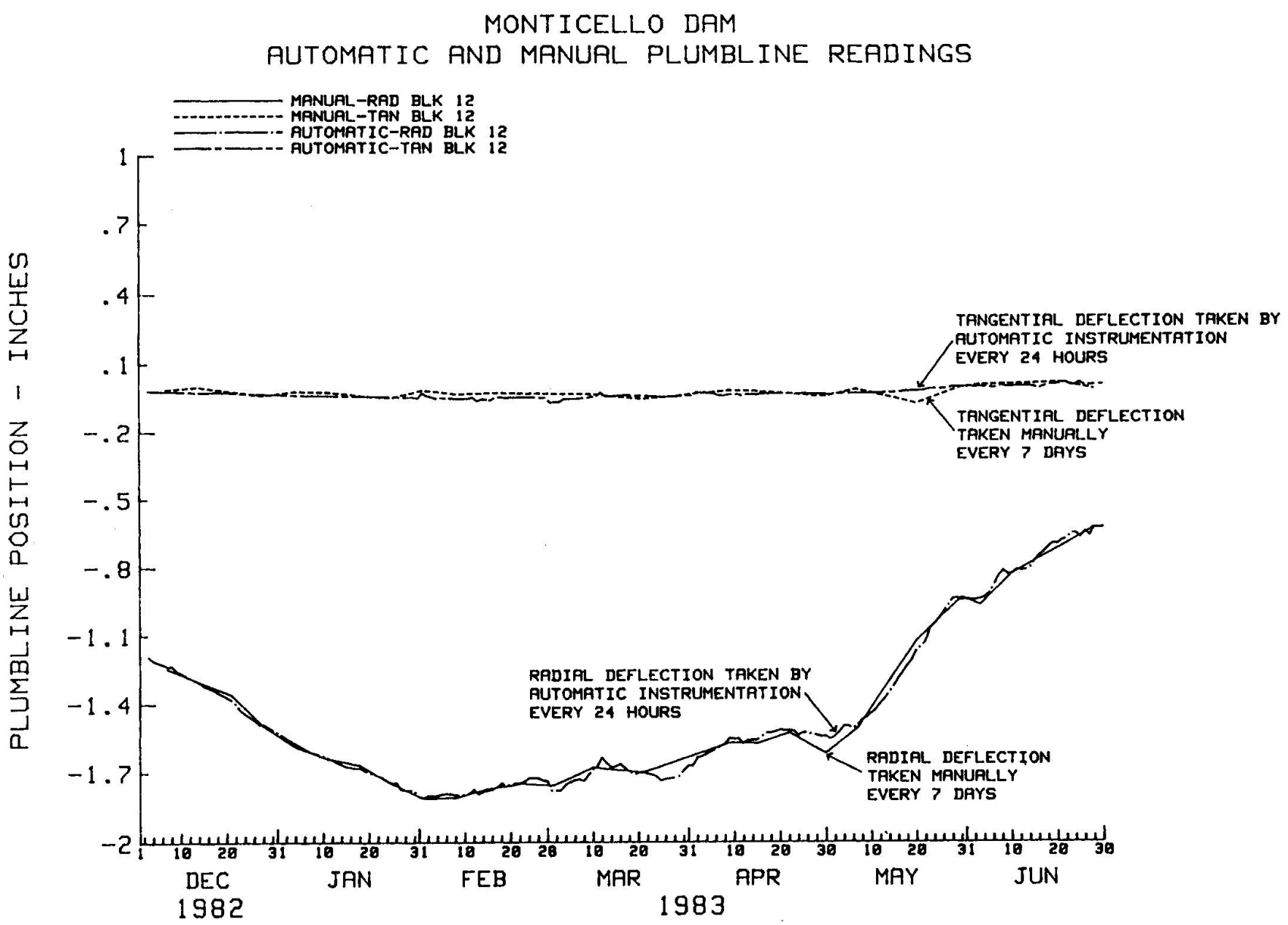

Fig. 3 Comparison of plumbline readings taken automatically and manually

Leere Seite
Blank page
Page vide

Bridge Behaviour Monitoring System on the Honshu-Shikoku Bridge

Système pour l'observation du comportement des ponts reliant Honshu et Shikoku

Das Brückenverhalten-Überwachungssytem der Honshu-Shikoku-Verbundbrücke

Takeaki IIJIMA

Born 1938, received his civil engineering degree at Waseda University, Japan. He was engaged in construction and administration of National Highway in Construction Ministry and Honshu-Shikoku Bridges in H.S.B.A. Now he is Head of Design Department, H.S.B.A.

Yuji KAGAWA

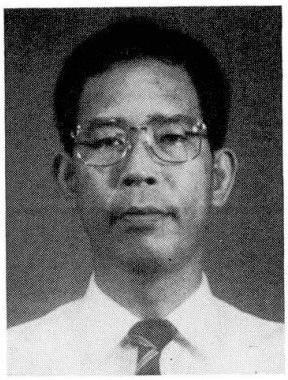

Born 1942, received his civil engineering degree at Ehime University, Japan. He was engaged in construction of Innoshima Bridge and Maintenance and Repair of Honshu-Shikoku Bridges. Now he a staff member of H.S.B.A.

Masahiko YASUDA

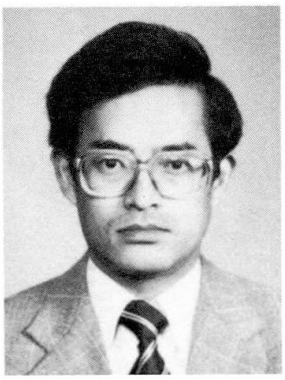

Born 1945, received his civil engineering degree at Kyoto University, Japan. He was engaged in construction of Ohnaruto and Iwakurojima Bridge. Now he is Manager of Design Section of 1st Construction Bureau, H.S.B.A.

Kozo HIGUCHI

Born 1950, received his civil engineering degree at Kyoto University, Japan. He was engaged in design and construction of Kojma-Sakaide route and planning of Monitoring on Ohnaruto Bridge. Now he is manager of Technical Affair Section in Tarumi Construction Office, H.S.B.A.

SUMMARY

In this paper, the monitoring of bridge behaviour of the Honshu-Shikoku Bridges is explained with regard to the purposes, items and configuration of the monitoring system, as well as examples of collected data. To this end, the Ohnaruto Bridge, which is subject to the most severe natural conditions, is used as an example.

RESUME

L'objet de cette monographie est de décrire les objectifs et les éléments de l'observation, la structure du système et quelques exemples de données de l'observation du pont d'Oonaruto, soumis aux conditions naturelles les plus sévères, à titre d'exemple de l'observation du comportement des ponts reliant les îles de Honshu et de Shikoku.

ZUSAMMENFASSUNG

Diese Abhandlung beschreibt die Honshu-Shikoku-Verbundbrücke (Brücke zwischen der japanischen Hauptinsel und der Insel Shikoku), eine Brücke, die den strengsten Naturbedingungen ausgesetzt ist. Sie ist ein Musterbeispiel für die Überwachung des Brückenverhaltens. Es werden Zweck, einzelne Gegebenheiten und die Struktur des Überwachungssystems sowie typische Messdaten dieser Brücke besprochen.

1. OUTLINE OF THE HONSHU-SHIKOKU BRIDGE PROJECT

The aim of the Honshu-Shikoku Bridge Project is to link Honshu with Shikoku via three highway and railroad routes by building long bridges over the Inland Sea, which has always been a major factor in the economy, industry, traffic, and culture of Japan from ancient times.

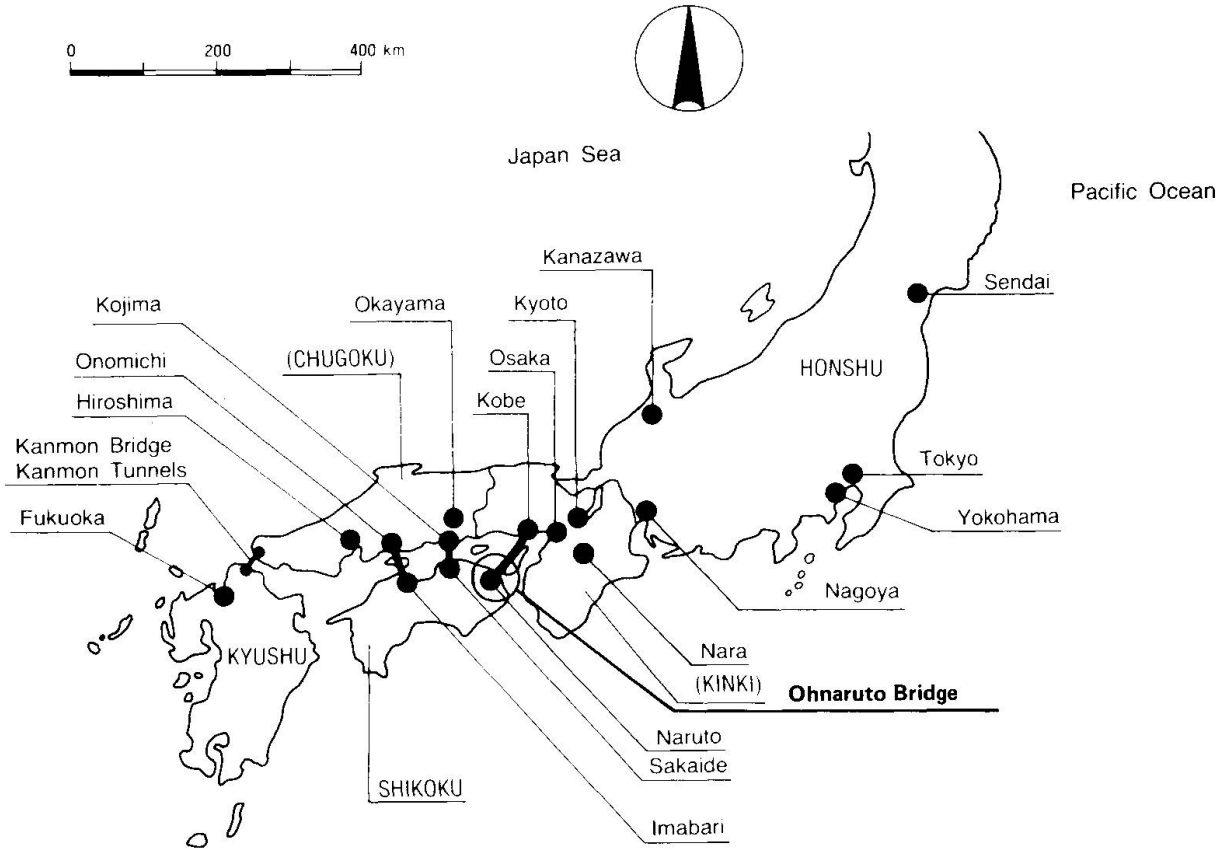

Fig. 1 Three Routes and the Location of the Ohnaruto Bridge

In general, the bridges are being built where the water is deep, currents are strong and natural disasters such as typhoons and earthquakes frequently take place. Also the straits over which the bridges will span are major sea routes which are congested with a great number of ships. Moreover, the construction sites are located in areas designated as national parks and where fishery is thriving. Accordingly, various mitigating measures have been taken for this project.

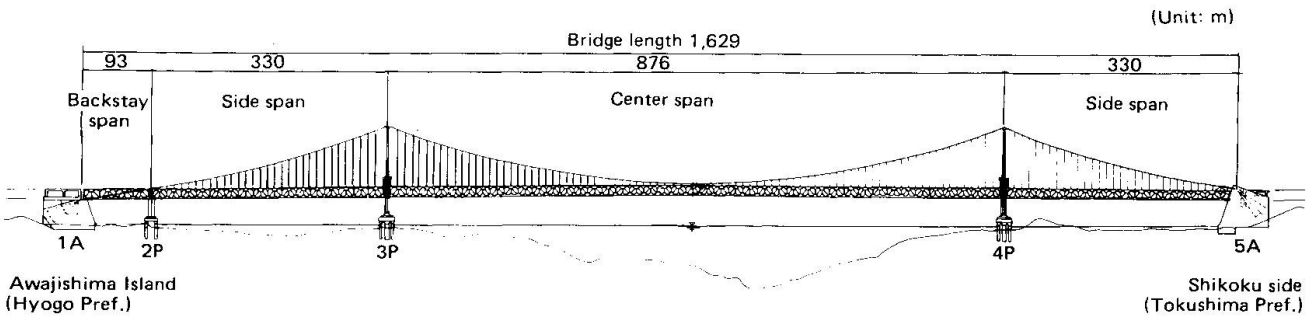

Fig. 2 General View of the Ohnaruto Bridge (Side View)

The Ohnaruto Bridge, a highway-railroad, dual-purpose suspension bridge, has been constructed initially. Only this bridge faces the open sea, and is subject to very severe wind conditions (basic wind velocity: 50 m/s). Further, this bridge is situated closest to the Tosa Sea and the sea area around the Kii Peninsula, both of which are expected to be the seismic origins of large-scale earthquakes, and thus will be built according to earthquake-resistant design standards of Honshu-Shikoku bridges.

Under these circumstances, the monitoring of bridge behavior (described below) has been conducted to verify the technical standards concerning resistance against wind and earthquake, including the measurement of response characteristics of the bridge under natural wind and earthquake.

2. PURPOSES AND ITEMS OF THE MONITORING OF BRIDGE BEHAVIOR

The purposes for monitoring the bridge behavior are shown in Table 1. As can be seen from this Table, methods and locations for recording data depend on purposes.

Table 1 Purposes of Monitoring of Bridge Behavior

<table>
<tr><th colspan="2">Purpose</th><th>Immediacy of Data</th><th>Location of Recording</th><th>Method of Data Recording (See Table 2)</th></tr>
<tr><td colspan="2">Traffic control</td><td rowspan="2">Required</td><td rowspan="2">Administrative office</td><td>Graphic display</td></tr>
<tr><td rowspan="2">Bridge structure control</td><td>Daily control</td><td>Operation monitoring table</td></tr>
<tr><td>Check of the soundness of bridge structure</td><td rowspan="2">Not required</td><td rowspan="2">1A</td><td rowspan="2">Magnetic tape</td></tr>
<tr><td colspan="2">Collection of data for future wind- and earthquake-resistant designs</td></tr>
</table>

- Traffic control:

  Data collected by anemometers and seismometers are transmitted regularly to the administrative office and monitored on a graphic display for restriction of traffic when necessary.

- Bridge structure monitoring:

  This comes under two categories: daily control use requiring real time data and checking of the soundness of bridge structure requiring accurate detailed long-term data.

  Maximum values of data detected at regular intervals by certain measurement instruments for wind, earthquake and vibration are transmitted to the operation monitoring table in the administrative office for daily check. To check the soundness of the bridge structure, for long-term maintenance purposes, the latest data is not required. Accordingly, raw data are recorded on magnetic tapes for later analysis via housed measurement instruments located at point 1A (see Fig. 2).

- Data collected for future wind- and earthquake-resistant designs are also analyzed later.

3. SYSTEM FOR MONITORING THE BRIDGE BEHAVIOR

The configuration of the monitoring system is diagrammed in Fig. 3. Measurement instruments are listed in Table 2. The spatial arrangement of the instruments is shown in Fig. 4.

A propeller anemometer, used mainly for traffic control provides data which are later analyzed for average wind speed, wind speed distribution for heights, maximum instantaneous wind speed, direction of wind, gust, intensity of turbulence and power spectrum of wind.

An ultrasonic anemometer yields data for analysis of factors such as power and cross spectra and spatial correlation of wind, as well as wind speed and direction (including angle of inclination).

The accelerometer was installed to measure responses of the bridge structure to external forces caused by wind, earthquake etc.

The system consists of sensors installed on the bridge structure and other elements, the measurement board and the monitoring instruments installed at 1A, the operation monitoring table installed in the administrative office, and a transmitter for the transmission and reception of data between devices.

Data are sent to the measurement board in the form of current or voltage through the transducer. The measurement instruments process data at all times, receiving, evaluating and storing all values.

Data necessary for monitoring are transmitted from 1A to the administrative office, a distance of approximately four kilometers, via optical fiber for supervision by ASTEC, the Automatic Supervisory Telemeter and Telecontrol System.

The operation, control and supervision of various processing devices can be executed not only via peripheral devices at 1A, but also by transmitting remote operation signals via the optical fiber line from the operation monitoring table in the administrative office.

In the case of earthquakes, the recording and storage of data on magnetic tapes are executed automatically when the scales of earthquakes exceed a certain Richter level, to ensure complete recording of sudden outbreaks. For winds, these operations are executed both automatically and manually. When earthquakes and winds occur simultaneously, the recording of earthquakes is executed preferentially.

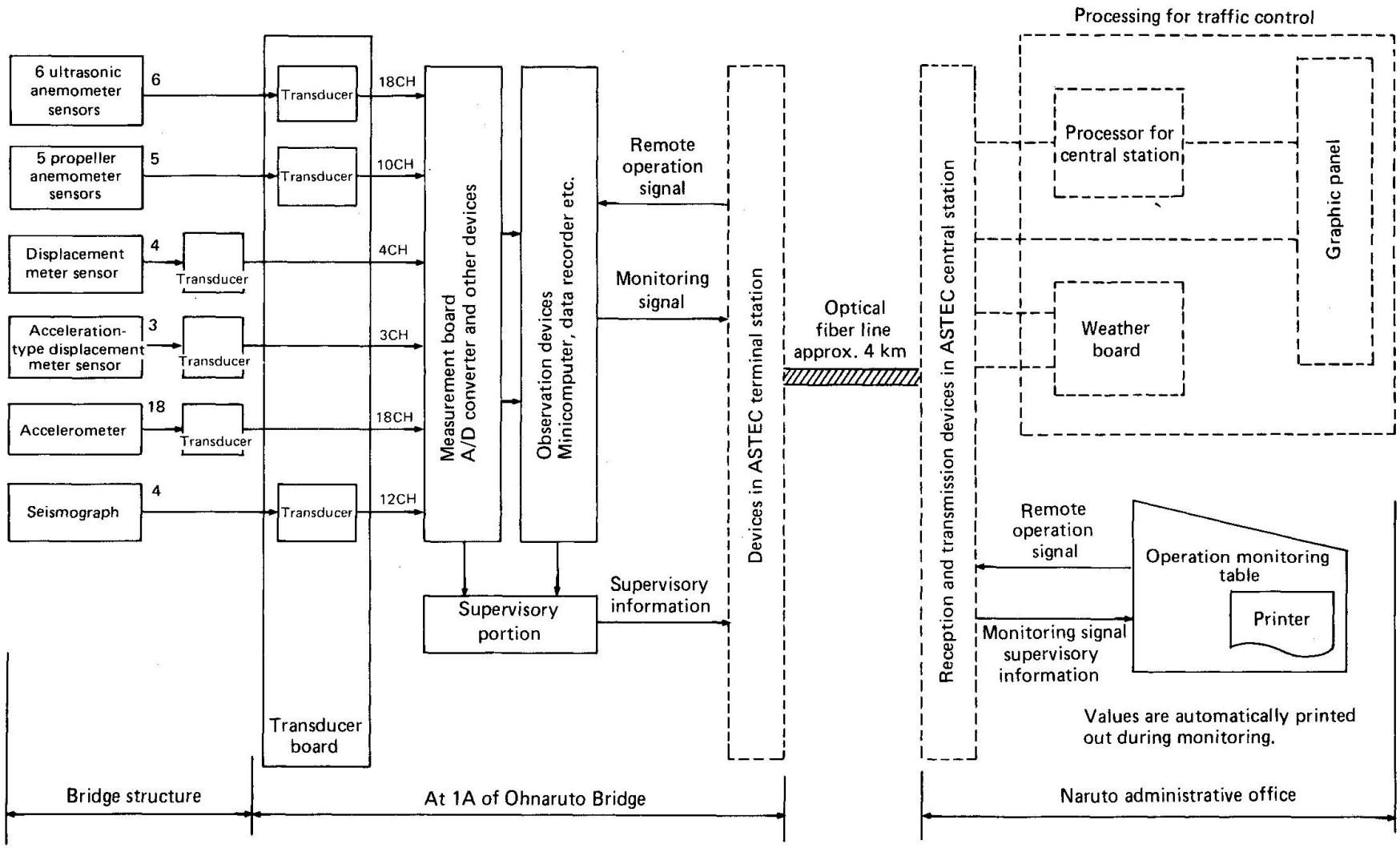

Fig. 3 System Configuration

Table 2 Measuring Instruments

Measuring Instrument					Data Recording	
Instrument	Quantity	Component	Number of Channels	Installation Location (See Fig. 2)	Monitor (Administrative Office)	Magnetic Tape Recording (1A)
Propeller anemometer	6**	Wind speed (horizontal), wind direction	12^{CH}	P_1 P_2 P_3, P_4, P_5, P_6	Graphic display → FDD Operation monitoring table	MT (10^{CH})
Ultrasonic anemometer	6	X, Y, Z (→ Main stream direction, angle of inclination)	18^{CH}	$S_1, S_2, S_3, S_4, S_5, S_6$	—	MT (18^{CH})
Seismograph	4	X, Y, Z	12^{CH}	G_1 G_2 G_3, G_4	Graphic display Operation monitoring table → P	MT (12^{CH})
Accelerometer	18	T (Transverse to bridge axis)	4^{CH}	3T 6T 4T, 10T	Operation monitoring table → P	For winds: MT (2^{CH}) For earthquakes: MT (4^{CH})
		L (longitudinal)	7^{CH}	2L, 5L, 6L 8L, 10L, 11L, 12L	Operation monitoring table → P	For winds: MT (3^{CH}) For earthquakes: MT (7^{CH})
		V (Vertical)	7^{CH}	3V, 4V 8V, 9V, 12V 1V 7V	Operation monitoring table → P Operation monitoring table → P	For winds: MT (7^{CH}) For earthquakes: MT (5^{CH})
Acceleration-type displacement meter	3	V (Vertical)	3^{CH}	1V, 3V, 4V	Operation monitoring table → P	—
Displacement meter	4	L (longitudinal)	4^{CH}	SSL, CSL, SNL, CNL	Operation monitoring table → P	—

* FDD: Floppy disc, P: Printer, MT: Magnetic tape
** One of the six units belongs to another system.

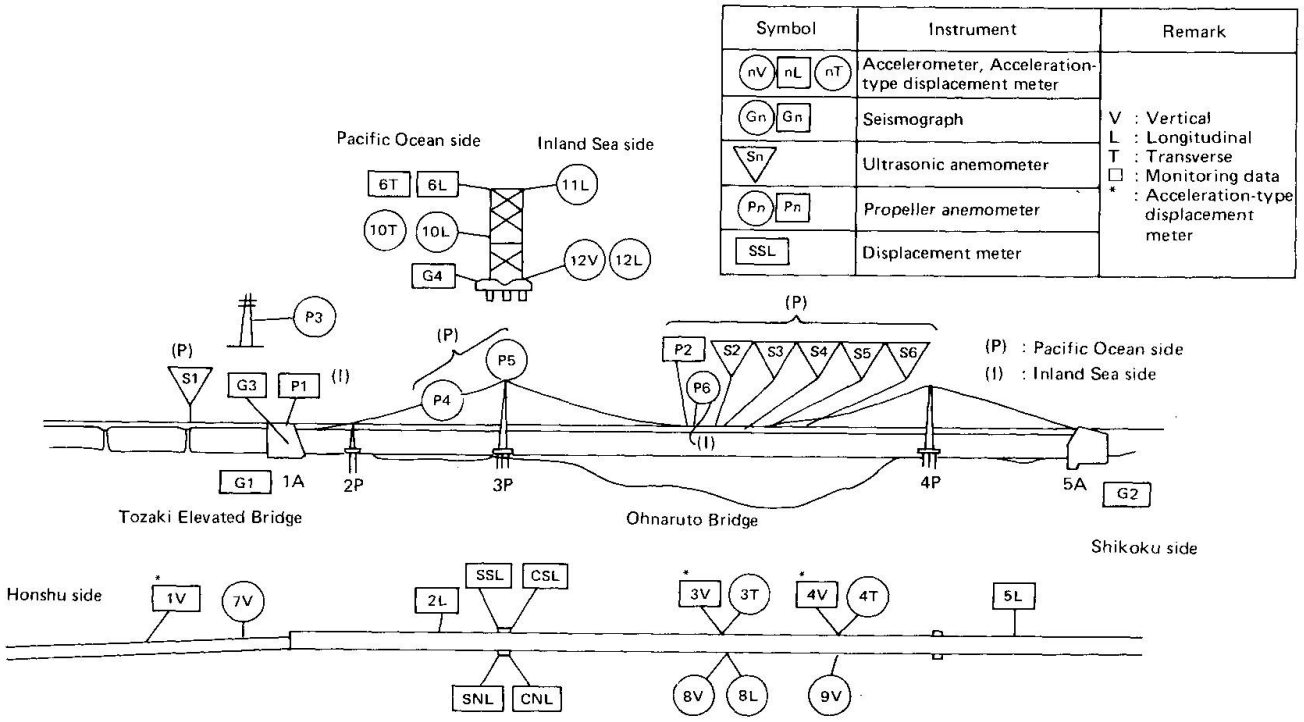

Fig. 4 Arrangement of Measuring Instruments

4. DATA ANALYSIS

Fig. 5 shows raw data collected by the propeller anemometer in the middle of the central span, and Fig. 6 shows an example of the analysis of the data. In Fig. 6, the solid line shows values calculated according to the Hino's Expression below, and the dotted line shows the result of the spectrum analysis. Fig. 7 shows accelerations measured in the direction transverse to the bridge axis, and Fig. 8 shows vibration displacements in the direction transverse to the bridge axis obtained by integrating data in Fig. 7 via FFT (Fast Fourier Transformation) using the band pass filter 0.04 to 2.5 Hz. These data, collected over two years since the opening of the bridge, are insufficient as the measurement period is short and neither strong winds nor large-scale earthquakes have occurred during this period. Accordingly, we will continue to collect data for verification regarding design.

Power spectrum of wind speed (Hino's Expression)

$$Su(f) = 0.476 \times \frac{\bar{u}^2}{\beta} \times \{1 + (\frac{f}{\beta})^2\}^{-5/6}$$

$$\bar{u}^2 = 6.0 \times Kr \times (U_{10})^2$$

$$\beta = 1.169 \times 10^{-3} \times \frac{\alpha U_{10}}{\sqrt{Kr}} \times (\frac{Z}{10})^{2m\alpha-1}$$

α : Wind speed exponent
Kr: Surface friction coefficient
f : Frequency
Z : Vertical altitude (meters)
m : Correction coefficient at the time of strong wind

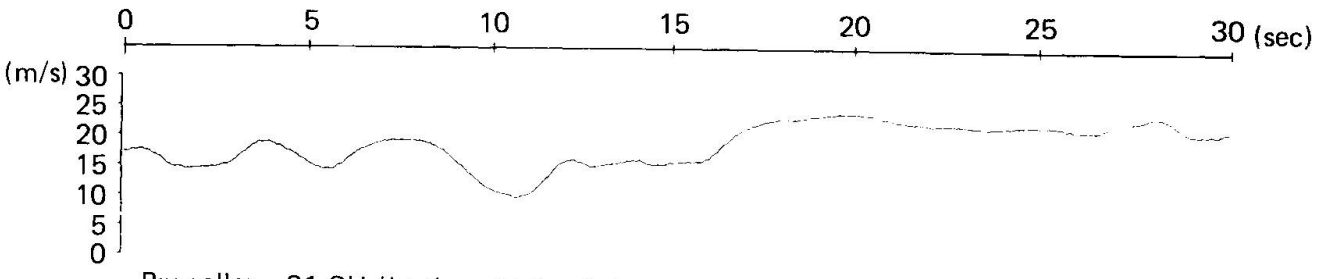

Propeller 31 CH (In the middle of the central span, U component, Pacific Ocean side)

Fig. 5 Wind Velocity

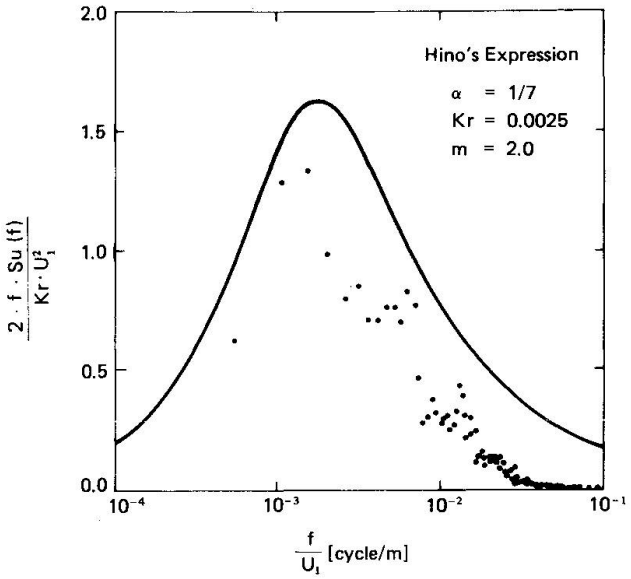

Fig. 6 Power Spectrum of Wind

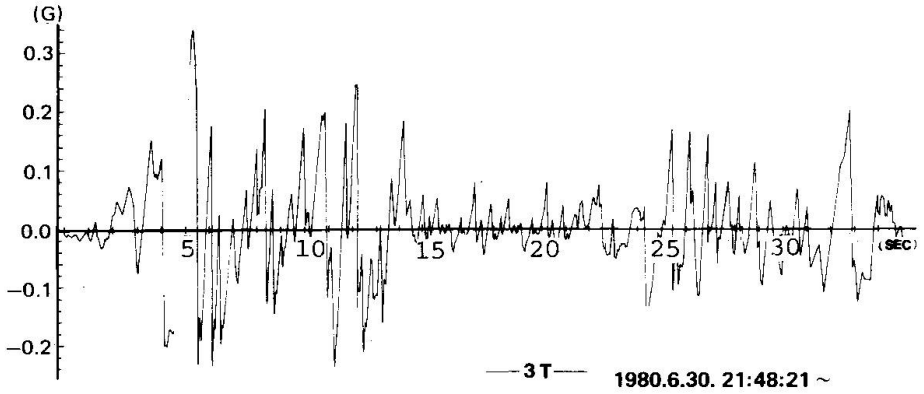

Fig. 7 Acceleration

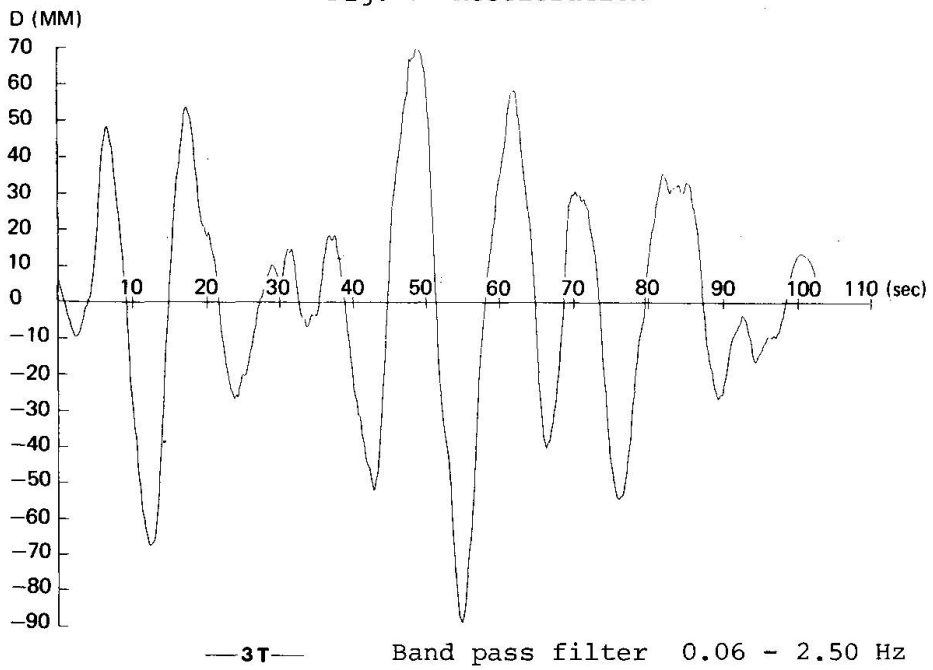

Fig. 8 Displacement

Instrumentation and Monitoring of Norddalsfjord Bridge, Norway

Instruments de surveillance et mesures sur le pont Norddalsfjord, Norvège

Instrumentierung und Ueberwachung der Norddalsfjordbrücke in Norwegen

Stein FERGESTAD
Civil Engineer,
Aas-Jakobsen A/S, Oslo

Kjell NAESS
Resident Engineer
Public Roads Adm.,
Sogn og Fjordane County

SUMMARY
Norddalsfjord bridge is a prestressed, 3 span concrete bridge, with a main span of 230.5 m. As an independant check of the structural analysis and planned jacking operations, monitoring instrumentation has been installed in order to verify the safety of the bridge. Strain gauges have been used in piers and superstructure, and hydraulic jacks between abutments and superstructure. During the construction period, good agreement has been obtained between theoretical calculations and measured values.

RESUME
Le pont de Norddalsfjord est un pont en béton précontraint à trois travées continues, construit par encorbellements successifs. La travée centrale est de 230.5 m. Pour vérifier la sécurite du pont et les calculs théoriqué on a installé des instruments de surveillance. Des extensomètres à cordes vibrantes sont encastrés dans les piles et dans le tablier. Les vérins hydrauliques sont installés entre les culées et le tablier. Pendant la périodique de les calculs théoriques ont été confirmés les instruments construction de surveillance.

ZUSAMMENFASSUNG
Die Norddalsfjordbrücke ist eine dreifeldrige, vorgespannte Betonbrücke mit einer Hauptspannweite von 230.5 m. Zur unabhängigen Ueberprüfung der statischen Analyse und zur Ueberwachung der Verschiebeoperationen mit Hydraulikzylindern zwischen Widerlagern und Oberbau wurde die Brücke instrumentiert. Dehnungsmesser sind in den Pfeilern und im Oberbau installiert worden. Während der Bauperiode sind die theoretischen Berechnungen durch die Messungen bestätigt worden.

1. NORDDALSFJORD BRIDGE

Norddalsfjord bridge is a 400 m long prestressed concrete bridge near Florø in Western Norway. The bridge was opened for traffic in the end of May 1987 after less than 2 years of construction. The main span is 230.5 m, constructed in free cantilevering, and for the time being the longest span for this type of bridge in Europe. A general view of the bridge is given in Fig. 1.

The main foundations are located in sea water at approximately 10 m depth. The main span superstructure is supported by twin wall piers, which are made monolithic with foundations and superstructure. The height of the piers between foundation and superstructure is 15 m in axis 2 and 2 m in axis 3. The piers in axis 2 are flexible enough so that an expansion joint at mid span is not required. During construction temporary walls were added in axis 2. This was done in order to make a box section with the required torsional stiffness to stand dynamic wind loads in the free cantilevered state before connection to the counterweight structure near axis 1. After the temporary walls were removed, jacking to obtain rotation and translation of the completed cantilevers before establishing continuity was performed as part of the design.

The width of the bridge deck is 8 m, refer Fig. 2. The box is 13.0 m deep over the piers and 3.0 m at centre of main span. Web thicknesses vary in steps from 0.35 m at piers to 0.25 m at mid-span. The thickness of the bottom slab decreases from 0.70 m at piers to 0.22 m at mid-span.

The main span and most of the side span between axis 1 and 2 are built in free cantilevering. The other side span is built on scaffolding to the ground. The counterweight structures are constructed on sand beddings. The sand was removed when the superstructure was completed. The counterweight structures are filled with rock, and they are supported on moveable bearings in axis 1 and 4.

2. REASONS FOR MONITORING AND CHOICE OF INSTRUMENTATION

2.1 Twin wall piers

The structural analysis and calculations are based on a finite element program. The calculations showed that the stability of the foundations and twin wall piers were sensitive to the stiffness of the double piers. Besides, the double pier design was new in Norway, and the client (Public Roads Administration) decided to spend some money on extra monitoring. Strain gauges were installed in the double piers as shown in Fig. 3, mainly to give a better assessment of the structure's safety. The design aim has been to create a balanced load distribution between the twin wall piers. This has partly been obtained by vertical jacking in axis 1 and horisontal jacking of the superstructure before continuity was established.

2.2 Main span

As an extension of the instrumentation program for the piers, strain gauges were installed also in the bridge deck and the compression slab of the main span as shown in Fig. 4. The purpose of these gauges is to give information about the moment redistribution in the superstructure due to creep and change in the statical system during the structure's lifetime. The moment redistribution is a feature which is common for all concrete bridges constructed according to the free cantilever method, and additional information from monitoring instrumentation was found very desireable.

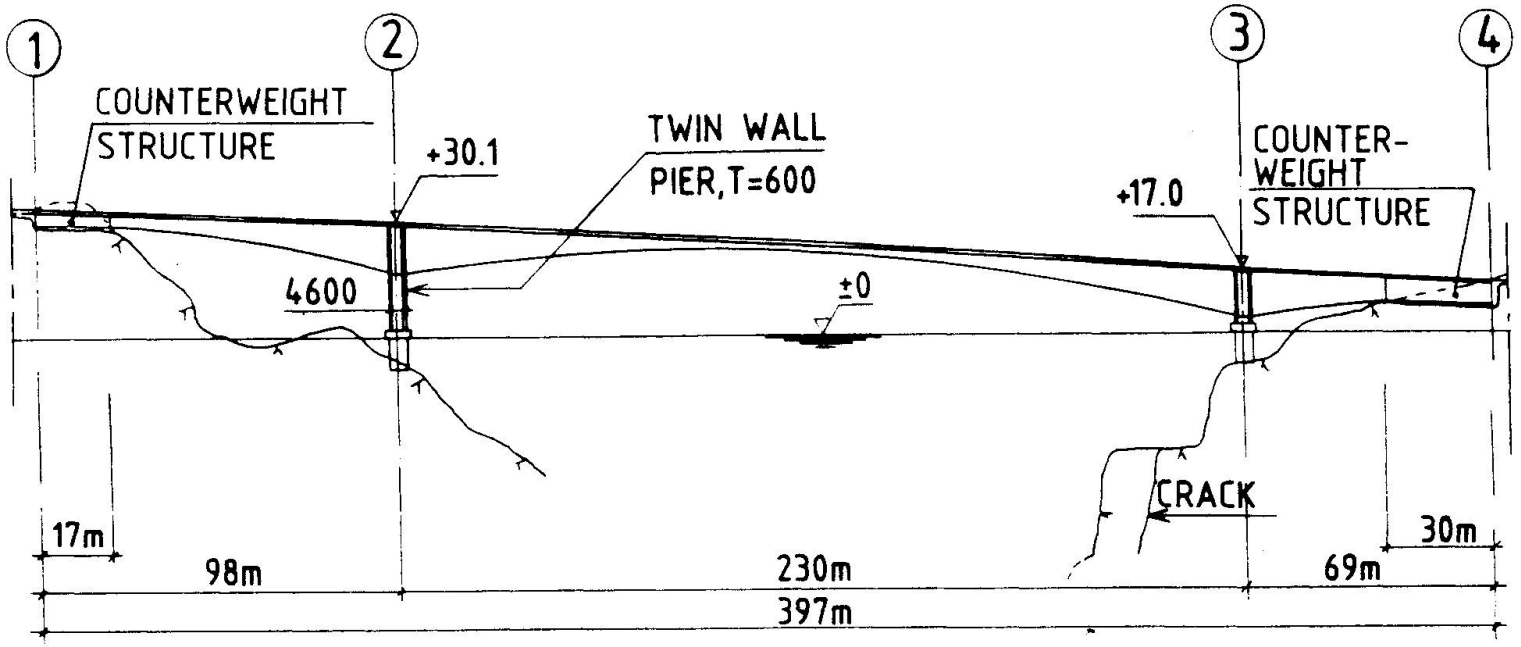

FIG. 1. NORDDALSFJORD BRIDGE. ELEVATION

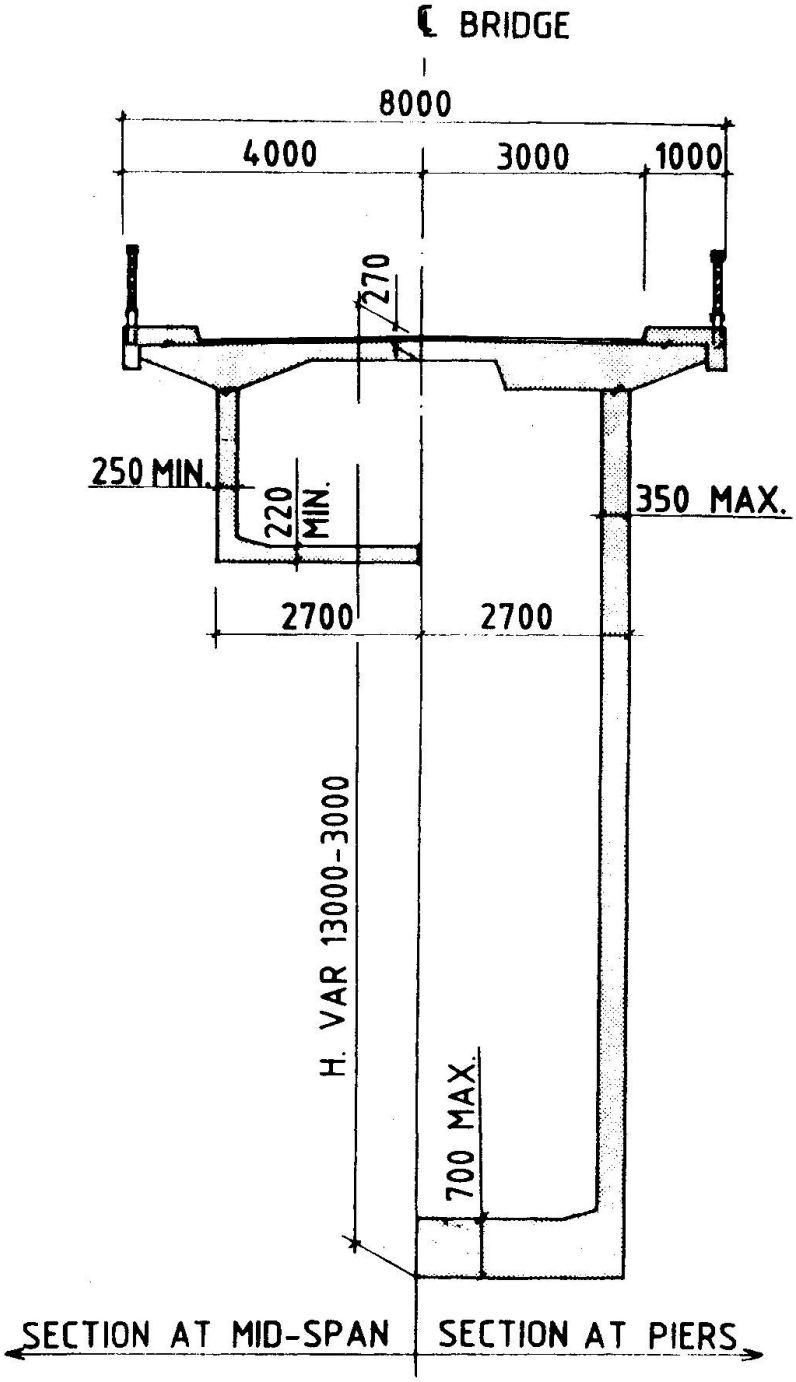

FIG. 2. NORDDALSFJORD BRIDGE. SECTION

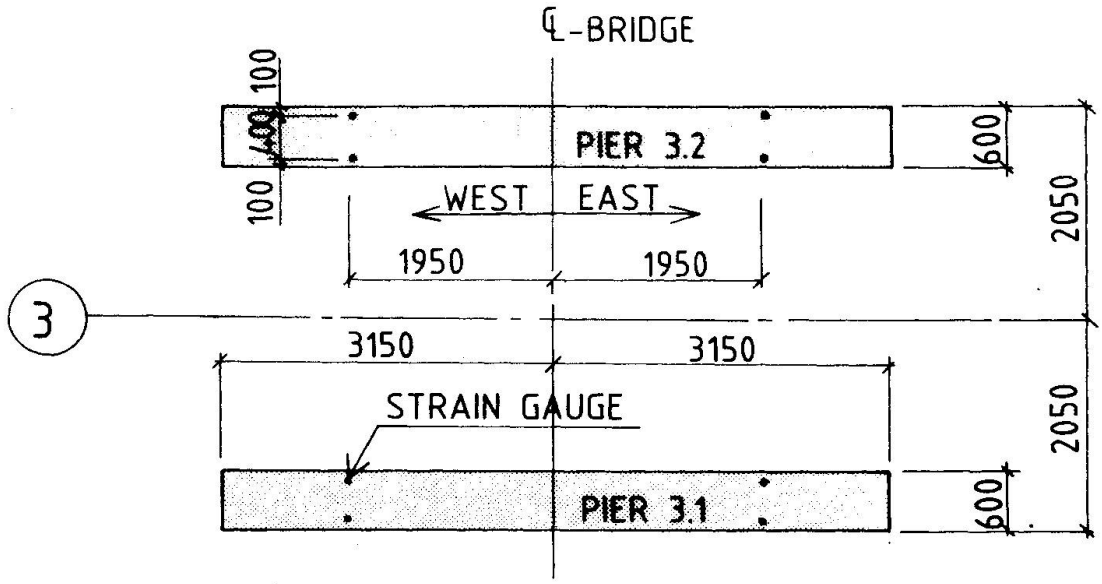

TWIN PIERS AXIS 3

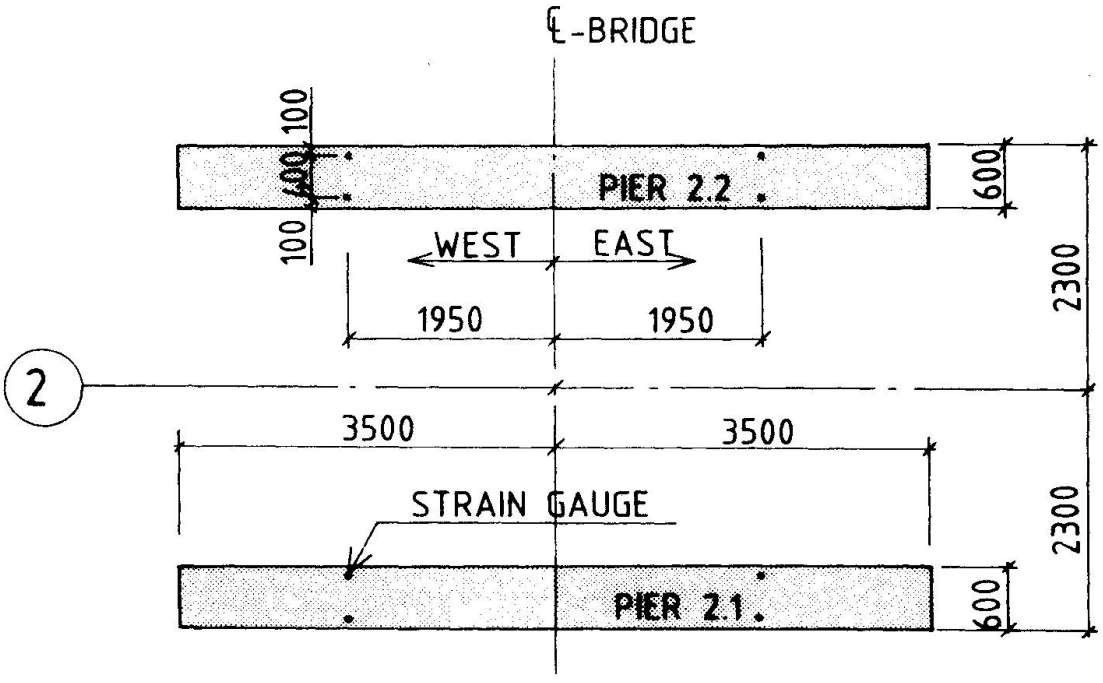

TWIN PIERS AXIS 2

FIG 3. LOCATION OF STRAIN GAUGES

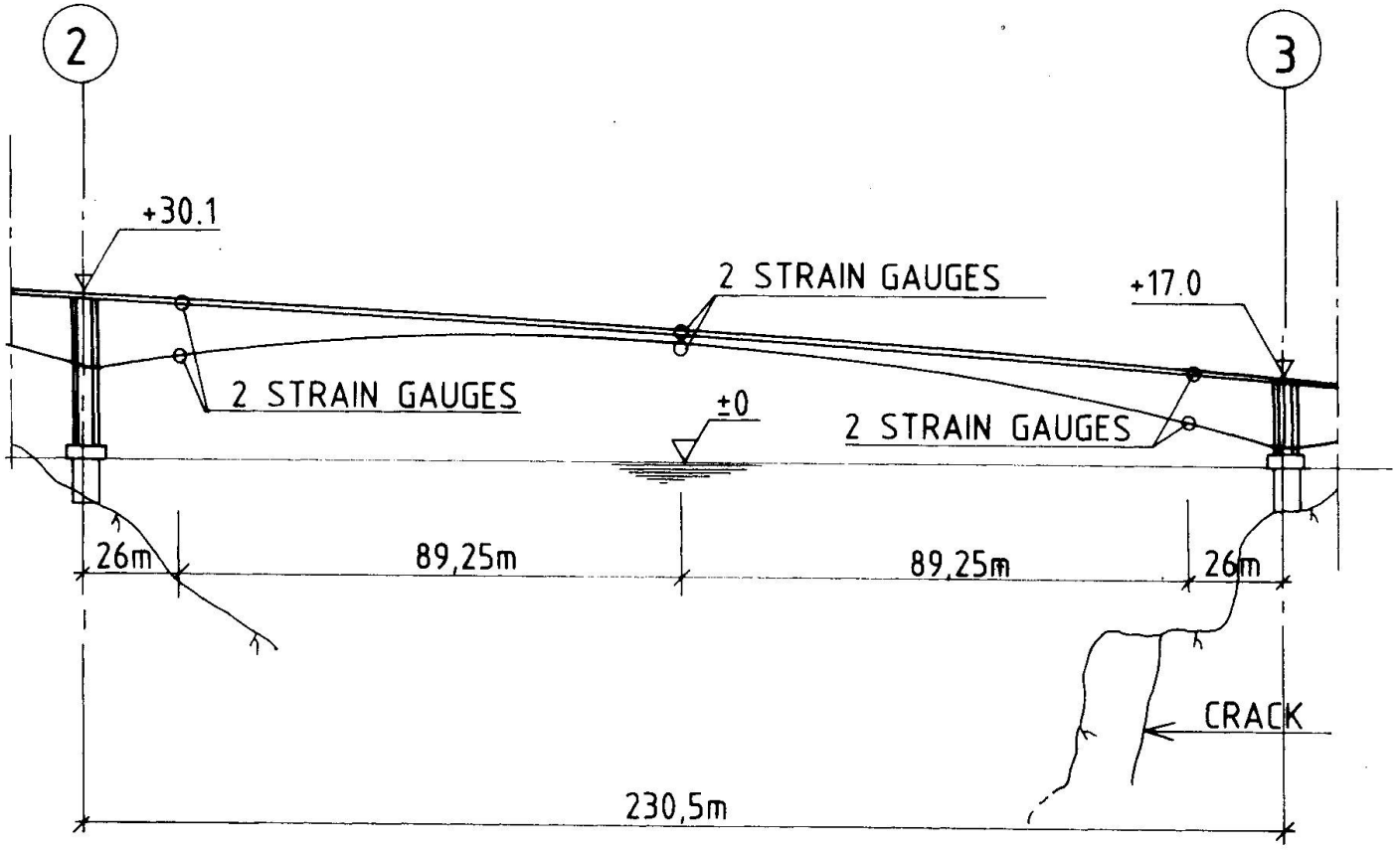

FIG. 4 STRAIN GAUGES IN DECK SLAB AND COMPRESSION SLAB

2.3 Counterweight structures

The counterweight structures filled with rock ballast are vital stabilizing elements. It is of safety reasons necessary to ensure that the total weight is higher than a certain design lower limit. On the other hand, having the bearings in axis 1 and 4 in mind, the total weight must be lower than a certain upper limit. In the actual design, a rather narrow interval was chosen between upper and lower limit. This was compensated by measuring the final load on the bearings by a battery of Enerpack cylinder-jacks. In addition, all the rock ballast was weighed before it was put into the counterweight structures. A little portion of sand and mass concrete was added to the rock to achieve the assumed design weight.

3. THE STRAIN GAUGE

The strain gauge is fabricated by Geonor AS, Norway. The gauge is essentially a vibrating-wire load cell welded to reinforcing steel, see fig. 5. The strain in the steel is a function of the frequency of the vibrating wire, and the frequency is measured by a separate indicator which can easily be connected and disconnected. The strain gauges will hopefully work through the entire lifetime of the structure. After the construction period, readings will be taken at certain intervals.

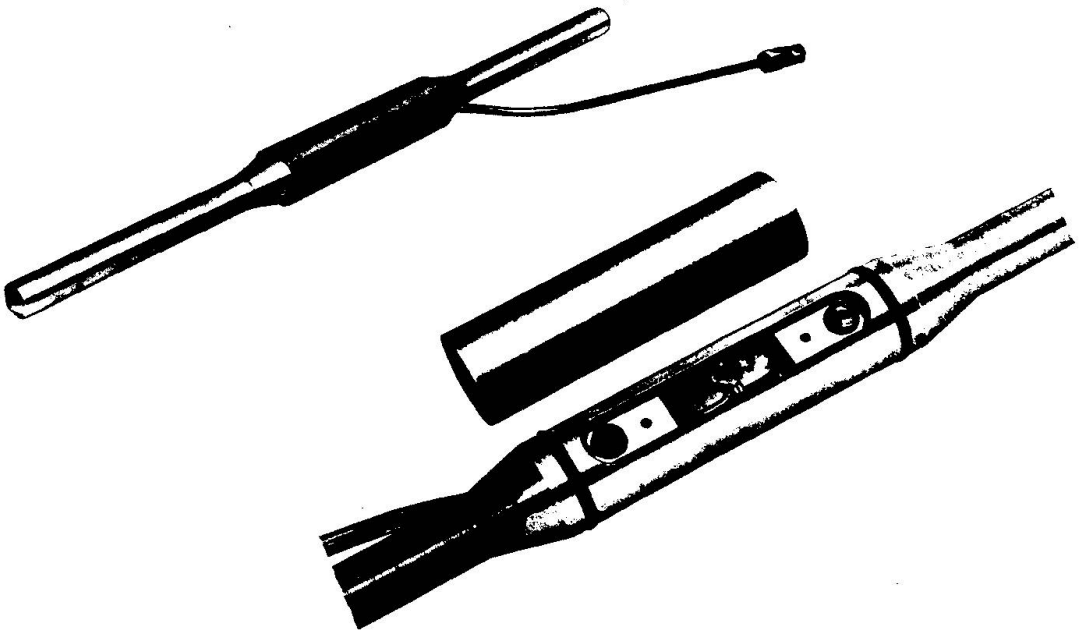

Fig. 5 STRAIN GAUGE

4. RESULTS FROM THE MONITORING INSTRUMENTATION, COMPARED TO CALCULATED VALUES

4.1 Twin wall piers, axis 2

State I: After symmetric free cantilevering, just before connection to the counterweight structure near axis 1.

State II: After completion of remaining unsymmetric free cantilevering until the longest cantilever has reached the middle of the main span.

State III: After jacking down the superstructure 200 mm in axis 1.

State IV: After horizontal jacking and prestressing continuity cables in mid-span.

State V: After installing superimposed dead load.

The strain values include strain due to shrinkage and creep in the concrete and elastic deformation in both reinforcement and concrete. Shrinkage and creep in the concrete is evaluated to account for approximately $\Delta\varepsilon$ = 150 μs in the reinforcement for state I-IV and $\Delta\varepsilon$ = 160 μs for state V. If these $\Delta\varepsilon$-values are subtracted from the measured ε-values, the total compression force in the piers may be computed. This compression force, called "measured force", is compared to the calculated force from the structural analysis.

	Pier 2.1			Pier 2.2		
State	Measured strain ε,(μS)	Measured force N,(MN)	Calcucated force N,(MN)	Measured strain ε,(μS)	Measured force N,(MN)	Calcucated force N,(MN)
I	352	20	21	349	20	21
II	320	17	15	528	38	39
III	457	31	30	364	21	24
IV	453	30	31	348	20	21
V	455	29	29	443	28	28

ε is the mean value of 4 strain gauges
μS = microstrain = 10^{-6}
N is the total axial load (compression) in mega-Newton (mN)

4.2 Twin wall piers, axis 3

State II: After completion of unsymmetric free cantilevering.

State IV: After prestressing continuity cables in mid-span.

State V: After installing superimposed dead load.

Measured force and calculated force are explained in chapter 4.1.

State	Pier 3.1			Pier 3.2		
	Measured strain ε,(μS)	Measured force N,(MN)	Calcucated force N,(MN)	Measured strain ε,(μS)	Measured force N,(MN)	Calcucated force N,(MN)
II	357	21	21	510	36	37
IV	342	19	19	512	36	39
V	468	31	28	543	38	35

ε is the mean value of 4 strain gauges
μS = microstrain = 10^{-6}
N is the total axial load (compression) in mega-Newton (mN)

4.3 Main span

The monitoring of the main span has just begun. The initial values from the six strain gauges are recorded. The development will be checked by taking readings at certain intervals in the future. In addition levelling of the bridge deck will be performed at the same intervals.

4.4 Counterweight structures

The total load on the bearings was checked by a battery of Enerpac cylinder-jacks before continuity in mid-span.

In axis 1 the superstructure was lowered 200 mm in order to stabilize the foundation in axis 2.

Axis	Measured load	Calculated load
1, before vertical jacking	3,60 MN	3,50 MN
1, after vertical jacking	2,82 MN	2,90 MN
4, before continuity	5,76 MN	5,70 MN

5. CONCLUSION, TWIN WALL PIERS

After completion of the bridge (State V), the piers nearest the abutments (piers 2.1 and 3.2) are left with higher compression than their twin pier towards the main span. This was also a design aim.

During construction, there has never been tension in any pier.

The results from the monitoring instrumentation has so far verified the theoretical calculations very well, specially in axis 2. Minor changes in dead load and prestressing force in cables over axis 3 may explain some of the differences between measured and calculated forces in piers 3.1 and 3.2.

Leere Seite
Blank page
Page vide

Instrumentation of glued segmental box girder bridges

Appareillage de mesure installé sur des ponts à caissons segmentés collées

Messgeräteeinrichtung auf geleimten Segmentkastenträgerbrücken

Ben I.G. BARR
Senior Lecturer in Civil and Structural Engineering
University College, Cardiff, UK

Ben Barr is a chartered civil engineer engaged in concrete materials research. His main interests are in the fracture processes in concrete and the fracture characteristics of fibre reinforced concrete materials.

Peter WALDRON
Lecturer in Civil Engineering,
University of Bristol, Bristol, UK

Peter Waldron is a chartered civil engineer engaged in structural concrete research. His main interests are in instrumentation, interpretation of experimental results, prototype testing and analysis of thin-walled structures.

H. Roy EVANS
Professor of Civil and Structural Engineering,
University College, Cardiff, UK

Roy Evans is head of department of civil and structural engineering at Cardiff. He is interested in composite construction and has conducted extensive research into all types of bridge and thin-walled structures.

SUMMARY

Glued segmental construction of post-tensioned concrete box girder bridges is a relatively new technique in the UK. Over the last year, three major bridge structures of this type have been instrumented to yield much needed information on (i) early shrinkage strains; (ii) time dependent effects, such as creep and loss of prestress; (iii) elastic strains during erection and early service life; (iv) temperature; and (v) formwork pressures during casting. The instrumentation schemes are briefly described and some early results are presented.

RESUME

La construction des ponts à caissons segmentés collés en béton postcontraint est une technique relativement récente au Royaume Uni. L'an dernier les structures de trois des plus importants ponts de ce type ont été équipées d'instruments de mesure afin de fournir des informations de première nécessité sur: (i) les dilatations de retrait primaire; (ii) les effets temporels, tels que le fluage et les pertes de précontrainte; (iii) les contraintes élastiques durant le montage et la première mise en service; (iv) les températures; (v) les pressions de coffrage durant le bétonnage. On décrit brièvement les schémas d'installation des instruments et on présente quelques premiers résultats.

ZUSAMMENFASSUNG

Im Vereinigten Königreich stellt die Herstellung von geilemten Kastenträgerbrücken ist eine ziemlich neuartige Herstellungstechnik dar. Während dem letzten Jahr sind drei solche grössere Brückentragwerke mit Messgeräte ausgestattet worden, um sehr mangelnde Nachweise zu erlanger über: (i) die Anfangsschwinddehungen; (ii) die zeiabhängige Wirkungen, wie das Kriechen und die Vorspannuns- verluste; (iii) die elastischen Spannungen während der Konstruktion und der ersten Dienststellung; (iv) die Temperaturen; (v) die Schalenpressungen während der Betonierung. Dieser Artikel beschreibt kürzlich die Messeinrichtungsschemas und präsentiert einige erste Ergebnisse.

1. INTRODUCTION

Segmental construction of concrete bridges was introduced into Europe in the 1950's. The method is particularly suitable for medium to long span bridges and is now commonly used in all parts of the world. For example, in North America, where the advantages inherent in this form of construction have long been recognised, over one hundred such bridges have been built since the 1970's. In the UK, the first segmental bridge was the Clifton Bridge, Nottingham, completed in 1957. Although over thirty such bridges have been built in the UK since then, the majority of these have been completed in the last decade. The increasing use of segmental techniques in recent years has occurred for a variety of reasons. These include improvements in materials, better analytical techniques and a growing awareness of the overall enonomic benefits.

1.1 Segmental construction techniques

The term segmental construction is very broad and refers to any concrete bridge structure that is cast in a number of distinct longitudinal segments. Several alternative techniques have evolved over the years. These are usually categorised according to the method of casting and erection of the segments [1] and include the (a) balanced cantilever method; (b) progressive placing method; (c) span-by-span method; and (d) incremental launching method.

1.2 Project description

By far the most significant construction technique is that employing balanced cantilevers in which the cost penalties of using segmental construction are more than offset by the savings brought about by the reduction in falsework. Fig. 1 provides an indication of the frequency with which each technique has been employed in North America, and the span lengths for which each is best suited [2]. It is apparent that 85% of all segmental bridges built to date are of balanced cantilever construction. Precast and cast in situ segments have been employed to about the same degree. In the UK, the pattern is similar with approximately two thirds of segmental bridges being of the balanced cantilever type of construction.

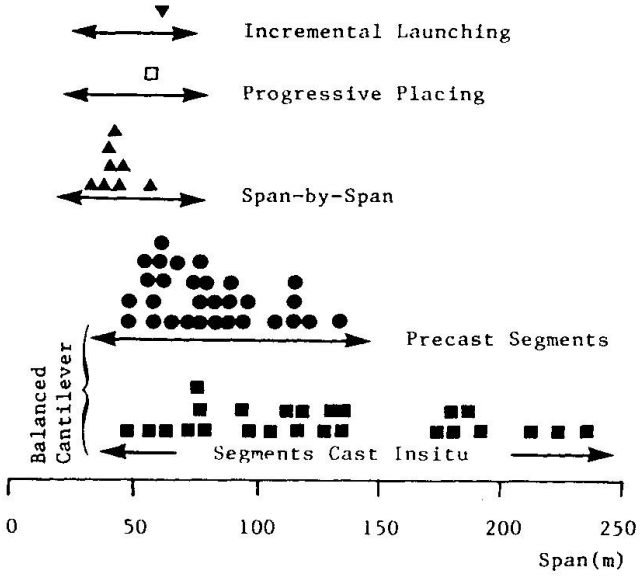

Fig. 1 Segmental bridge types

1.2.1 Limitations

The research project described here concentrates on the balanced cantilever method as the predominant structural technique. More specifically the investigation is centred on glued segmental construction in which match-cast precast segments are prestressed together separated by a thin layer of epoxy resin. This technique is becoming increasingly competitive especially for medium span viaducts. Despite these restrictions much of the research should be of equal value to the other forms of segmental construction.

1.2.2 Objectives

One of the most important considerations in the design of segmental bridges by balanced cantilever is the effect of the time-dependent properties of the materials employed in construction. These include shrinkage and creep of the concrete, and relaxation in the prestressing steel. Since each segment is cast from a different batch of concrete on a different day, each segment may then be expected to respond uniquely to the application of construction loads during and immediately after erection. Moreover, since each balanced cantilever may take several weeks to erect, continuity at midspan will not generally be achieved until one half-span has been subjected to much higher levels of creep, shrinkage, etc..

In bridges employing cast insitu segments or precast segments with thick mortar joints there is some opportunity for adjusting the vertical profile during erection. However, in glued segmental bridges formed from match-cast segments, vertical profile must be decided at the time of casting and is very difficult to adjust during erection. For this reason all deformations due to time-dependent effects and elastic response under varying construction loads must be accurately calculated at the design stage.

A further consideration in all thin-walled concrete bridges is the effect of differential temperature distributions across the wall thickness. This can be of particular significance in box girders for which the volume of air enclosed inside the box may have the effect of accentuating the thermal gradients across the walls. In such cases, deformation may not be restricted to longitudinal movement only but may include significant longitudinal and transverse bending effects.

Finally, in segmental bridges of this type employing precast segments, dimensional accuracy during casting is of paramount importance. Deformation of formwork due to self-weight of wet concrete and the vibrations created during compaction must therefore be closely controlled.

In summary the main objectives of the research programme are to investigate the following:

(i) early shrinkage strains in concrete segments;
(ii) time-dependent effects, such as creep and loss of prestress;
(iii) elastic strains and deflections during erection and early service life;
(iv) thermal effects due to temperature differentials across the walls; and
(v) formwork pressures caused by external vibration during casting.

A dearth of information exists in these areas, particularly with respect to the climatic and environmental conditions prevailing in the UK. A major initiative has recently been established to investigate these effects. Analytical and computational aspects of the research are being verified and calibrated by monitoring the performance of three major glued segmental bridges. It is the instrumentation and early measurements from this field investigation which are described in some detail here.

2. DESCRIPTION OF INSTRUMENTED BRIDGES

Three glued segmental bridges were identified for instrumentation, each with a very different structural configuration. The first bridge was straight in plan with varying section depth; the second and third had almost constant cross-sectional depth but displayed very different levels of horizontal curvature.

2.1 River Torridge Bridge

The River Torridge Bridge, located 1km north of Bideford, North Devon, forms part of the 8.4km Bideford bypass on the A39 trunk road between Taunton and Freddon. Completed in May 1987 it carries two lanes of traffic 29m above mean high water level over the Torridge tidal estuary.

The bridge consists of eight continuous spans, each up to 90m in length, with a total length of 645m. The general arrangement and elevation of the bridge is shown in Fig. 2. The superstructure is straight in plan and is formed from 251 segments weighing up to 105 tonnes each. Its cross-section, Fig. 3(a), is that of a single cell box girder with wide side cantilevers, varying in depth from 6.1m at the supports to 3.1m at midspan.

Segments were match cast on site by the short-line method at a rate of approximately five per week. After curing for several months, each unit was transported to the western end of the partly completed bridge and erected using a purpose built launching girder itself weighing 150 tonnes. As each segment was positioned, a thin layer of epoxy resin was applied by hand to the matching faces immediately prior to prestressing, thus ensuring water-tightness and a uniform transfer of stress across the joint.

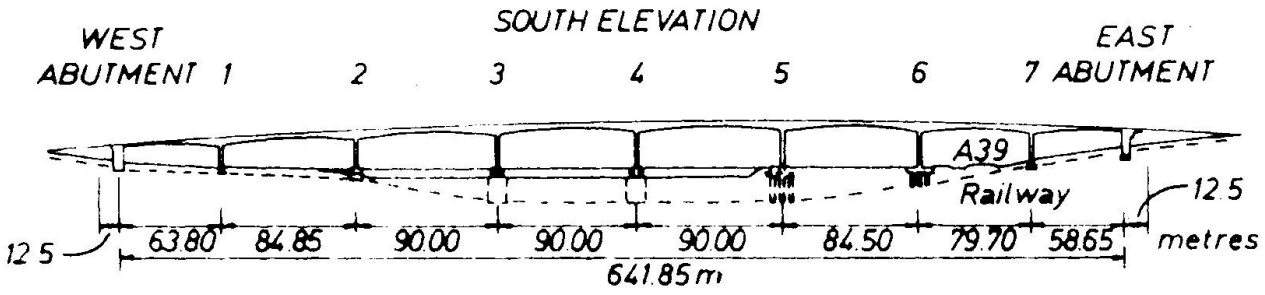

Fig. 2 Elevation of River Torridge Bridge.

2.2 Grangetown Viaduct

The second and third viaducts to be monitored are both located on the peripheral distributor road currently being constructed around the city of Cardiff. The required alignment, together with the frequency and spacing of the obstacles, made the choice of viaducts a logical solution for this part of the scheme. Both viaducts were designed to carry the Department of Transport's HA loading and were checked for 45 units of HB loading. This design loading was used in order that the viaducts could be used to meet the needs of the adjacent docks and also to cater for future industrial development along the peripheral distributor road.

The Grangetown Viaduct, which is over 1km long, is the longest post-tensioned glued segmental viaduct in the United Kingdom. The twin trapezoidal box girder superstructure is made up of a total of 641 segments weighing between 43.5 and 74 tonnes. Typical cross-sections for a mid-span segment and a pier segment are shown in Fig. 3(b). Between the abutments, each deck is supported by 14 circular 3m diameter columns varying in height from 8.5m to 18m. The columns in turn are supported by means of hexagonal pile caps.

2.3 Cogan Viaduct

The second post-tensioned glued segmental viaduct to be instrumented at this site is the Cogan Viaduct. Although the Cogan Viaduct is shorter in length it

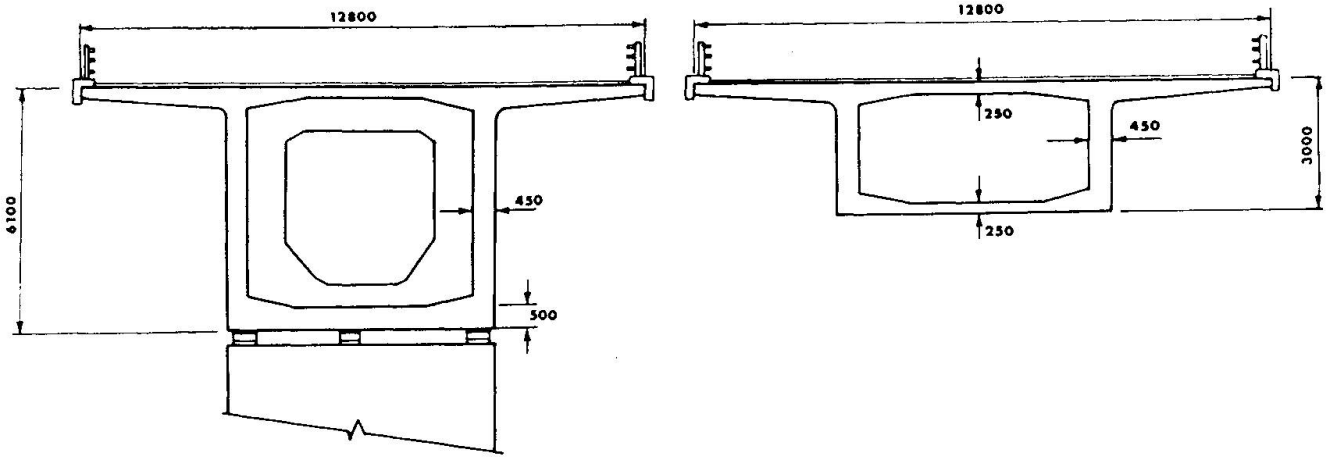

Fig. 3(a) Typical sections through River Torridge Bridge

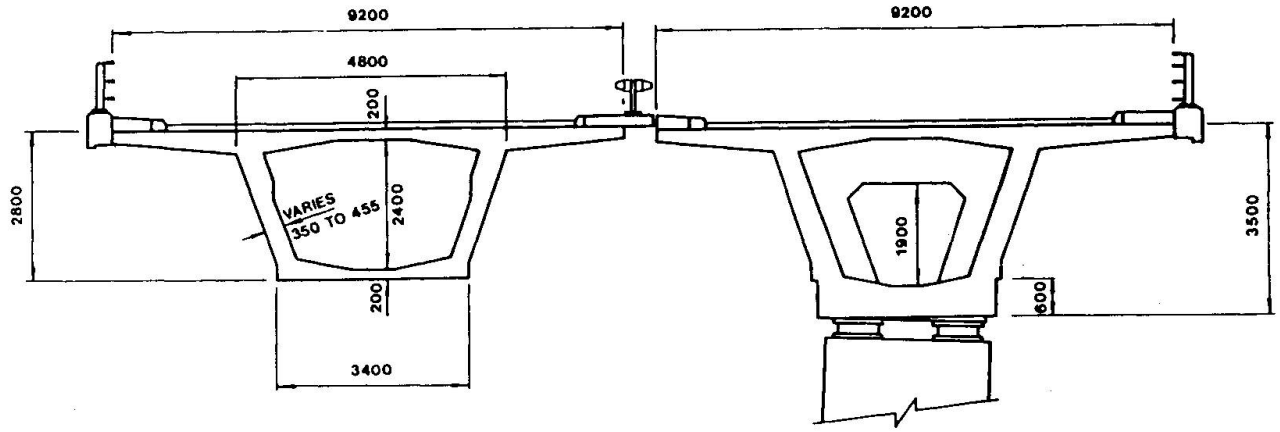

Fig. 3(b) Typical sections through Grangetown Viaduct

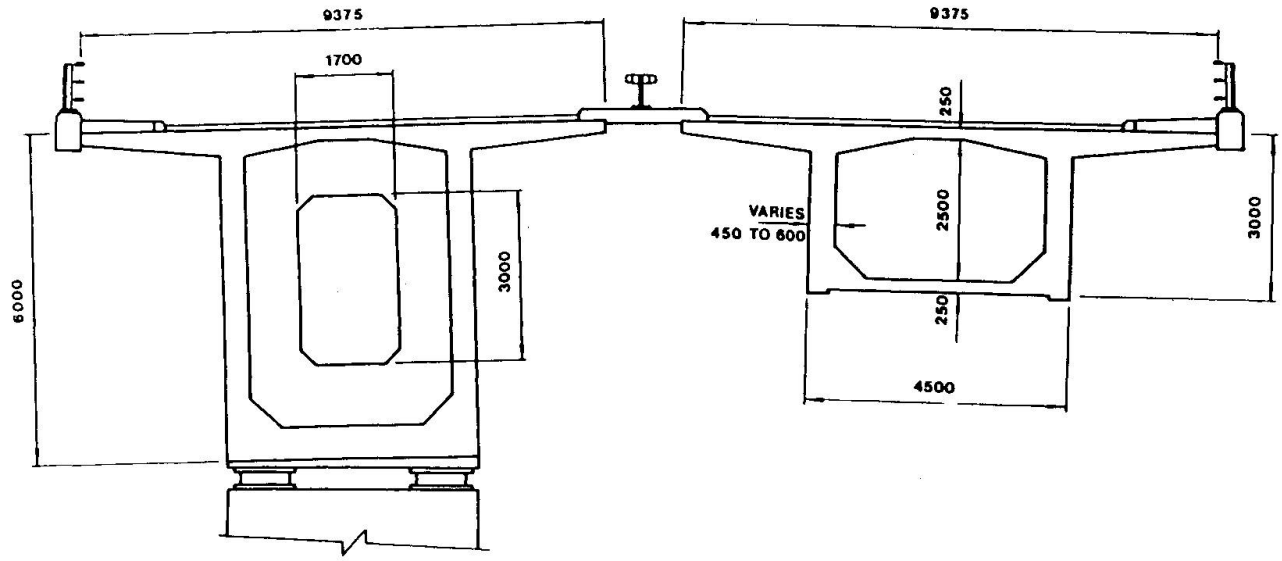

Fig. 3(c) Typical sections through Cogan Viaduct

is more complicated than the adjacent structure since it has a main span of 95m and a radius of curvature of only 285m for some of the approach spans. Cogan Viaduct differs from Grangetown Viaduct in that the deck is based on a rectangular box section due to the curved soffit of the 95m main span. Typical cross-sections for a mid-span segment and a pier segment for the Cogan Viaduct are shown in Fig. 3(c). The viaduct has 6 spans for each carriageway and will be built from 300 segments, approximately 2.5m long and weighing between 43 and 117 tonnes. The pier segments to the main span are 6m deep and during their construction some additional monitoring of formwork pressures was carried out.

As for the two previous bridges, the precast deck segments were manufactured on site by the short-line match-cast method. In order to meet the construction programme and ensure independence from weather conditions, a purpose built three-bay portal frame factory was erected. The casting cells in each bay were capable of producing one segment per day and hence only a limited amount of time was available for the installation of the gauges in any given segment. The instrumented spans of the Grangetown and Cogan Viaducts were both erected by crane.

3. INSTRUMENTATION SCHEMES

3.1 Concrete strain

Instrumentation for the measurement of concrete strain was similar in all three bridges. In the River Torridge Bridge four bridge segments were chosen within one of the central 90m spans (Span 5). Their locations, identified in Fig. 4, were designated P4-1E, P4-6E, P4-10E and P4-16E, corresponding to their positions relative to Pier 4. Three further segments within a single half-span were chosen in both the Grangetown and Cogan Viaducts, at approximately mid-span, quarter-span and support sections.

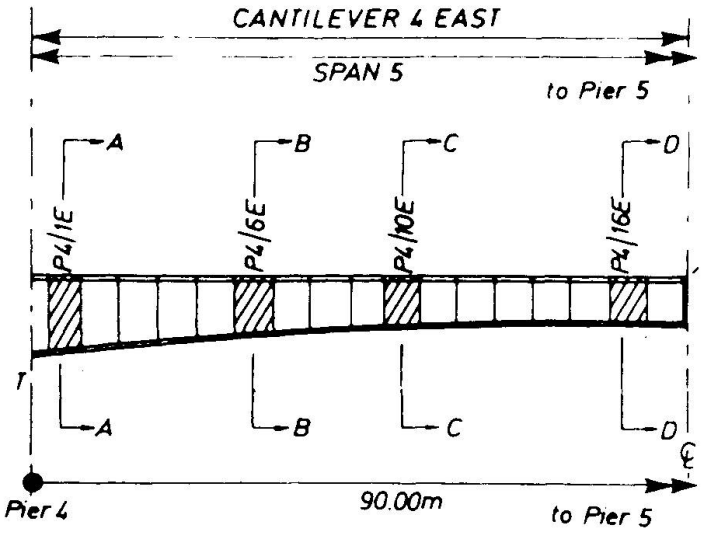

Fig. 4 Instrumented segments

Concrete strain was measured using embedment type vibrating wire strain gauges with a 140mm gauge length. This type of gauge was chosen because of its robustness during installation and casting but also because, unlike electrical resistance gauges, its readings remain unaffected by disconnection. This is essential for field investigations when a complete strain history is required but where it is impracticable to leave data recording equipment permanently attached. This type of gauge has been used extensively for bridge tests and has proven to be reliable and accurate. It has a sensitivity of less than one microstrain and displays very low long term drift.

Each segment was instrumented for measurement of strain at a number of discrete points around the cross-section on the median line of the walls. For segment P4/1E, both single and rosette gauges were used at the positions indicated in Fig. 5. All gauges were fixed to secondary steel attached to the main reinforcement before casting. Axial strains were monitored at six positions, namely the four corners and at the cantilever tips. Three-element rosette gauges were deployed at each of the three intermediate positions in each flange and web

element. These yielded additional information on the distribution of axial strain as well as in-plane shear strain around the box section. A similar arrangement was used for segment P4/6E. The remaining two segments in the River Torridge Bridge were instrumented less fully with only single element axial strain gauges.

A similar instrumentation scheme was adopted for the other two bridges. In the three instrumented segments in Grangetown Viaduct, gauges were positioned at eighteen similar locations to those identified previously in Fig. 5. However, in this instance, only the central gauge in each flange and web element was a rosette. In the Cogan Viaduct segments, the six axial gauges in the box corners and cantilever tips were retained with two 120° rosette gauges at intermediate points along each wall element forming the box.

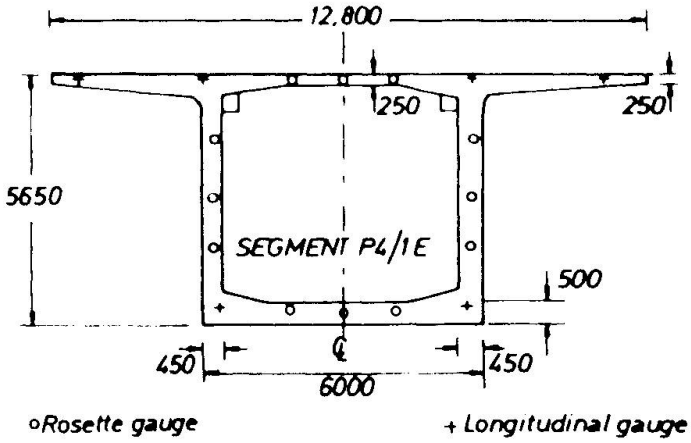

Fig. 5 Strain gauge positions within Segment P4/1E

3.1.1 Instrumentation success rate

In each of the three structures several additional gauges were installed across the thickness of the various wall elements. Since direct strain in this direction is likely to be negligible, these gauges should yield valuable information on long-term concrete shrinkage strains.

A total of 289 vibrating wire strain gauges were deployed in this way in the three structures, as indicated in Table 1. The overall failure rate of approximately 1% was extremely low considering the difficult installation and casting operations.

Structure	Axial	Rosette	Shrinkage	Total	Failures
River Torridge Bridge	40	24	4	116	1
Grangetown Viaduct	42	12	3	81	2
Cogan Viaduct	18	24	2	92	0
Total	100	60	9	289	3

Table 1 Vibrating wire gauge deployment

3.1.2 Material properties

In addition to this programme of monitoring strain behaviour in the bridge structures, a parallel laboratory investigation into the various time-dependent material properties was also initiated. Numerous prism specimens, each with a single axial vibrating wire gauge embedded on the centreline, were manufactured from the batches of concrete used for construction of the instrumented segments. Some have been fully sealed against loss of moisture, for control purposes; the remainder have either been left unsealed or have been partially sealed, to represent more accurately the environmental conditions at the various bridge sites. A number of these specimens are being used to determine

Young's modulus, Poisson's ratio and the coefficient of thermal expansion and their variations with age. The remainder are being used for the long-term assessment of creep and shrinkage effects.

3.2 Temperature monitoring

Copper-constantan thermocouples were used throughout because of their robustness and reliability over long periods of time. They are also relatively cheap and are not greatly affected by the severe environment of the concrete.

The aims of the thermal investigation were twofold. Firstly, to adjust the concrete strain readings obtained at each vibrating wire gauge position for a standard reference temperature; secondly, to measure variations in thermal gradient across the walls of the cross-section and along the length of the superstructure resulting from different solar and environmental conditions. For the former purpose, single thermocouples were attached to the gauges at all gauge positions; for the latter, arrays of thermocouples were placed across the thickness of each wall element in two selected segments only. One of these was Segment P4-10E (River Torridge Bridge) in which the thermocouple arrays supplemented the vibrating wire gauges previously described. The other segment

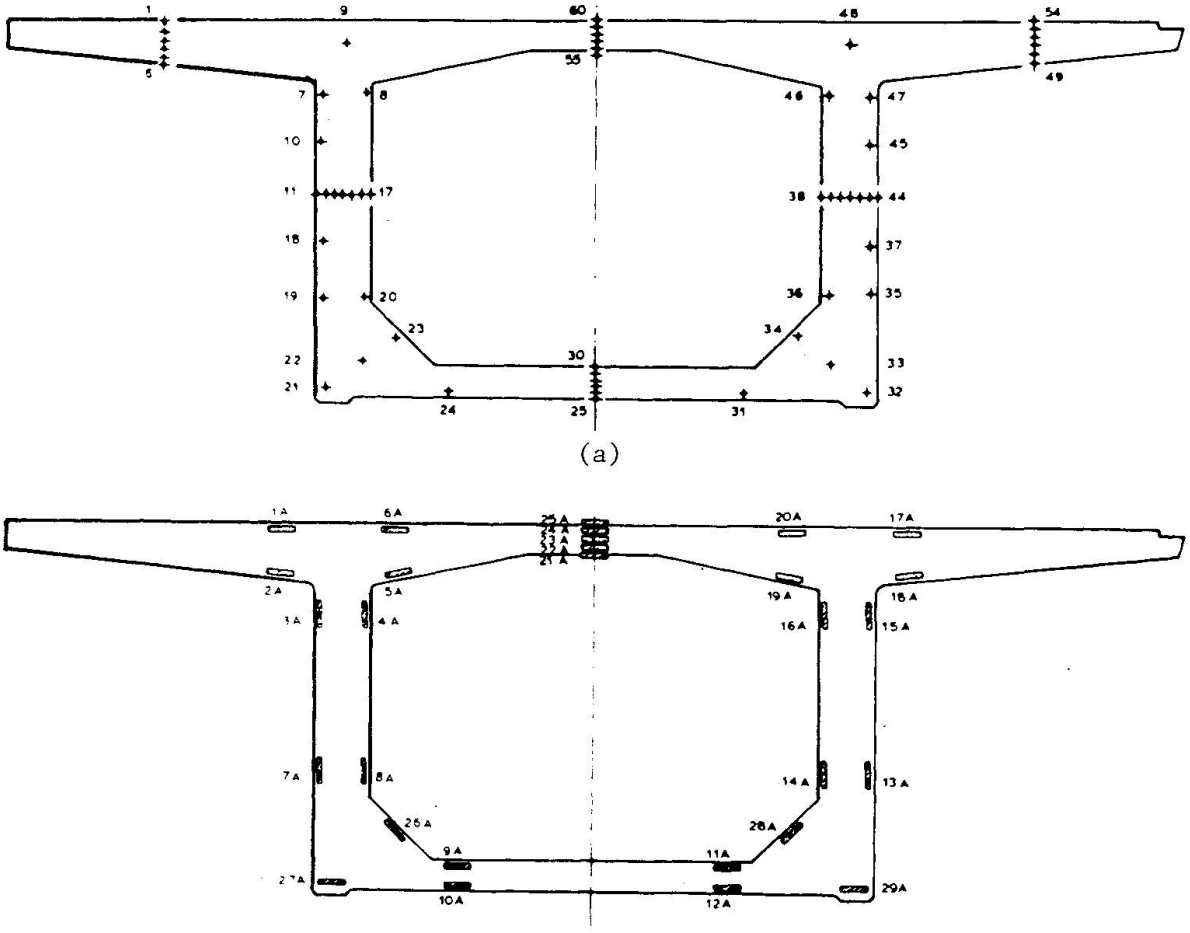

Fig. 6 Positions of (a) thermocouples, and (b) electrical resistance strain gauges, in a segment of the Cogan Bridge.

selected for thermal investigation was in the Cogan Viaduct within the same half-span but additional to the three segments previously instrumented with vibrating wire gauges. This segment was also heavily instrumented with electrical resistance strain gauges placed in pairs near opposite faces of the walls for the purpose of monitoring short-term longitudinal and transverse strains due to diurnal temperature variations. Fig. 6 shows the positions of thermocouples and electrical resistance strain gauges in the Cogan Viaduct.

Lead wires of the installed gauges and thermocouples were bundled together and fixed securely with cable ties to the sides of reinforcement bars so as to avoid, as far as possible, contact with poker vibrators during concreting. The wire ends were protected during casting in two plastic trays suitably spaced off the main reinforcement of the inner faces of the webs so as to be flush with the inner surface of the finished concrete. The trays were later replaced by electrical switch boxes into which reading instruments could be plugged to obtain results.

3.3 Monitoring of pier reactions

After continuity has been established at mid-span the structure becomes indeterminate. Deformations due to subsequent time-dependent effects, settlement or superimposed loading will then result in the creation of additional secondary bending moments and reactions. In order to determine the magnitude of these effects, an attempt has been made to monitor pier reactions. To date this aspect of the investigation has been limited to Grangetown Viaduct. However, if it proves to be successful, the technique will also be applied during erection of Cogan Viaduct.

During construction of Grangetown Viaduct, each balanced cantilever was supported by a single 3m diameter column. After erection of the pierhead unit, the design required a balanced pair of segments to be permanently stressed prior to erection the next pair. Ten such pairs of segments were constructed per column. Finally, an additional segment was added leaving a gap of 300mm between adjacent cantilever tips to be filled by an in-situ joint. The bearings used for the two viaducts were designed with additional top and bottom plates, machined to match the bearings, to be cast into the soffit of the pierhead segment and the top of the column.

During installation of the two bearing plates at the top of the appropriate columns, a vibrating wire gauge was cast vertically immediately under the centre of each. The objective of introducting these two gauges was to monitor the strains due to the known self-weight of the individual segments during erection. It should then be possible to use these results as a calibration curve during subsequent loading and deformation of the structure. Three columns were instrumented in this way; the intermediate pier supporting the balanced cantilever containing the instrumented segments (Pier 3), together with the pier either side.

The results from the two gauges installed at Pier 3 of the Grangetown Viaduct are shown in Fig. 7. The shape of the two curves is similar, although the numerical values differ substantially from one another. The difference in the strain readings is thought to be due to the two gauges being located at at different positions relative to the bearings. The strain concentration immediately below the bearing plates change rapidly and even small variations in the position of the gauges will result in large variations in the recorded strain. At a later stage these results will be related to the corresponding dead load on the structure and will be utilised to monitor the pier reactions during the passage of a test load across the structure and during its early service life.

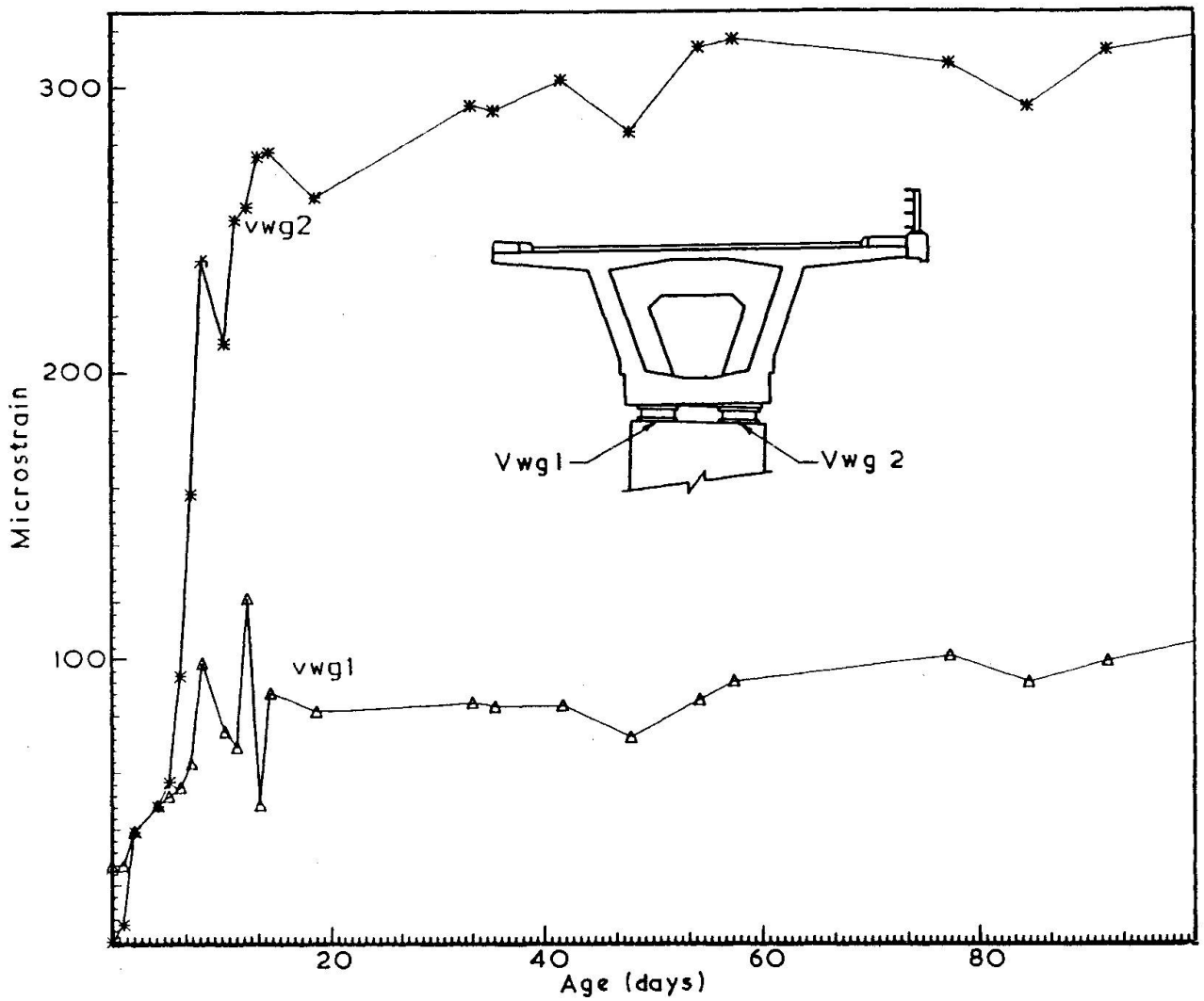

Fig. 7 Calibration curve for pier reactions

4. INITIAL RESULTS FROM STRAIN MONITORING

It was not possible to use remote automatic data logging equipment for a variety of reasons. These included difficult site conditions during erection, the distance between instrumented segments within the same span and the geographical location of the three structures. Approximately 20,000 strain readings from the bridge segments and prism tests were recorded manually in the first 12 months of the project. These have been entered in to a computer data base for subsequent reduction and analysis.

4.1 Shrinkage strains

Approximately 70% of the total expected shrinkage takes place in the first 28 days. The phenomenon is thus of much greater significance to insitu construction than to the glued segmental technique described here. In Fig. 8, two typical shrinkage strains recorded from Segment P4/10E in the River Torridge Bridge before erection are compared with those from two partially sealed prism specimens. As expected, one of the prisms stored outdoors displayed shrinkage strains approximately 15% higher than the other prism stored indoors at a relatively high humidity of 85%. Both prisms, however, over-estimated the true shrinkage strains as measured in the bridge segments by approximately 30%..

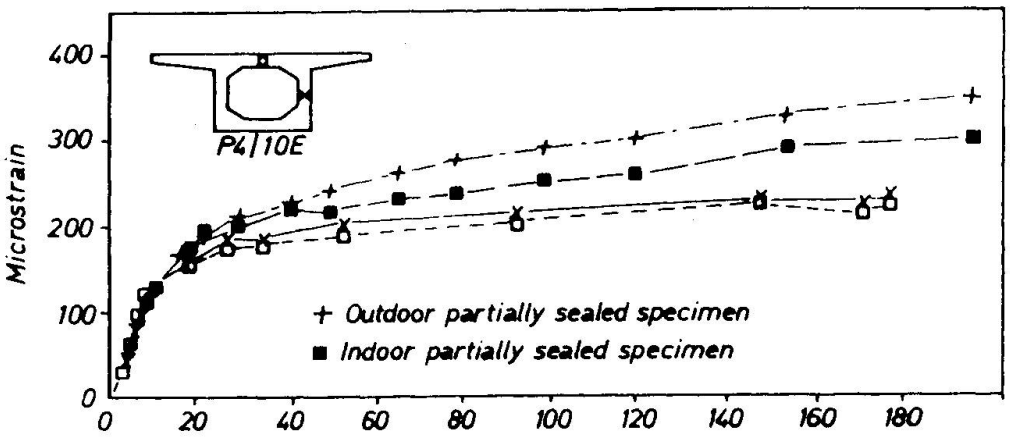

Fig. 8 Typical concrete shrinkage strains

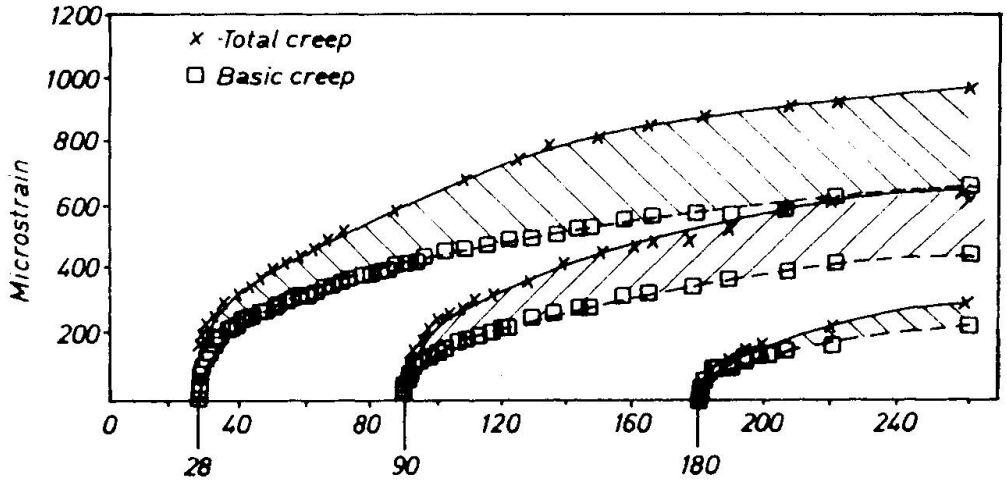

Fig. 9 Typical results from concrete creep tests

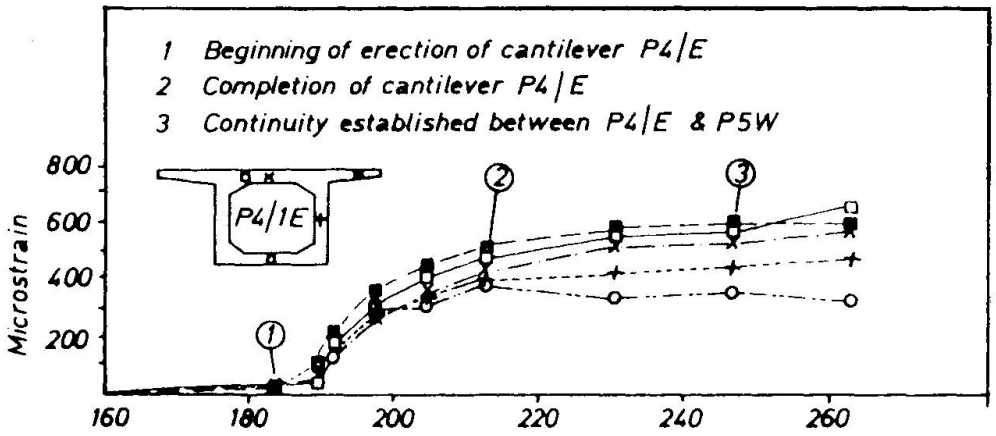

Fig. 10 Concrete strains measured during erection

4.2 Creep strains

Concrete creep is likely to be a more significant effect than shrinkage since it occurs as a result of self-weight stresses during erection and due to the subsequent application of external loads. Fig. 9 illustrates typical results of creep tests on prism specimens prepared with concrete from Segment P4/1E. From these results, corresponding to initial loading at ages of 28, 90 and 180 days, it is apparent that the level of creep strain is significantly reduced if the load is applied at a later age.

Two separate measures of creep are shown in Fig. 9. Basic creep is obtained from fully sealed specimens and may therefore be considered to occur in the absence of shrinkage. Total creep, which is approximately 30% higher, represents the creep of partially sealed specimens which thus enable the creep and shrinkage mechanisms to occur interactively.

4.3 Erection strains

Results from five typical gauges distributed around the cross-section of Segment P4/1E in the River Torridge Bridge are shown in Fig. 10 for the period including erection of Span 5. All strains are compressive and increase throughout erection of the balanced cantilever to a maximum of approximately 500 microstrain in the top flange. Thereafter, some change in these values of strain are apparent due to the combined effects of creep, shrinkage and the establishment of continuity with the previous span. The situation is further complicated by the application of additional construction loads caused by movements of the launching girder.

5. FORMWORK PRESSURE MEASUREMENTS

At the time of the manufacture of the 6m deep Cogan bridge pierhead segments, the authors and the engineer for the scheme were not aware of any work which would give an indication of the concrete pressures developed due to external vibration of the shutter. All the data available to date related only to static pressures developed on formwork during construction using internal vibrators. Hence a small additional study was initiated to monitor the formwork pressures during the manufacture of the deeper segments for the Cogan Viaduct.

5.1 Static pressure tests

In the first series of tests, all four load cells in the formwork were connected to a switch box, the concrete pressures being recorded on a digital readout unit. Four tests were carried out using the simple procedure illustrated in Fig. 11. The main conclusions were as follows:

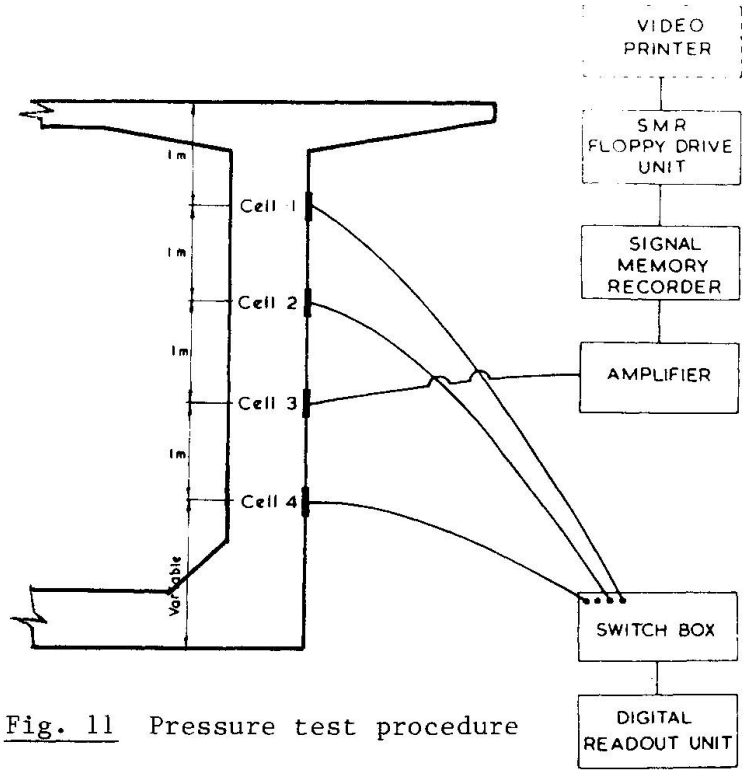

Fig. 11 Pressure test procedure

(a) The results were reproducible but did not show the dynamic pressures generated by external shutter vibration.

(b) Over short periods of time, the recorded mean concrete pressures were related directly to the hydrostatic head of concrete. Over longer periods, the pressures were reduced due to the setting of the concrete.

(c) The maximum pressures were recorded by Cell 3. The maximum pressure recorded was 72 kN/m^2.

5.2 Dynamic pressure tests

In a second series of pressure tests, an attempt was made to monitor the dynamic effects of the external vibration of the concrete. Since the maximum static pressures had been recorded by Cell No. 3, the instrumentation used in this part of the study was connected as shown in Fig. 11. In this case, Load Cell No. 3, was connected to a Signal Memory Recorder (SMR) via an amplifier. Although the SMR had the ability to monitor and register transient signals automatically, in this study it was triggered manually at the appropriate times when the shutter was being vibrated.

Typical results from these tests are given in Figs. 12 and 13. Fig. 12(a) shows a four-second burst of recorded pressure variations. The mean pressure recorded during this time was 17kN/m^2. By using a zoom facility it was possible to enlarge any part of the recording on the screen which allowed further analysis of small details to be carried out. Fig. 12(b) shows that the maximum pressure recorded was 23.0kN/m^2; the minimum pressure was 9.1kN/m^2.

Figs. 13(a) and (b) show the corresponding graphical displays for pressure variation when the mean pressure had increased to 74kN/m^2. Eight four-second bursts were recorded at various times during the manufacture of the elements; the pressures recorded are summarised in Table 2. The main conclusions from this part of the study are as follows:

(a) Pressure variation does take place where external vibration is used.

(b) The range of pressure variations is at a maximum when the mean pressure is relatively low.

(c) The range of pressure variation is reduced as the mean pressure is increased. This could be due to a number of factors including the damping effect of the head of concrete and the setting of the concrete.

Test Number	Mean Pressure kN/m^2	Max. Pressure kN/m^2	Min. Pressure kN/m^2	Pressure Range kN/m^2
1	6.5	11.0	-1.9	12.9
2	17	23.0	9.1	13.9
3	57	63.4	51.4	12.0
4	74	77.8	68.6	9.2
5	75	78.7	73.9	4.8
6	75	76.8	73.4	3.4
7	74	74.9	73.0	1.9
8	74	74.9	72.0	2.9

Table 2 Pressure variations during external vibration

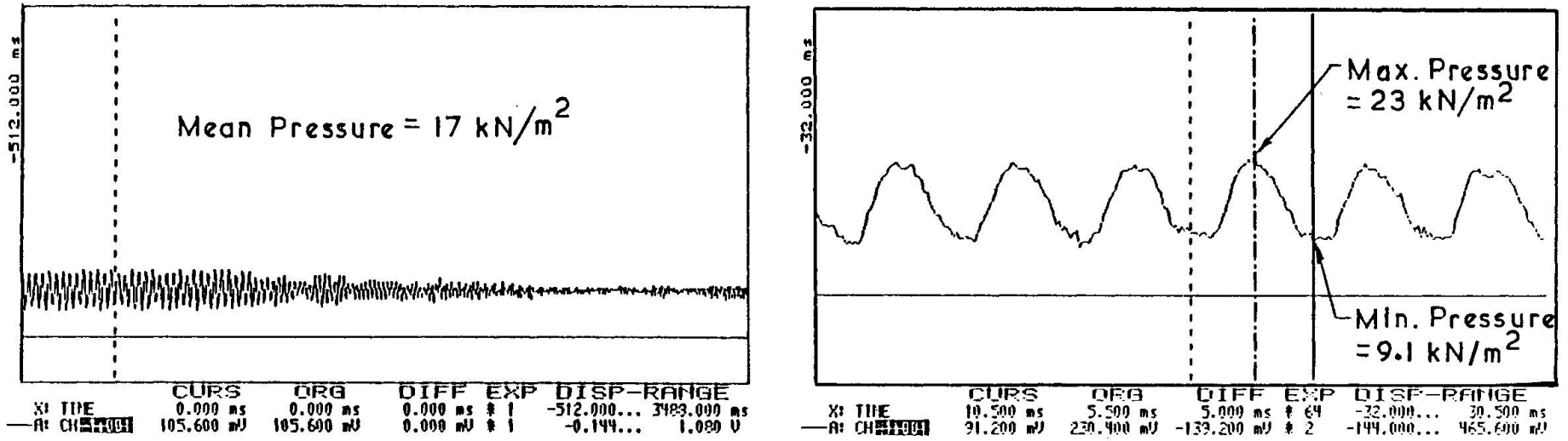

(a) (b)

Fig. 12 Results recorded at a mean pressure of 17kN/m²

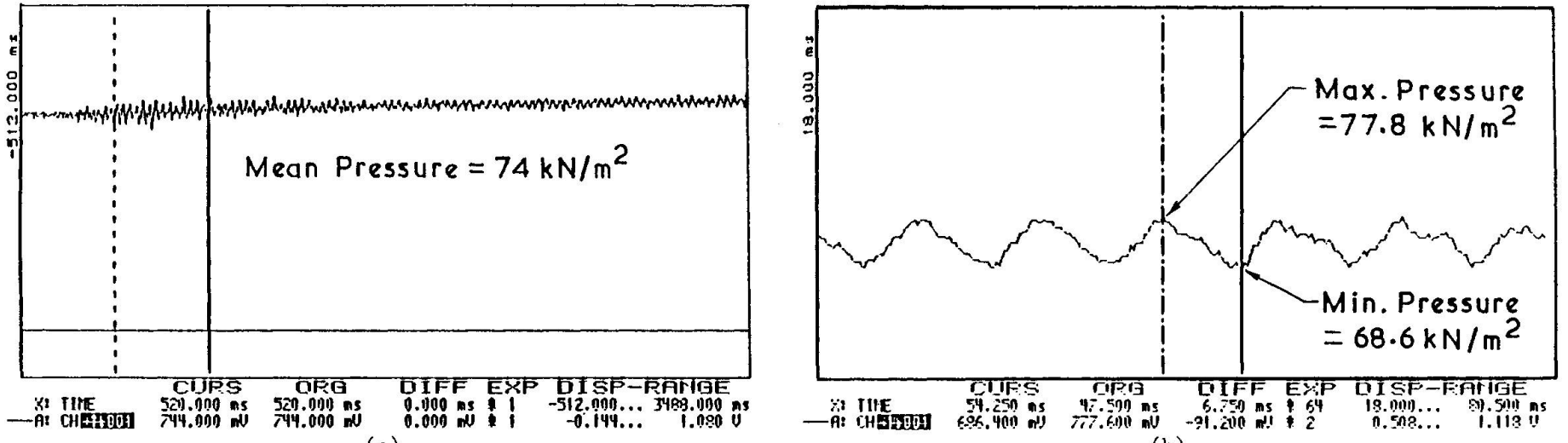

(a) (b)

Fig. 13 Results recorded at a mean pressure of 74kN/m²

ACKNOWLEDGEMENTS

The field work described was funded by the Science and Engineering Research Council (UK) as part of its coordinated programme of large and full scale testing of structures. Additional support was provided by the County of South Glamorgan.

REFERENCES

1. ZIADAT G.S. and WALDRON P. Segmental Construction - a State-of-the Art Report. Dept. of Civil Eng., Univ. of Bristol, UK, Report No. UBCE/C/86/1, Déc. 1986, 159 pp.

2. KULKA F. and THOMAS S.J. Feasibility Study of Standard Sections for Segmental Prestressed Concrete Box-girder Bridges. Journal, Prestressed Concrete Institute, Sept./Oct. 1983, 54-77.

3. WALDRON, P., ZIADAT, G.S. and SALFITY, R.R., Early Results from the Instrumentation of a Glued Segmental Bridge. Proc. Inst. Struct. Engrs./ Building Res. Establishment Seminar on Structural Assessment, Garston, Watford, UK, April 1987.

Leere Seite
Blank page
Page vide

Aerodynamic Monitoring of the Cable-Stayed Mississippi River Bridge

Contrôle de la réponse aérodynamique d'un pont à haubans le Mississippi

Überwachung des aerodynamischen Verhaltens einer Schrägseilbrücke über der Mississippi

Robert BRUCE
Boh Professor
Tulane Univ.
New Orleans, USA

Robert Bruce, PhD, born in 1930, is Chairman of the ACI-ASCE Committee on Prestressed Concrete.

Robert DRAKE
Professor
Tulane Univ.
New Orleans, USA

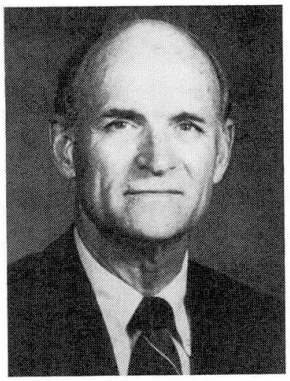

Robert Drake, PhD, born in 1926, is now researching nondestructive testing of cable faults.

Claude SPERRY
Professor
Tulane Univ.
New Orleans, USA

Claude Sperry, MS, born in 1925, is the Principal Investigator of this project.

Hugh THOMPSON
Dean, School of
Engineering Tulane Univ.
New Orleans, USA

Hugh Thompson, PhD, born in 1935, continues research combined with administration.

SUMMARY
Results of monitoring of the aerodynamic response and wind climate of a cable-stayed bridge across the Mississippi River at Luling, Louisiana, USA, are presented. Typical measurements made of wind spectra and wind induced motions of the cable stays and bridge deck are compared with predictions.

RESUME
Les résultats d'un programme de contrôle et de mesures de la réponse aérodynamique d'un pont à haubans sur le Mississippi près de Luling en Louisiane (USA) et des vents sur le pont sont présentés. Des valeurs typiques des spectres mesurés des vents et des déplacements des haubans et du tablier causés par le vent sont comparés aux valeurs prédites.

ZUSAMMENFASSUNG
Die Resultate der Ueberwachung von Windverhältnissen und Bauwerksreaktion infolge Wind bei der seilverspannten Brücke über den Mississippi in Luling, Louisiana, USA, werden vorgestellt. Typische Messwerte der Windspektren, sowie der Bewegungen von Pfeilern und Brückenträgern werden mit den vorausberechneten Werten verglichen.

1. INTRODUCTION

Early in the preliminary design of the cable-stayed Mississippi River bridge at Luling, Louisiana, it was decided that the bridge should be instrumented to measure its dynamic response to wind and to obtain the characteristics of the wind at the site. The bridge was to be erected in an area exposed to hurricane winds. Potentially, there were opportunities for enhanced understanding of the aerodynamic response of the cable stays and deck under moderate and extreme winds.

The bridge was completed in 1984 and data acquisition began that same year. The responses presented here cover a range of wind speeds up to 15.6 m/s. The bridge has not yet experienced a hurricane.

The work described herein was sponsored by the Louisiana Department of Transportation and the United States Federal Highway Administration.

2. DESCRIPTION OF THE BRIDGE

The Mississippi River bridge at Luling, Louisiana is the first large steel cable-stayed structure to be built in the United States. It consists of a five-span superstructure, made entirely of weathering steel. Measuring 372.5 m center-to-center between support towers, the navigation channel span was the longest of its kind in the western hemisphere at the time it was opened to traffic. Worldwide, the channel span is the second longest of its type, the longest being the 404 m span across the Louri River at St. Nazaire in France. The Luling bridge lies in the North American hurricane belt and is designed to withstand the static and dynamic loads of hurricane force winds.

Deck support is provided by continuous twin trapezoidal box girders having a constant depth of 4.27 m. For the main span there are six rectangular cross girders where additional support is provided by the connection of cable stays. To improve aerodynamic performance, the main span is equipped with fairing plates. The total length of the bridge is 837 m; while the deck measures 25 m in width providing four lanes of traffic flow plus outside shoulders. The towers are of all-welded cellular construction and rise 122 m above the mean low water level of the river. A number of these details are summarized in Fig. 1.

The cable system consists of 12 stays per tower arranged in two identical radiating patterns. Each stay contains two or four cables. Each stay terminates both at the cross girder and at the tower top in a Hi-Am anchorage. The individual cables are built from parallel 0.635 cm diameter wires bundled in groups of 103, 211, 271 or 307 wires, depending on load and location. These wires are cold drawn stress relieved and prestressed with a design strength 45% of the ultimate. The bundle is wrapped with 0.635 cm diameter wire on a 1.83 m pitch along its entire length. This wrapping contained the bundle during shipping and installation and holds a polyethylene pipe away from the wire bundle, providing an annulus which is filled with grout. The polyethylene pipe and grout provide weather protection for the bundle. Grout was injected after the stays had been tensioned on the bridge.

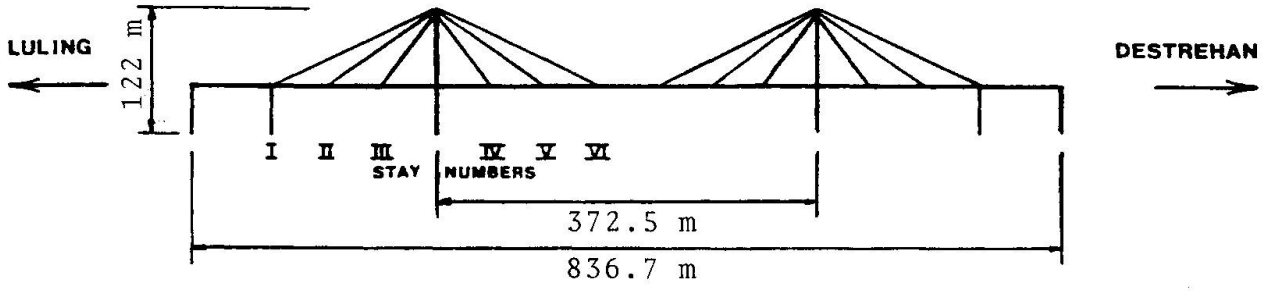

ELEVATION OF LULING BRIDGE

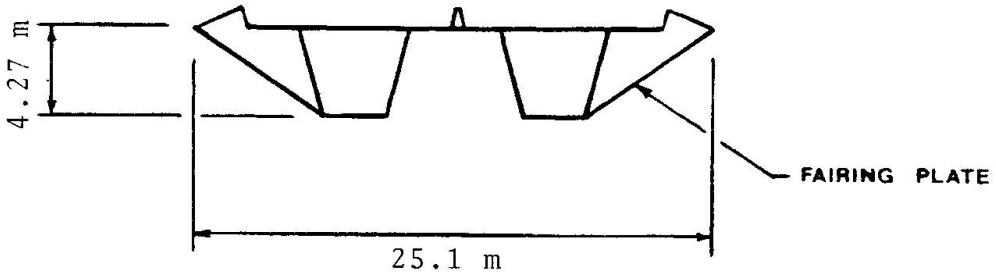

CROSS SECTION OF MAIN SPAN DECK

Fig. 1 Bridge details

3. INSTRUMENTATION

The upriver stays on the Luling side of the bridge were instrumented with pairs of accelerometers. Each pair of accelerometers was mounted with sensitive axes mutually perpendicular and also perpendicular to the axis of the cable. The displacement spectrum of the major axis of the eliptical path of each pair of accelerometers was computed from acceleration data.

Acceleration of the bridge deck was monitored at the center of the two approach spans on the Luling side of the main span and at the center and quarter points of the main span. These data provided displacement spectra of the vertical and torsional modes of deck motion. Anemometry located at the same points as the deck monitoring equipment provided measurements of the three mutually perpendicular components of the wind. The top of the tower supporting the instrumented stays also was provided with an accelerometer in order to record the tower motion in the direction of the longitudinal axis of the bridge. Detailed descriptions of the data acquisition instrumentation and techniques, as well as the computer software used for data reduction and analysis, may be found in [1] and [2].

4. STAY MOTION

As an example of the data acquired from the stays, Fig. 2 is a graph of the motion of the longest backstay in a wind having an average speed of approximately 4 m/s and a turbulence intensity of 15% [3]. These data were recorded at an accelerometer station located at a point equivalent to 11% of the stay span length above the bottom anchorage point of the stay, and processed by a computer to achieve the desired spectral format. The position of the accelerometer stations on the stays was selected for convenience and accuracy in estimating the antinodal amplitudes of the first twenty modes of cable motion [4]. The equally spaced peaks in Fig. 2 represent the natural frequencies of the stay as it responds primarily to vortex shedding. The peak heights represent a 13.65 minute average of the peak amplitudes of the major axis of the elliptical displacement trajectory at the various frequencies. Measured fundamental frequencies of the stays were in all cases slightly less than the analytically predicted values, with the greatest error being 9.3% [4].

The stay numbering system is indicated in Fig. 1 where the longest backstay is identified as I and the remaining stays are numbered sequentially through the longest forestay which is identified as VI.

The aerodynamic response of cable stay I to wind is summarized in Fig. 3. The figure is a plot of antinodal displacement amplitude versus mode number or, indirectly, vibratory frequency. Additional parameters shown on the figure are the average wind speed during the time of the measurement and the horizontal direction of the wind. In this connection, a value of the angle θ equal to zero degrees indicates a wind blowing perpendicularly to the longitudinal axis of the bridge and coming from the upriver direction; 90° indicates a wind originating from the Luling side of the river and oriented along the longitudinal axis of the bridge.

The mode number or frequency necessary to resonant vibration of the cable stay with vortex shedding, that is, aeolian vibration, is indicated at each wind speed by a black circle. These frequencies were calculated by assuming a Strouhal number equal to 0.20, and using the measured frequencies of the stays as well as the component of the mean wind which was perpendicular to the stay. Where the circles do not appear on the graph for a particular wind speed, the critical frequency was greater than 20 Hz. The instrumentation system does not respond beyond 20 Hz.

As the wind speed and forcing frequencies increase, the response frequencies increase and their amplitudes decline. At the lower frequencies - second and third modes - the 13.65 minute average antinodal displacement amplitudes associated with vortex shedding are less than 1.0 mm, while at the higher mode numbers the amplitudes are less than 0.2 mm. Using the methods set forth by Doocy, et al, [5] these amplitudes suggest bending stress amplitudes in the individual rods of the stays of less than 1050 kN/m^2. Such stress levels are not likely to pose fatigue problems. It is also unlikely that greater displacements or stresses caused by vortex shedding will be measured in future studies since the large displacements induced by vortex shedding are associated in these data with wind speeds of the order of 4.5 m/s or less.

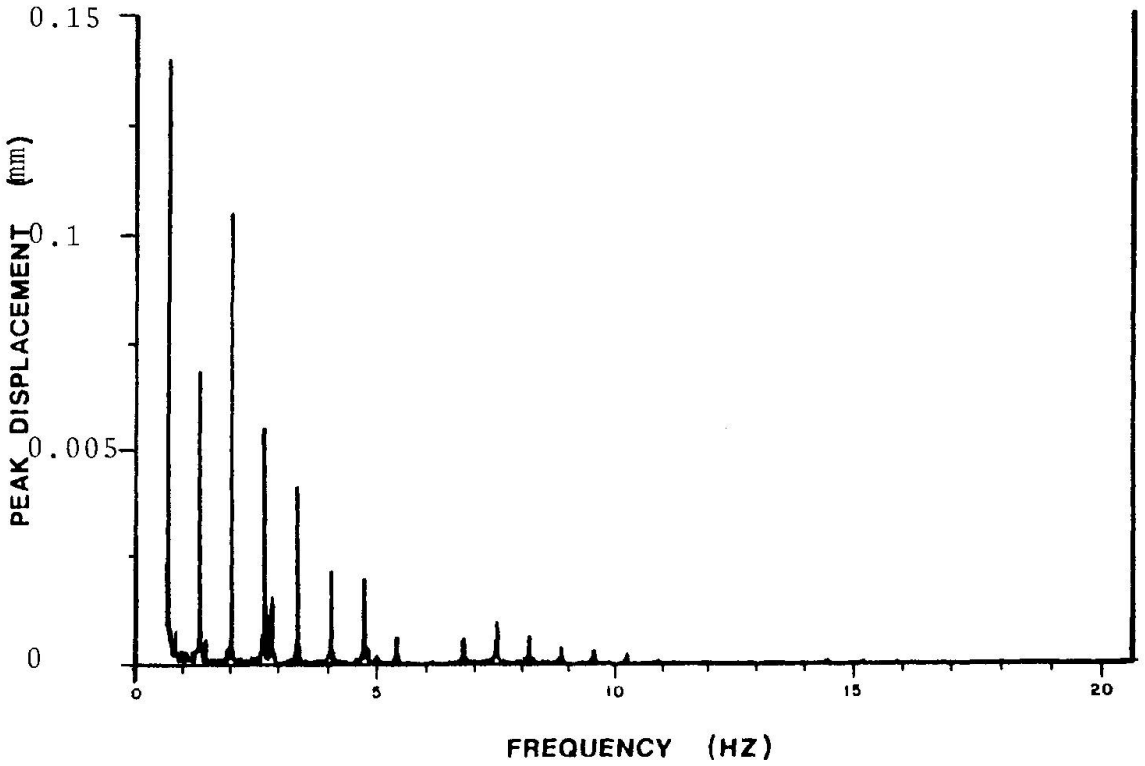

Fig. 2 Displacement spectrum of inboard cable of stay I for a wind speed of 4 m/s

Based on the correlation model described by Blevins [6], these data also suggest that the logarithmic decrement of the cable stays ranges from 0.03 at the lower frequencies upward towards 0.10 at the higher levels. In magnitude and functional dependency upon frequency such values are comparable to data reported by Edwards and Livingston for self damping electrical conductors [7].

The largest measured amplitudes occur in the fundamental mode of the longest backstay at wind speeds in excess of 10 m/s. As will be demonstrated below these large amplitudes in the motion of the stays coincide with the onset of deck resonance in the vertical mode caused by shedding of vorticies from the bridge. The largest recorded 13.65 minute average displacement amplitude of the stay is approximately 3.0 mm at a mean wind speed of 14 m/s. Because of the low frequency of the motion, this amplitude should produce bending stresses of approximately 1140 kN/m^2 at the socket faces.

Three of the six instrumented stays, I, IV and V, are comprised of four identical cables arranged on a pattern measuring 60 cm by 150 cm horizontally. The lower two cables of stays I and V were instrumented primarily to observe the effects of wake induced vibration. Some evidence of wake induced excitation was obtained. For the first three modes of motion of stay I, Fig. 4 presents a plot of the ratio of the displacement amplitude of the leeward cable to that of its windward companion. Nominally, 10 to 25% greater amplitudes are in evidence on the leeward stay. In the worst case there is a 40% increase in activity associated with the 14 m/s wind speed. However, these large percentage increases in amplitude are associated with very low levels of displacement, as may be seen by referring to Fig. 3.

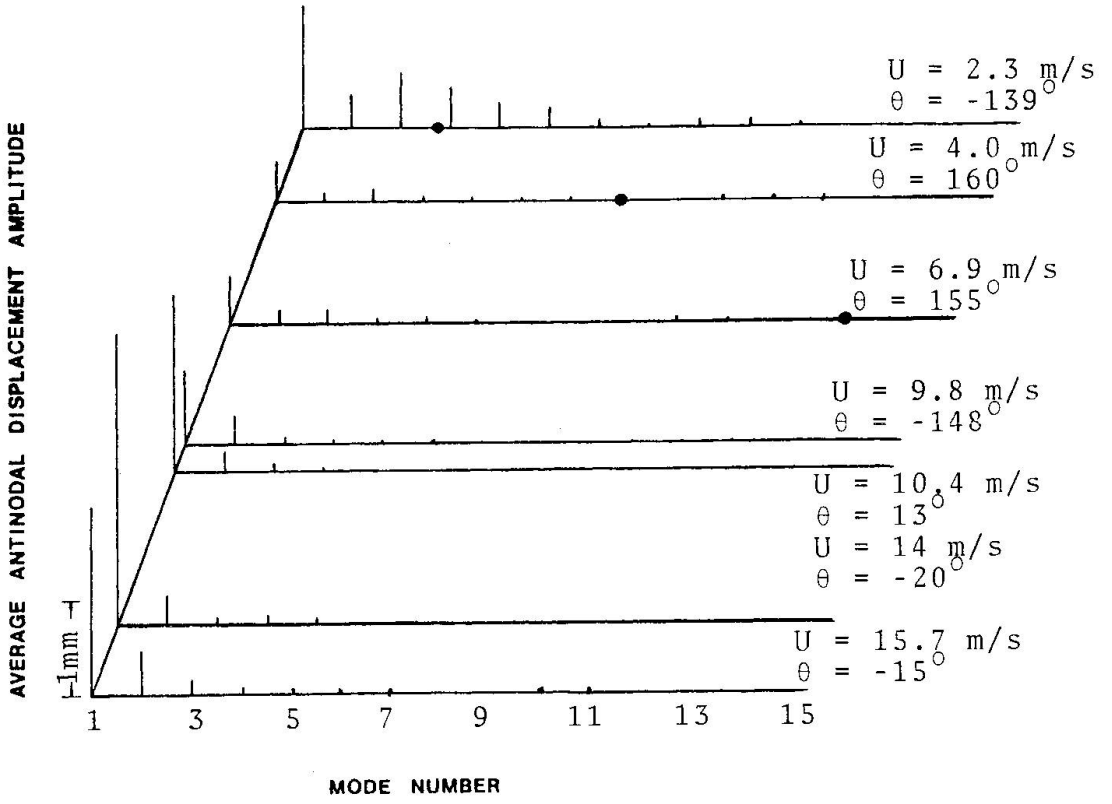

Fig. 4 Aerodynamic response of stay I

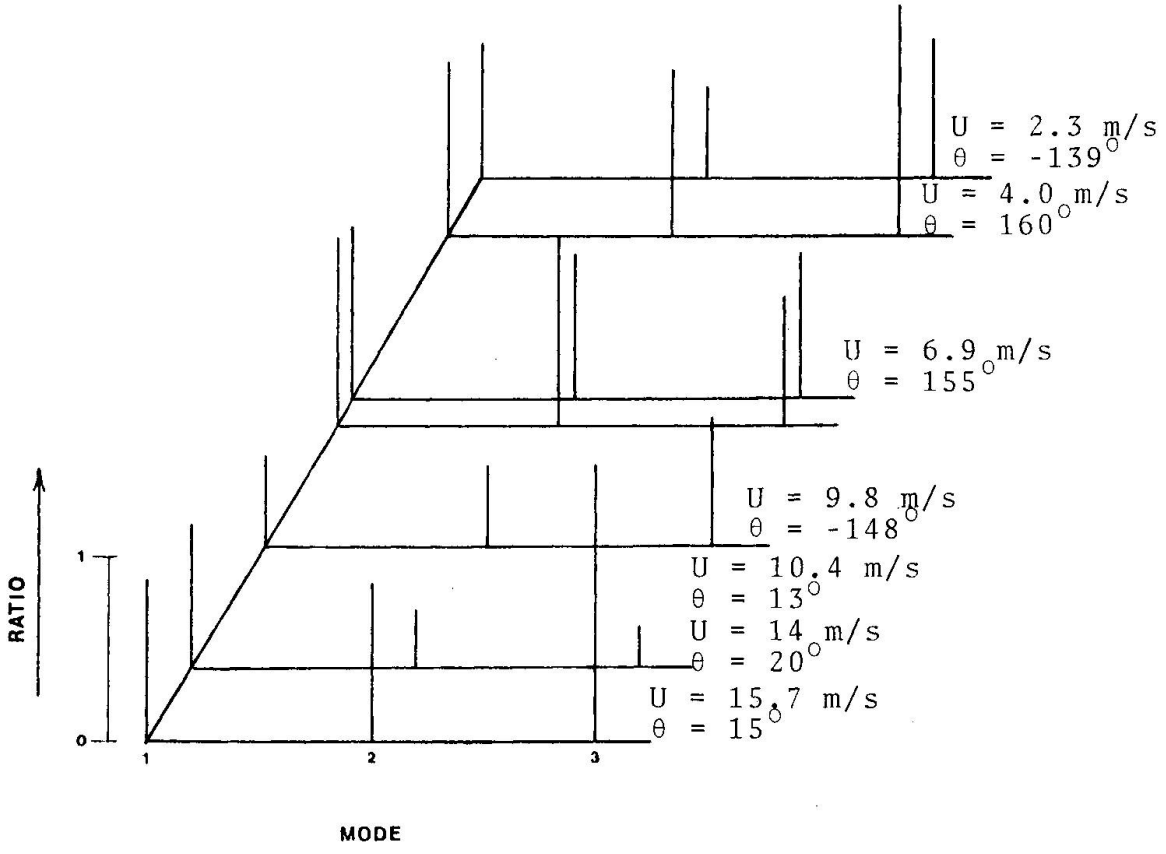

Fig. 4 Ratio of downwind to upwind displacement of stay I

5. DECK MOTION

Spectra of the peak vertical motion of the center section of the main span were obtained for various wind speeds and directions [3]. The fundamental frequency of the first vertical mode of deck motion measured 0.35 Hz; this is to be compared with a value of 0.369 Hz which was anticipated during the preliminary design and wind tunnel studies for the bridge [8].

The variation of the vertical, first mode displacement amplitude of the bridge deck as a function of position on the bridge and wind speed is shown in Fig. 5. This figure summarizes data taken from a number of spectra. Station 4 identifies the instrumentation located at the center of the main span; Stations 3 and 5 are at the quarter points of the main span; and Stations 1 and 2 are at the center of the two side spans on the Luling side of the main span. The abrupt increase in displacement amplitude between 9.8 and 10.4 m/s heralds the onset of resonance between the first vertical mode of deck motion and the shedding of vorticies from the deck. In the most common case, the resonance would cease at some wind speed beyond 15 m/s, and the amplitudes would decline [8]. Thus, it is not clear that the maximum displacement amplitudes of this resonant condition have been measured in the current series of observations. However, at this frequency the time averaged maximum measured displacement amplitude of 3.6 mm is equivalent to an acceleration of 0.00175g, far below the levels of 0.02g which has been suggested as the point where bridge users begin to feel discomfort because of deck motion.

Comparison of Fig. 5 with Fig. 3 indicates that the increase in the displacement of the cable stay in its first mode is coincident with wind speeds of 10.4 m/s and above. Thus, it appears that the increased activity may arise in the resonant interaction of the vertical mode of deck with the shedding of vorticies. There also remains the possibility that the wind has exceeded a critical level necessary to the onset of stay galloping because of departures from circularity in cross section or eccentricities in aerodynamic center and center of rotation.

Estimates of the critical wind speed for vortex excitation of the deck vertically and the amplitude of the resultant motion were prepared during the design phase of construction of the Luling bridge [8]. The estimated values were 7.5 m/s and 6.6 cm at mid span. These estimates rest on the conservative assumptions of bridge damping at one percent, coherent vortex shedding along the entire length of the span, and a uniform, low turbulence intensity wind normally incident upon the bridge. As shown in Fig. 5 the vertical resonance begins between the 9.8 and the 10.4 m/s wind speeds. Neither of these are normally incident winds; their angles to the axis of the bridge are 58° and 77° , respectively, producing components of the wind normal to the bridge of 8.3 and 10 m/s. Thus, the wind tunnel indications of the critical wind speed may be accurate, although additional data are needed to obtain more precision in this regard. Clearly, the estimate of displacement amplitude was high. However, it is more than likely that the damping of the bridge is greater than the conservative figure of one percent [9], and most unlikely that the shedding is coherent along the length of the bridge. Unfortunately, current protocols do not include measurements of bridge damping nor the opportunity to estimate the degree of coherence of vortex shedding along the bridge length.

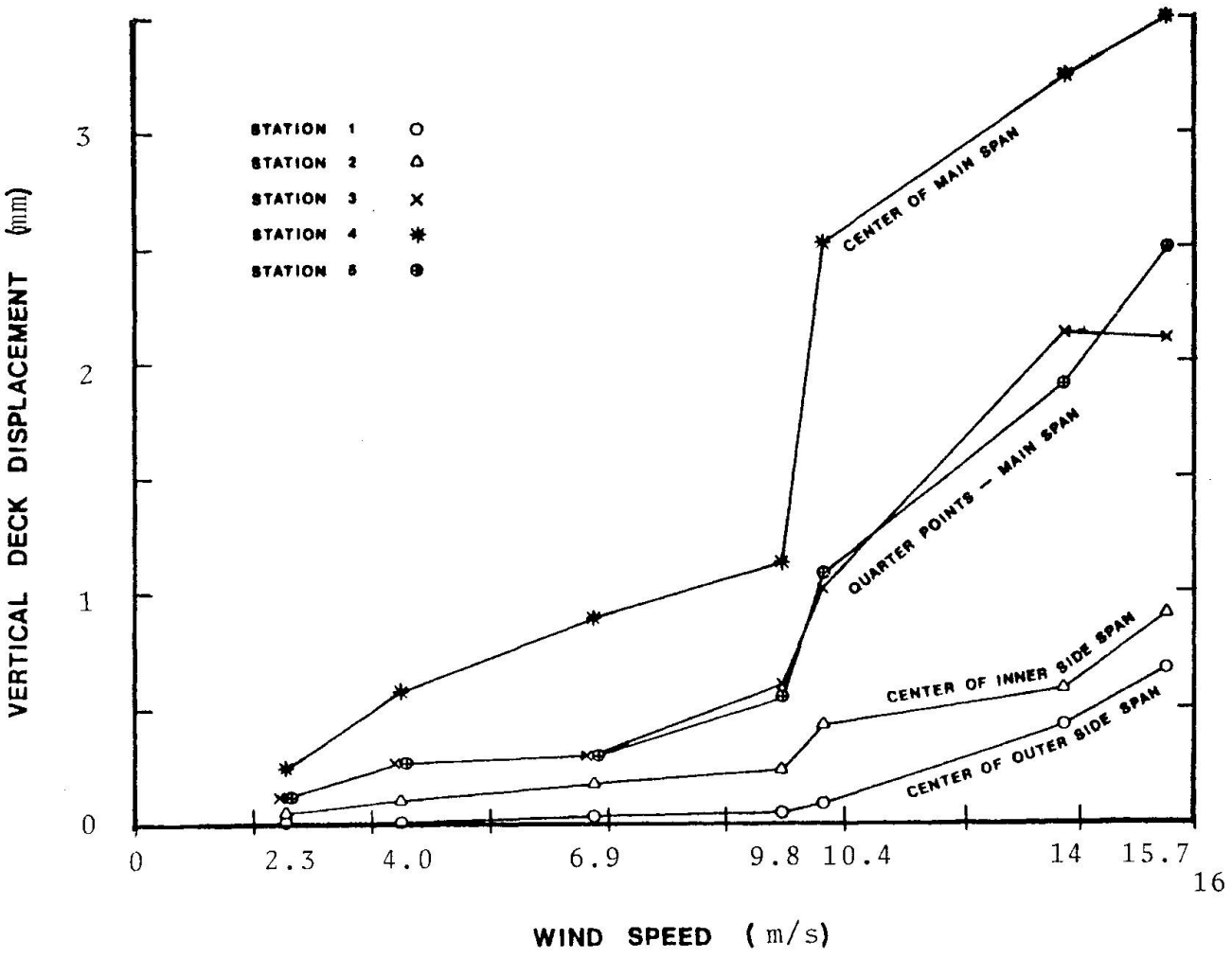

Fig. 5 Vertical deck displacement

The torsional displacements of the bridge deck were quite small by comparison with the values associated with the vertical modes at all wind speeds encountered. The first natural frequency of the torsional mode of the deck was measured at 0.937 Hz. This is to be compared with a pre-construction estimate of 1.238 Hz.

The contribution of the torsional displacement may be seen in the representation of Fig. 6. This figure properly scales the total displacement at the center of the main span and at the deck edge. The proportion of the height of the vertical mode displacement and the height contribution to the edge of deck from the torsional mode are preserved. Differences in the frequencies of the two modes are readily apparent. In all cases observed the contribution of the torsional mode was on the order of 10% of the total displacement of the edges of the bridge deck. There was no evidence of torsional resonance with the shedding of vorticies from the girders, which is consistent with design studies indicating excitation of the torsional mode at wind speeds in the vicinity of 32.5 m/s [8].

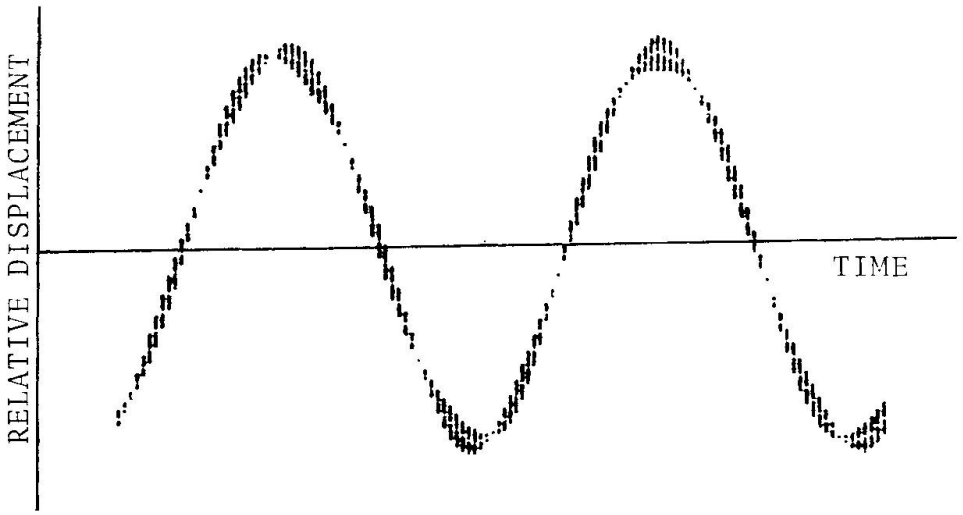

Fig. 6 Relative vertical and torsional displacements

6. TOWER MOTION

An accelerometer was placed in the top of the tower carrying the instrumented stays. The orientation of the device provides measurements of tower motion parallel to the axis of the bridge. Data were taken during the same time as the previous spectra for the vertical and torsional motion of the bridge deck. The largest time averaged displacement amplitude occured at a frequency of 0.350 Hz which coincides with the frequency of the deck in its first vertical mode. Clearly, this component of the tower motion is a part of the first mode vibration of the entire structure moving in response to the shedding of vorticies from the deck and supporting girders. At this wind speed, displacements for other modes were negligible.

None of the stay spectra show any response in the vicinity of 0.35 Hz. This suggests that the tower is largely coupled to the deck through the axial, and not the transverse, mode of cable vibration. Because the transverse vibrations of the stays were a matter of first priority, the placement of the accelerometers on the cables is such that axial motion of the cable elicits no response.

Amplitudes of the tower motion at the frequency of the vertical deck vibration are shown in Fig. 7 as a function of windspeed. Although the onset of deck resonance is still apparent in this figure, it is not as pronounced as in the graphs of deck displacement.

The changes in cable stay tension and stress because of the combined motion of deck and tower are a matter of interest because of the possibility that the fatigue limit of the stay rods might be exceeded. An estimate of this change may be obtained by assuming that the longest backstay, Stay I, is fixed in place at its lower end; such an assumption is at least partially justified by the fact that this stay is connected to the bridge at a pier; the other backstays are attached to cross beams on the first approach span where greater flexibility is available. Also it may be assumed conservatively that the tower does not foreshorten under increased compressive load, and that all elongation of the backstay is drawn from the axial mode of stay motion, without effect upon transverse

sag. Under these assumptions the maximum tower displacement at 0.350 Hz, which was measured as 0.9 mm, produces a stress amplitude of 1170 kN/m² in the cable rods, again an insignificant variation vis-a-vis fatigue.

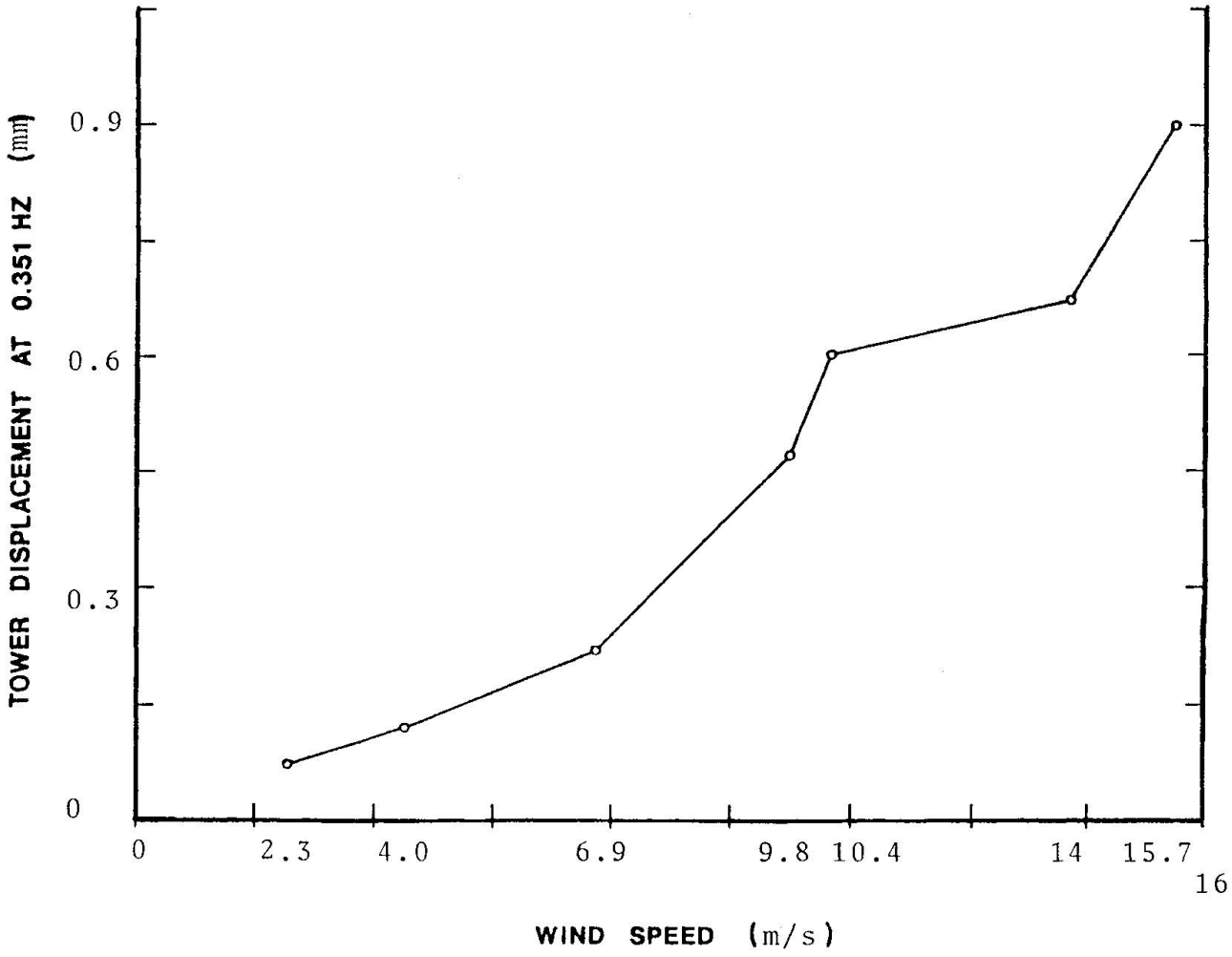

Fig. 7 Tower displacement

7. WIND CHARACTERISTICS

Some of the principle properties of the wind which produced the responses in Fig. 3, Fig. 4, Fig. 5, and Fig. 7 are summarized in Table 1. The mean wind values averaged over 13.65 minutes are given along with their horizontal and vertical angles. Winds originating from the upwind direction normally incident upon the bridge are assigned values of $\theta = 0$. The angle θ is measured positively as it turns towards the Luling end of the bridge. The angle ϕ is measured from the perpendicular; values of ϕ of less than 90° indicate an upward component in the mean wind velocity. The turbulence intensity is of interest because of its possible role in eliminating coherent shedding of vorticies from the deck and cable stays. The declining turbulence levels shown with increasing wind speed reflect in part the elimination of currents driven by thermal convection. At the 4% level, the turbulence intensity is approaching the kinds of turbulence associated with wind tunnel tests where 0.5 - 1.0% may be expected.

Wind Speed m/s	θ, degrees	φ, degrees	Turbulence Percent	Roughness Factor[10]
2.28	-139.0	88.9	20.6	-
4.02	160.0	84.6	12.7	0.0153
6.93	155.0	87.0	7.9	0.0059
9.79	-148.0	88.0	6.1	0.0030
10.4	12.9	85.8	5.6	0.0029
14.0	-19.6	87.0	4.1	0.0021
15.7	-14.6	87.0	4.0	0.0017

Table 1 Wind Characteristics

Representative measured and theoretical wind spectra along the wind direction for a wind speed of 9.6 m/s are shown in Fig. 8. The smooth curve is the spectrum suggested by Davenport [10]. At wave number values of the order 10^{-3} inverse meters, there remains considerable uncertainty, because at this wind speed the associated period of the low frequency waves is of the order of two minutes and the sample period is only 13.653 minutes. With the exception of the low wave number portion of the curve, the Davenport spectrum provides a reasonably good approximation to the spectrum measured at the bridge site, although it does overestimate the high frequency components, as suggested by Simiu and Scanlan [11].

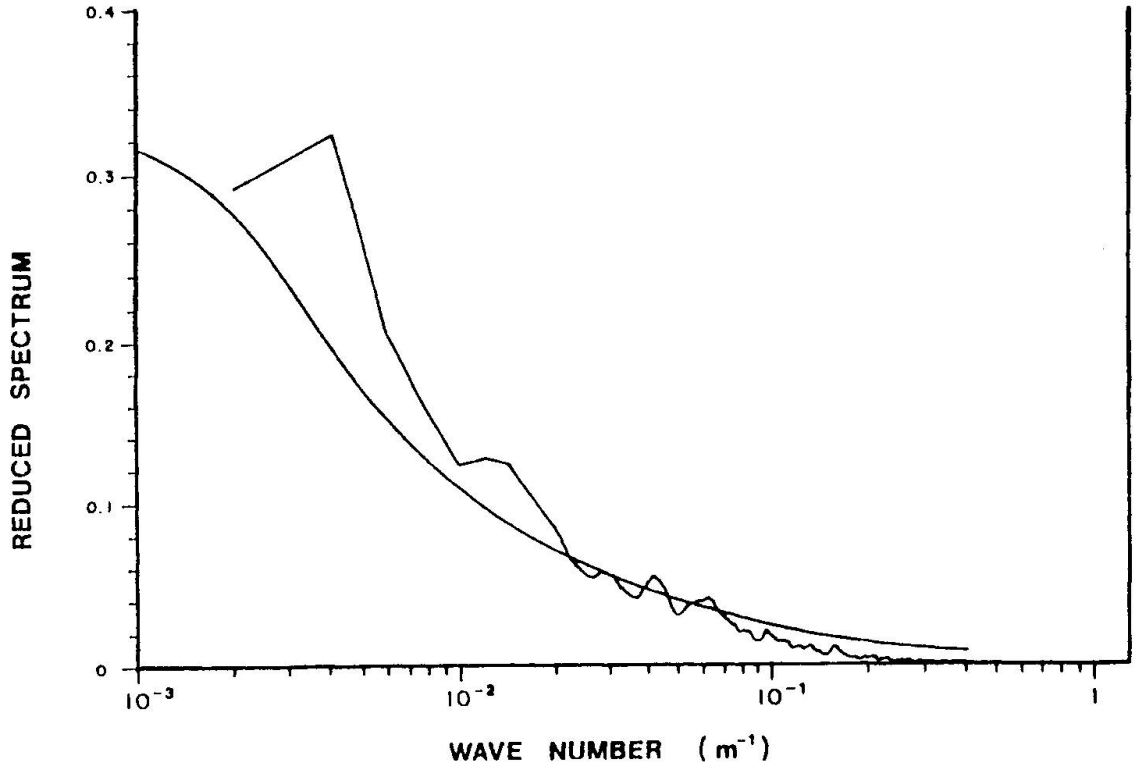

Fig. 8 Wind spectra

The coherence of the longitudinal component of the turbulence is shown in Fig. 9. Data for this figure were taken from the anemometers at the center and quarter point of the main span for a normally incident wind speed of approximately 10 m/s. Curves for decay constants equal to 1.5 and 2.0 are drawn on the figure. These values are to be compared with values of 6 and 7 proposed by Davenport, and with values of 3.5 at 21 m/s and 8.8 at 33 m/s quoted by Simiu and Scanlan [11] from the work of Shiotani. These findings serve to further reinforce their assertion that decay constants are functions of the mean wind speed.

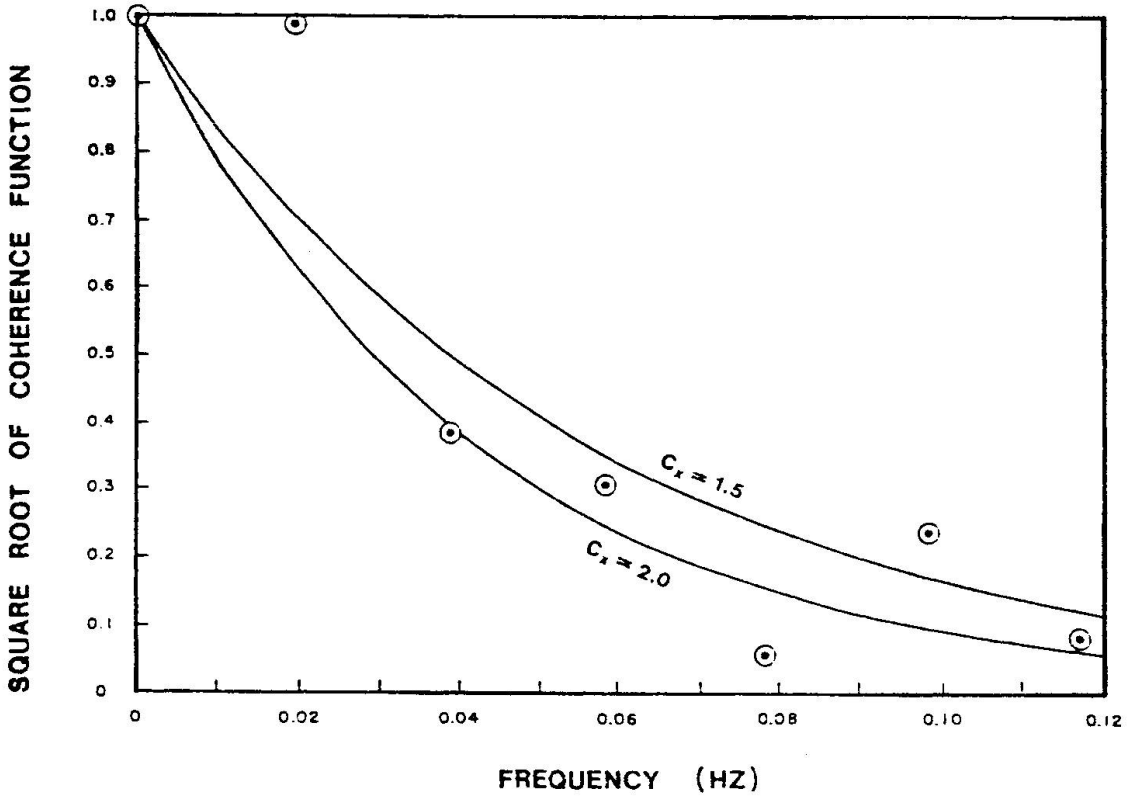

Fig. 9 Coherence of wind turbulence

8. CONCLUSIONS

Systematic measurements have been made of the response of cable stays to vortex shedding and wake induced forces. In addition a first mode response of stays to either galloping or bridge deck motion has been recorded. Both the displacements and stresses from these three sources are small in the range of wind speeds monitored since 1984. First mode vertical and torsional displacements of the main span also have been observed, the vertical displacement arising from a resonant vibration of the deck with vorticies shed from the box girders. Although the onset of this resonance is in accord with predictions from wind tunnel studies, the acceleration and displacement amplitudes are much less than values predicted on the basis of assumptions of bridge damping of one percent of the critical value and coherent vortex shedding along the entire length of the main span. The vertical motion of the deck is transferred by the cable-stays into the principal oscillation observed at the tower tops. Various parameters and spectra characterizing the wind turbulence at the bridge site were measured and found to be within the expected range of values for such data.

REFERENCES

1. BOURGEOIS, B.S.;BRUCE, R.N.; DRAKE, R.L.; SPERRY,Jr., C.J.; and THOMPSON, H.A.; "Wind Instrumentation of the Luling Bridge, Luling, Louisiana, Vol. I", METHODS AND RESULTS, Report No. FHWA/LA79-1st, Louisiana Department of Transportation and Development, Baton Rouge, Louisiana, March, 1982.

2. BOURGEOIS, B.S.; BRUCE, R.N.; DRAKE, R.L.; SPERRY,Jr., C.J.; and THOMPSON, H.A.; "Wind Instrumentation of the Luling Bridge, Luling, Louisiana, Vol. II", PROGRAM USER'S GUIDE, Report No. FHWA/LA79-1st, Louisiana Department of Transportation and Development, Baton Rouge, Louisiana, March, 1982.

3. BRUCE, R.N.; DRAKE, R.L.; SPERRY,Jr., C.J.; and THOMPSON, H.A.; "Dynamic Response to Wind and Wind Climate of the Luling-Destrehan Bridge at Luling, Louisiana, Vol. II": REDUCED FIELD DATA FROM THE LULING BRIDGE, 1984-85, Report No. FHWA/LA82-1st, Louisiana Department of Transportation and Development, Baton Rouge, Louisiana, July, 1986.

4. BRUCE, R.N.; DRAKE, R.L.; SPERRY,Jr., C.J.; and THOMPSON, H.A.; "Dynamic Response to Wind and Wind Climate of the Luling-Destrehan Bridge at Luling, Louisiana, Vol. I": OBSERVATIONS FROM THE 1984-85 PERIOD, Report No. FHWA/LA82-1st, Louisiana Department of Transportation and Development, Baton Rouge, Louisiana, July, 1986.

5. DOOCY, E.S.; HARD, A.R.; RAWLINS, C.B.; and SKEGAMIR, R.; "Transmission Line Reference Book - Wind Induced Conductor Motion," Electric Power Research Institute, Palo Alto, California, 1979.

6. BLEVINS, Robert D., "Flow-Induced Vibration," Van Nostrand Rinhold Company, New York, 1977.

7. EDWARDS, A.L. and LIVINGSTON, A.E.; "Self-Damping Conductors for the Control of Vibration and Galloping of Transmission Lines," IEEE Symposium on Conductor Vibration and Galloping, Chicago, Illinois, June 26, 1968.

9. OHLSSON, Sven, "Dynamic Properties of the Tjorn Bridge," Experimental Investigation, Chalmers Tekniska Hogskola, Institutionen for Konstruktionsteknik, Stal-och Trabyggnad, Publ S 81:3, Goteborg 1981.

10. DAVENPORT, A.G., "The Spectrum of Horizontal Gustiness Near The Ground in High Winds," Quarterly J. Royal Meteorological Society, Vol. 87, 1961, p. 194-211.

11. SIMIU, Emil and SCANLAN, Robert H., "Wind Effects on Structures: An Introduction to Wind Engineering," John Wiley & Sons, New York, 1978. p. 53-62.

Leere Seite
Blank page
Page vide

Monitoring of Structural Behaviour of Cable-Stayed Bridge

Contrôle du comportement des structures d'un pont à haubans

Konstruktionsüberwachung einer Schrägseilbrücke

Henrik E. LANGSOE
Civil Engineer Ph.D.
Cowiconsult, Consulting
Engineers and Planners AS.
Copenhagen, Denmark.

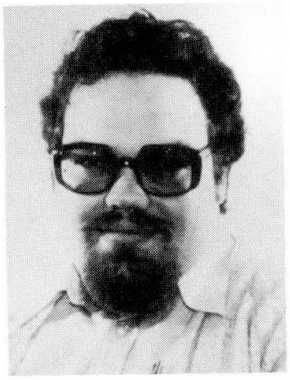

Henrik E. Langsoe, born 1950, got his civil engineering degree at the Technical University of Denmark. He has specialized in instrumentation and measuring techniques and has a Ph. D. degree in surveillance of structures with special reference to structural safety.

Ole Damgaard LARSEN
Consulting Engineer.
Cowiconsult, Consulting
Engineers and Planners AS.
Copenhagen, Denmark.

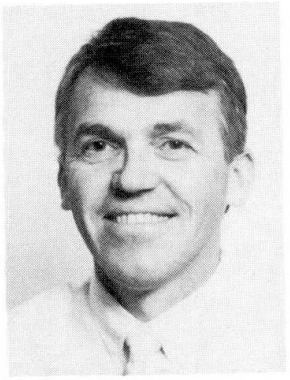

Ole Damgaard Larsen, born 1942, got his civil engineering degree at the Technical University of Denmark. He is presently head of the special structures department in Cowiconsult. He has been in charge of research and development studies as well as detailed design projects mainly within the bridge and offshore sector.

SUMMARY

The Faroe Bridges in Denmark, inaugurated in 1985, are permanently monitored by means of a computerbased monitoring and control system. The system checks structural conditions such as movements of the bridge superstructure at the expansion joints, rotation of the superstructure etc. The system further has a number of service functions such as monitoring the hydraulic system for torsional fixation of the superstructure and controlling the corrosive climate within the closed box girder superstructure.

RESUME

Les ponts de Faroe, inaugurés en 1985, sont surveillés en permanence par un système informatisé de surveillance et de contrôle. Le systéme contrôle les conditions structurelles telles que les mouvements de la superstructure du pont aux joints de dilatation, la torsion de la superstructure etc. Le système dispose de plus de certaines fonctions de service comme la commande du système dispose de plus de certaines fonctions de service comme la commande du système hydraulique pour la fixation rotationelle de la superstructure, et le contrôle des conditions climatiques corrosives dans le caisson fermé de la superstructure.

ZUSAMMENFASSUNG

Die Faröbrücken in Dänemark, im Verkehr seit 1985, sind permanent überwacht durch ein computerbasiertes kontroll- und Warnungssystem. Die Überwachung beinhaltet Konstruktionszustände wie u.a. Überbaubewegungen an Lagern und Brückenfugen, Trägerrotationen etc. Darüber hinaus hat das System eine Reihe von Service-funktionen wie die Überwachung des hydraulischen Systems für die Torsionsstabilisierung des Trägers und die Kontrolle des Luftklimas im geschlossenen Stahlträger.

1. INTRODUCTION

The Faroe Bridges in Denmark were built in connection with the rerouting of the E4 motorway and were inaugurated in 1985. They consist of two separate bridges, one connecting Zealand with Faroe (the ZF bridge) and one connecting Faroe with Falster (the FF bridge), cf. fig. 1, 2 and 4.

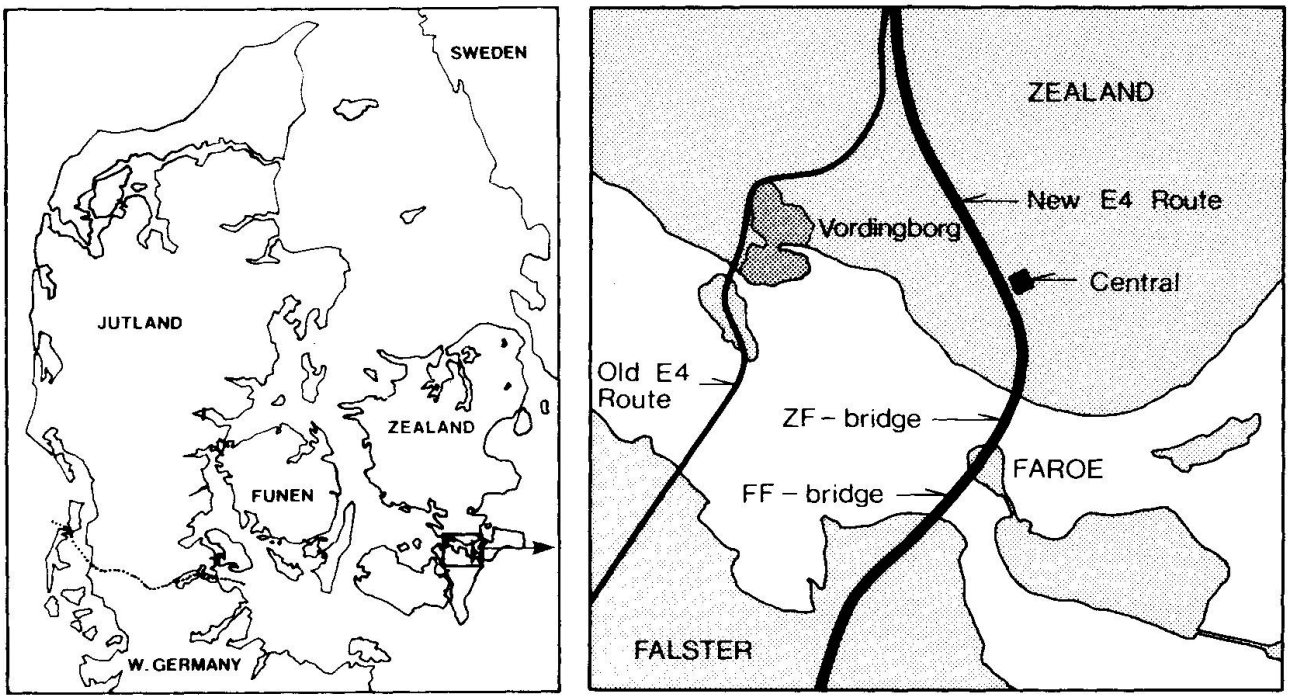

Fig. 1 Bridge location

The ZF bridge is 1.6 km long. The bridge superstructure is a continuous steel girder from coast to coast, fixated in the longitudinal direction at pier nos. 9 and 10, cf.fig. 4.

The FF bridge is 1.7 km long and the superstructure of this bridge is also continuous from coast to coast. It is fixated in the longitudinal direction at pier no. 9, cf. fig. 4. The 3 central spans of the bridge are cable stayed sections. The main span is 290m, the side spans 120m each. The cables are all located in the vertical symmetry plane of the bridge, being supported by A-shaped pylons, cf. fig 2 and 7.

A general description of the bridge project can be found in [1].

The bridges are permanently monitored by means of a computerbased monitoring and control system. The purpose is to ensure that the structure is functioning properly and to establish an optimum inspection and maintenance programme for important components. The computer central is located approximately 3 km North of the ZF-bridge, refer to fig. 1.

The present paper gives a short description of the monitoring system itself and describes the tasks of the system as well as its daily operation.

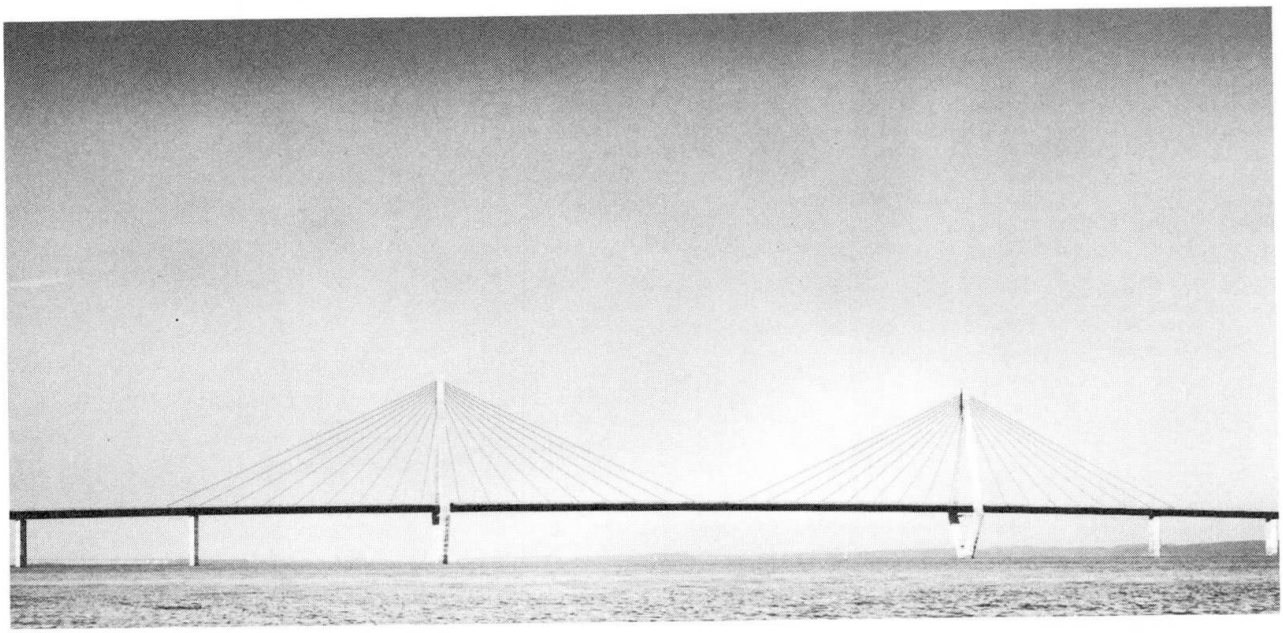

Fig. 2 Photograph of the cable stayed Faroe-Falster bridge.

2. TECHNICAL LAYOUT OF THE MONITORING SYSTEM

The principal layout of the system is a distributed process control system as shown on fig. 3:

- Two central computers in tandem operation, with automatic schwitching from one to the other in case of failure.

- Completely independent monitoring systems for each of the bridges, connected to the central by means of a common transmission line.

  Breakdown of one monitoring system does not affect the other. In case of transmission line failure or break down of the central computers each monitoring system will continue operation on its own.

- Each independent monitoring system consists of a subcentral and 3-4 substations placed in the abutments, bridge girders and pylons. In case of breakdown of a substation, the rest will continue their tasks.

- Signal input/output is controlled by the substations.

The central control room is in addition to the central computers equipped with console for communication with the operator, printer and plotters for printouts of messages, alarms, statistics and measurements.

The communication between computers and substations is based on a local area network for industrial use, modified for communication via modems.

The system has been designed with only 40% of its capacity (software as well as hardware) used. The reason for this is to make the addition of future tasks

a relatively simple matter. One of the future tasks will be the monitoring of the Guldborg tunnel, which is presently being constructed 20 km from the bridge as part of the rerouting of the motorway.

3. TASKS OF THE MONITORING AND CONTROL SYSTEM

3.1 Tasks of relevance to maintenance and traffic safety.

These tasks consist of the following:

- Monitoring for malfunction in computers, substations, transmission lines and electric system (distribution boards).
- Monitoring for malfunction in illumination of bridge girders, pylons and piers in the navigation channel passing the ZF-bridge.
- Monitoring for malfunction of traffic signs.
- Monitoring for malfunction of marine lanterns and fog horn.
- Monitoring for malfunction of, or alarm from lifts and work platforms.
- Control of illumination of both bridges (on/off,intensity).
- Control of marine lanterns and fog horn (on/off).
- Control of traffic signs (on/off).
- Monitoring and control of air humidity within both bridge girders. (The inside of the girders is not painted, but protected against corrosion by keeping the air humidity within certain limits).

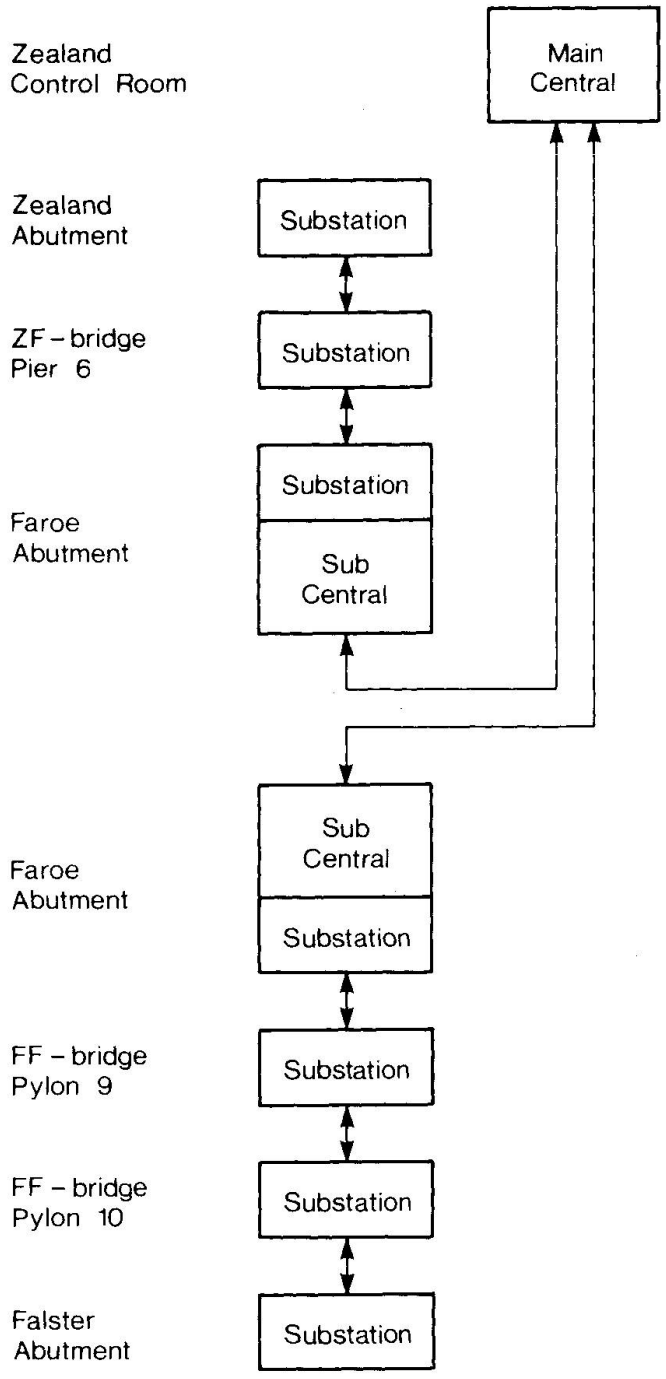

Fig. 3 Principal layout of monitoring system.

These tasks are more or less trivial and will not be commented further upon.

3.2 Tasks of relevance to structural safety.

These tasks, which are summarized on fig. 4, consist of the following:

1 Monitoring of oil pressures in the hydraulic pendulums at the pylons combined with monitoring of the transverse inclination of the bridge superstructure.

2 Monitoring of the displacements of the bridge girders at the abutments.

3 Inclination transducers were installed during the building period, for use during construction of the bridge girder. It is planned to connect these tranducers to the monitoring system.

4 Monitoring of the inclination of the anchor piers in the ZF-bridge has been planned, but not yet installed.

Since these tasks are special to the Faroe Bridges, they will be further described in the following.

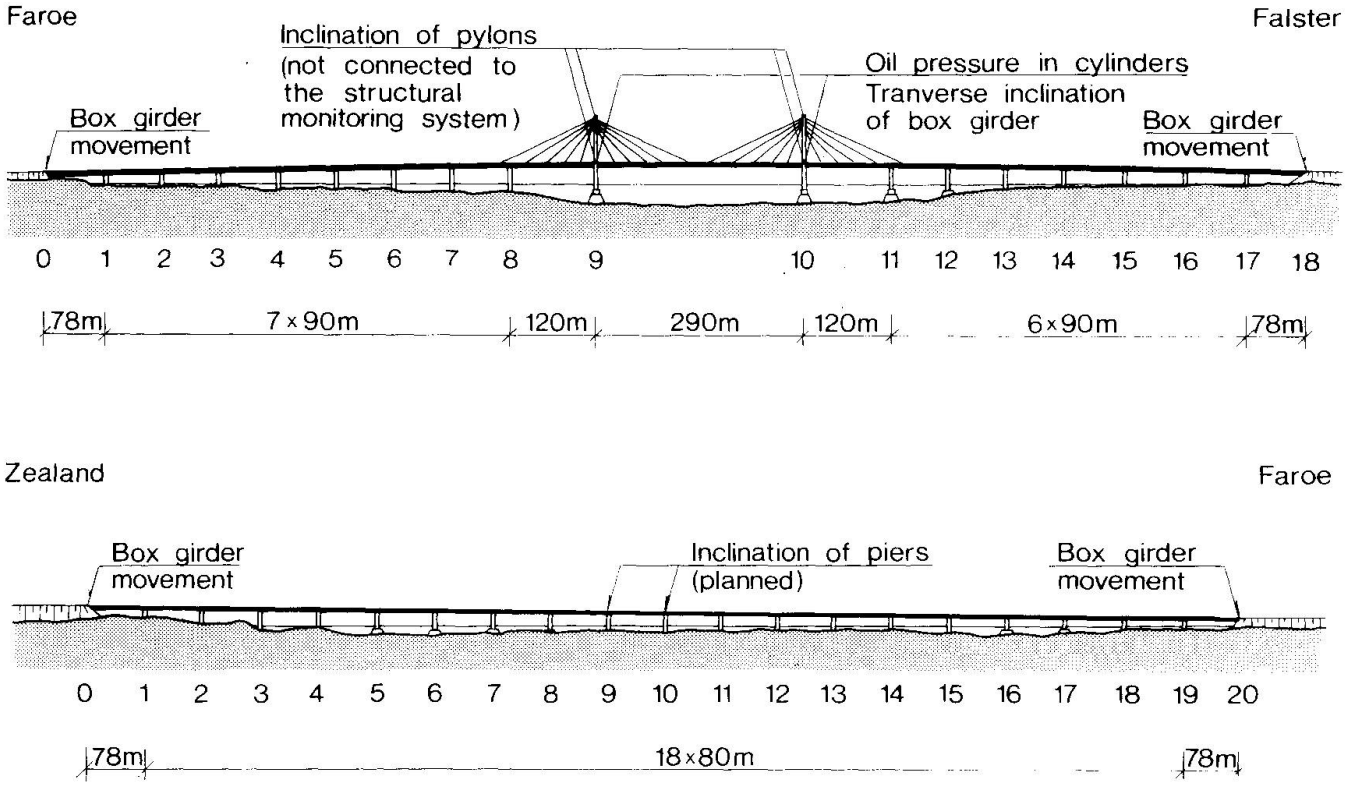

Fig. 4 Monitoring of structural parameters with relevance to safety.

3.2.1 Oil pressure i hydraulic pendulums and inclination of bridge girder.

At the pylons, the bridge girder is free to move in the vertical direction, but fixed against rotation in order to give the girder sufficient torsional stiffness. This is done by the use of interconnected oil filled cylinders as shown on fig. 5.

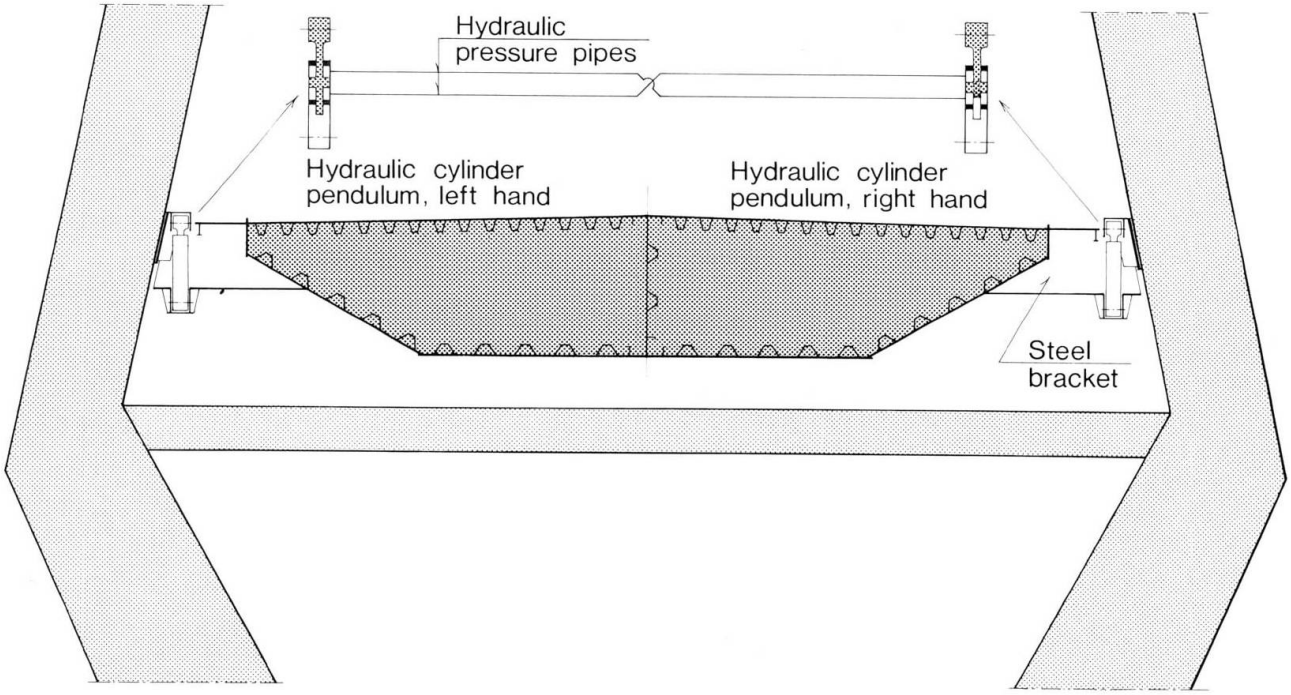

Fig. 5 Arrangement of hydraulic pendulums for torsional fixation of bridge superstructure at pylons.

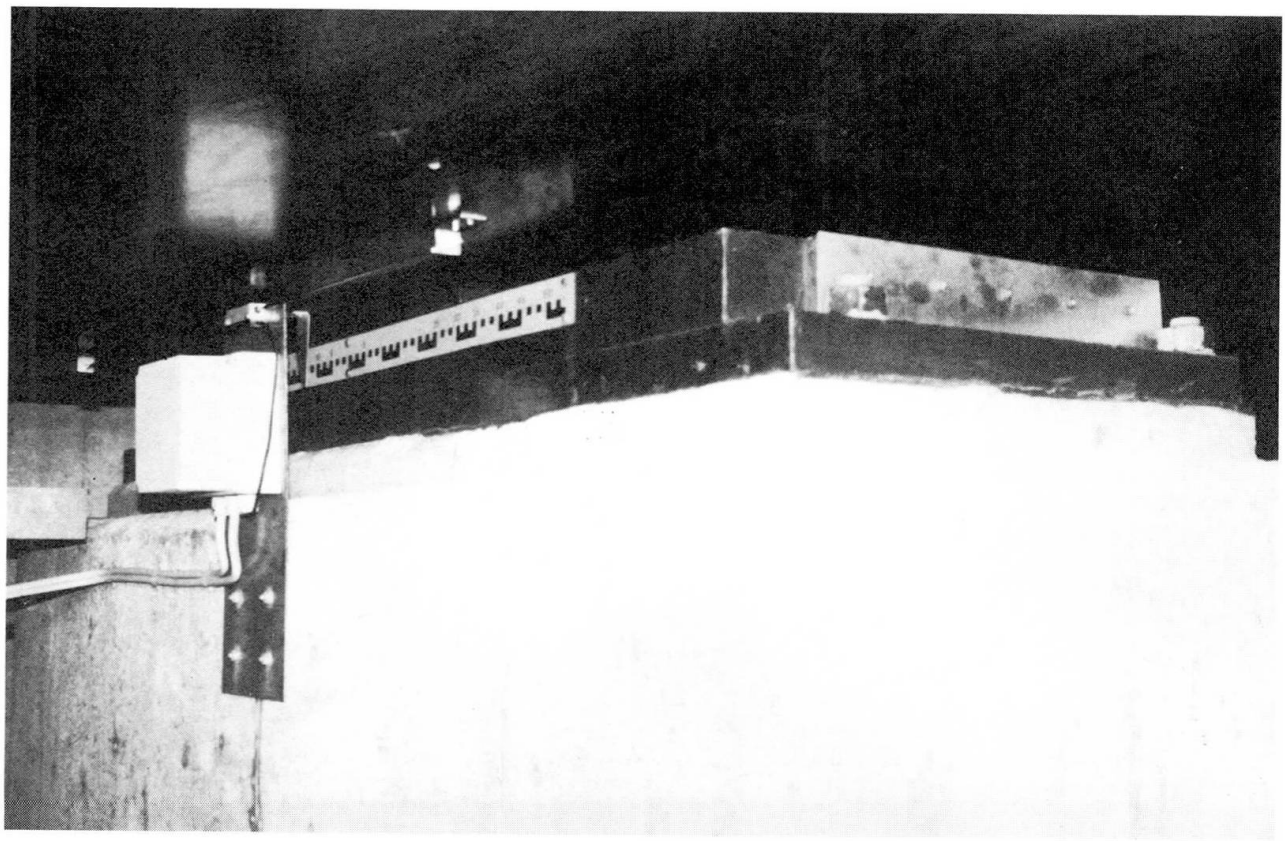

Fig. 6 Photo of displacement transducer at abutment.

In order to check the functioning of the cylinders and to measure the effect of excentric loading of the bridge deck, pressure sensors are installed in each cylinder.

The system can malfunction in two ways. Rupture can occur resulting in immediate loss of oil pressure and consequently the superstructure will experience a critical decrease in torsional rigidity. This is detected directly by means of monitoring the oil pressures in the hydraulic pendulums.

In case of uneven load distribution on the cylinders, however, too large inclination of the bridge girder in the transverse direction can result from leakage of oil past the pistons in the cylinders. This will not necessarily show on the oil pressures, but is detected by means of inclinometers located within the bridge girder.

In case of low or high oil pressure or too high inclination, an alarm massage is printed in the control room.

3.2.2 Girder displacements at abutments.

The expansion joint movements at the abutments can become very large for both bridges because of the continuity of the bridge superstructure. Allowance is made for a total travel of up to 1 m at each abutment.

In order to follow the movements in relation to box girder temperature, displacement transducers have been installed at the abutments, see fig. 6.

The computer registers

- The position of the box girder at each abutment. If a girder end is outside the allowable interval, an alarm message will be given in the control room.
- The accumulated travel at each abutment. This gives useful information upon the wear of the bearings and is of importance for the determination of inspection intervals and perhaps the initiation of special maintenance works.

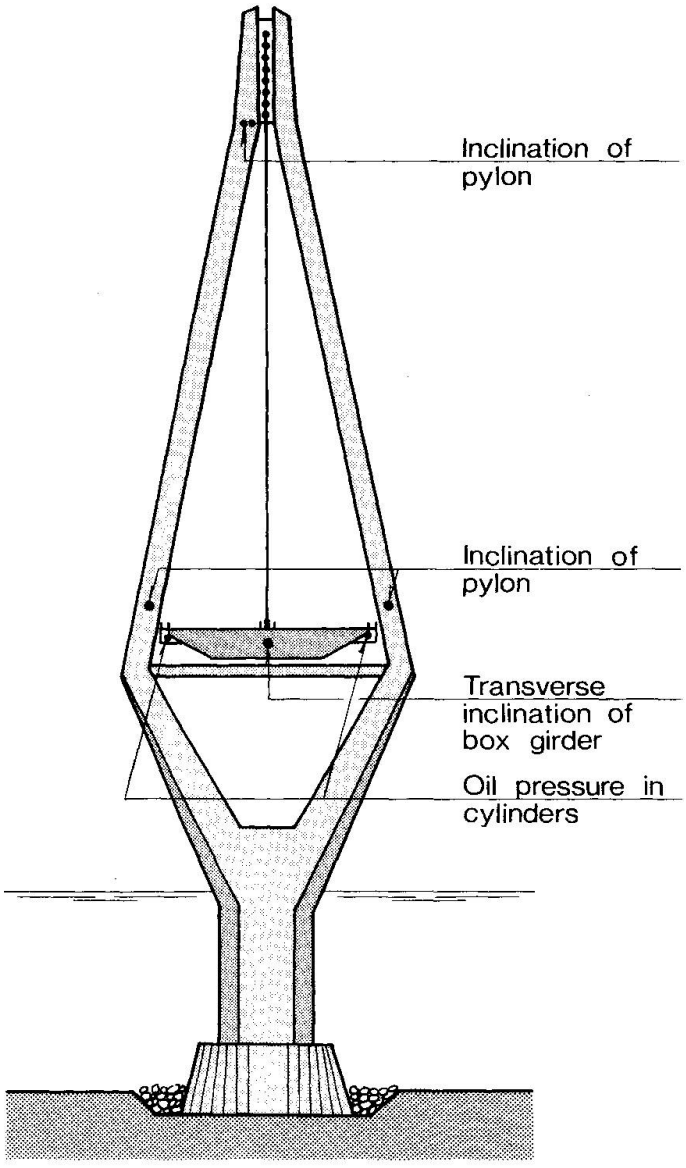

Fig. 7 View of pylon with instrumentation.

3.2.3 Inclination of pylons.

Inclination transducers have been installed in both pylons in two levels as shown on fig. 7. They are presently set up for manual measurements, but can be connected to the monitoring system if time should prove it nescessary.

The inclination of pylon 9 gives a direct measure of the horizontal differential force from the two cable planes.

As the transducers are of the wibrating wire type, they provide an excellent long term stability. Therefore, they are very well suited for monitoring the long-term stability of the pylons. Fig. 8 shows one of the inclino-meters.

3.2.4 Inclination of anchor piers in ZF-bridge.

It is planned to use the incli-nation of the the anchor piers in the ZF bridge to monitor the horizontal force on them from the bridge girder, just as the inclination of pylon 9 could be used as such an indicator for the FF bridge.
Such equipment has however not yet been installed.

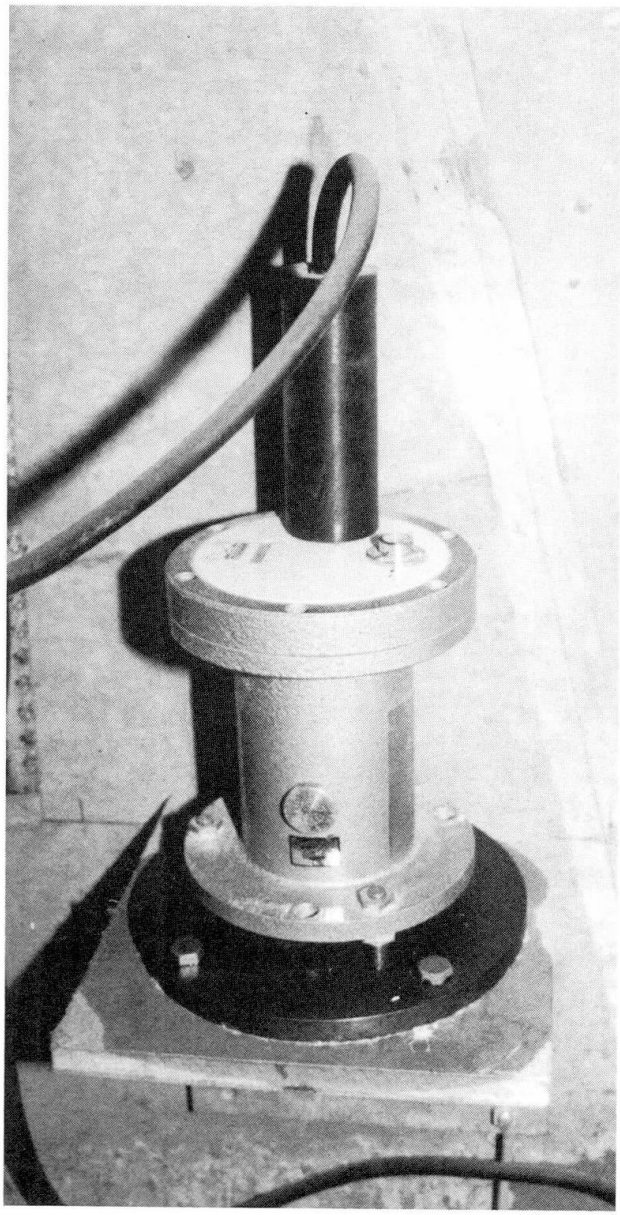

Fig. 8 Photo of an inclinometer (protective shield removed).

4. OPERATION OF THE MONITORING AND CONTROL SYSTEM.

The system performs automatically the tasks mentioned in section 3. Automatic control can however at any time be overridden manually. This gives the possi-bility of

- Enabling a special test mode for the system.
- Controlling all installations manually, which is important during main-tenance and repair of the installations.
- Controlling all measurements, e.g. starting printing of selected data on plotter etc.

Fig. 9 gives a view of the control room.

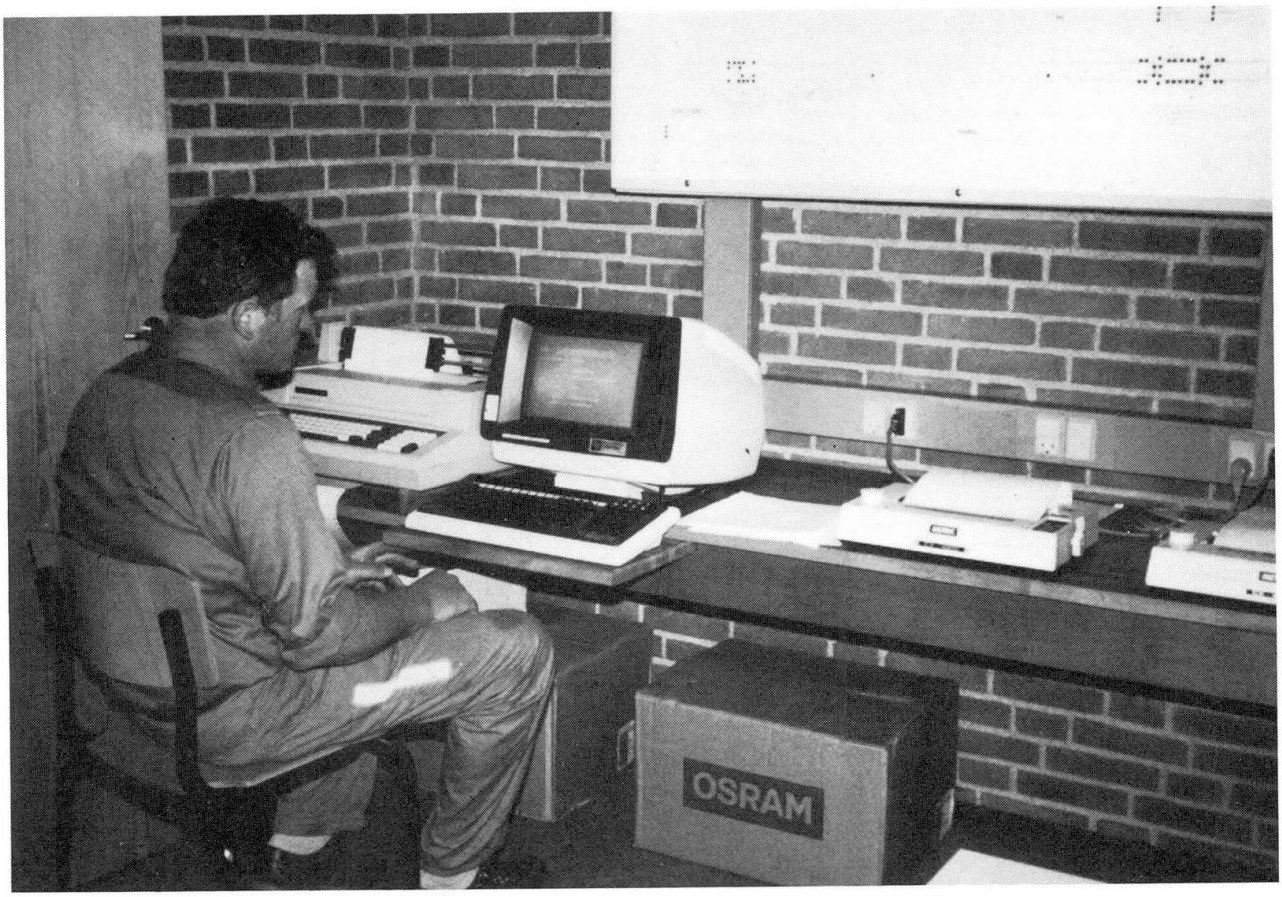

Fig. 9 Control room.

5. EXPERIENCES.

The system has at present been in service for two years. Experiences from use of the system from start-up time till now are however sparce, since some initial technical problems have had to be overcome.

The system is at present working to its best, and there is no doubt that it will fulfill the expectations to it.

REFERENCES.

1. HAAS G., OSTENFELD K.H. and JENSEN G., Die Stahlüberbauten der Farø-Brücken, Dänemark. Stahlbau, Heft 12, December 1985.

Leere Seite
Blank page
Page vide

Structural Monitoring of a Large Space Frame

Contrôle structural d'un treillis tridimensionnel de grande dimension

Überwachung eines grossen Raumfachwerks

R. E. WEST
Senior Consultant
Wiss, Janney, Elstner
and Associates
Princeton, NJ, USA

A. E. N. OSBORN
Consulant
Wiss, Janney, Elstner
and Associates
Princeton, NJ, USA

G. P. RENTSCHLER
Senior Engineer
Wiss, Janney, Elstner
and Associates
Princeton, NJ, USA

SUMMARY
The glass walls and the roofs of the recently completed New York Convention Center are supported by a large space frame. The computer-aided design was highly optimized. Retroprisms for optical surveys and a system for automated sensing of impact, wind, snow, temperature, joint movement, column tilt, and strain at important members have been installed. Software has been developed to check related data for normal structural behavior.

RESUME
Les parois de verre et les toits du Centre de conférence de New York qui vient d'être achevé reposent sur un treillis tridimensionnel de grande dimension. Conçu sur ordinateur, ce treillis a été fortement optimisé. Il comporte des prismes à vision rétrograde pour les études optiques et un système de détection automatique des chocs, du vent, de la neige, de la température, du mouvement des joints, de l'inclinaison des colonnes et des dilatations exercées sur les membres principaux. Un logiciel a été mis au point pour vérifier, à partir de cet ensemble de données, que le comportement de la structure est normal.

ZUSAMMENFASSUNG
Die Glaswände und Dächer des vor kurzem fertiggestellten New York Convention Centers werden von einem grossen Raumfachwerk getragen. Der computerunterstützte Entwurf wurde auf das Höchste optimiert. Retroprismen für optische Messungen und ein System zur automatischen Erfassung von Aufprallen, Wind, Schnee, Temperatur, Fugenbewegungen, Neigung der Pfeiler und Dehnungen der wichtigsten Komponenten wurden installiert. Speziell entwickelte Software überprüft die gemessenen Daten mit denjenigen für ein normales Verhalten der Struktur.

1. INTRODUCTION

1.1 Background

The Jacob K. Javits Convention Center in New York City, designed by I. M. Pei, was first occupied in April 1986. Distinguished by the interplay of large horizontal and vertical planes of black reflective glass, the great hall in this modern "Crystal Palace" vaults from elevation 6 to 23 m, then to 32, 41, and 56 m at the top (see Fig. 1). The space frame roof covers 53 400 m^2, and another 18 600 m^2 of vertical space frame support the glass walls.

Because the details of the space frame are unusual, and because the Center is an exhibition hall and place of public assembly, concerns have been raised for the integrity and safety of the structure. To address these concerns, extensive tests of materials, controlled inspection during erection, full-scale load tests, peer reviews, and independent computer analyses have been performed. To increase confidence in the continued satisfactory performance of the space frame, an ongoing monitoring program has been instituted.

1.2 Description of the Structure

1.2.1 General

The space frame was detailed by the firm PG Structures, subcontractor to the successful bidder for the structural steel, Karl Koch Erectors. Some 75 500 bar elements, each typically a threaded rod within a tube, are joined at about 18 000 hubs to form the space truss. The space truss is generated from square

Fig. 1. Jacob K. Javits Convention Center - East Elevation

grids of 3,05 m elements in two planes, with the nodes of the bottom surface centered under the open areas of the top surface 1,52 m above [2]. Four diagonals and four bars in plane join at each hub. The design process was computer-aided both for selection of members and for analysis of behavior under various conditions of loading.

1.2.2 Special features

The space frame has a number of special features:

-It is divided into several large regions (see Fig. 2) that are continuous in each direction over several spans of 27,43 m; the space frame, 1,52 m in depth, is supported by "diamond trusses" 3,05 m deep by 6,1 m wide at the column strips.

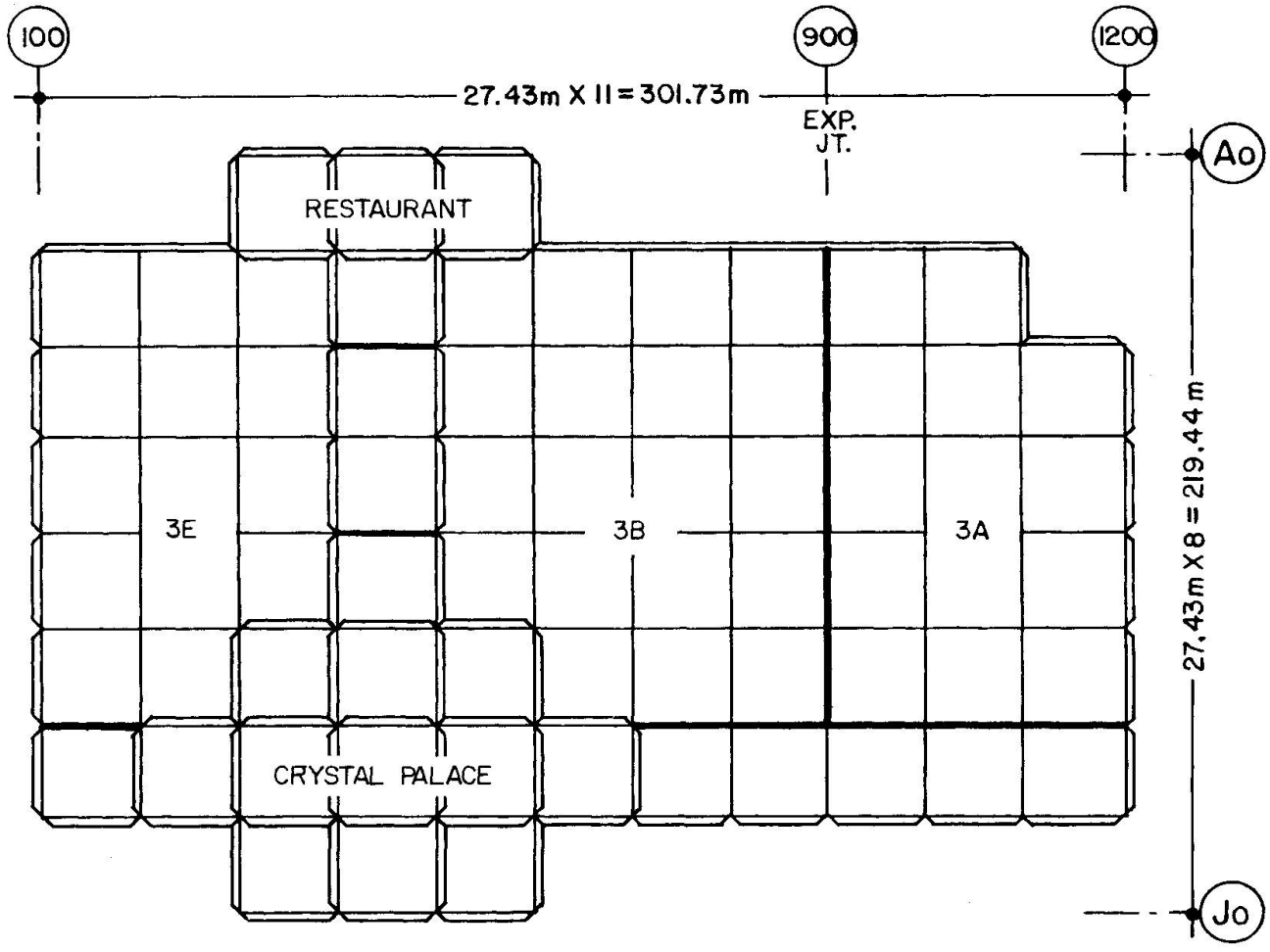

Fig. 2. Key Plan

-High-strength (900 MPa yield) quenched and tempered steels of limited ductility were used for the threaded tension rods. The rods were not upset at the ends; threads were rolled on the body which was the pitch diameter. Since the net area for tension is then less at the thread, yielding is mostly restricted to the unused thread length inside the nuts at the ends of the bars. The factor of safety is 2,0 for yield of the tension members at design load.

-Member sizes are varied so that the structure is "optimized", i.e., with the exception of the smallest, no member is 10 percent larger than it need be, for tension or compression, according to the design methods used. Some light members result, e.g. 13 mm tension rods or tubes 76 mm diameter by 3 mm wall thickness.

-The space frame is composed of separate hub, tube, and threaded-rod elements secured by nuts and washers inside the spherical hubs. Each tube is clamped between two hubs by a single tension-rod connection. In a sense, two threaded connections now depend on the integrity of one nut.

1.2.3 Redundant or alternate load paths
The part of the frame that is only 1,52 m deep is highly redundant: should any member become unavailable to carry load, the load path readily passes to neighboring members without much loss of load capacity. However, those diamond trusses that support exterior spans together with several heavy air-conditioning units, often have a single line of five bare rods, 6 to 8 cm diameter, at the bottom chord in the regions of positive moment. If one of these rods should become unavailable to carry load, only dead load plus some small live load could be carried by the frame.

1.2.4 Dimensional changes
Because regions of the space frame are as large as 137 by 110 m (see Fig. 2), sliding bearings were designed to accommodate changes in dimension due to temperature variation and live loading. Since the section used for tension members is less than half that used for compression members, the tension elements of the space frame will elongate more under load than the compression elements will shorten.

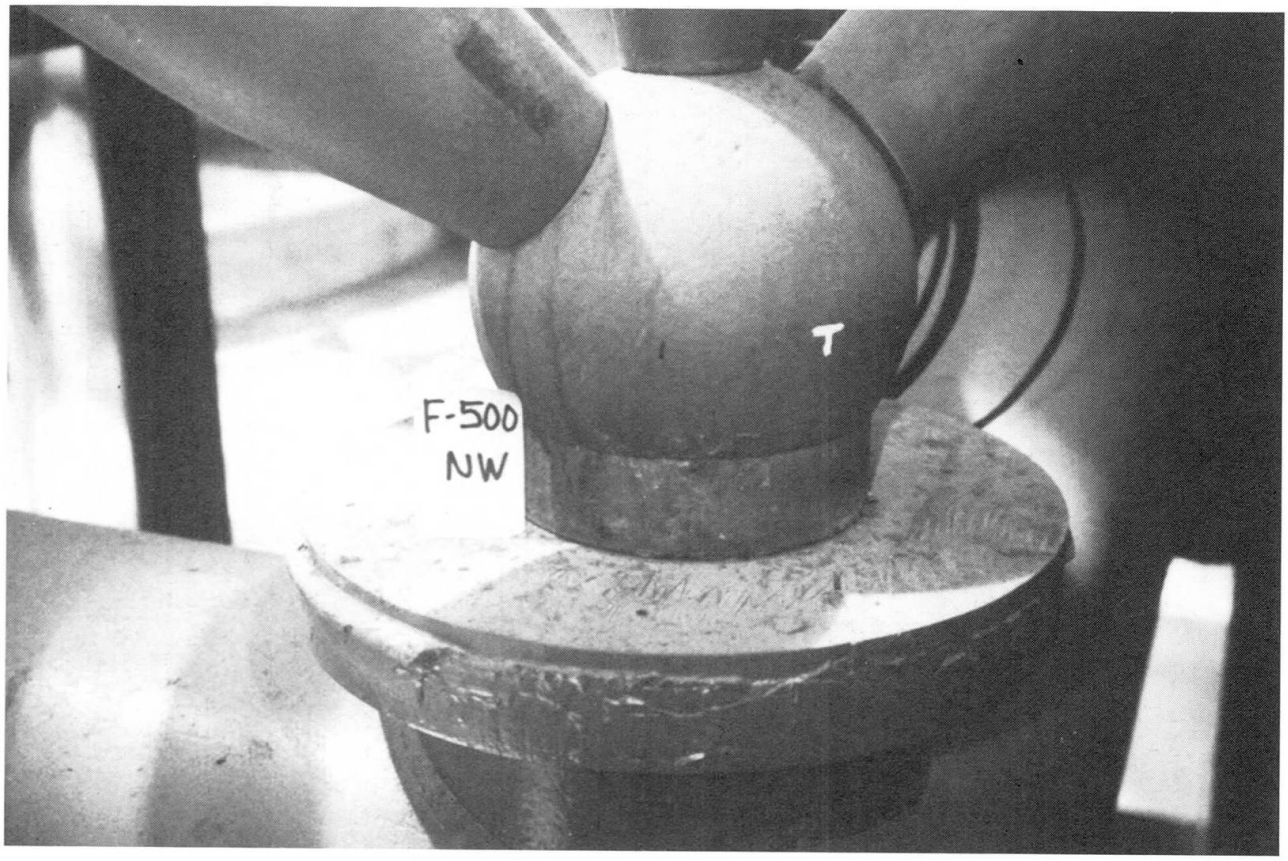

Fig. 3. One of Four Bearing Hubs at Top of "Champagne Column"

1.2.5 Columns and bearings
The horizontal portions of the space frame are supported by the diamond trusses along the column lines. Columns with four-legged towers support the trusses. Each leg terminates in a hub, which bears on the outstretched pipe frame 3 m square at the top of a column assembly (see Fig. 3). The 10 m high columns are

assembled from four pipes of 41 cm dia. filled with concrete and joined by cruciform plate weldments in the center. The shape is said to resemble a long-stemmed champagne glass (see Fig. 4). These assemblies are relatively flexible: the horizontal spring factor at the top is about 10 kN/mm. As the space frame is loaded, either by rising temperature or by gravity loads, the bearings push out from the center toward the edges of the structure. Although designed to slide, some friction occurs. If the friction is too great, loads could build up in the space frame members and in the columns beyond the loads considered in design. While bearings at corners are free to slide in all directions, others are confined to linear motion: this requires all four legs to slide in concert even though they are not rigidly connected to one another. All sliding bearings are unrestrained against uplift.

1.2.6 Rotation of the diamond trusses

Since the diamond trusses in the column strips are continuous over several spans, there will be somewhat more deflection in the exterior spans even when the roof is subjected to uniform load. The unequal deflection will produce a slight rotation of the truss. The four-point bearing at the top of the "champagne column" will then be subject to eccentric load.

Fig. 4. Interior of "Crystal Palace" (looking southwest)

1.3 Concerns

1.3.1 Fire

Fire is a serious hazard in any place of public assembly, particularly in a large exhibit hall. The Convention Center is fully equipped with sprinklers, has a full-time fire brigade on site, and stringent rules for temporary occupancy are imposed. An extensive array of smoke detectors and heat sensors

has been provided to alarm the fire department. Local heating of a high-strength tension bar, even to 400 degrees C., could seriously reduce its strength.

1.3.2 Impact
Impacts are a hazard at the Center because heavy lift equipment and large trucks are constantly used to move exhibits in and out of the show floor areas. A sudden vibration could also result from the fracture of a tension rod in the roof truss. During the recent installation of test equipment in Area 3A, it was observed that a lower chord member of a diamond truss had been struck from below and bent 4 cm out of line.

1.3.3 Concealed damage
Most of the tension rods are concealed within tubes; all connections are typically concealed inside hubs. A flaw in a cast steel hub or in a threaded rod, a missing nut, or ongoing corrosion cannot be directly or conveniently detected.

1.3.4 Design error
Many of the design details, particularly at bearings and other moving joints, but also at other connections, are unprecedented. Experience leads one to expect that some will not behave as intended.

1.3.5 Falling objects
The structure is relatively large, and is in the flight path of two major airports and a nearby heliport. Risk analysis shows that the annual probability of occurrence of an aircraft's hitting the roof is about 1:1 000 000.

1.4 Monitoring Program

To allay concern for "damaged members" -- whether flawed when built into the structure, suffered while in service, or resulting from malfunction of design details [1] -- the State of New York proposed an extensive plan for formal inspections twice a year, once in the winter and again in the summer. Special inspections would be made when an unusual load was encountered. The plan also includes continuous automated sensing by some 150 transducers to characterize the behavior of the space truss under thermal, wind, snow, or impact load.

2. MONITORING BY PERIODIC AND SPECIAL INSPECTIONS

2.1 Exterior Low Roof Deflections

To obtain the response of the space frame to thermal or snow load, and any time-dependent behavior, the deflected shape of the roof will be measured by optical survey. In order to conduct the survey when the exhibit space is occupied, 99 precast concrete monuments 58 x 58 x 14 cm with bronze tablets were set on the roof deck in place of the insulation and ballast layer of the inverted roofing system. Each slab is cemented to a spare piece of EDPM rubber laid on the roofing membrane. Since the slab weighs 100 kg, and the coefficients of friction are about 0.8, the locations can be expected to be reasonably permanent, and will improve the accuracy of benchmark leveling runs. About 350 additional elevations will be taken from points located on concrete slabs that support HVAC units.

2.2 Interior High Roof Drift and Deflection

To obtain both drift and vertical deflections in the glazed high roof areas of the Crystal Palace, Galleria, and Restaurant, 45 pentaprism targets have been situated in the space frame. These retro-prisms allow distance measurements to be made by EDM with about 3 mm accuracy over the typical distance of 50 m or so. A Topcon Geodetic Total Station GTS-3B tacheometer is used to obtain distances to the nearest 2 mm and angles to 1 second of arc. Horizontal control is referenced to 19 survey markers embedded in the floor of the three areas.

2.3 Bearing Movements

Periodic monitoring of bearing-hub movements on the chromed plates atop the "champagne columns" will be facilitated by scratch gages fabricated from stainless spring steel with a hardened stylus at the end to provide a trace on a soft brass tablet, 8 x 8 cm. An approximate record of movement since April 1986 has been provided by means of a coat of paint inadvertently applied over the chromed surface of the bearing plates and by observation of the disruption of recent dust layers.

3. MONITORING WITH AUTOMATED SENSING

3.1 General Description

The system includes some 150 transducers to measure both environmental loadings -- due to snow, wind, solar radiation, and temperature -- and building response to these loads, including strains in roof structural members, lateral building movements, and impacts to the structure, should they occur. Electrical power for excitation, signal conditioning, and analog/digital conversion is provided no more than 20 m distant from each transducer by a distributed system of special data loggers. These are wired in turn to the host computer, nearly a kilometer away from the furthest transducer. The host may be accessed remotely by telephone modem.

3.2 Trial Subsystem

3.2.1 Purpose

The trial subsystem was installed to select sensors and mounting hardware and to provide a real base for the development of data acquisition software. Twenty-seven different sensors were installed in and on the roof structure. Three more were placed in the monitoring office for direct observation and periodic calibrations. Some 2 000 m of cable and three data acquisition units were installed.

3.2.2 Initial studies

-Electrical noise (EMI) from operating HVAC units, lighting, or hand-held radios can interfere with analog signals in transducer leads. Cables with braided shield and with less expensive foil shield were tested at the Convention Center with full-bridge strain gaging and found reasonably noise free.

-Vibrational characteristics of the structure were studied using both accelerometers and velocity transducers. Accelerometer outputs were amplified by a charge amplifier and fed into a Wavetek spectrum analyzer. Natural frequencies of the space truss were about 2.5 Hz; of the individual bar elements, about 29.5

Hz at dead load. The influence of HVAC operation or wind gusts on background vibrations was also recorded.
-Impacts were simulated by dropping a 10 kg steel weight through 0,6 m on bottom chord members of diamond trusses. Impacts were well transmitted about 50 m through the space frame; the log-log plots of distance vs. the unfiltered Power Spectral Density response of the vibration sensors were reasonably linear.
-At first, sensors were placed on bare rod bottom chords of the diamond trusses since these members are the most exposed to impact. It was found that the signal was attenuated if the vibration had to travel past a column and then turn a right angle to arrive at the sensor. Also, even small impacts to the instrumented member caused the sensor to go off scale. Better results were obtained when the sensor was placed on the upper roof structure, just below the roof deck (Elevation 23).
-Since about 25 vibration pick-ups are needed to monitor the space frame that supports the low roof, it is impractical to record and analyze all of the spectral data that could be collected. Instead, a peak-read circuit was developed to monitor each vibration sensor. This circuit is reset after each reading, i.e. once per second.
-The vibration studies were made with a small impact rather than a damaging one, thus it is difficult to set appropriate alarm levels initially. Instead, "soft" alarm thresholds, set low in the beginning, will be raised as experience dictates.

3.3 Measurements and Sensors

3.3.1 Strains in diamond trusses

The bare tension rods, compression chords, and a diagonal compression strut were instrumented as full-bridge load cells using bonded strain gages. These gages are used to indicate live load stress in important structural members. The system determines whether this stress is within allowable limits, and whether it is consistent with the measured loading on the roof. It also determines whether dead load stresses have been released (e.g. fracture of a tension rod in the bottom chord of a diamond truss). Micro-Measurements Series EA strain gages, bonded with AE-10 epoxy, were used for good long-term performance characteristics. Another epoxy adhesive, EPY150 by BLH, was also used. Two tee element gages were used for full-bridge configuration on axially loaded members.

3.3.2 Snow load on roof deck

Strain gages installed on the roof deck and its supports are intended to measure the direct vertical loading (snow load) on the roof. To avoid the problem of arching over a sensor plate, the bending in a top chord that directly supports the roof deck is gaged. HITEC Model HBW-35-125-06-10GP weldable gages in a full-bridge configuration were used for convenience and reliability. Simple load tests were used to calibrate the system.

3.3.3 Temperature

Platinum resistance temperature devices (RTD), Type 100W30 by Omega, were used rather than thermocouples, because RTD's are more compatible with the data loggers used. Temperature is monitored in various locations, including the data logger cabinets, to pick up any significant gradients.

3.3.4 Building side-sway

The roof structure of the building is expected to move laterally in response to wind pressure and temperature fluctuation. Relative building side-sway is measured at expansion joints with Model LRT 150-B linear potentiometers by Waters. The maximum stroke is 150 mm; the maximum positional error is 0,15 mm.

3.3.5 Wind speed and direction
Wind speed and direction are monitored by J-TEC Model VA320 ultrasonic vortex anemometers and wind vanes at the top of 10 m towers located on both the north and south roofs.

3.3.6 Solar radiation
Movements can also be caused by solar radiation that induces temperature changes in the roof deck and curtain walls, which may not be properly measured by the RTD's. Therefore, Hollis MR-5 silicon-cell pyranometers are installed near the anemometer towers to measure total sun and sky radiation.

3.3.7 Bearing movements
Sliding structural bearings located at the column tops should be able to move horizontally to assure that roof structural components are being loaded as the designers intended. Bearing movements are monitored with linear potentiometers to determine whether these movements are actually occurring.

3.3.8 Inclinometers
To resolve lateral movements of the column capital of less than 0,025 mm, tiltmeters that have an accuracy of about 8 arc seconds are installed at 12 columns where bearings seem to be locked. Model QA-1400 servo-accelerometers by Sundstrand are accurate to about 4 arc seconds.

3.3.9 Pressure transducers
The barometric differential on the roof deck is a small but significant part of live load. Setra Model 261-1 pressure sensors range from -0,3 to +0,3 kPa.

3.3.10 Vibration transducers
Impact to important structural members is sensed by Geo Space Model HS-1 vertical velocity transducers. Frequency response is from 4.5 to 200 Hz.

3.3.11 Sensor locations
The deployment of the various sensors is:

Device	3A	3B	3E	High Bay Areas	Total
Strain gaged bare rods	17	15	11	5	48
Strain gaged roof deck	2	3	2	1	8
Strain gaged tubes	3	0	0	0	3
Temperature sensors (RTD's)	7	9	8	7	31
Exp. joint movement (potentiometers)	2	7	5	4	18
Tiltmeters (inclinometers)	4	4	4	0	12
Vibration sensors (velocity type)	7	11	7	4	29
Wind stations (3 sensors ea.)	3	0	3	0	6
Bearing movement potentiometers	2	2	2	0	6
Air pressure transducers	1	1	1	0	3
Power supply voltage	2	2	2	0	6
Totals	50	54	45	21	170

3.4 Data Acquisition System (DAS)

3.4.1 Data Logger: Isolated Measurement Pods (IMP's)
-Data loggers monitor the DC voltage outputs from each sensor. Because of the size of the Center, a distributed system was needed in which data loggers located near the sensors transmit digital signals to a host computer. The Isolated Measurement Pod (IMP), Model 35951B, by the Solartron Divison of Schlumberger is designed to provide both excitation voltage and bridge termination for 10-channels of strain gage signals.

-A 20-channel voltage IMP, Model 35951C, is used where the pulsed 2 VDC supply to strain gages does not provide suitable excitation.
-The IMP's convert the analog voltage signals produced by the sensors to digital signals, which are transmitted over a pair of wires to the computer.
-This is a serial system in which a single pair goes from the computer to the first IMP, from there to the second IMP, and so on. Having only a single line has the disadvantage that should that line be cut, all data from instruments located beyond the cut are temporarily lost. However, the location of the break is easily determined and can be readily repaired provided an exhibition is not in progress.
-Up to 30 IMP's are possible in one net; the system at the Center has 18. All IMP's are scanned once per second, for this system an effective scan rate of some 170 channels per second.

3.4.2 Power supplies
The IMP's are powered from the host location on a protected uninterruptable circuit. Each transducer in turn is powered on an isolated circuit to assure that a short in one line does not have an effect on other lines powered from the same supply. A partial solution is to use only strain gage IMP's, but external +/- 15 VDC supplies are provided for the vibration sensor circuits and other devices.

3.4.3 Network wiring
The communications net supplies DC power to the IMP's and transmits signals both outbound from the host and inbound from the IMP's. Data are transmitted at 163 kilobaud superimposed on the DC power. Each incoming zero bit is divided into four parts: a positive pulse, a negative pulse, and two settling periods. The outgoing zero-bit signals are the reverse: two waits, a positive pulse, and a negative pulse. This accomplishes two purposes: it prevents saturation of the IMP I/O transformers, and it distinguishes between incoming and outgoing data. It does impose fairly high frequency requirements on the transmission line. Current specifications from Solartron for network cable are:

Characteristic impedance	100 ohms +/- 25 ohms
Attenuation at 160 KHz	less than 15 dB/km
Mutual Capacitance	50 pf/m (typ.); 60 pf/m (max.)
Velocity of Propagation	66 percent (typ.)

Alpha No. 9820 is a shielded 2-conductor #16 AWG cable that is said to meet this specification. Attempts to operate the system using other cable that was not impedance matched were unsuccessful.

3.4.4 Host computer
The host computer is a Compaq 386 (IBM-PC AT-compatible) with 1.2 megabyte floppy-disk drive, 130 megabyte hard-disk drive, 1 megabyte of expanded memory (RAM), 80287-8 math co-processor chip, Quadram high resolution monitor and controller card, and an Epson F286 dot-matrix printer.

3.4.5 Software: RTM 3500
The host computer monitors, stores, and prints displays of data collected on the IMP network, using a software package called Real Time Multi-tasking RTM-3500 by Micro Specialty Systems (MSS), Northampton, Pennsylvania to interface with the Schlumberger IMP system. Part of the output format is a spread-sheet that displays the incoming voltage data converted to engineering units on multiple screens. Formulas can be inserted in the spreadsheet to perform conversions and some statistical measures. These can then be used to trigger several types of alarms such as deviation, rate, or limit set-points. The software package is very comprehensive and has proven adaptable to our needs.

3.4.6 Storage of data
An archival data storage rate of once per hour is planned. This will create monthly files of about one megabyte. Data will be stored more frequently if alarm conditions occur. For rapidly changing readings such as vibration or wind, only maximum values will be saved.

3.5 Reports

3.5.1 Software: Shell program
We are currently developing a "shell" or "application" program in Basic [3] that uses the RTM-3500 program in background to gather data, set initial alarms, and save data on disk. The shell program will make data comparisons in real time, allow displays of specific data in graphic and tabular formats, and diagnose alarm conditions for the operator. The program will also analyze historical data (stored on disk) and make possible a variety of presentations, including the automatic generation of monthly reports. As we become more familiar with the data and the relations among the observed behaviors at related sensors, we intend to implement computer programs to interpret the data and produce simplified reports.

3.5.2 Daily
All the reports will be available continuously on the monitors in the Convention Center Control Room and at the engineer's office by modem, including diagnostic reports.

3.5.3 Monthly
Printed monthly reports will summarize the conditions imposed on the space structure and highlight any unusual events.

3.5.4 Emergency
It is expected that, at first, most alarm conditions will be false. Emergency response plans are being formulated.

4. CONCLUDING REMARKS

4.1 Findings to date

4.1.1 Optical Surveys
An optical survey conducted on January 27, 1987, with about 480 Pa snow on the roof found deflections of 3 to 20 mm, less than half that expected.

4.1.2 Damaged Members
The damaged member observed in the lower chord of the diamond truss on Column Line 10 was reportedly damaged by the contractor installing the moveable partition on Line 9 during March 1986. It is remarkable that this damage, although clearly visible from the floor, had not been repeatedly noticed. It is our opinion that the impact which caused the damage would result in an alarm condition on the automated monitoring system. It is fortunate that the damage was located near a point of contraflexure where loss of capacity does not endanger the space frame seriously.

4.1.3 Bearing Movements
Automated monitoring of the bearings has shown less than predicted movements and a tendency to move in jumps. To obtain forces under conditions of no movement, our computer model was modified to lock the bearings instead of using zero

friction as in design. Only one member was overstressed for 10 degrees C. change. This run also provided the effect of temperature changes on roof deck elevations.

4.1.4 Other data collected
-The complete installation was completed in July 1987. Strain, temperature, expansion joint movement, bearing movement, wind and solar radiation data were collected for March 1987 during a trial of the subsystem.
-No snow fell on the roof during March and there are no load related strain gage readings. Usetul information was gathered, however, which indicates gage drift and response to other environmental loadings such as wind, temperature, and HVAC system pressure. Drift of gage sensors, at least during the first months of operation, was very low, not more than a few microstrain over the period.
-Temperature changes of 10 degrees C. induce movements at the expansion joints of roughly 10 mm. This amount of movement is about that expected.
-The absolute movement is not vital unless it exceeds the gap provided. So far there is no tendency evident for movement in one direction more than the other, which might indicate ratcheting or walking off supports.
-Total movement of the bearing at Column Go, 1200 was about 1.5 mm which occurred in two jumps. For 6 degrees C., a north-south movement of at least 4 mm was expected.
-An inclinometer with a resolution of less than 10 arc seconds was installed at Column Go, 1200. After transforming the rotation to horizontal movement of the column capital, the response was found to be linear vs. temperature but with considerable noise, which is characteristic of accelerometers used as inclinometers.
-Other data collected provided no anomalies.

5. FURTHER DEVELOPMENT

5.1 Expert System

Logical comparisons of values obtained from sensors that should respond to the same loading will form the basis of an "expert system". As experience develops the patterns of normal behavior for the space frame, we expect to write adaptive software that can reach decisions for alarming at several levels of significance. If non-linear behavior can be resolved, it may be possible to develop the software to include some level of artificial intelligence to assess damage. For the near term, it appears unlikely that the space frame will receive loadings sufficient to provide the "shake-down" conditioning needed for predictable response.

REFERENCES

1. YAO, JAMES T. P., Safety and Reliability of Existing Structures, Pitman, London, 1985, pp. 7-15.

2. AGERSKOV, H., Optimum Geometry Design of Double-Layer Space Trusses, ASCE Journal of Structural Engineering, Vol. 112, No. 6, June 1986, pp. 1454-1463.

3. KEMENY, J. G., and T. E. KURTZ, True Basic, Addison-Wesley, Reading, MA, USA, 1985.

Full-Scale Dynamic Testing of ENEL Power Plant Structures

Essais dynamiques des structures des centrales électriques - ENEL

Dynamische Versuche an den ENEL Grosskraftwerkbauwerke

Emanuele F. RADOGNA
Ordinary Professor,
University of Rome, Italy

Emanuele R. Radogna, born 1930, Professor of Civil Engineering. Research work deals mainly with: — dynamic response of structures in service; — probabilistic analysis of safety versus fatigue; — problems of fracture mechanics of concrete; — redesign of concrete structures.

Eduardo FALLETTI
Hydraulic Engineer,
ENEL Rome, Italy

Eduardo Falletti, born 1940, got his hydraulic engineering degree at the University of Napoli in 1966 and joined ENEL in 1967. At first involved in the design of the power plants' hydraulic and marine structures, he is now responsible for the design of thermoelectric and nuclear power plants' major structures.

Ennio Mario DA RIN
Civil Engineer,
ISMES S.p.A.
Bergamo, Italy

Ennio M. DaRin, born 1947, got his civil engineering degree at the University of Liege (B), joined the staff of Professor Ch. Massonnet and was involved in plastic structural analysis and testing. After some design and site construction practice, he was engaged by ISMES and has been since concerned with full-scale dynamic structural testing.

Umberto ROSSI
Hydraulic Engineer,
ENEL Rome, Italy

Umberto Rossi, born 1947, got his hydraulic engineering degree at the University of Rome in 1972. Since 1975 he has been employed at ENEL and involved in the design of the hydraulic and marine structures of thermoelectric power plants.

Stefano STEFANI
Civil Engineer
ENEL Rome, Italy

Stefano Stefani, born 1955, got his civil engineering degree at the University of Rome in 1980. He has since been employed at ENEL and involved in the design of thermoelectric power plants's various structures.

SUMMARY

The ENEL Power Plants' major steel or concrete structures have been the object of dynamic investigations. This paper gives a short overview of some of these investigations undertaken to verify the design and construction qualities.

RESUME

Le comportement des plus importantes structures des centrales électriques de l'ENEL a été examine au moyen d'essais et relevés dynamiques effectues. Le present article donne un aperçu de ces investigations entreprises dans le but de verifier la qualité du projet et de la construction.

ZUSAMMENFASSUNG

Das Verhalten der wichtigsten Strukturen der ENEL Grosskraftwerken ist mit dynamischen Verfahren experimentell untersucht worden. Dieser Artikel gibt einen Überblick über die zus Qualitätssicherung vorgenommenen Prüfungen.

1. INTRODUCTION

In structural design, the assessment of safety is performed in three different steps:

- calculation of the "response" S of the mathematical model of the structure to the applied actions;
- calculation of the "resistance" R, provided by the geometrical dimensions of the structural system, the mechanical properties of the materials, the restraint conditions,etc.;
- comparison between the quantities R and S: the structure is "safe" if $R - S > 0$.

Each quantity involved in the above calculations has to be estimated in the design stage: the extrapolation of the data acquired from past experiences to future actions, materials and constructions involves a number of uncertainties which require an adequate margin between R and S.
The basic formulations of safety analyses are the following:

- starting from the upper and lower p - fractiles of the random variables R and S, the ratio R_k/S_k is computed providing the characteristic safety factor ("Level 1" methods);
- the performance function $Z = R - S$ is defined allowing to express the limit state condition as $Z = 0$; then the distance between the average μ_z of the probability density function of the random variable Z and the $Z = 0$ point is expressed through s_z, the standard deviation of Z : $\mu_z = \beta s_z$. The reliability index $\beta = \mu_z/s_z$ is adopted as a measure of the safety ("level 2" methods);
- with reference to the inequality $S > R$, which expresses the failure, considering S and R as random variables, the probability of failure is given by:

$$P_{fail} = \text{Prob}\,[S > R] = \iint_{[S>R]} p_{R,S}(S,R)\,dS \cdot dR$$

where $p_{R,S}(S,R)$ is the joint probability density function of the random variables S and R. ("Level 3" methods).

For structures prevailingly exposed to randomly fluctuating environmental actions, the largest uncertainties concern precisely the modelling of the external actions (wind, waves, earthquakes etc.). The monitoring of these structures after their construction yields directly the action effects without any knowledge of the applied actions and the technological quantities, depending on the structural system geometry and the actual material characteristics.
The structural survey allows hence to answer two different questions:

- the improvement of the statistical distribution of environmental actions and of their correlative probabilistic models;
- the assessment of the integrity of a structure during its lifetime with special concern for progressive damaging phenomena.

In the present paper, some typical full-scale investigations are briefly described, as examples of the increasing interest in structural dynamic investigations. Some of these investigations have already been performed by ISMES, on behalf of ENEL, at the Torvaldaliga Nord Power Plant (four thermoelectric groups of 660 Mw each), and some others are planned by ENEL to be conducted at the Termini Imerese and at the S.Filippo del Mela Power Plants (both consisting of two Thermoelectric groups of 320 Mw each).
In all cases, initial dynamic testing provides first of all a set of useful reference data for allowing future evaluations of the structural integrity. Repeating the dynamic testing of the structure during its lifetime and measuring

the response quantities as before, an eventual deviation between subsequent corresponding outputs will indicate structural deteriorations.
In some cases, a further aim of the measurements is the improved knowledge of the environmental actions. In this respect, the recently performed testing must be considered as preliminary investigations and further efforts will be made by ENEL to gain more information.

2. GENERAL ASPECTS OF THE EXPERIMENTAL PROGRAMS

Three classes of quantities are involved in the structural problems:

a) input quantities describing external actions;

b) technological quantities depending on the structural system geometry and the material characteristics;

c) output quantities representing the action effects.

In the design stage, the quantities (a) and (b) are given and the quantities (c) are calculated by means of the structural mechanics methods.
During the acceptance tests of the constructions, the response is measured to given loadings, applied to a well identified structure. The comparison between the calculated and measured response gives the required information on the conformity of the as-built construction with respect to the idealized structure.
The system identification technique applied to civil structures requires the knowledge both of (a) and (c) quantities. It is then possible to identify the characteristic parameters of (b) and to recognize if some changes of them are still running: these goals can be attained more directly in the frequency domain through the application of the powerful modal and transfer analyses techniques.
Moreover, having measured the output quantities (c) and knowing the technological quantities (b), an evaluation can be made of the external actions (a).

3. OUTLINE OF THE EXPERIMENTAL TECHNIQUES

It is well known from the theory of linear systems, that the dynamic characteristics of a structural system can be inferred if its response (output) to some given excitation (input) is measured. In forced vibration tests, this excitation is provided artificially by means of one or more structural vibrators, of the electro-mechanical or hydraulic type, placed at the appropriate points on the structure to be tested. In general, these vibrators are used for generating a sinusoidally varying force of adjustable amplitude and controlled slowly sweeping frequency between the limits of a consistent frequency range.
In some cases it is possible to take advantage of the natural excitation provided by ambient wind, wave or traffic forces; without requiring the installation of structural vibrators, ambient vibration surveys can yield valuable data on the actual performance of as-built structures under the true environmental conditions. Yet, forced harmonic vibration tests will usually produce more complete and more accurate information about the dynamic structural parameters, mainly because of the precise control of the excitation characteristics possible with this method.
The structural response to the applied excitation is measured by means of various transducers: accelerometers, seismometers, displacement or strain-gauges mounted on the tested structure at appropriate locations.
For the simultaneous recording of the transducer signals, use is made of a computerized data acquisition and processing system, developed by ISMES and the hardware of which is located in a Mobile Laboratory. Data from the various installed transducers are fed to signal conditioners which drive, after on-line analog-to-digital conversion, into the computer memory. During the acquisition process, single channels may be observed in real time on an oscilloscope and, at the end of it, pre-processing of the test data can be undertaken directly on site to obtain preliminary information in the form of response curves or transfer functions plots. All the collected data are finally driven into a multichannel tape recorder and may thus be subsequentely played back to a

computer for the more thorough analysis to be made at the Central ISMES Laboratories.

4. FULL-SCALE INVESTIGATIONS

4.1 Turbogenerator foundation

A steam turbogenerator concrete foundation (50.60 x 16.00 m in plant and 12 m in height) was subjected to forced harmonic vibrations by means of a mechanical vibrator covering an overall frequency range from 1 to 50 Hz (the frequency corresponding to the rotational speed of the machine). The structural response was measured using 40 seismometers located at appropriate points of the structure; the analysis of the response allowed to identify the 8 lowest natural frequencies, modal shapes and corresponding damping ratios: these frequencies appeared to be sufficiently low indicating thus satisfactory design and construction qualities. Further amplification peaks,without clearly defined corresponding vibration shapes, were noticed at higher frequencies, because of the limited number of measurement positions: the vibration behaviour at higher frequencies is the most significant for this structure subjected to the steady-state operating forces caused by inevitable unbalanced masses of the rotor: in order to check the satisfactory serviceability of the machine-foundation system, the actual vibration levels must hence be investigated by direct measurements during operating conditions.

4.2. Machine Hall

The Torvaldaliga Nord Power Plant machine hall overall structure was also subjected to forced harmonic vibrations. This industrial building, 276x62 m large and 34 m high,is composed by 17 steel portal frames laterally connected by longitudinal beams and braced with diagonal trusses; a thermal expansion joint provides a structural disconnection between two nearly symmetric halves of the complete machine hall.
The aim of this investigation was in fact to make an evaluation of construction quality through the determination of its dynamic characteristics, although the machine hall structural service is prevailingly static. The tests, executed during the licensing process, allowed to evaluate the quality of the connections through the measured damping ratios associated with the fundamental vibration modes. The vibration tests were executed symmetrically on the two halves of the building; the construction quality could thus be appreciated by comparing the corresponding responses of the two half structures; this was expecially interesting considering that the two parts of the machine hall were constructed by two different contractors.

4.3. Multiflue chimney

Finally, the Torvaldaliga Nord Power Plant multiflue chimney was analyzed under dynamic excitation of artificially produced harmonic forces and high natural wind forces excitation as well. This chimney is composed of an outer slightly tapered concrete shell 243 m high and four inside steel flue liners; each liner is divided into five elements hinged one to another and supported individually by steel platforms.
The chimney's dynamic characteristics were first investigated through analysis of the structure response to harmonic varying forces applied to the tip in two orthogonal directions. The first three natural vibration modes of this cantilever-type structure were thus identified in two orthogonal vertical planes (natural frequencies, modal shapes and related damping ratios). Due to the eccentricity of the excitation force, the characteristic of the fundamental torsional vibration mode could also be determined.
These modal parameters showed to be in satisfactory agreement with the ones computed in the design stage. Moreover,making reference to a lumped masses stick-model, the actual rocking impedance of the overall foundation (raft, piles and participating soil) was evaluated: this by computing the ratio of the measured foundation raft rocking to the actual total dynamic moment acting upon

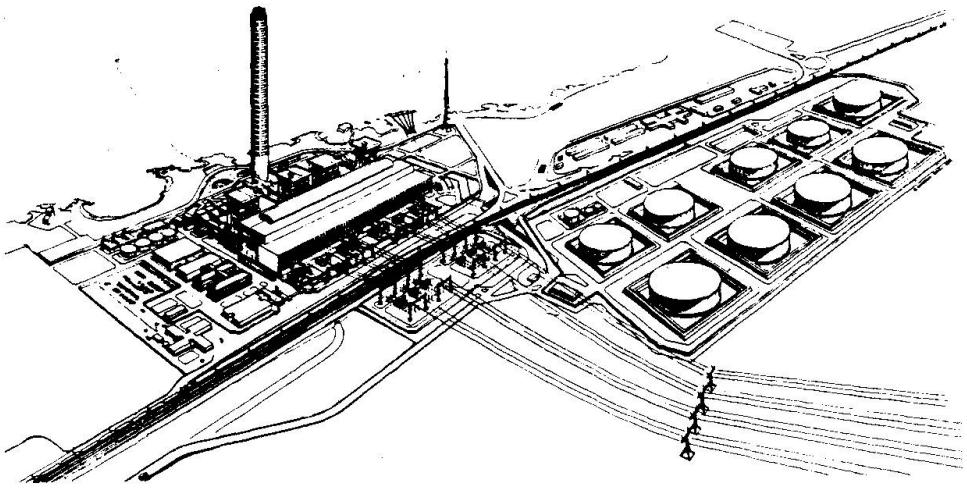

Fig.1 TORVALDALIGA NORD POWER PLANT

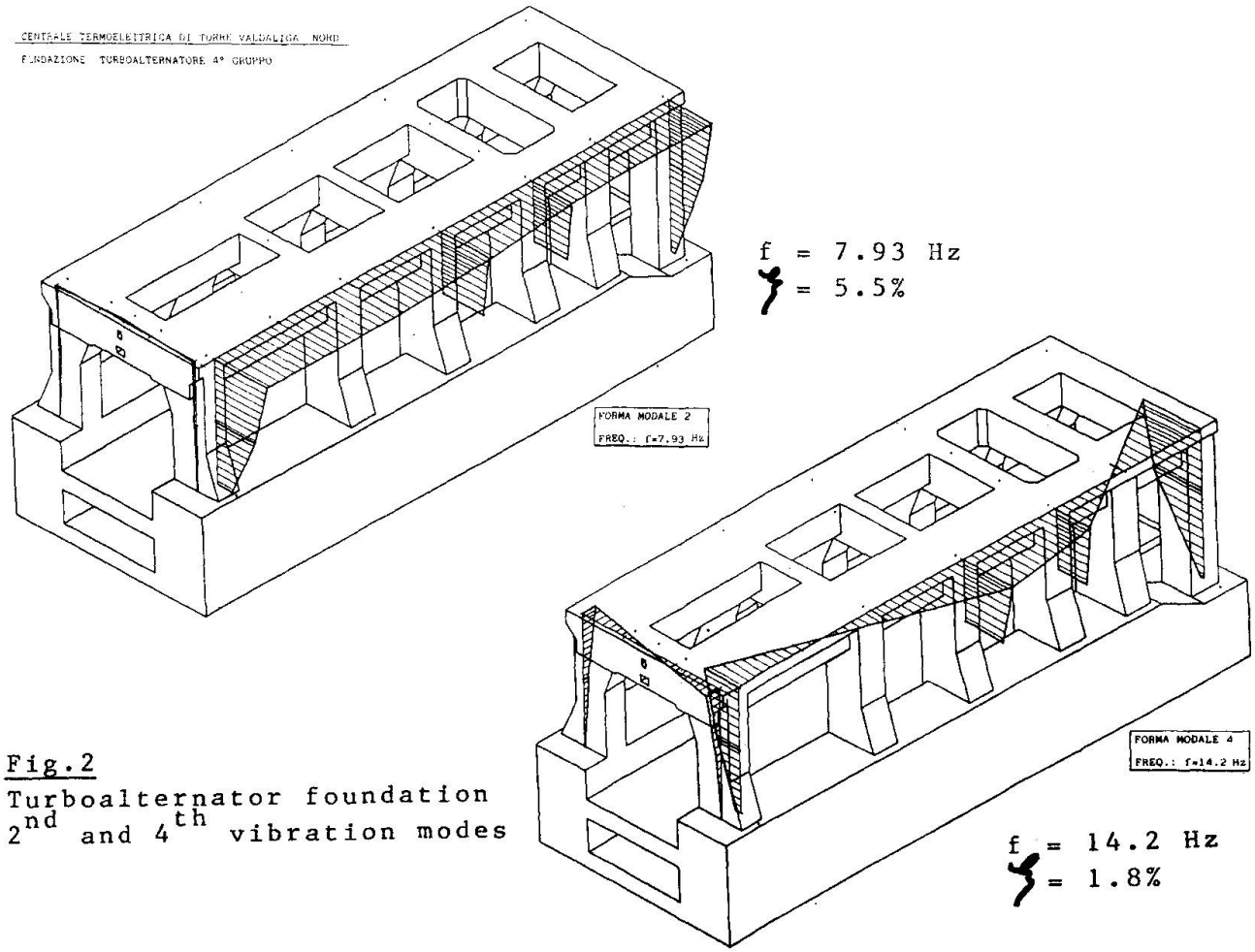

f = 7.93 Hz
ξ = 5.5%

f = 14.2 Hz
ξ = 1.8%

Fig.2
Turboalternator foundation
2nd and 4th vibration modes

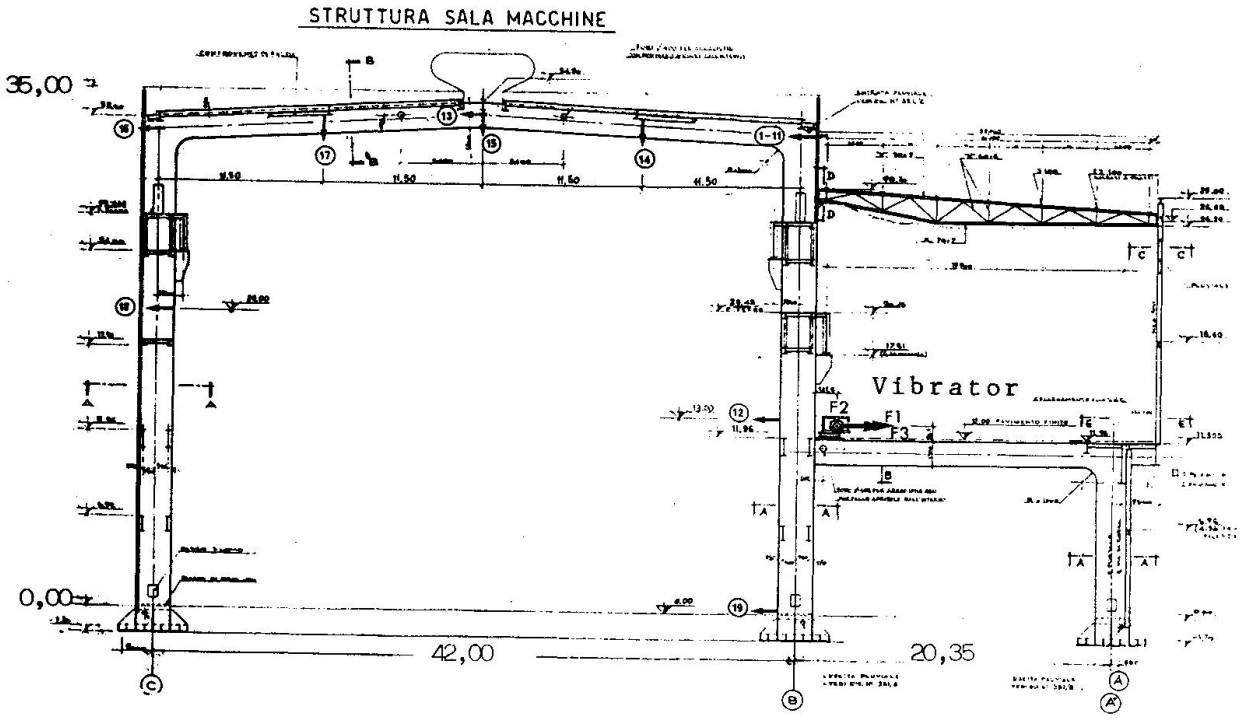

Fig.3 Torvaldaliga Nord Machine Hall structure

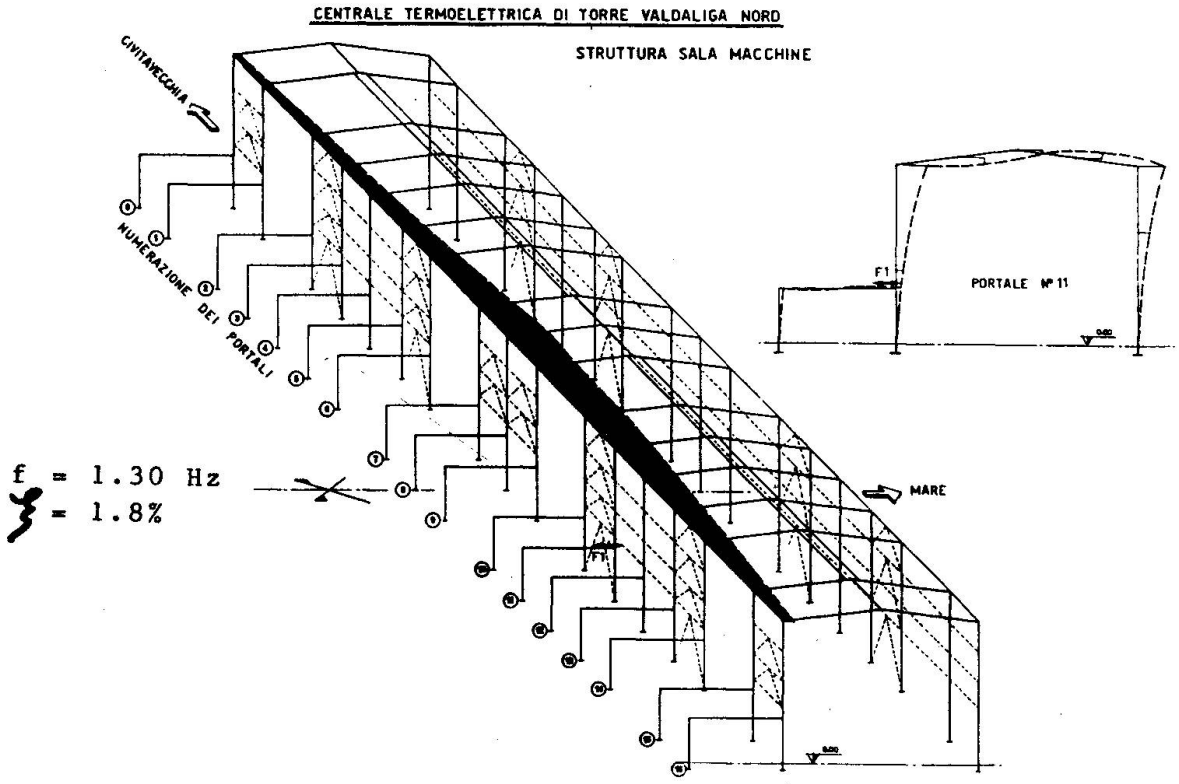

Fig.4 First lateral vibration mode

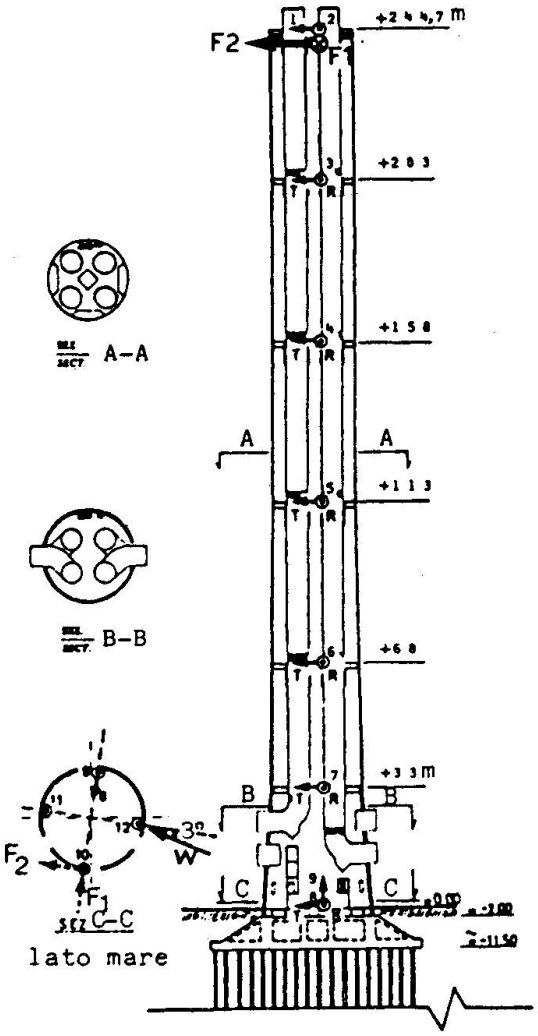

Fig.5 Torvaldaliga Nord multiflue chimney

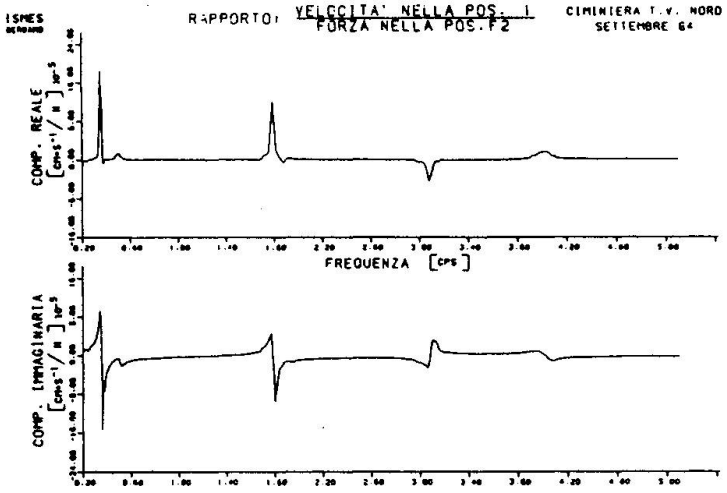

Fig.6 Tip velocity response transfer function

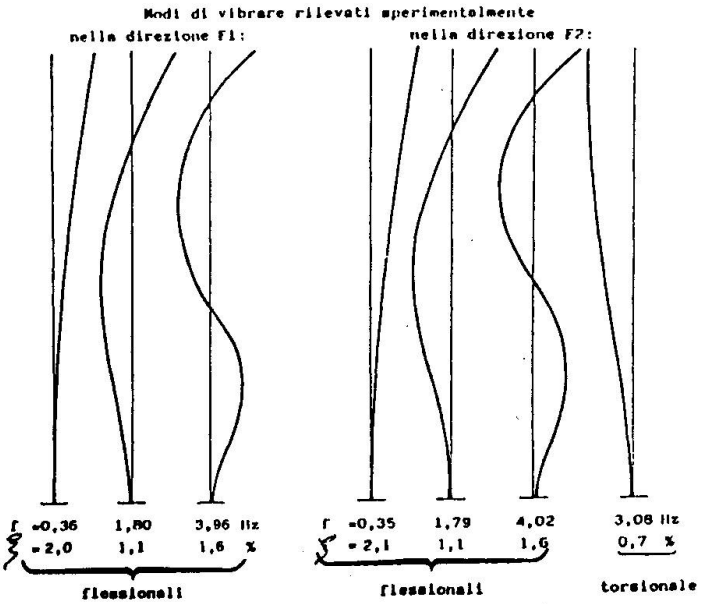

Fig.7 Experimental modal shapes, frequencies and damping ratios

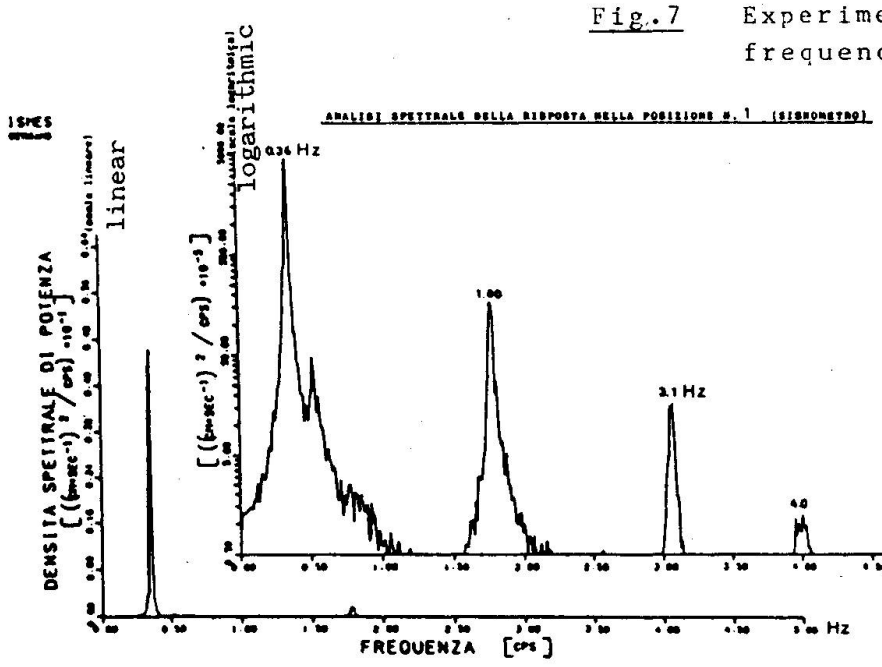

Fig.8 Power spectral density of the chimney's tip wind induced vibrations

it. The obtained resulting stiffness, although somewhat larger, appeared to be of the same magnitude as the value computed through the usual design assumptions.
The spectral analysis of the chimney's response to strong environmental wind excitation (with an average wind speed of about 21 m/s) showed evident peaks at the same frequencies found previously. The chimney's response to the wind resulted, almost entirely, in being due to the fundamental vibration mode: the fundamental torsional mode appeared to be, although very slightly, excited too. The vibration response intensity was found to be of the same order of magnitude as well in the along-wind direction as in the cross-wind one.

4.4. Cooling water intake

To provide the cooling water of the machines, in Torvaldaliga Nord Power Plant the sea water is drawn by means of a subsea concrete channel starting with an intake 300 m off from the coast and 16 m under the sea-level.
In view of evaluating the waves actions on the intake, 26 pressure transducers were set up on the walls and under the foundation slab of the structure, as well as wavemeters and anemometers for the measurement of the high waves and wind speed and direction. The main aim of these experiments was the investigation of the local actions of the waves, a physical phenomenon at present time not representable in a mathematical form, owing to the particular geometry of the intake. The need of full-scale tests came from the difficulties of reproduction of local actions on a reduced scale physical model: the greatest difficulties derive from the scale-effect of the water-air interface (shock action of the waves). From the full-scale measurements, information is expected, moreover, about sub-pressure variations, caused by the waves, on the foundation soil; this phenomenon could hardly be reproduced on a reduced-scale physical model, because of its strong dependence on the nature and stratigraphy of the foundation soil.

4.5. Coal/oil-ships jetties

In both S.Filippo del Mela and Termini Imerese Power Plants, an off-shore jetty is at present time under construction: the S.Filippo del Mela jetty, designed for the dock of up to 120.000 WT coal-ships, is located in open sea, in non constant sounding depth, up to 33 m, and is composed of ø 1500 and ø 1800 concrete piles and an overcapping concrete plane frame; the Termini Imerese jetty, designed for the dock of up to 50.000 WT oil-tanker, is located in open sea, in about 14 m sounding depth and is composed of ø 1422 steel piles and an overcapping steel frame.The design live loads are mainly the waves actions (design wave height 9 m), the bollard pull and the tacking ship impact (design tacking speed 0.15 m/s).
Dynamic in situ investigation tests are foreseen as well on insulated elements (piles) as on the overall construction, by means of artificially forced excitation: through the former, by measuring the displacement and the rocking of the pile at tip section and at ground-sea interface section, the translational and rotational stiffnesses and damping ratios of the infixed part of the pile are expected; through the latter, a complete dynamic characterization is expected, which will allow a comparison with the design forecast (first modal frequencies in the range from 0.5 up to 1.6 Hz) and a collection of some reference dynamic parameters for future checks especially after an eventual severe loading such as sea-storm or ship collision.

5. REMARKS

The disposal of a numerical reference model of the tested structure allows to deduce more complete and more significant information from the experimental data. This, not necessarily very refined reference model, must allow:

- a rational interpretation of the response of the tested structure;
- the evaluation, by applying the system identification techniques, of the main technological parameters;

- a sensitivity analysis of possible variations of these parameters with the aim of making a rational interpretation of observed eventual deviations in time of the periodically repeated dynamic investigations results.

The full-scale dynamic testing or monitoring of large constructions gives information about the actual but overall structural behaviour; if necessary this overall structural behaviour assessment can be integrated by local testings of the actual material properties or conditions.
The past monitoring experiences have revealed that nowadays the structural response measuring instruments are much more reliable than the external action measuring instruments: there appeared, in particular, the need of gust anemometers to obtain the dynamic wind speed characteristics and pressure-transducers to obtain directly the dynamic wind actions. Concerning the dynamic measurement of wave actions, the pressure transducers have also a fundamental role, as indicated by the on-going technological progress of these instruments.

6. CONCLUSIONS

In the last three decades,major advances have been made in structural design and construction technology. In particular, design procedures were fundamentally improved by the introduction of the probabilistic concept of safety. Making use of continously refined computational techniques of static and dynamic structural analyses it is thus nowadays possible to design large civil or industrial engineering structures according to more precise specifications, in order to meet in particular definite serviceability requirements. Nevertheless, uncertainties remain in what concerns the actual engineering performance of the as-built structure, under the true environmental conditions, due to constitutive material properties, construction quality, foundation behaviour, numerical modelling idealization, etc.
There is, thus, a strong need for a postconstruction verification of the design assumptions and execution criteria in order to finally check the actual serviceability, safety and thus the quality of the construction. In this respect,the recent development of dynamic testing and analysis techniques has provided an efficient means for getting the required valid information.

7. REFERENCES

1. MEIROVITCH L. "Analytical methods in vibrations", The Macmillan Company, New York, 1967

2. AUGUSTI G.,BARATTA A.,CASCIATI F., "Probabilistic methods in structural engineering", Chapman and Hall, London, New York, 1984

3. CASTOLDI A. et al., "Analisi sperimentale delle strutture", from "Costruzioni in zona sismica", Coordinatore CASTELLANI A., Masson/Tamburini Milano, 1982

4. DA RIN E.M. "Dynamic structural testing of Torre Valdaliga Nord Power Plant's 250 m high multi-flue chimney", XXV Cicind Meeting, Venice 1986

5. FALLETTI E.,ROSSI U. et al., "Sistemi di controllo e monitoraggio adottati dall' ENEL per le strutture a mare", Aiom Congress, Venezia 1986

6. DA RIN E.M.,RADOGNA E.F.,STEFANI S.,"Indagine sperimentale sul comportamento dinamico di una ciminiera multiflusso alta 250 m", XIII Convegno AIAS, Bergamo 1985

7. CASTOLDI A.,PAGANI ISNARDI G.,VITIELLO E., "Esperienze di sollecitazione dinamica e identificazione su strutture per centrali elettriche", II Convegno Nazionale di Ingegneria Sismica in Italia, Rapallo 1984

8. ISMES Report n. 2344, "Indagine sperimentale sul comportamento dinamico di una struttura di sostegno dei turboalternatori della Centrale Termoelettrica di Torrevaldaliga Nord", 1984

9. ISMES Report n. 2619, "Indagine sperimentale sul comportamento dinamico della struttura sala macchine della centrale termoelettrica di Torrevaldaliga Nord", 1985

10. ISMES Report n. 2567, "Indagine sperimentale sul comportamento dinamico della ciminiera multicanne della Centrale Termoelettrica di Torrevaldaliga Nord", 1984

11. ISMES Report n. 3282, "Centrale Termoelettrica di Torrevaldaliga Nord. Elaborazione dei dati memorizzati dal sistema automatico installato sull'opera di presa", 1986

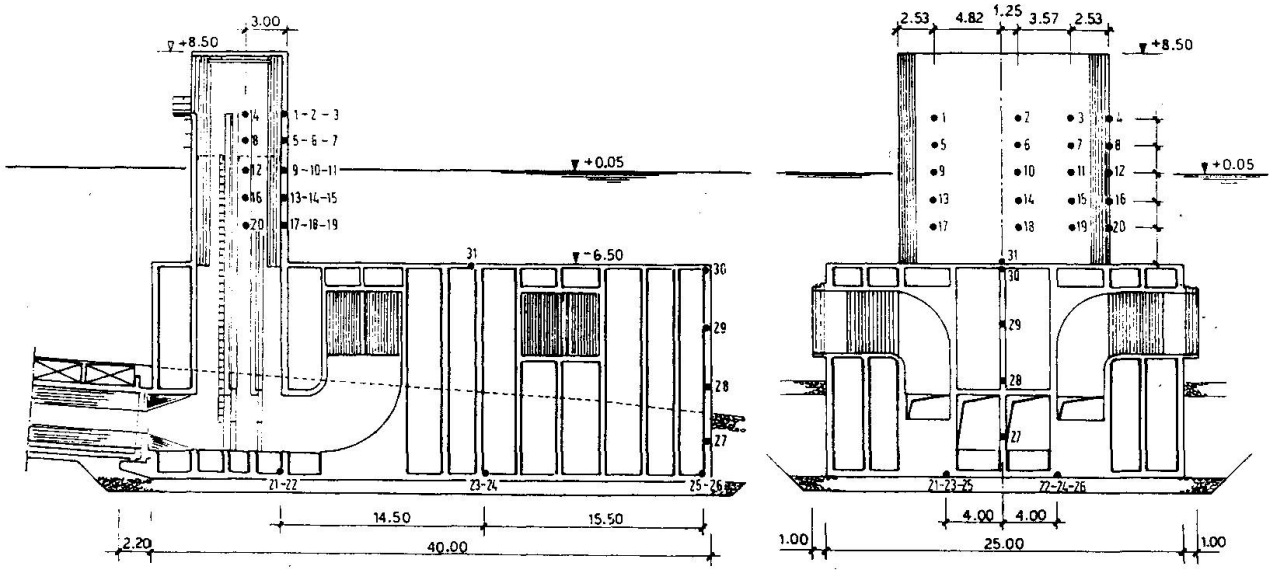

Fig.9 Torvaldaliga Nord cooling water intake (lateral and front view).

Structural Integrity Monitoring of Fixed Offshore Platforms

Surveillance de la tenue structurale des plate-formes marines fixes

Gebrauchsfähigkeitüberwachung von festgesetzten Seeplattformen

V.G. IDICHANDY
Sr. Scientific Officer Gr. I
Ocean Engineering Centre
Indian Institute
of Technology
Madras 600 036, India

V.G. Indichandy, born in 1946, got his Master's degrees in Physics and Engineering Mechanics and Doctoral degree in Ocean Engineering. For the last 18 years, he has been working at IIT Madras in various capacities and his areas of interests are Experimental Techniques and Instrumentation applied to Model and Prototype testing of fixed and floating structures.

C. GANAPATHY
Professor & Head
Ocean Engineering Centre
Indian Institute
of Technology
Madras 600 036, India

C. Ganapathy, born in 1937 obtained his doctorate in Civil Engineering from the IIT Madras. He was engaged in teaching and research for about 25 years. His area of specialisation is Structural Engineering with particular interest in Steel Structures, Offshore & Ship Structures. He has been professor in Ocean Engineering since 1978.

P. SRINIVASA RAO
Professor
Structural Engineering
Laboratory - Indian
Institute of Technology
Madras 600 036, India

P. Srinivasa Rao, born in 1936, got his B. Tech and M. Tech in Civil Engineering from the IIT Kharagpur and his Dr.-Ing. degree from the Technical University of Munich. Since 1972 he has been Professor of Structural Engineering at the IIT Madras. In addition to being very active in teaching and research with well over 60 publications to his credit, he is also a leading Consulting Engineer in the field of Concrete Structures in India.

SUMMARY

This paper describes a comprehensive study on Structural Integrity Monitoring of Fixed Offshore Platforms based on their dynamic response. Analytical and experimental investigations have been carried out to identify factors in dynamic response most sensitive to structural damages, despite the presence of changes in parameters other than damages, affecting dynamic response. Based on this study, a scheme for integrity monitoring has been proposed which has the potential to replace, if not, at least reduce the frequency of the present uneconomical and hazardous diver inspection.

RESUME

Cet article decrit une étude de la surveillance de la tenue structurale des plate-formes marines fixes sur la base de leur réponse dynamique. Des recherches théoriques et expérimentales ont été effectuées en vue d'identifier les éléments de la réponse dynamique qui sont les plus sensible à des dommages structuraux. On en a déduit un plan de surveillance de la tenue pouvant remplacer, sinon au moins réduire la fréquence des dispendieuses et hasardeuses inspections sous-marines habituelles.

ZUSAMMENFASSUNG

Dieser Beitrag beschreibt ein Studium der Gebrauchsfähigkeit von festgesetzten Seeplattformen auf Grundlage deren dynamischen Antwort.
Analytische une experimentelle Forschungen wurden unternommen um die zu den Tragwerksschäden empfindlichten Elementen in der dynamischen Antwort zu bestimmen.
Von dieser Forschungen ist ein Überwachungschema abgeleitet worden, welches die kostspieligen und unsicheren gewöhnlichen Untersee-besichtingungen wenn nicht ersetzen, wenigstens deren Häufigkeit vermindern kann.

1. INTRODUCTION

Majority of the offshore oil production platforms belongs to the jacket type of fixed structure, a welded steel tubular space frame. These platforms and many more to be installed in future are designed for all types of environmental loads and for a useful life span of more than two decades. Such a long service in a very hostile environment prevailing in the ocean, makes it necessary to inspect these structures for identifying and locating possible structural defects for timely maintenance and repair.

At present, all over the world trained divers are being utilized for this inspection. But, poor visibility, concealment of damages by excessive marine growth, non-availability of trained divers, prohibitive cost and dependence of diver inspection on weather conditions, limit the viability of this hazardous operation both technically and economically. Consequently, a need has been felt to develop better techniques, preferably operated from the deck of the platform to monitor the structural integrity of the installation periodically and an instrumented integrity monitoring based on dynamic response was proposed by many researchers as the best alternative.

1.1 Integrity monitoring based on dynamic response

Structural integrity monitoring based on dynamic response is not new to civil engineers, as this method has been made use for land-based structures after seismic activity or fire hazards. The method itself is based on the fact that any structure, regardless of the type, has natural modes of vibration which are fundamental characteristics of the structure and do not change unless there are changes in its stiffness or mass distribution. In the case of an offshore structure, these modes are continuously excited by wind and wave forces and periodic determination of modal characteristics with the help of proper instrumentation and measurement techniques can reveal the integrity of the structure.

Thus it appears that integrity monitoring reduces to determination of modal parameters of the structure. However, it should be kept in mind that there are certain other factors apart from structural damages e.g. variation in mass distribution that could possibly alter the modal characteristics and this can lead to serious difficulties including erroneous conclusions while interpreting the measured data. Based on investigations by some organisations on simple theoretical and physical models, different approaches had been suggested to overcome this difficulty.

1.2 Background information

Organisations involved in the research of this topic are certification agencies, research establishments on behalf of offshore oil industry as well as universities. Some of the important among them are American Bureau of Shipping, Lloyds Register of Shipping, Det Norske Veritas, Norske Agip and Technomare, Structural Monitoring Ltd., Keith Feibush Associates, Aerospace Corproation, GKSS Forschungs Zentrum, Institute Francais du Petrole, The Massachusetts Institute of Technology, University of Maryland and University of California.

These investigators used analytical and physical models for their work and many of them also took measurements on actual production platforms. Apart from the global frequency monitoring, some authors suggested changes in mode shapes as well as shift in modal vectors in all six degrees of freedom of different modes and these organisations are: The Aerospace Corporation [1,2] and the University of Maryland [3]. However, both these organisations based their conclusions on very simple analytical and physical models and suggested further detailed work including analysis using 3-D finite element model of actual platforms to fully understand and develop the potential of the method as a tool for structural integrity monitoring.

1.3 Scope of present work

As a result of these suggestions, it was felt that there was a need for study all the aspects of integrity monitoring, incorporating every factor influencing the dynamic response of the structure with the help of a 3-D finite element model and to prove the results obtained in the laboratory with the help of a physical model. Consequently the present work is executed in the following sequence.

Formulate a 3-dimensional FE model of an existing well platform consisting of the full deck structure, distributed deck mass, jacket, grouted piles, launch truss, marine growth, hydrodynamic added mass, effect of pile foundation etc., for dynamic analysis using structural analysis package SAP IV, so as to determine the modal parameters like natural frequencies and mode shapes for various conditions of the factors influencing the dynamic response of the platforms. Based on the results of the analysis, test a physical model of the platform under different types of excitation to study the efficiency of the measuring system in identifying the modal parameters and to prove the results of the analysis. Finally, to propose a scheme for integrity monitoring based on the results of these investigations [4].

2. ANALYTICAL INVESTIGATION

2.1 Features of the platform

The well platform selected for analysis consisted of a jacket, deck with machinery and had four main piles and an equal number of skirt piles. The outer diameter of each leg was 1.335 m and wall thickness 0.020 m. Two of the main legs had a batter of one in eight in two perpendicular directions and the other two had the same batter only in one direction. A key plan of the jacket is shown in Fig.2.

On the deck of the platform were located a crane, helideck, test separator, fuel storage tank, generators and other essential machineries. The total deck load inclusive of the live load was 503 t.

All the eight piles were steel tubulars of external diameter 1.220 m with a wall thickness of 0.025 m and these were driven through the legs to a depth of 72 m below mud level. The annular space between the leg and the pile was grouted with cement.

This platform was situated in a water depth of 85 m. The overall height from mud-level to the top of the deck was 107 m.

2.2 Formulation of the FE Model

In the FE model all the members were idealised as 3-D beam elements having all six degrees of freedom. Nodes were located at the centroidal axes of the intersecting members. Figs.1 and 2 show the vertical framing, launch trusses, horizontal framings and other deck frames. As can be seen, almost the entire structure was represented in the mathematical model and only a very few unimportant members at horizontal levels were left out.

Additional mass due to equipments on the deck, grout in the pile-leg annular space, water inside the pile etc. were included in the model as lumped masses in the respectives nodes.

The effect of the entrained water or added mass was included as lumped mass in the model as the mass of the water displaced by the submerged members. Depending on the orientation of the member the mass was lumped by resolution of vectors in the respective directions.

The soil-pile interaction and their lateral restraints were adequately represented by linear spring whose stiffness was worked out based on the slope of the load deflection curves. These springs were treated as boundary elements in the analysis.

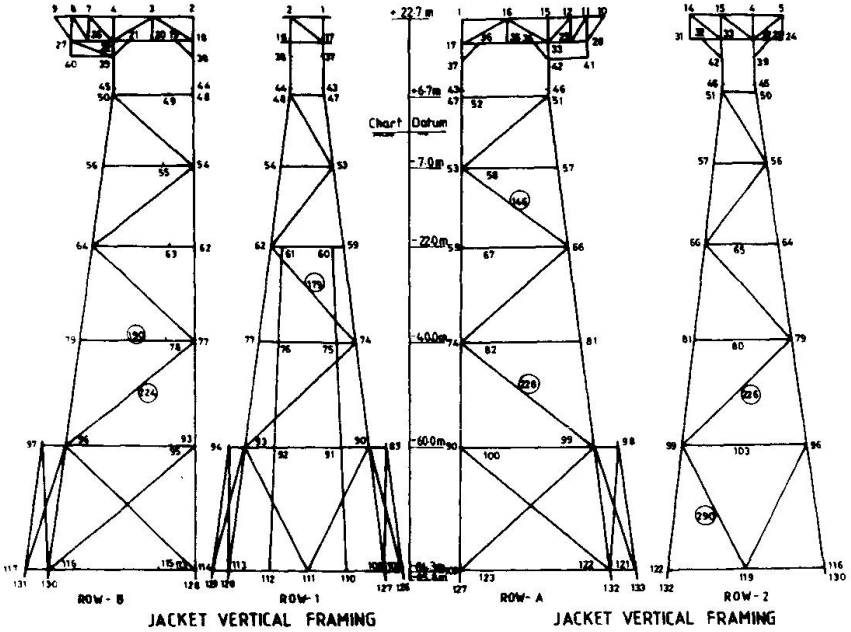
+22.7m
Chart Datum
-7.0m
-22.0m
-40.0m
-60.0m
ROW - B
ROW - 1
ROW - A
ROW - 2
JACKET VERTICAL FRAMING
JACKET VERTICAL FRAMING

Fig.1

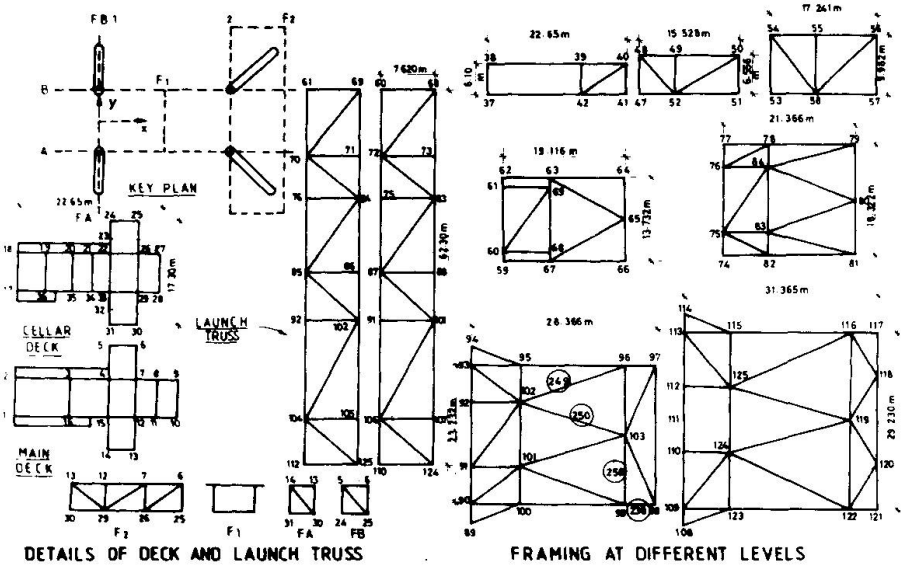
KEY PLAN
CELLAR DECK
MAIN DECK
LAUNCH TRUSS
DETAILS OF DECK AND LAUNCH TRUSS
FRAMING AT DIFFERENT LEVELS

Fig.2

A build up of marine growth on any structure produces an increase in mass without any significant change in stiffness. This causes a reduction in natural frequency. Additionally an increase in geometric dimension due to marine growth results in corresponding increase in added mass. As an excessive marine growth could be expected in tropical waters, marine growth distribution as given in CIRIA report [5] was assumed. This assumes for example a growth of 0.300 m at the interface. Effect of this additional mass was included in the model as lumped mass and added mass arising from the changed dimension in all cases of analysis of platform with marine growth.

2.3 Final model and details of computation

The final model used for the analysis had 253 nodes, 373 beam elements, 88 boundary elements representing lateral restraints of the piles, 24 different sections, lumped mass data representing deck mass and added mass of submerged members. Structural Analysis Program SAP IV was utilized for dynamic analysis of this problem.

Total number of linear simultaneous equations to be solved for the eigenvalue problem was 990 and the CPU time required for the solution of 10 eigenvalues was 20 min. and 12.5 min. for 5 eigenvalues on an IBM 370. This naturally involved a lot of computer time and hence majority of the problem analysed was for 5 eigenvalues.

2.4 Parametric study

Dynamic response and modal parameters of an offshore platform are dependent on different factors. From the reported results of a detailed study by ABS [6], the following parameters were identified for parametric study.

i) Deck mass, a change of ± 5 and $\pm$ 10 percent.

ii) Foundation change in top layer springs to simulate scour or soil build up. A combination of scour and build up at different legs was also considered.

iii) Marine growth, an excessive growth is assumed as expected in tropical waters.

iv) Damage in members, complete severance were simulated by reducing all sectional properties to a value 10^{-15}, thus making it ineffective. Simulation of a half-through-cut in a member was achieved by modifying sectional properties to those of a semicircular open section.

In the analysis, initially, the basic structure with 'NO CHANGE' in any of the parameters was analysed. To estimate the individual effects of parameters listed above they were varied and analysis carried out. Finally combined effect of all these parameters including damages in members were analysed in order to identify characteristics which could be used for monitoring structural integrity. Members damaged in the analyses were selected depending on its location as well as redundancy.

2.5 Results and Discussions

The results obtained in each analysis were natural frequencies, for different modes and modal vectors in all the 6 degrees of freedom representing the shapes of each mode. Because of certain limitations a few important results alone are presented here. These results presented here are representative and explain the general behaviour and the trend.

The following results are presented.

Change in natural frequencies for different conditions including structural damages

in Tables 1, 2 and 3.

Translation perpendicular to the predominant modal direction for various cases in Tables 4, 5 and 6.

Ratios of modal vectors in two perpendicular direction in Table 7.

Changes in mode shapes in Figs.3,4,5,6,7,8,9 and 10.

2.5.1 Natural frequency and structural damage

There are a few important conclusions that could be derived from the results in Tables 1, 2 and 3. Missing diagonal members which are shear connectors change the natural frequencies of the platform depending on their location and their contribution to the overall stiffness of the structure, e.g. a missing member 224 introduces a change of 2.7 percent in the II mode whereas a missing 290 or even a half through cut in 290, the change is 15.4 in the IV mode. Another striking feature is the nonuniformity in the change in natural frequencies unlike in the case of a change that affects the structure as a whole, e.g. marine growth or a change in deck mass. For instance, a complete severance of a very important diagonal member 290 does not affect the frequencies of modes II, VIII and IX whereas the change is 15.4 percent for the IV mode. In other words a missing member changes the modal characteristics of those modes for which it is of importance. As expected severance of horizontal level members which do not substantially contribute to the lateral stiffness of the structure, had no effect on the natural frequencies. This is illustrated by the results for missing members 190, 250, 258 and 249. When combined situations are considered, an excessive marine growth masks completely the marginal changes in frequencies even due to complete severance of important members. However, the non-uniformity of changes in different modes are still maintained. Thus integrity monitoring based on frequecy shift alone, becomes impractical on platforms where there are excessive marine growth unless the severed member is very important like member 290 when the change in frequency in the IV mode is considerably larger than the rest.

2.5.2 Mode shapes for various situations

Results presented in Figs.3 to 10 show changes in mode shapes for different situations for the most affected main leg. Change in deck mass, scour or soil build up do not change the mode shape considerably and what is more important is that the basic form of the mode is maintained with very minor changes, while an excessive marine growth shifts the modes to a large extend despite the retention of the basic shape of the mode. All these indicate that these changes are general to the structure and affects the overall dynamic behaviour. This is in sharp contrast to the changes in mode shapes where damages are present. The results presented are mainly for load bearing members. No drastic change in predominant mode shape was expected with failure in redundant members. The table below shows a comparitive study of change in the mode shape vector in the predominant modal direction for the most affected mode for certain missing members.

Member	Node No.	Percent change	
		I Flexural mode	II Flexural mode
146	57	9.9	4.9
179	62	6.5	17.4
224	77	9.6	86.1
226	81	53.5	99.2
228	81	22.3	54.2
290	99	99.8	99.0

Description	Frequencies in Hz for Mode No									
	I	II	III	IV	V	VI	VII	VIII	IX	X
No change	0.5597	0.6131	0.8304	1.119	1.245	1.332	1.485	1.655	1.751	2.068
Deck Mass + 5 percent	0.5465 (-2.4)	0.6049 (-1.3)	0.8175 (-1.6)	1.106 (-1.2)	1.229 (-1.3)					
Deck Mass + 10 percent	0.5367 (-4.1)	0.5971 (-2.6)	0.8063 (-2.9)	1.095 (-2.2)	1.213 (-2.6)					
Marine Growth	0.5105 (-8.8)	0.5189 (15.4)	0.7193 (-13.4)	1.003 (-10.4)	1.094 (-12.1)					
2 m scour on all legs	0.5584 (-0.23)	0.6082 (-0.08)	0.8249 (-0.7)	1.101 (-1.6)	1.224 (-1.7)	1.228 (-3.3)	1.472 (-0.9)	1.619 (-2.2)	1.749 (-0.6)	2.046 (-1.1)
Marine growth &+5 per cent DM	0.5026 (-10.2)	0.5137 (-16.21)	0.7101 (-14.5)	0.9880 (-11.7)	1.091 (-12.4)					
Marine growth & 2 m scour	0.5070 (-9.4)	0.5149 (-16.0)	0.7115 (-14.3)	0.9897 (-11.6)	1.059 (-14.9)					
Marine growth, 2 m scour & +5 percent deck mass	0.5001 (-10.7)	0.5091 (-17.0)	0.7026 (-15.4)	0.9752 (-12.9)	1.056 (-15.2)					
Marine growth & Diff. support	0.5098 (-8.9)	0.5182 (-15.5)	0.7223 (-13.0)	1.007 (-10.0)	1.077 (13.5)					

TABLE 1 Change in natural frequencies for changes other than damages

Values in bracket give percent change

Description	Frequencies in Hz for Mode No.									
	I	II	III	IV	V	VI	VII	VIII	IX	X
No change	0.5597	0.6131	0.8304	1.119	1.245	1.332	1.485	1.655	1.751	2.068
Missing member 179	0.5596 (0)	0.6131 (0)	0.7938 (-4.4)	1.100 (-1.7)	1.245 (0)					
Missing member 224	0.5459 (-2.5)	0.5963 (-2.7)	0.8293 (-0.1)	1.100 (-1.7)	1.222 (-1.9)	1.319 (-1.0)	1.485 (0)	1.653 (-0.1)	1.746 (-0.3)	2.036 (-1.6)
Missing member 228	0.5516 (-1.5)	0.5904 (-3.7)	0.8223 (-1.0)	1.119 (0)	1.218 (-2.2)	1.314 (-1.35)	1.485 (0)	1.655 (0)	1.746 (-0.3)	2.040 (-1.4)
Half through out in 290	0.5438 (-2.8)	0.6124 (-0.1)	0.7949 (-4.3)	0.9467 (-15.4)	1.195 (-4.0)					
Missing member 290	0.5438 (-2.8)	0.6124 (-0.1)	0.7944 (-4.3)	0.9463 (-15.4)	1.188 (-4.6)	1.260 (-5.4)	1.481 (-0.3)	1.655 (0)	1.751 (0)	2.040 (-1.4)
Missing member 190	0.5597 (0)	0.6131 (0)	0.8304 (0)	1.119 (0)	1.245 (0)					
Missing member 250	0.5594 (0)	0.6131 (0)	0.8304 (0)	1.119 (0)	1.245 (0)	1.332 (0)	1.484 (0)	1.655 (0)	1.750 (0)	2.067 (0)
Missing member 258	0.5587 (0)	0.6131 (0)	0.8300 (0)	1.118 (0)	1.245 (0)	1.332 (0)	1.484 (0)	1.655 (0)	1.750 (0)	1.990 (0)
Missing member 249	0.5594 (0)	0.6131 (0)	0.8304 (0)	1.119 (0)	1.245 (0)	1.332 (0)	1.485 (0)	1.655 (0)	1.750 (0)	2.067 (0)

TABLE 2 Change in natural frequencies and structural damages
Values in bracket give percent change

Description	Frequencies in Hz for Mode No.									
	I	II	III	IV	V	VI	VII	VIII	IX	X
No change	0.5597	0.6131	0.8304	1.119	1.245	1.332	1.485	1.655	1.751	2.068
Half through out in 290 & Deck mass + 5%	0.5322 (-4.9)	0.6131 (0)	0.7860 (-5.4)	0.9341 (-16.5)	1.185 (-4.8)					
Marine growth & missing member 290	0.4829 (-13.7)	0.5163 (-15.8)	0.6967 (-16.1)	0.8493 (-24.1)	1.011 (-18.8)					
-do- & Deck mass + 5%	0.4766 (-14.9)	0.5121 (-16.5)	0.6866 (-17.3)	0.8421 (-24.8)	1.000 (-19.7)					
Marine growth, scour and missing member 290	0.4793 (-14.36)	0.5108 (-16.7)	0.6902 (-16.9)	0.8355 (-25.3)	0.9931 (-20.2)					
Marine growth, soil buildup & missing member 290	0.4853 (-13.3)	0.5200 (-15.2)	0.7010 (-15.6)	0.8585 (-23.3)	1.025 (-17.7)					
Missing member 228 & Deck mass + 10 percent	0.5290 (-5.5)	0.5757 (-6.1)	0.7591 (-8.6)	1.096 (-2.1)	1.186 (-4.7)	1.307 (-1.9)	1.436 (-3.3)	1.613 (-2.5)	1.671 (-4.6)	1.990 (-3.8)
Missing member 228, marine growth & soil buildup	0.4888 (-12.7)	0.5126 (-16.4)	0.7076 (-14.8)	1.011 (-9.7)	1.072 (-13.9)					
Missing member 228, marine growth & deck mass +5%	0.4818 (-13.9)	0.5028 (-18.0)	0.6947 (-16.3)	0.9874 (-11.8)	1.051 (-15.6)					

TABLE 3 Change in natural frequencies for combined situation
Values in bracket give percent change.

Node No.	Missing member			
	Nil	146	224	228
15	-0.085	2.59	2.35	2.81
33	-0.19	2.62	2.17	2.82
42	-0.206	2.55	2.04	2.71
46	0.287	1.89	2.26	1.99
51	0.369	1.80	2.28	1.87
57	0.353	1.71	2.00	1.71
66	0.170	0.76	1.58	1.76
81	0.087	0.53	1.09	1.61
99	-0.087	0.47	0.50	0.57
122	0.093	0.28	0.16	0.32
132	-0.050	0.14	0.07	0.16

TABLE 4 x-Translations of first flexural mode in y direction for different conditions

Node No.	Missing member			
	Nil	146	224	228
15	2.043	-0.31	4.636	-0.91
33	1.872	-0.22	4.259	-0.85
42	1.645	-0.29	3.731	-0.73
46	1.262	-0.19	2.802	-0.49
51	1.201	-0.18	2.647	-0.45
57	0.978	-0.16	2.043	-0.25
66	0.749	-0.29	1.501	-0.13
81	0.636	-0.21	1.138	0.04
99	0.377	-0.21	0.817	-0.17
122	0.121	-0.08	0.300	-0.09
132	0.049	-0.03	0.124	-0.04

TABLE 5 x-Translations of first flexural mode in y-direction for different conditions

Node No.	No change	Deck mass +10%	Marine Growth	Missing member 228	Deck mass 10% and missing member 228	Marine growth, deck mass +10% & missing member 228
15	-0.085	-0.25	3.60	2.81	2.394	2.21
33	-0.190	-0.34	3.38	2.82	2.416	2.04
42	-0.206	-0.35	3.18	2.71	2.238	1.91
46	0.287	0.15	3.11	1.99	1.653	2.01
51	0.369	0.24	3.09	1.87	1.540	2.02
57	0.353	0.24	2.66	1.71	1.414	1.750
66	0.170	0.08	2.12	1.76	1.496	1.362
81	0.087	0.03	1.53	1.61	1.384	0.972
99	-0.087	-0.12	0.87	0.57	0.469	0.503
122	0.093	-0.11	0.42	0.32	0.268	0.239
132	-0.05	-0.05	0.20	0.16	0.136	0.112

TABLE 6 X-Translation of first flexural mode in Y-direction

Node No	No change			Missing member 250		
	x	y	y/x	x	y	y/x
4	3.75	7.5	2.0	3.75	7.53	2.01
22	3.13	5.86	1.87	3.11	5.89	1.89
39	2.18	3.51	1.61	2.18	3.53	1.62
45	0.16	-0.06	-0.37	0.15	0.09	0.60
50	-0.17	-0.40	2.35	-0.18	-0.38	2.11
56	-0.17	-0.98	5.76	-0.19	-0.96	5.05
64	0.32	-0.76	2.37	0.29	-0.74	2.55
79	0.75	-0.45	0.60	0.71	-0.44	0.62
96	0.89	-0.72	0.81	0.84	0.35	0.41
116	0.78	0.04	0.06	0.73	0.13	0.179
130	0.39	0.07	0.173	0.37	0.07	0.19

TABLE 7 Ratio of y to x-Translation of X mode for missing member 250

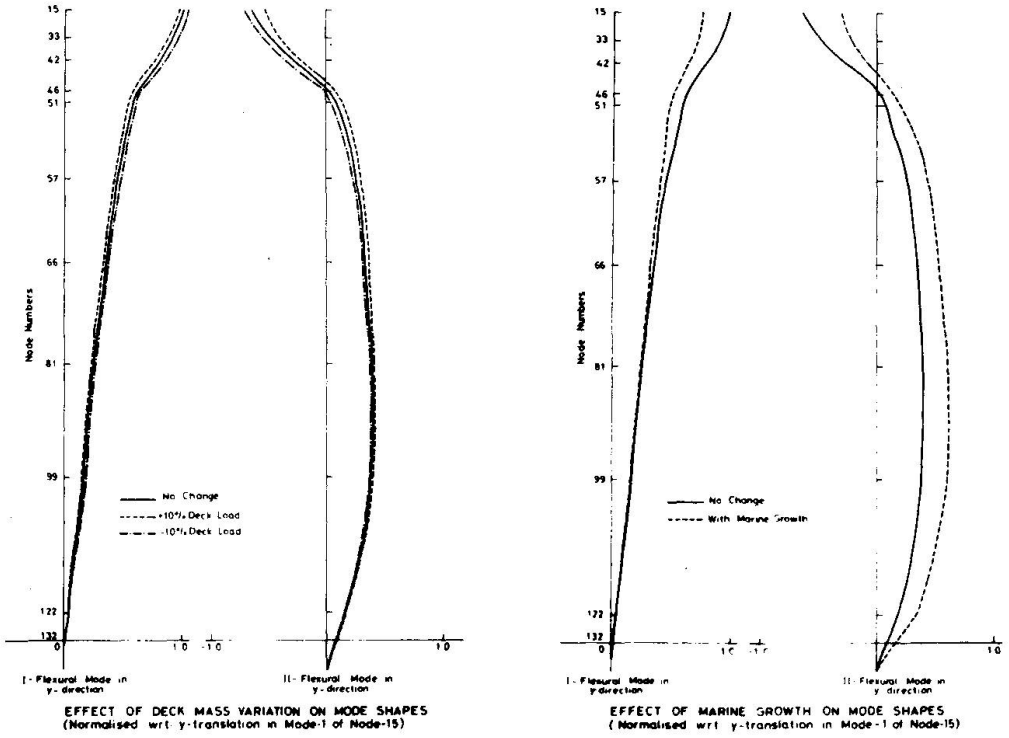
Node Numbers
No Change
+10% Deck Load
-10% Deck Load
I- Flexural Mode in y-direction
II- Flexural Mode in y-direction
EFFECT OF DECK MASS VARIATION ON MODE SHAPES (Normalised wrt y-translation in Mode-1 of Node-15)
No Change
With Marine Growth
EFFECT OF MARINE GROWTH ON MODE SHAPES (Normalised wrt y-translation in Mode-1 of Node-15)

Fig.3

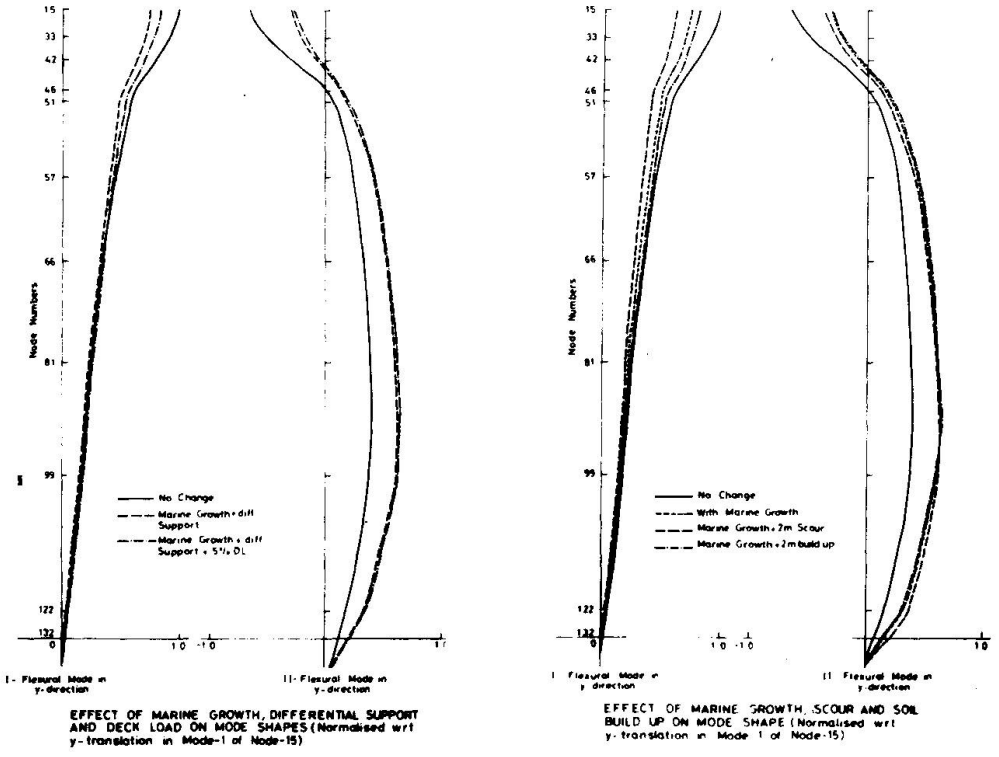
Node Numbers
No Change
Marine Growth + diff Support
Marine Growth + diff Support + 5% DL
I- Flexural Mode in y-direction
II- Flexural Mode in y-direction
EFFECT OF MARINE GROWTH, DIFFERENTIAL SUPPORT AND DECK LOAD ON MODE SHAPES (Normalised wrt y-translation in Mode-1 of Node-15)
No Change
With Marine Growth
Marine Growth + 2m Scour
Marine Growth + 2m build up
EFFECT OF MARINE GROWTH, SCOUR AND SOIL BUILD UP ON MODE SHAPE (Normalised wrt y-translation in Mode 1 of Node-15)

Fig.4

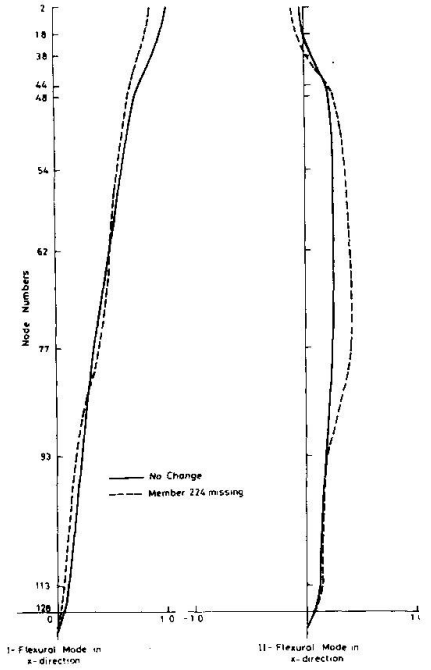

EFFECT OF DAMAGE ON MODE SHAPES
(Normalised wrt. x-translation in Mode-1 of Node-2 undamaged)

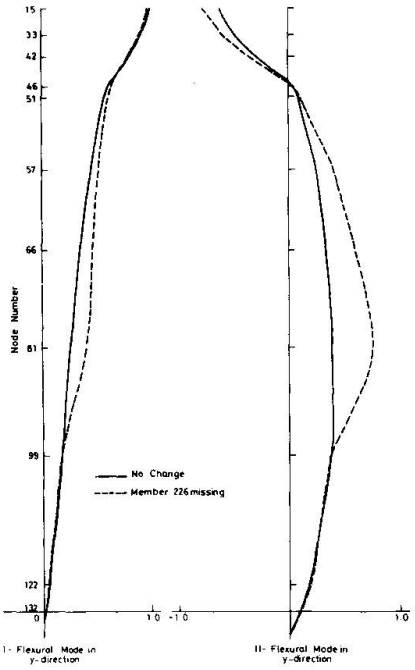

EFFECT OF DAMAGE ON MODE SHAPES
(Normalised wrt. y-translation in Mode-1 of Node-15 undamaged)

Fig.5

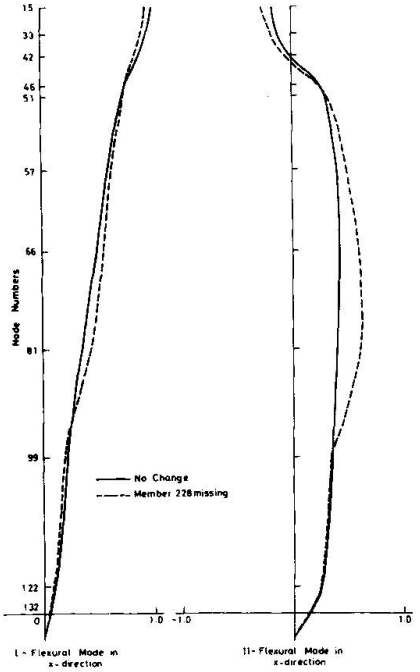

EFFECT OF DAMAGE ON MODE SHAPES
(Normalised wrt. x-translation in Mode-1 of Node-15 undamaged)

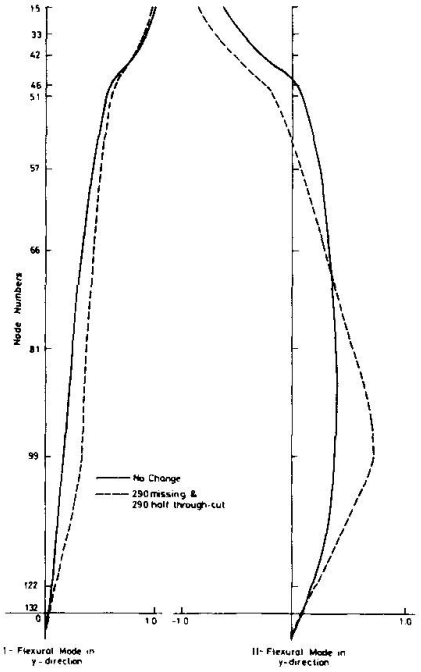

EFFECT OF DAMAGE ON MODE SHAPE
(Normalised wrt y-translation in Mode-1 of Node-15, undamaged)

Fig.6

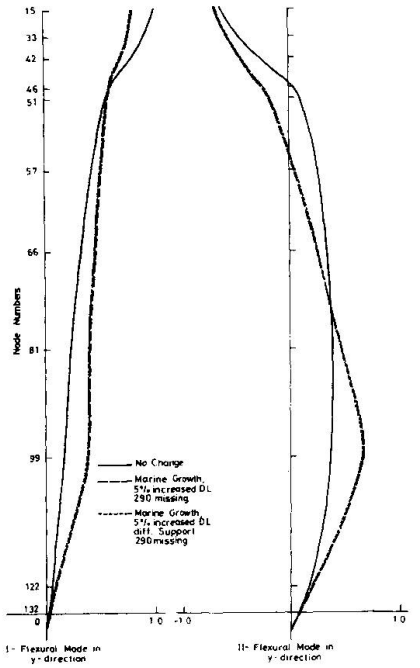

COMBINED EFFECT OF MARINE GROWTH, DIFFERENTIAL SOIL SUPPORTS, INCREASED DECK LOAD ON MODE SHAPES (Normalised w r t y-translation in Mode-1 of Node-15, undamaged)

Fig.7

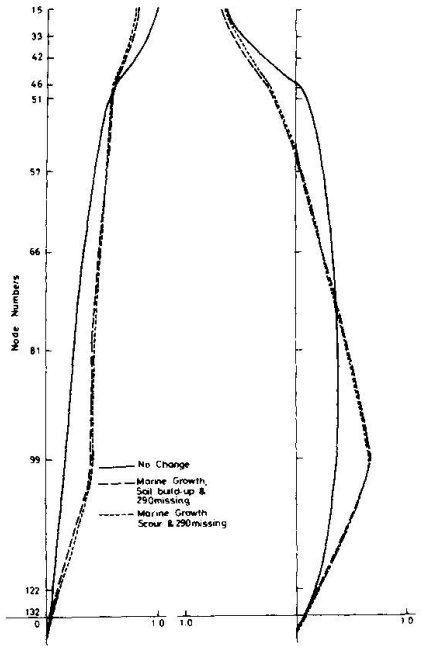

COMBINED EFFECT OF MARINE GROWTH, SOIL BUILD-UP, SCOUR AND DAMAGE ON MODE SHAPES (Normalised wrt y-translation in Mode-1 of Node-15, undamaged)

Fig.8

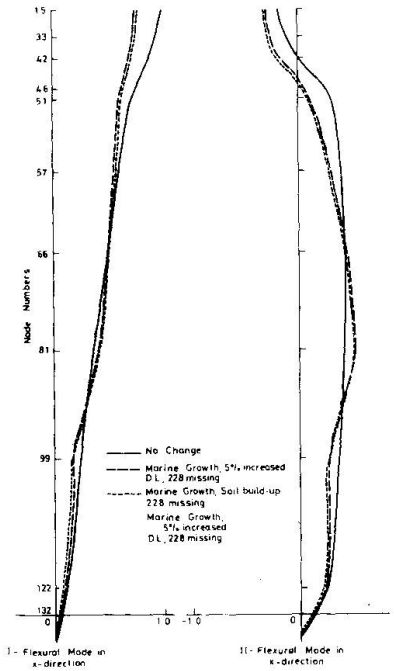

COMBINED EFFECT OF MARINE GROWTH, PILE SPRING, DECK LOAD, SOIL BUILD-UP & DAMAGE ON MODE SHAPES (Normalised w r t x-translation in Mode 1 of Node 15, undamaged)

Fig.9

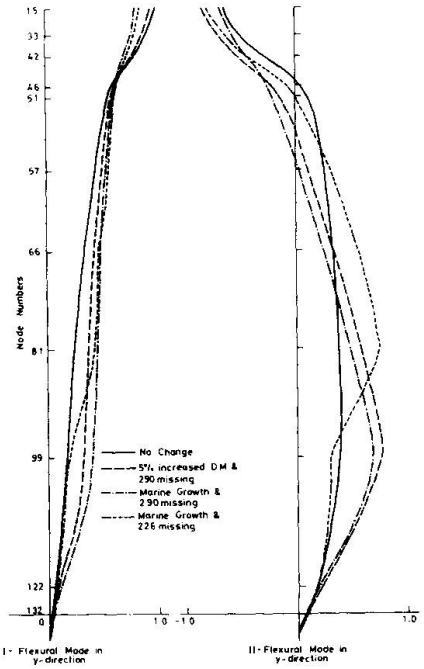

COMBINED EFFECT OF CHANGE IN DECK LOAD, DAMAGE AND MARINE GROWTH ON MODE SHAPES (Normalised wrt y-translation in Mode-1 of Node-15, undamaged)

Fig.10

The failure of 146 and 179 does not change the mode shape drastically because 146 is located close to the free end of the structure and 179 though located at the third level has two additional members close by belonging to the launch truss making it redundant.

The figures giving the combined effect of different situation on mode shape clearly indicate that they are more or less same as if the damage alone were present. Thus changes in any of the parameter were taken together with damages in members, the mode shapes remain unaltered and are same as though damages alone were present. Or in other words, changes in mode shape due to damages cannot be masked by changes in any other parameter affecting dynamic response.

2.5.3 Change in modal vector perpendicular to predominant modal direction

In the search for factors that are maximum affected by damages in members, it has been found that modal vector perpendicular to the predominant modal direction is a very sensitive factor which can be of use in monitoring. Tables 4-7 present these results. The tables are self explanatory. The changes are very drastic; in one case it is almost 33 times the value for undamaged situation. Even when there are changes in other parameters this translation remains to be very much different from the no change situation.

It is also seen that these results can provide clues for the condition of highly redundant horizontal level members. One typical result alone is presented here. The ratios of x to y translation of X mode are presented for nodes in one of the legs for missing member 250. The value of this ratio changes from 0.81 to 0.41 and 0.06 to 0.179 for the most affected nodes. It may be noted that these changes are seen only at higher modes and hence the real significance of this effect will depend very much on the capability of the measuring system to measure the translations at higher modes. If the results of measurements already reported are any indication, this must be possible with the usual methods of measurements.

3. EXPERIMENTAL INVESTIGATION

Experimental investigations were found necessary to verify the observations of the analyses as well as to prove the measurement procedure to be adopted to obtain the required information. For this limited objective, tests on a geometrically similar model, an analysis of the same with SAP IV and a comparison of both the results obtained would be sufficient. Moreover, it is almost impossible to design and test an elastic model of a jacket with available material and testing methods. The linear scale of the model was decided to be 1:35 based on the 2.5 m depth of water in the flume available. The model was made out of PVC tubes and the fundamental period of the model with deck load was nearly 4 Hz when fixed in water.

3.1 Test program

Though the model was planned to be tested in a flume under wave loading, considering the water depth in the flume and the difficulties in simulating damages in members as well as joining them back for further damages in other members, it was decided to restrict the number of experiments to be done in the flume to a minimum and to carry out the tests involving damages in more members in air by exciting the model with an electrodynamic excitor. In this case, any way, the results necessary were not dependent on the nature of excitation. As a result, tests were conducted for 5 damage situations in air and for 2 in the wave flume. In both these tests, the deck mass alone was varied because in the analysis, it was very clear that change in mass either in the deck or distributed on the structure was contributing maximum to the uncertainity in interpreting the data.

The physical model was excited with the help of an electrodynamic excitor. 6 accelerometers were used to measure the response at all the nodes of one of the main legs. 5 strain gauges were also fixed at these nodes. Accelerometer output was analysed in frequency domain with the help of FFT analyser to get

the auto power spectrum of the response and the strain gauge data wasrecorded on a strip chart recorder. Results obtained were natural frequencies and amplitudes from FFT analyses and strains at the nodes. Experiments were also conducted in a flume under wave loading. Two views of the experimental set-up are shown in Figs.11 and 12.

3.2 Dynamic Analysis of the Model

As in the case of the well platform a finite element equivalent of the physical model was formulated for dynamic analysis using SAP IV. The principles governing the modelling was exactly same as those for the well platform. There were 74 nodes and 170 beam elements for the model which was assumed to be fixed at eight points, representing the four main legs and four skirt legs. Damages were simulated in the same way as in the case of the well platform. Figs. 13 and 14 show the FE model of the Physical model.

3.3 Results and discussions

The results obtained in the analysis and the experiments are presented in Tables 8, 9 and 10 and Figs.15 to 22 for various cases. The informations on frequencies as well as mode shape vectors clearly indicate the close agreement between the analytical and experimental results. Though there are differences in the exact magnitude of the frequency values by around 10 percent, the shift dueto damage in members are in good agreement. Strains in members were however, not obtained analytically and as a result, only results of measurements alone are presented. For the limited objectives already explained in the beginning of the chapter, the experimental results validate the behaviour predicted by analysis and also proves the adequacy of measurements for determining the required informations.

4. A SCHEME FOR INTEGRITY MONITORING OF FIXED OFFSHORE PLATFORMS

The results of the analytical and experimental investigation clearly indicate that Integrity Monitoring based on dynamic response can be viable, if it is carried out with a lot of care at every stage. Though it is desirable to restrict the measurements to deck alone, the results show that mode shape information which involves under water measurements will be necessary not only to establish the integrity but to locate the damages, if any, as it is evident from the figures that the mode shape deviates from the original near the vicinity of the damage. The scheme proposed below for integrity monitoring has obviously two stages, viz., analytical as well as field measurements on platform.

4.1 Analysis of the platform

A detailed three dimensional analysis of the platform is naturally the first step in this operation and this should be available before any measurements are taken. For the purpose of the analysis, a well proven general purpose structural analysis program can be made use of. As far as possible, complete structural and all hydrodynamic aspects of a partially submerged structure should be represented in the analytical model. The representation of the lateral restraints of pile should be based on the soil investigation data of the site. Once the model is ready, a parametric study can be carried out and the results of this study would later prove useful when actual measurements are undertaken. Natural frequencies, mode shapes of at least 10 modes and informations on modal vectors in all six degrees of freedom for all the modes are the results required at the end of this first stage of integrity monitoring.

4.2 Measurements on platform

Recording of acceleration response simultaneously at diagonally opposite legs and spectral analysis of this data forms the next stage. Biaxial accelerometers are advisable, as it was seen in analysis that the data of translation perpendicular

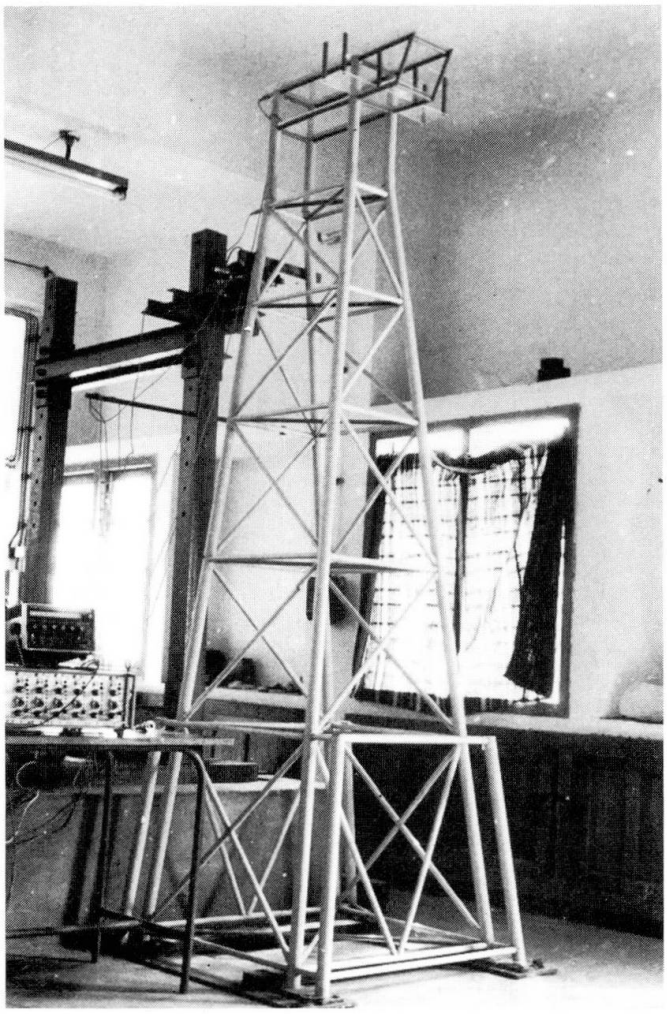

Fig.11
Model under external excitation

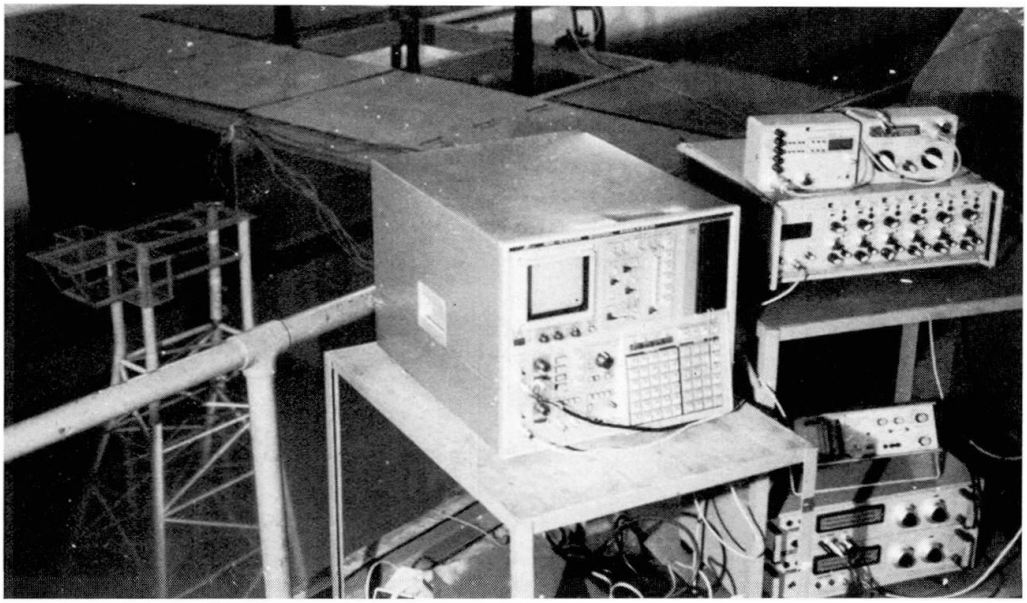

Fig.12 : Model fixed in wave flume for wave loading

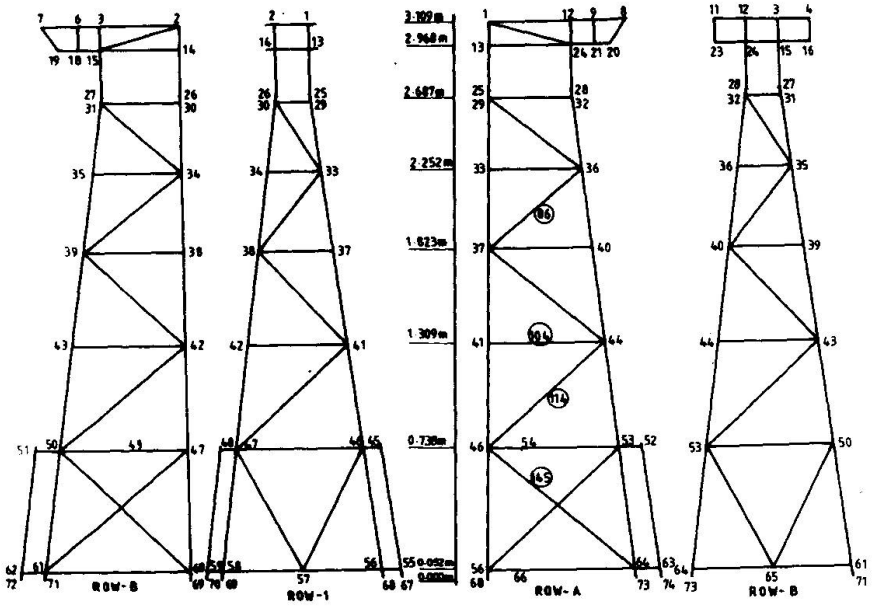

FIG. VERTICAL FRAMING OF JACKET MODEL

Fig.13

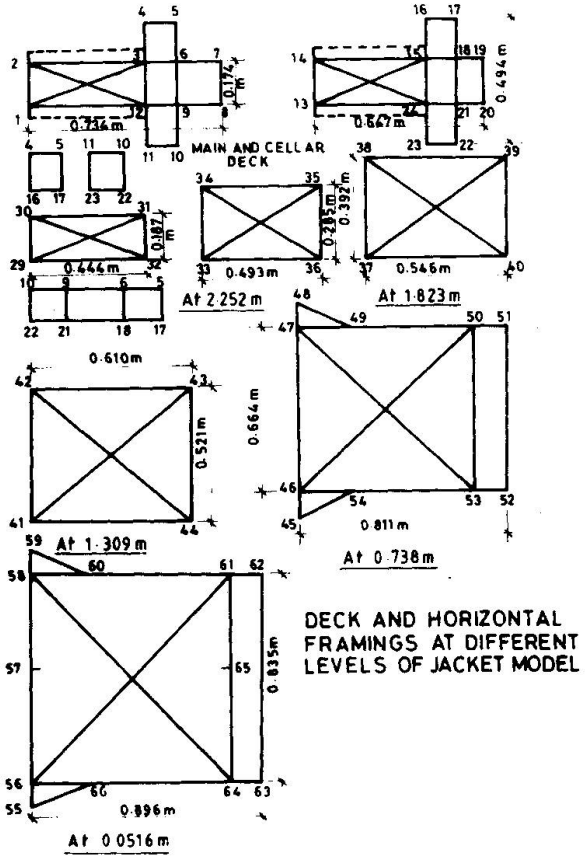

DECK AND HORIZONTAL FRAMINGS AT DIFFERENT LEVELS OF JACKET MODEL

Fig.14

Deck Load	Description of Model	Analysis		Experiment	
		I Flexure	II Flexure	I Flexure	II Flexure
M	No damage	5.727	30.59	5.15	27.5
M	Half through cut 114	5.704 (0)	29.71 (-2.9)	5.15 (0)	26.5 (-3.6)
M	Missing member 114	5.556 (-3.0)	24.13 (-21.1)	4.9 (-4.9)	21.0 (-23.6)
M	Missing member 145	5.708 (0)	29.53 (-3.5)	5.10 (0)	26.2 (-4.7)
M	Missing member 86	5.576 (-2.6)	30.22 (-1.2)	5.05 (-.19)	27.0 (-1.8)
M	Missing Member 104	5.727 (0)	30.57 (0)	5.15 (0)	27.5 (0)
M+10%	No damage	5.457 (-4.7)	30.43 (0)	4.95 (-4.9)	27.0 (-1.8)
M+10%	Half through cut 114	5.438 (-5.1)	29.58 (-3.3)	4.9 (-4.9)	26.0 (-5.5)
M+10%	Missing member 114	5.297 (-7.5)	24.08 (-21.3)	4.65 (-9.7)	20.5 (-25.5)
M+10%	Missing member 145	5.443 (-5.0)	29.46 (-3.7)	4.85 (-5.8)	25.8 (-6.2)
M+10%	Missing member 86	5.334 (-6.9)	30.03 (-1.8)	4.90 (-4.9)	26.5 (-3.6)
M+10%	Missing member 104	5.457 (-4.7)	30.40 (0)	4.95 (-3.9)	27.0 (-1.8)
M-10%	No damage	6.044 (5.5)	30.78 (0)	5.5 (4.9)	27.0 (1.8)
M-10%	Half through cut 114	5.855 (2.2)	29.88 (-2.3)	5.22 (1.4)	27.0 (-1.8)
M-10%	Missing member 114	6.019 (5.1)	24.27 (-20.7)	5.40 (4.9)	21.25 (-22.7)
M-10%	Missing member 145	6.024 (5.2)	29.69 (-2.9)	5.38 (4.5)	26.0 (-5.5)
M-10%	Missing member 86	5.903 (3.1)	30.40 (0)	5.30 (2.9)	27.0 (-1.8)
M-10%	Missing member 104	6.044 (5.5)	30.75 (0)	5.40 (4.9)	27.0 (-1.8)

TABLE 8 Natural frequencies in Hz of Model - Comparison of results
Values in bracket give percent change

Mode	Node No	No change		Half through cut in 114		Missing member 114		Missing member 86		Missing member 145	
		SAP IV	Expt	SAP IV	Expt	SAP IV	Expt	SAP IV	EXpt	SAP IV	Ex pt
I Flexure in X-direction	1	403.04	385.68	77.58	86.91	9.36	7.38	8.34	8.78	232.5	256.90
	29	541.11	528.90	82.02	71.33	10.41	8.52	9.22	10.59	123.0	150.82
	33	39.67	51.76	118.07	105.24	11.13	9.78	12.76	13.88	91.25	98.53
	37	627.5	659.83	43.83	36.78	7.51	6.35	21.36	20.56	37.29	46.59
	41	7.56	5.85	11.54	10.50	12.74	14.61	9.85	7.38	12.33	14.55
	46	47.0	47.80		18356.0	9.75	9.33	45.0	42.1	15.75	18.78
II Flexure in X-direction	1	81.33	72.52	13.72	12.53	3.02	2.98	11.86	10.53	22.0	25.03
	29	174.11	195.31	12.03	9.80	2.614	1.88	11.28	8.73	42.8	39.85
	33	75.68	85.66	12.09	11.88	2.84	2.57	16.86	15.88	345.6	402.85
	37	31.54	32.59	13.56	11.77	3.18	2.92	28.30	25.78		14678.5
	41	10.18	9.80	29.43	30.53	3.94	3.24	8.40	7.53	320.5	356.8
	46	17.00	13.59	47.60	50.86	2.47	2.52	12.33	9.79	14.77	16.88

TABLE 9 Ratio x to y translations of I & II mode of model - Comparison of results

Mode	No change				Missing Member 86				Missing Member 114			
	10 kg deck load		12 kg DL		10 kg DL		12 kg DL		10 kg DL		12 kg DL	
	SAP IV	Expt	SAP IV	Expt	SAP IV	Expt	SAP IV	Ex pt	SAP IV	Expt	SAP IV	Expt
I Flexure in X-direction	4.94	4.25	4.66 (-5.67)	3.95 (-7.1)	4.79 (-3.02)	4.1 (-3.5)	4.52 (-8.46)	3.87 (-8.9)	4.66 (-5.63)	4.02 (-5.4)	4.42 (-10.52)	3.79 (-10.8)
II Flexure in X-direction	13.91	11.55	13.78 (0)	11.5 (0)	13.87 (0)	11.3 (-2.2)	13.74 (-1.2)	11.2 (-2.6)	10.62 (-23.7)	8.5 (26.4)	10.47 (-24.73)	8.5 (-26.4)

TABLE 10 Natural frequencies in Hz of model fixed in water - Comparison of results

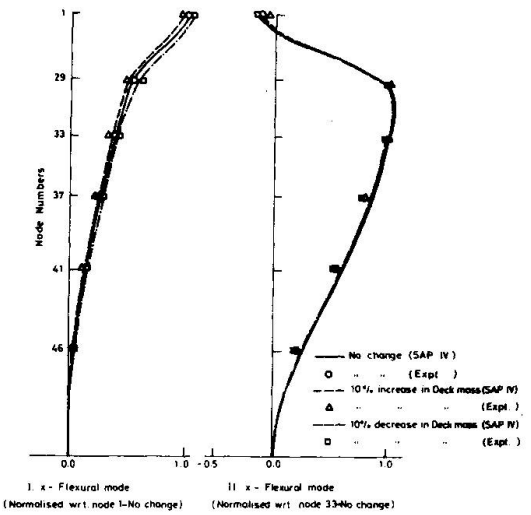

MODE SHAPES - EFFECT OF DECK LOAD VARIATION

Fig.15

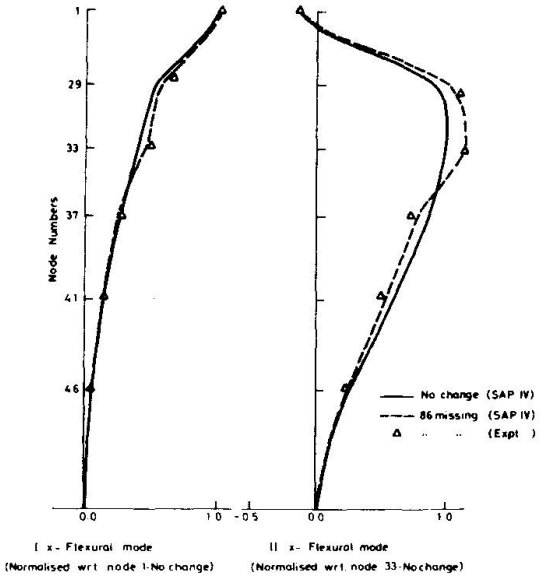

MODE SHAPES - EFFECT OF DAMAGE IN MODEL

Fig.16

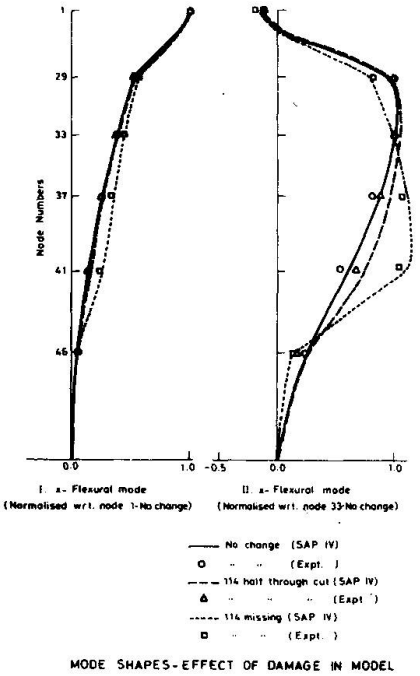

MODE SHAPES - EFFECT OF DAMAGE IN MODEL

Fig.17

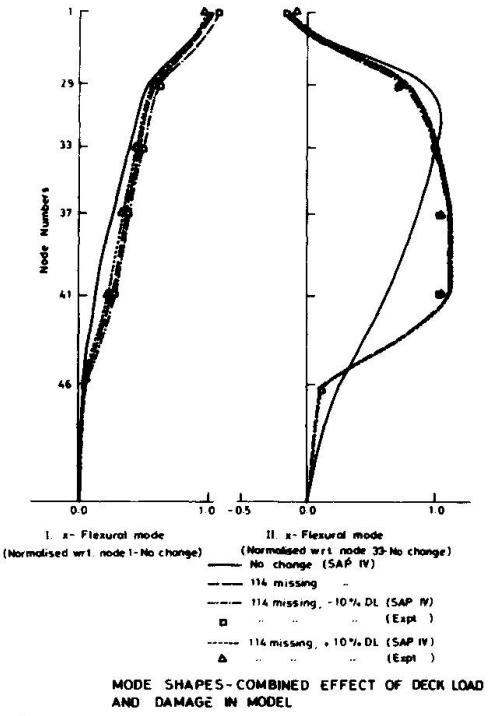

MODE SHAPES - COMBINED EFFECT OF DECK LOAD AND DAMAGE IN MODEL

Fig.18

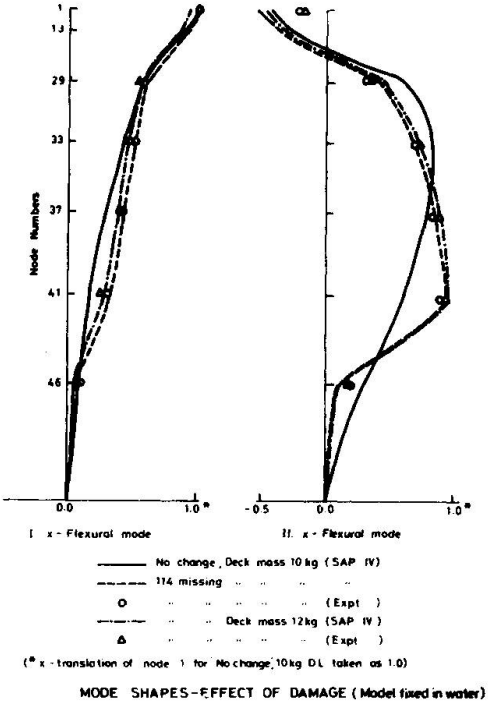

Fig.19

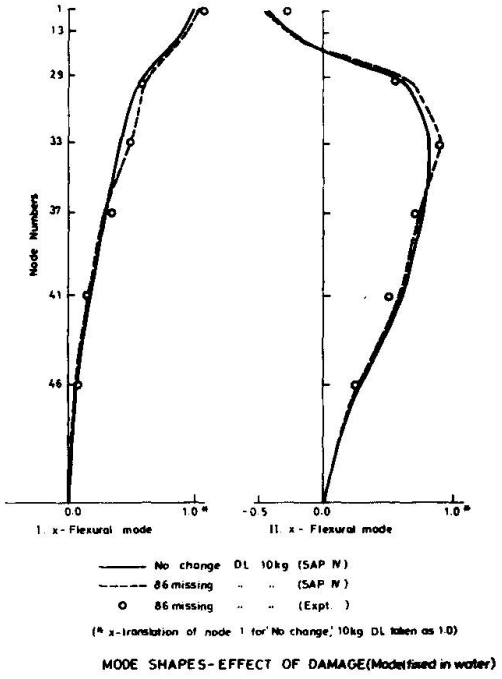

Fig.20

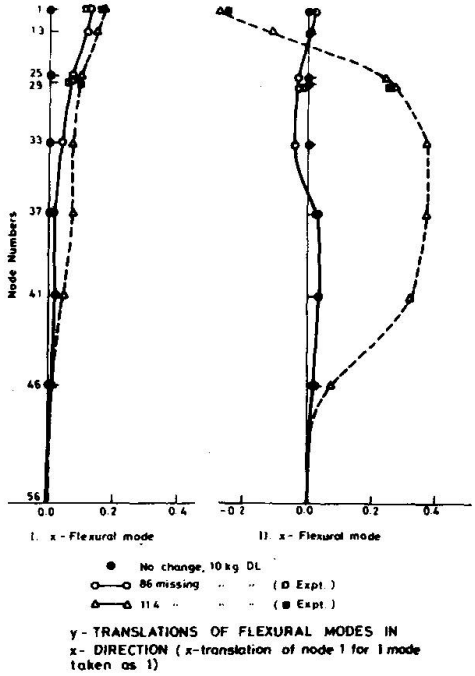

Fig.21

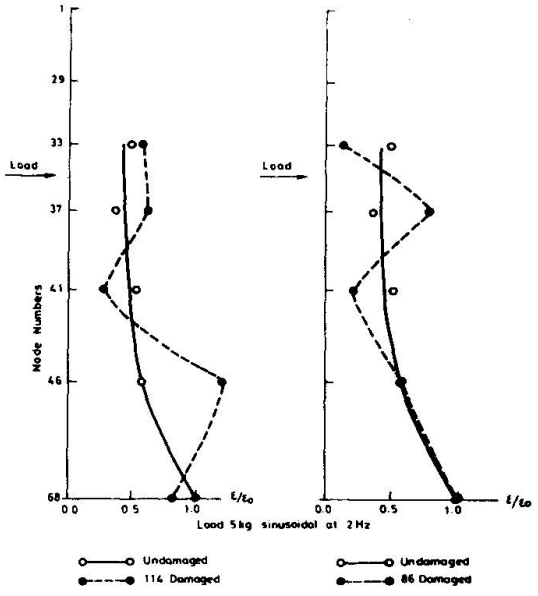

Fig.22

to predominant modal direction can provide very valuable informations with regard to the integrity of the structure. The data from the accelerometers are analysed with the help of a signal analyser having capabilities of auto-spectral analysis of data using FFT or any other proven data processing technique. It is advisable to take this data on all the nodes above water so that identification of modes is possible with the help of phase information. The frequencies thus obtained are compared with those of the analyses and every effort should be made to identify the analytical system which compares well with those of measurement. The next step is the comparison of modal vectors. Modal vectors normalised with some reference points for the predominant modal direction and the direction perpendicular toit should be compared with the theory. If the agreement is good with the identified system, it may not be necessary to venture into any underwater measurements. If the mode shape vectors in different directions are not in agreement, detailed underwater measurement would become necessary. For this purpose too biaxial accelerometers on diagonally opposite legs are to be deployed with the help of divers. If these informations are available (mode shapes) for as many modes as possible, all mode shapes can be plotted and the shape of each can give a good insight into the state of thestructure. As a confirmation, the modal vector perpendicular to the predominant modal direction can also be compared. The main advantage of determining mode shapes with the help of under water mesurement is that, these information can immediately locate the position of damage, if there is any.

4.3 Some additional suggestions

System identification of analytical model with the help of measured data may prove to be the most important phase of this monitoring procedure and perhaps the most difficult. This can however be overcome by taking a complete set of required information on modal characteristics either soon after the installation of the platform or immediatley after a physical inspection by divers. This can form the basis for all future measurements and comparison. If a set of data is available from a healthy platform, it would serve as a signature for comparison for all future measurements.

Temporary deployment of biaxial accelerometers underwater is another difficult phase, and can be criticised as a drawback as in the case of diver inspection. This, however, is not very true because there is a lot of difference between a diver inspecting a structure underwater and installing an instrument for measurements.

At least in the case of new platforms, diver dependence can be overcome, if some accelerometers are installed during the fabrication stage itself. For safety considerations, the most suitable location would be the annular space between the pile and the main leg. Once this area is grouted, the installation will be permanent and development of suitable biaxial accelerometers are well within the reach of the instrumentation industry. Periodic measurements from these accelerometers would be the best indicators of the integrity of the structure and has the potential to replace the physical inspection, if carefully carried out. Though this investigation was carried out with special emphasis on offshore platforms which, except for the deck, is submerged, the method can be easily applied to any tall structure like TV towers, tall chimneys, mooring dolphins, multistoreyed buildings etc. to assess structural deterioration in course of time. A permanent installation to evaluate structural response on these expensive structures can generate valuable data to evaluate the actual factor of safety to help engineers to design economic structures.

5. CONCLUSIONS

Based on a detailed analytical and experimental investigation modal parameters of a well platform has been evaluated and feasibility of its measurement proved.

Simulating various changes in quantities that can affect these parameters, it has been shown that they indicate the integrity of the structure. Based on the investigation, a scheme for integrity monitoring of fixed offshore platforms is proposed which can reduce the frequency of physical inspection, if not completely replace this uneconomical procedure. Of course, these conclusions are based on a laboratory investigation and field measurements on platforms and the capability of the analytical techniques of spectral analysis to determine natural frequencies and magnitudes for mode shape evaluation of as many modes as possible have to be proved to completely exploit the potentialities of this technique. But, if the results available from the reported literature on field measurements on plaform, are any indication, it may not prove to be a very difficult task.

REFERENCE S

1. COPPOLINO, R.N. and RUBIN, S., Detectability of structural failures in offshore platforms by ambient vibration monitoring. Offshore Technology Conference, Texas, 3865, 1980, pp 101-110.

2. RUBIN, S. and COPPOLINO, R.N., Flexibility monitoring of offshore jacket plaforms. OTC, Texas, 4535, 1983, pp 201-208.

3. SHAHRIVAR, F. BOUWKAMP, Damage detection in offshore platforms using vibration information ASME symposium on Offshore Mechanics and Arctic Engineering, 1984, pp 174-185.

4. IDICHANDY, V.G., Integrity monitoring of fixed offshore platforms, Ph.D. Thesis, Indian Institute of Technology, Madras, 1986.

5. HALLAM, M.G., HEAF, N.J. and WOOTTON, L.R., Dynamics of marine structures - Methods of calculating the dynamic response of fixed structures subject to wave and current action, CIRIA Underwater Engineering Group report, UR8 Oct. 1978.

6. WOJNAROWSKI, M.E., STIANSEN, S.G. and REDDY, N.E., Structural Integrity evaluation of a fixed platform using vibration criteria, OTC 2909, Texas, 1977, pp 247-256.

Leere Seite
Blank page
Page vide

Vibrating-Wire Reinforcement Strain Gauges for Performance Monitoring of Large Concrete Structures

Jauge de déformation à corde vibrante et mesures de performance de grandes structures en béton

Dehnungsmessungen am Bewehrungsstahl mit schwingenden Saiten zur Überwachung grosser Betonbauwerke

G. SØRUM
Norwegian Geotechnical Institute

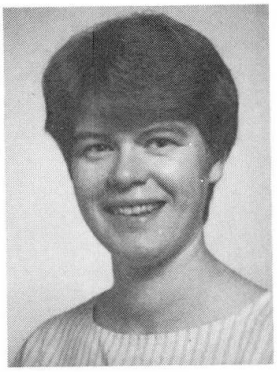

T. DYKEN
Norwegian Contractors

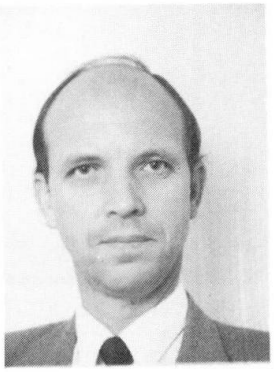

SUMMARY
The Norwegian Geotechnical Institute's vibrating wire reinforcement strain gauge is presented and the performance record of the instrument discussed. Application of the gauge in a wide variety of instrumentation projects is described in order to give an indication of the usefulness of the instrument in performance monitoring. As an example of the data that has been collected with help of the gauge, strain and creep data from Norwegian Contractors' Condeep structures are discussed briefly.

RESUME
Il s'agit de la présentation de la jauge de déformation à corde vibrante de l'Institut Géotechnique de Norvège, et des performances de cet instruement. La description de ses domaines d'application dans de très nombreux projets différents montre son utilité dans les mesures. A titre d'exemple de données recueillies à l'aide de cette jauge, un rapide exposé des données de déformation et fluage des structures Condeep de Norwegian Contractors est presenté.

ZUSAMMENFASSUNG
Die schwingende Saite des Norwegischen Geotechnischen Institutes, montiert auf Armierungsstahl, wird vorgestellt und die Messgenauigkeit des Instrumentes diskutiert. Die Anwendbarkeit des Meßgerätes auf unterschiedliche Instrumentationsprojekte wird beschrieben um die Brauchbarkeit für Kontrollmessungen zu demonstrieren. Als Beispiel für Daten welche mit Hilfe dieses Meßgerätes gesammelt wurden, werden Dehnungs- und Langzeitkriechdaten der Norwegian Contractors' Condeep Plattform kurz diskutiert.

1. INTRODUCTION

Monitoring programs for large concrete structures will generally include instruments for determining strain and/or stress in the concrete. For measurement of strain, there are three basic types of instruments that can be used; surface-mounted strain gauges, embedded strain gauges, or strain gauges attached to the reinforcing steel. The best approach for a given application depends on details of the structure and the specific information that is required.

All three types of strain gauges are used at the Norwegian Geotechnical Institute (NGI). Embedded and surface-mounted gauges are used primarily where it is necessary to determine principal stresses and stress concentrations. The technique of strain-gauging the reinforcing steel is usually preferred when the objective is to monitor the actual loading on the structure. In this case the instrumented reinforcement is located in a part of the structure where the strain measurements can be related to the applied loads. The majority of the projects that NGI has been involved with are of this kind.

In the mid-1960's a vibrating-wire strain gauge for monitoring stress in reinforcing steel was delevoped at NGI. The instrument was orginally designed and used to measure the distribution of axial loads in precast concrete friction piles. Since then the instrument has been used on a great variety of projects, and has been a valuable tool for monitoring the performance of reinforced concrete structures.

The main objectives of this paper are: to describe the NGI vibrating-wire reinforcement strain gauge, to comment on its performance, and to illustrate its use. Selected applications are presented from projects involving different types of concrete structures where it has been beneficial to monitor stress or strain in reinforcing steel as an alternative to the use of surface-mounted or embedded strain gauges.

The paper does not present results of measurements in detail, but typical data is given for most of the examples. One of the examples includes a unique 9-year record of strain measurements in an offshore concrete structure subjected to cyclic loading. Since little is known about the effects of long-term cyclic loading on the creep of concrete, a brief discussion of this data has been included.

2. THE VIBRATING-WIRE REINFORCEMENT STRAIN GAUGE

2.1 Description

Principal features of NGI's reinforcement strain gauge used to monitor axial load or stress/strain in steel reinforcement are shown in Fig. 1. The instrument is basically a small-diameter load cell welded in series with the reinforcing steel, Fig. 1(a).

The sensing element in the load cell is a vibrating-wire strain gauge. The sensor is of the constant vibration type; that is, the gauge-wire oscillates continuously and at constant amplitude as long as the gauge is connected to the external exciter electronics. The change in frequency of the gauge-wire is a measure of the axial strain or stress in the load cell as well as in the

reinforcing steel attached to it.

There are two versions of the reinforcement strain gauge. One has a single vibrating-wire sensing element, Fig. 1(b), and the other has two sensing elements, Fig. 1(c).

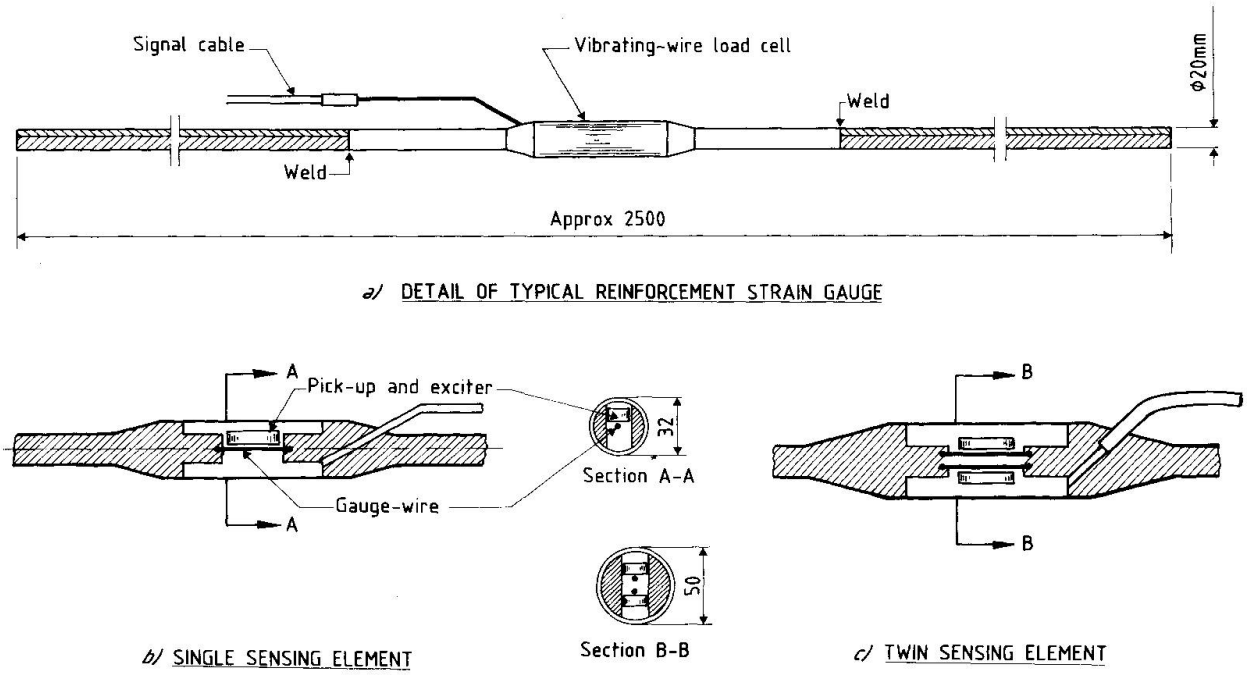

Fig. 1 NGI's vibrating-wire reinforcement strain gauge

The body of the load cell is machined from a single piece of high strength steel. It is dimensioned to have approximately the same cross-sectional area as the renforcing steel. The gauge-wire and magnet system used to excite the gauge-wire and make the frequency measurements are mounted axially in a milled slot in the gauge. For the single sensing element gauge, the axis of the gauge-wire is coincident with the longitudinal axis of the reinforcing steel. For the twin sensing element gauge, two independent gauge-wires and magnet systems are mounted either side of the longitudinal axis of the load cell. Since the load cell is fabricated of a higher strength steel than normal reinforcing steel, it operates within its elastic range even after the reinforcing has started to yield.

The gauge-wire is sealed in a small metal tube and furthermore the entire load cell is sealed with O-rings and an outer thin-walled sleeve so that the entire instrument is completely watertight. Electrical connections are made via a specially designed compression gland.

The outer sleeve separates the body of the load cell from the concrete. Thus it eliminates concrete bond and transfer of shear stresses along the side of the load cell. The sleeve is held in place only by O-ring friction. Transfer of stresses from the concrete to the tapered ends of the load cell is minimized by means of a layer of soft rubber at the interface which separates the gauge from the concrete.

2.2 Advantages

NGI's system design philosophy is to use vibrating-wire type instruments wherever possible for geotechnical and structural field instrumentation applications of a complex nature. Typical conditions for such projects are long cable runs, integration into a complicated construction sequence, construction activities that are potentially hazardous to delicate instruments and system components, the need in some cases to install instruments several years before actual use, and submergence in salt water under relatively high pressure.

The primary reasons for using vibrating-wire type instruments are:

- proven reliability
- proven long-term stability
- mechanical robustness
- frequency output signal (minimal noise problems)
- minimum of electronics within the transducer
- uncomplicated cabling procedures, and
- relative ease of production of small series of instruments

NGI has concentrated on the development and use of reinforcement gauges as opposed to embedded gauges for measuring strain in concrete because measured strains in reinforcement appear to give more consistent results for the types of projects that NGI is involved in. The instrument can be calibrated directly in terms of stress or strain and the modulus of elasticity is constant.

The reinforcement strain gauge is robust and easier to install than embedded gauges. It can be shop-welded to short lengths of reinforcing steel and installed as a "sister bar" with minimum disturbance to other construction operations.

The reinforcement strain gauge with two sensors, Fig. 1(c), makes it possible to discriminate between axial stresses and bending stresses carried by the reinforcement. This can be an important advantage for some applications. If, however, bending stresses are negligible, the second vibrating-wire provides a back-up or redundant sensor.

2.3 Performance record

2.3.1 Accuracy

The accuracy of the vibrating-wire reinforcement strain gauge will depend on the range of measurements that is required, but generally speaking it is better than 1 percent of full scale for non-conformity, hysteresis and repeatibility errors combined.

2.3.2 Temperature sensitivity

The temperature sensitivity of the reinforcement strain gauge depends on the type of steel used to fabricate the instrument since it depends on the difference in the coefficients of thermal expansion between the gauge-wire and the body of the instrument. Typical temperature sensitivity ranges from

0.2 to 0.6 με/°C. The value 0.2 με/°C is typical for the most commonly used instruments.

2.3.3 Dynamic response

The dynamic response of the vibrating-wire strain gauge is suitable enough for most civil engineering applications. The principal limitation lies in the electronic circuitry used to determine the frequency of the output signal and not in the strain gauge itself.

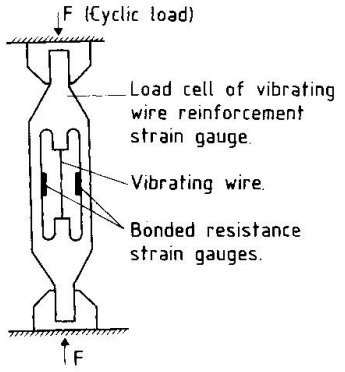

a/ TEST ARRANGEMENT

Frequency of loading Hz	Difference as % of indicated value *
4.0	+0.33
6.7	-0.61
8.3	-1.73
10.0	-1.04

*Difference between measured change in load for vibrating-wire strain gauge compared to resistive gauge, given as a % of the value indicated by the resistive gauge.

b/ TEST RESULTS

Fig. 2 Dynamic response test of reinforcement strain gauge

Satisfactory operation of the vibrating-wire reinforcement strain gauge has been confirmed by controlled tests up to 10 Hz. This was done in 1974 in order to qualify instruments for use on offshore structures. In these tests the dynamic response of the vibrating-wire reinforcement strain gauge and bonded electrical resistance strain gauges were compared using the test specimen shown in Fig. 2(a). The gauges were subjected to cyclic loading in steps up to 10 Hz (limited by the testing machine). No significant differences were found between the vibrating-wire reinforcement strain gauge and the resistance strain gauge, Fig. 2(b).

2.3.4 Long-term stability

The excellent zero point stability of vibrating-wire instruments is well known, and this explains their wide spread use in long-term monitoring programs. Stability tests started at NGI in 1967 using 12 vibrating-wire strain gauges show a long-term zero point drift corresponding to 0.3 percent of full scale after 20 years.

The long-term stability of a reinforcement strain gauge, over an 8-year period has been established by ongoing measurements on an actual project. A "dummy" reinforcement strain gauge was installed as part of the instrumentation for a concrete tunnel lining. The dummy gauge is installed in such a way that it is not loaded but is otherwise subjected to the same environmental conditions as

the other instrumentation. Data from this in-situ test is presented in Fig. 3 and shows that the long term drift of the instrument is less than 2 microstrain over 8 years.

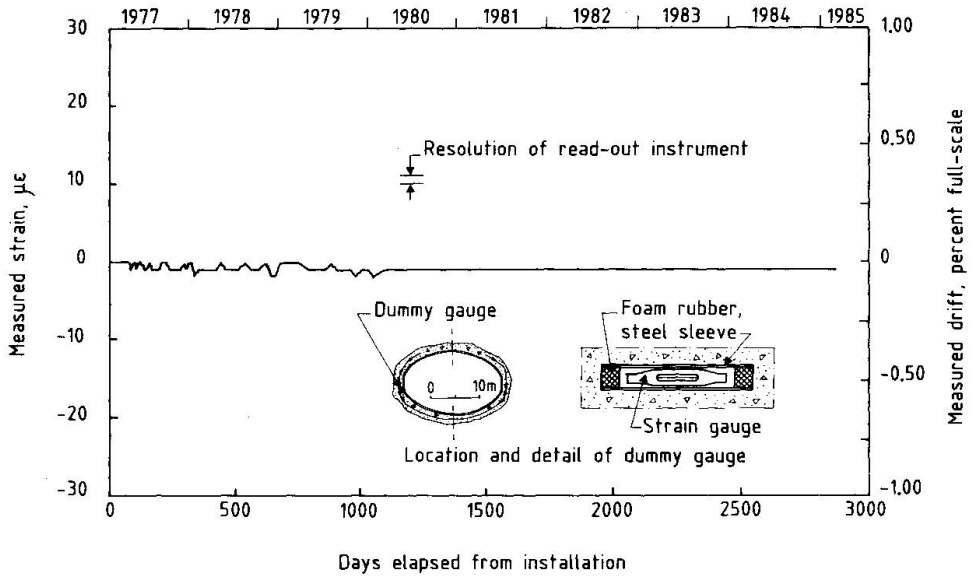

Fig. 3 Measured zero point drift of vibrating-wire reinforcement strain gauge

2.3.5 Long-term reliability

Except for some offshore applications most of the structures instrumented by NGI have been observed for only a few years. For this reason there is little information regarding the long-term reliability of the reinforcement strain gauges. Performance data spanning over a 6 to 7 year period is available from one offshore structure. Sixty strain gauges were installed on this structure during construction in 1979-80. When last checked at the end of 1986, all 60 instruments were operating normally and giving data that appears reasonable in every respect.

3. APPLICATIONS

Although strain monitoring programs for concrete structures may differ significantly from structure to structure, the main objectives are usually design verification and documentation of adequate safety of the structure. Three common circumstances where strain measurements can provide information of practical or economical value are outlined below.

- The loading on the structure is well defined and understood, but the effects of the loads on the structure are uncertain. Thus, the function of the instrumentation is to determine the response of the structure to the applied loads. This generally requires that critical parts of the structure be

instrumented to measure the stresses that occur. In this case the results of the measurements enable the structural engineer to compare predicted stresses with observed values and thereby verify the integrity of the structure.

- The uncertainty is in the loading on the structure and not the integrity of the structure itself. The monitoring program in this situation may be entirely different from one intended to provide structural response data. In this case the instrumented structure functions in reality as a load measuring system. The results of the measurements are used to verify design estimates of the loading and to provide information regarding soil/structure interaction.

- Some construction procedures may cause special loading conditions on the structure as it is being built. When this is so, it is essential to monitor and control the construction process to ensure that the work is progressing safely and that no damage occurs to the structure. In this case instrumentation is used actively as a construction control tool, and the monitoring program has to be designed to detect unacceptable performance in time to initiate contingency action if the situation is judged to be critical.

NGI has used the reinforcement strain gauge on a wide variety of projects both onshore and offshore. The following examples have been selected to illustrate various uses of the gauge in monitoring programs of the type outlined above. In each case the use of the gauge is briefly described and where possible some typical data presented.

3.1 Retaining wall

The reinforcement strain gauge has been used to optimize the design of retaining structures. The retaining wall shown in Fig. 4(a) was the first of a number of concrete structures to be constructed for bulk storage of chemical fertilizer.

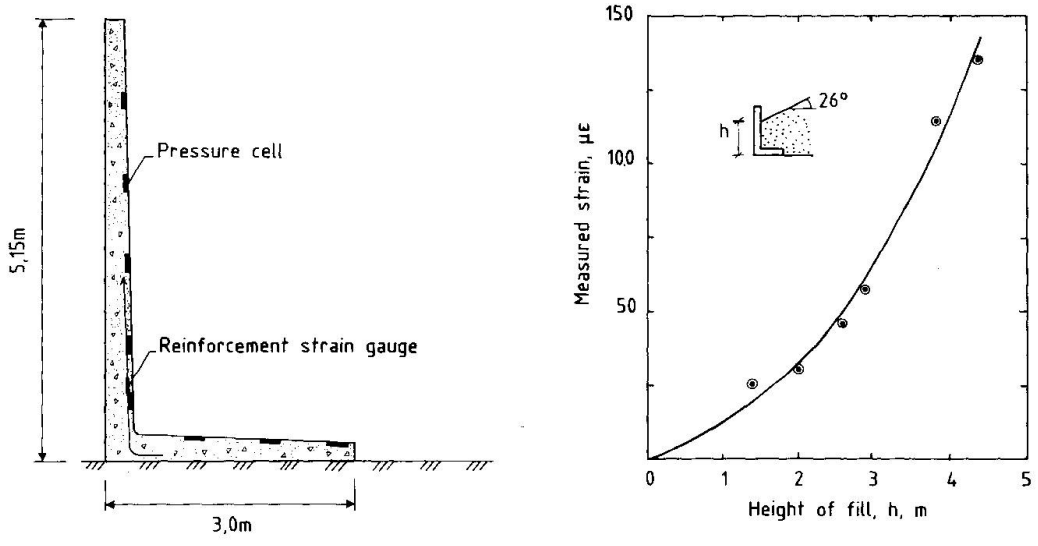

a/ CROSS SECTION OF RETAINING WALL

b/ MEASURED STRAIN IN REINFORCEMENT

Fig. 4 Strain measurements in a retaining wall

A full scale test was carried out on the first structure to provide a basis for the design of the other storage bins that were to be built. The instrumentation consisted mainly of pressure transducers since the aim of the investigation was to find the pressures acting on the wall during the filling of the storage area. The reinforcement strain gauge was used to monitor the stress developed in the reinforcing steel near the base of the wall. The moment at the base of the wall determined from the strain gauge readings, Fig. 4(b), provided an overall check on the loading. On the basis of the measurements empirical rules were developed for the design of the storage bins.

3.2 Friction piles

A series of loading tests [1] have been carried out using cylindrical and conical precast concrete friction piles driven into a very loose deposit of homogeneous sand, Fig. 5(a). One of the main objectives of the test program was to determine the magnitude and distribution of skin friction along the piles. This was done by using reinforcement strain gauges to measure the axial load at regular intervals along the piles. In order to correlate the strain gauge readings to axial load, the piles were calibrated in a loading frame before and after the tests. Typical results from the pile load tests are shown in Fig. 5(b).

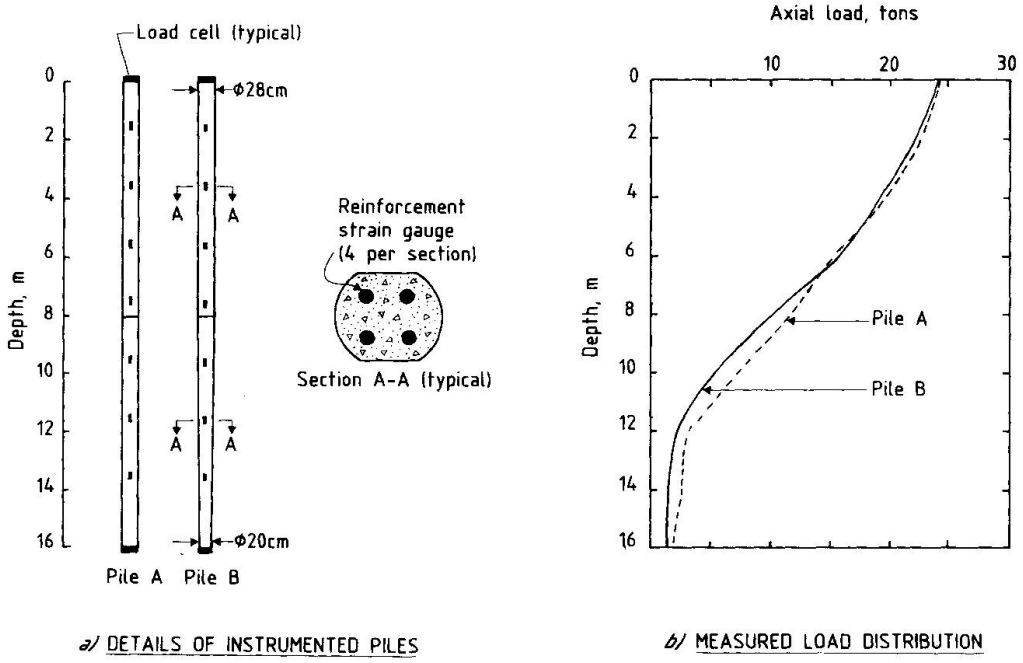

Fig. 5 Measurement of axial load in friction piles

3.3 Tunnel lining

One of the underground stations on the Oslo east-west railway line consists of a rock tunnel with a reinforced concrete lining. The first section of the tunnel was instrumented in order to monitor the stresses developed in the lining, Fig. 6(a). On this project both vibrating-wire reinforcement strain gauges and vibrating-wire embedded strain gauges were cast in the concrete lining of the tunnel.

Results from an embedded strain gauge and a reinforcement strain gauge installed at the same location are shown in Fig. 6(b). The measured strains are in good agreement for the two types of instruments. The "dummy" gauge used to obtain the long-term performance data reported in Fig. 3 was part of this instrumentation program.

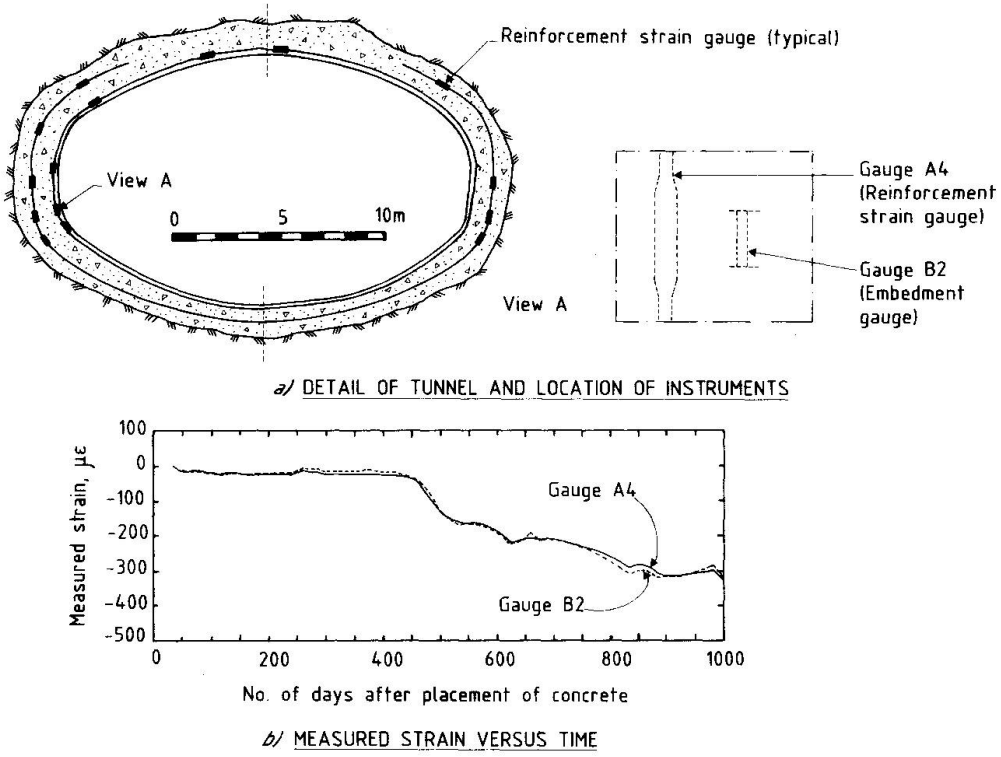

Fig. 6 Strain measurements in a reinforced concrete tunnel lining

3.4 Prestressed concrete reactor vessel

A model prestressed concrete reactor vessel was built as part of a Scandinavian nuclear energy research project. The test vessel, Fig. 7, of a scale of 1:3, was thoroughly instrumented to determine the effects of high internal pressure and temperature on the integrity of the structure. This is an example where the loading on the structure is known but the response of the structure to these loads has to be verified by measurements. The objectives of the project were to test the design of the removable lid and the adequacy of the thermal insulation system. In the final phase of the test program the vessel was pressurized hydraulically to failure. Measurements of thermal stress and stress concentrations near the penetrations through the base of the vessel and around the removable lid were of prime concern. These were measured with embedded strain gauges, 250 in all, since they are better suited for measurements of the state of stress at a point within the concrete. The monitoring program also included vibrating-wire reinforcement strain gauges installed at mid-height of the vessel as indicated in the figure for monitoring axial and circumferential strains.

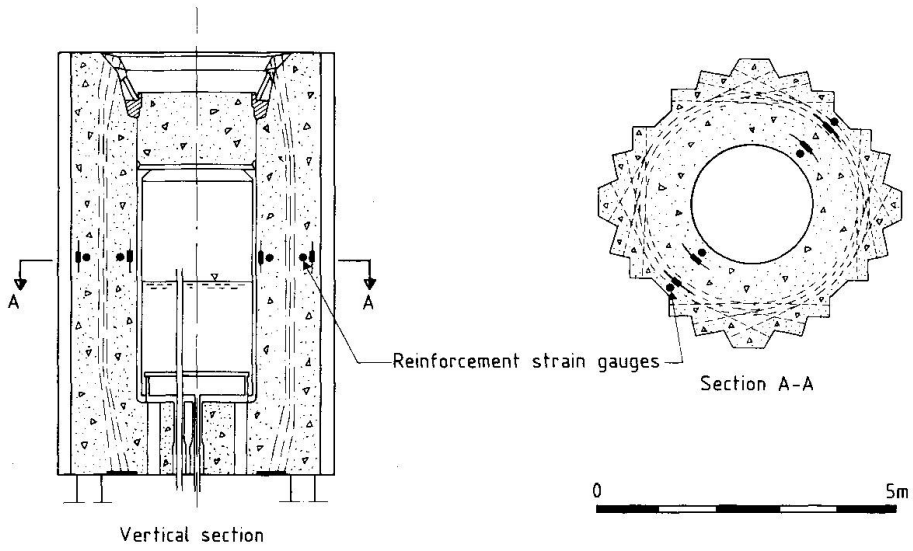

DETAIL OF TEST STRUCTURE AND LOCATION OF INSTRUMENTS

Fig. 7 Strain measurements in a prestressed concrete pressure vessel

3.5 Slurry-trench walls

The deepest part of the underground or subway system in Oslo was constructed in soft clay by the cut and cover method using slurry trench techniques [2]. This

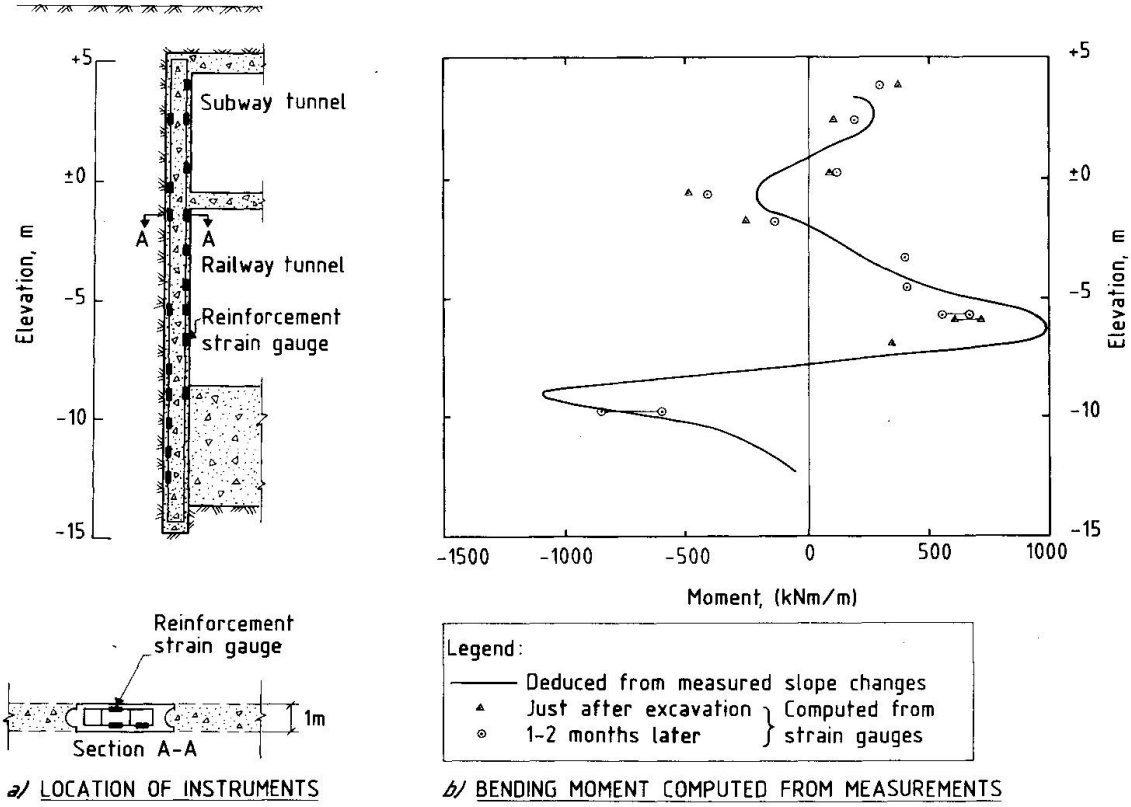

a/ LOCATION OF INSTRUMENTS

b/ BENDING MOMENT COMPUTED FROM MEASUREMENTS

Fig. 8 Monitoring of strain in reinforcement of a slurry trench wall

involves the use of a slurry to stabilize the trench during excavation and then replacing the slurry with concrete to form an in-situ wall element. A unique excavation and bracing procedure had to be followed during excavation of the clay between the longitudinal walls of the subway tunnel. An extensive construction control program was carried out on this difficult project. This included instrumenting one of the first sections of the slurry-trench wall with reinforcement strain gauges, Fig. 8(a), as part of an extensive monitoring program to determine the loading on the tunnel during construction. An example of the bending moments in the wall derived from the reinforcement strain gauge data is given in Fig. 8(b).

3.6 Bridges

Fig. 9 presents two examples of the use of the reinforcement strain gauge in bridge structures. In both cases measurements of the load and moment carried by the bridge piers were needed to monitor and control construction operations. To measure the loading, the piers were instrumented with reinforcement strain gauges, one in each corner. The relative locations of the strain gauges used on these structures are shown in the figure. Fig. 9(a) shows the unsymmetrical Norddalsfjord bridge [3] which has short, ballasted cantilevered spans towards land. It was instrumented in order to assess the safety of the structure during the free cantilevering construction procedure that was used. Fig. 9(b) shows Nordsund bridge which was instrumented because of torsional effects on the main span and support during construction of the curved approach span.

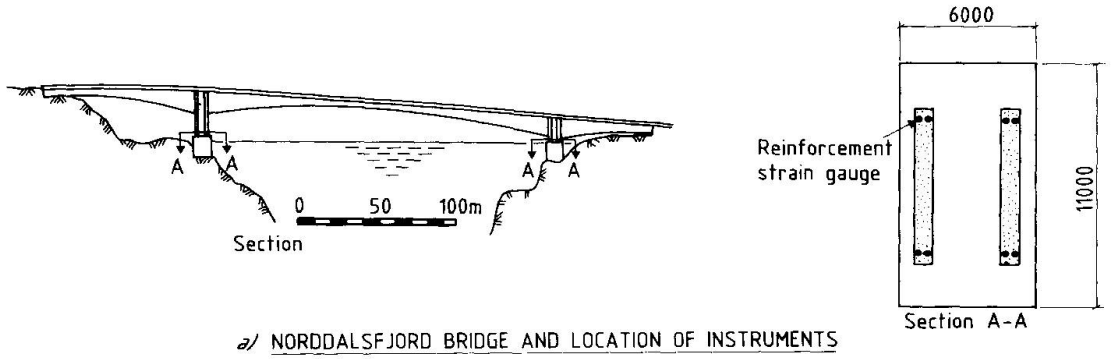

a/ NORDDALSFJORD BRIDGE AND LOCATION OF INSTRUMENTS

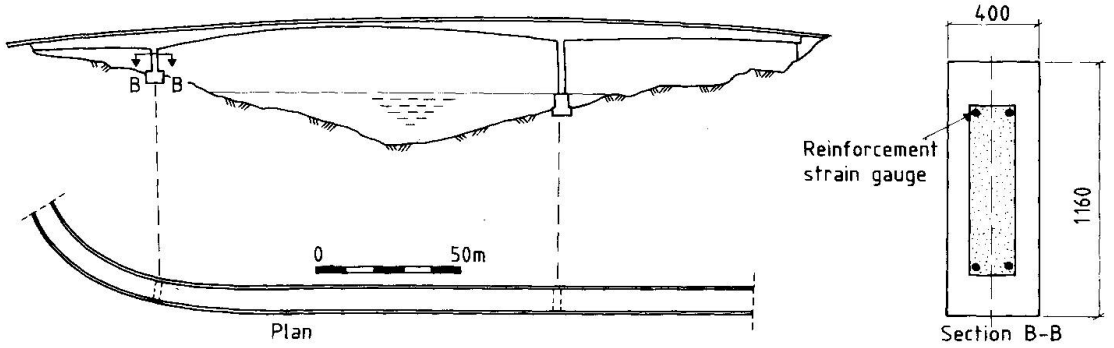

b/ NORDSUND BRIDGE AND LOCATION OF INSTRUMENTS

Fig. 9 Instrumentation for monitoring bridge construction

3.7 Gullfaks C test structure

A large scale soil penetration test was carried out in the North Sea in 1985. In more than 200 m of water a concrete test panel, 2.4 m wide, 0.4 m thick and 23 m long was penetrated 22 m into the seabed to provide important design information for Statoil's Gullfaks C platform [4]. The base of this Condeep structure is fitted with 1400 running metres of concrete foundation skirts that must penetrate 22m into the soil. The large scale test was carried out to confirm that penetration of the 22m long skirts of the structure would be possible. Fig. 10(a) shows overall details of the 360 ton test stucture, and Fig 10(b) shows the maritime operations during the penetration test. Included in the instrumentation program were four vibrating-wire reinforcement strain gauges installed in the corners of the test panel, 3 m above the tip. These instruments were used to determine if any significant bending moments were developed in the cantilevered part of the test panel as it penetrated into the soil. As it turned out, at a particular stage in one of the tests rather large bending moments were developed in the tip of the concrete panel. The strain gauge readings showed this quite convincingly. Fig. 10(c), for example, shows some data from the test at a stage where the moment is decreasing but there are still large tensile strains in the reinforcing steel on one side of the test panel.

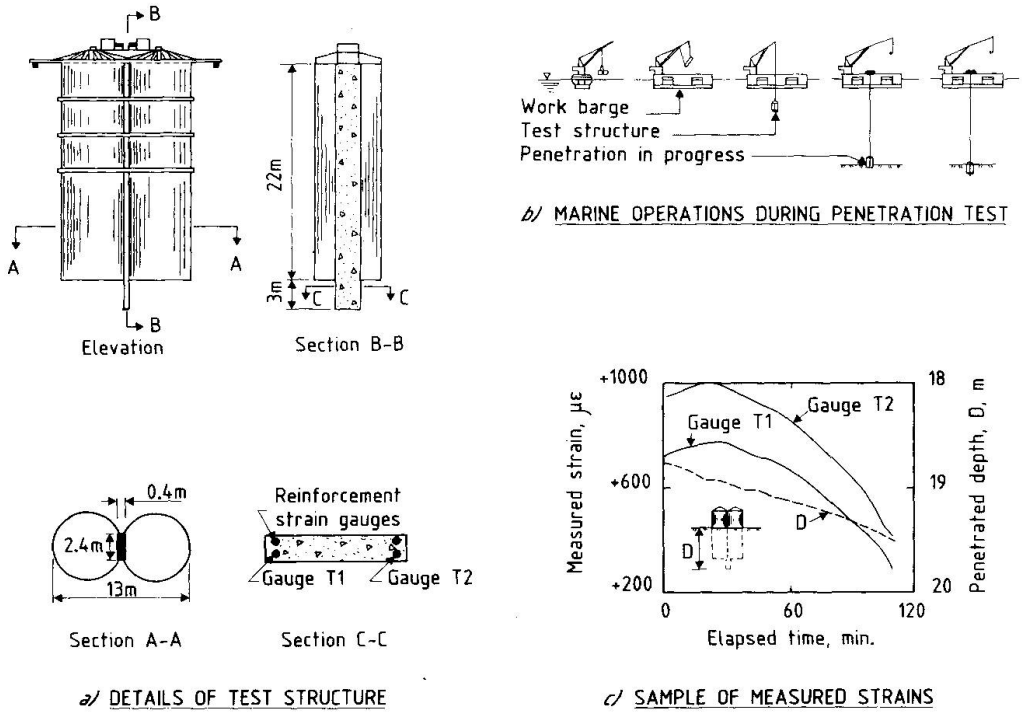

Fig. 10 Strain measurements in the Gullfaks C test structure

3.8 Condeep structures

One of the principal uses of NGI's vibrating-wire reinforcement strain gauge has been offshore on the Condeep gravity base structures built by Norwegian Contractors [5]. The instruments have been used both to ensure safe installation of the structures and for long-term performance monitoring needed for design veri-

fication purposes and to confirm the integrity of the structures. Three different examples are given below to illustrate why and how the reinforcement strain gauges have been used on these structures.

3.8.1 Monitoring forces in parts of the structure

One structure was designed with a concrete slab around the periphery of the base to increase the foundation area. This slab is supported by massive inclined prestressed concrete struts as shown in Fig. 11(a). Selected concrete struts were instrumented with reinforcement strain gauges to satisfy requirements imposed by the certifying authority. The primary objective of the measurements was to obtain quantative and qualitative information concerning mud line forces caused by wave loading. These instruments have been incorporated into the long-term monitoring program for the structure and static and dynamic strains in the struts have been monitored systematically.

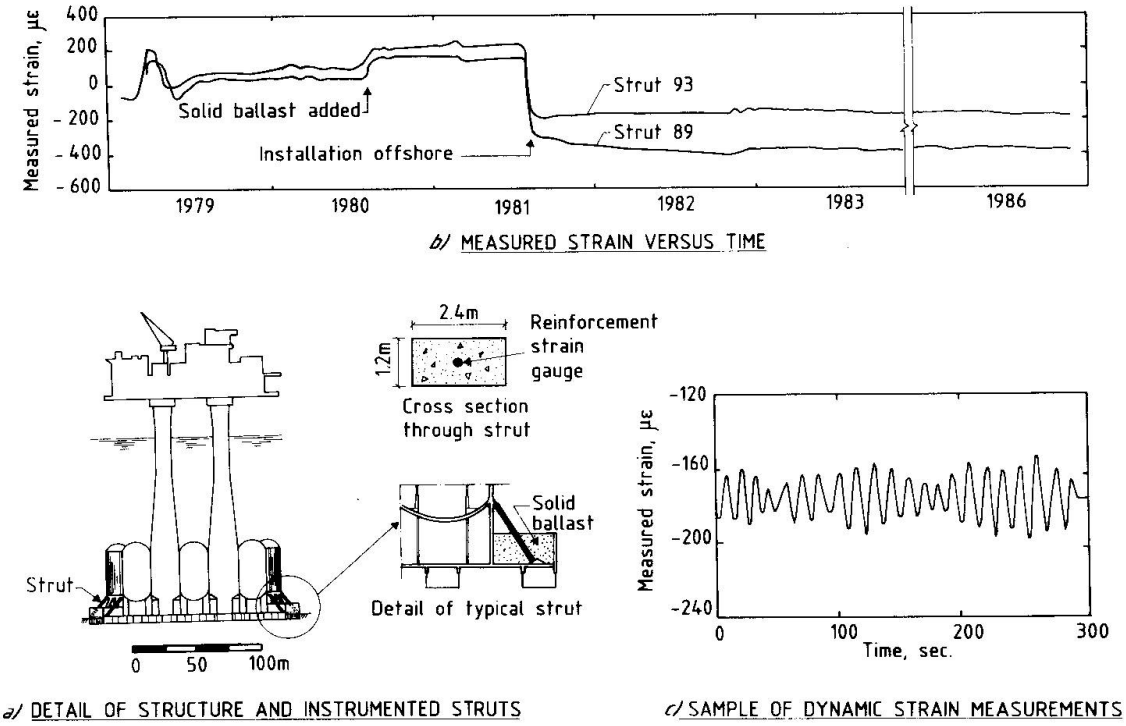

Fig. 11 Monitoring forces in the struts of a Condeep structure

Typical data from the reinforcement strain gauges in the struts are given in Fig. 11(b). Two important activities which had significant bearing on the measured strains are indicated on the figure although others, such as prestressing of the cables and the effects of increased hydrostatic pressure on the caisson during deep submergence and deck mating operations are readily identified. A sample of dynamic strain measurements from a typical strut is given in Fig. 11(c). Such data forms the basis for an evaluation of the mudline forces mentioned above.

3.8.2 Monitoring critical operations during installation

The base of most Condeep structures consists of a cluster of spherical domes that are generally penetrated slightly into the foundation soil. It is

desirable to press the platform as deep into the seabed as possible because this means a reduction in the amount of underbase grout that is injected between the seabed and the undersisde of the platform. While seating the domes during installation of the structure it is therefore important to monitor that the domes are not overstressed.

Monitoring the safety of the domes is not a simple task because the contact area and penetration resistance change as the dome penetrates into the soil. Three different techniques have been used to monitor dome seating. As shown in Fig. 12(a), reinforcement strain gauges are used to monitor the strain in the centre of the domes and/or at the base of the cell wall where the resulting hoop stresses can be correlated to the loading on the dome. In addition, the contact pressure between the dome and soil is measured directly by means of an earth pressure transducer mounted flush at the centre of the dome. By using the instrumentation to monitor the loading, the safe and economical installation of the structures have been ensured.

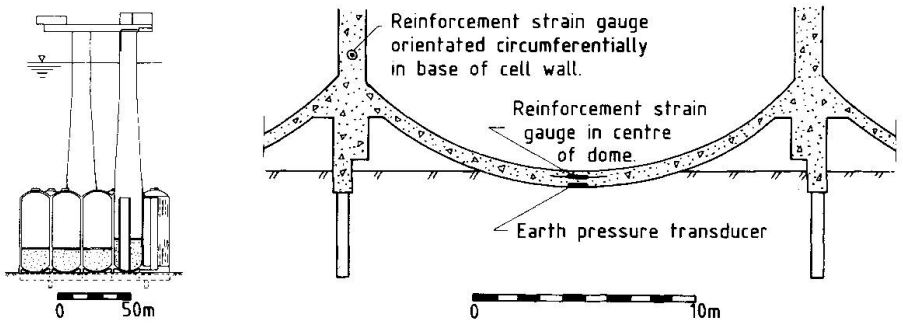

a/ DETAIL OF STRUCTURE AND TYPICAL INSTRUMENTATION, LOWER DOMES

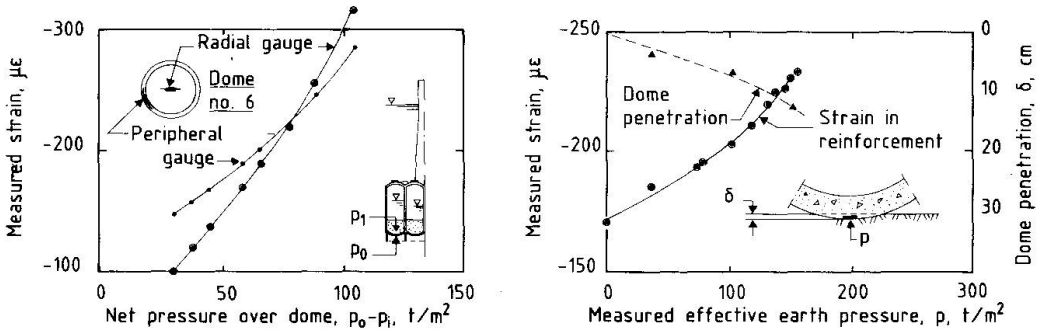

b/ STRAINS DUE TO CHANGES IN HYDROSTATIC LOADING DURING TEST SUBMERGENCE

c/ TYPICAL MEASUREMENTS WHILE SEATING DOMES DURING INSTALLATION OF STRUCTURE

Fig. 12 Strain measurements in the lower domes of Condeep structures

Fig. 12(b) presents typical data from the test submergence of a Condeep structure, which is carried out as preparation for the deck-mating operation. During the test submergence it is possible to verify the operation of the instruments in the dome by comparing the strain gauge readings to the known hydrostatic loading on the lower domes. Fig. 12(c) presents data from seating of one of the domes during installation of a structure.

3.8.3 Monitoring of environmental loading and creep in the concrete

Long-term performance programs for several Condeep structures have included vibrating-wire reinforcement strain gauges for measurement of the static and dynamic axial strains in the shafts.

The first measurements of this kind were initiated as an alternative to direct measurement of the hydrodynamic pressures on the structure [6]. By instrumenting the shaft with strain gauges, Fig. 13(a), it has been possible to determine the resulting environmental loading on the shafts and to use this information to check computational models used during the design. In addition, measured long-term variations in strain have made it possible to study the effects cyclic loading on creep in the concrete.

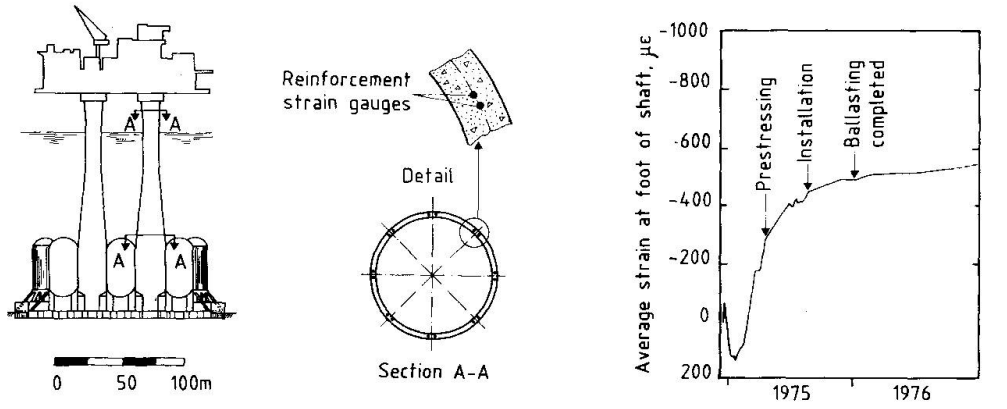

a/ DETAILS OF TYPICAL STRUCTURE AND INSTRUMENTED SHAFT

b/ MEASURED STRAIN IN SHAFT

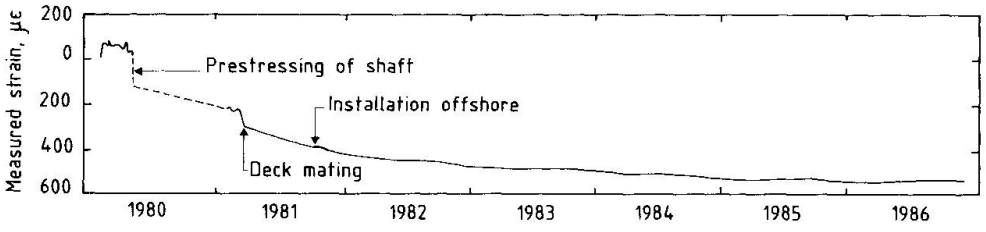

c/ AVERAGE MEASURED STRAIN AT TOP OF SHAFT VERSUS TIME

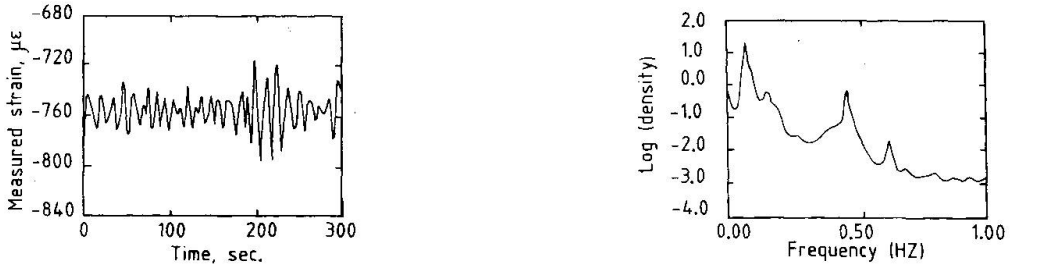

d/ SAMPLE OF DYNAMIC STRAIN MEASUREMENTS

e/ TYPICAL GENERALIZED STRAIN SPECTRA

Fig. 13 Strain measurements in the shafts of Condeep structures

Typical data from the vibrating-wire reinforcement strain gauges in the shaft are given for two different structures in Fig. 13(b) and (c), with important activities indicated. Considerable data have been collected over the years and outstanding material for creep analysis is now available. This is discussed further in the next section.

Dynamic measurements, Fig. 13(d), obtained with the reinforcement strain gauges have been used in a design verification study to compare actual response of the structure to the calculated response. Spectral density plots from the reinforcement strain gauges in the shaft, of which a typical plot is given in Fig. 13(e), and information about displacements and curvatures were obtained from the data.

4. REVIEW OF STRAIN AND CREEP DATA

Some Condeep structures have been extensively instrumented for performance monitoring and data from several years have been collected. Much of the structural data have not been analysed to their full potential. This is unfortunate especially when the extent of the data that exists is considered: data from construction periods, time histories, dynamic response during storms, long-term cyclic loading, etc. In order to give an indication of the potential of the data collected, the following is a comparison between measured values and calculated values of strain in the shaft of one structure.

4.1 General

Reinforcement strain gauges were placed vertically in the centre of the shaft wall 5 metres above the base of the shaft, see Fig. 13(a). The distance from the fixed end was chosen in order to reduce the influence of end effects.

The measured values are presented in Fig. 14(a) showing the development of strain subsequent to completion of slipforming. The calculated values shown in the figure are based on the formulae and curves presented in CEB-FIP Model Code of 1978.

4.2 Concrete

The 28-day cube strength for the concrete used in the shafts was 60.7 MPa. Portland cement with increased fineness was used to achieve a faster slipform-rate and higher compressive strength. The cement content was 400 kg/m^3. The aggregates were fragments of gneisses and granites quarried from large moraine deposits. The water/cement ratio was about 0.40. A superplasticizing admixture, 5 l/m^3 was used. The slump was about 200 mm. A modulus of elasticity of 29 GPa for the concrete was measured by standard tests at 28 days.

4.3 Loading history

The slipforming of the shafts started in January 1980. The first loading on the instrumented cross section was the weight of fresh concrete. After a few hours the heat of hydration caused a temperature rise. Temperature measurements made

in another shaft show a maximum temperature in the centre of +45 deg. C. As the air temperature was about zero, the cooling of the section caused a significant tensile strain in the centre of the wall which can be seen from the measured curve, Fig. 13(c). This tensile strain diminished after some time due to relaxation. In May, once the slipforming had been completed, the ring beam on top of the shafts was cast and then 122 prestressing tendons, which are terminated in the lower part of the shaft, were stressed. The remaining 40 tendons which extended to the top of the shaft were stressed, from both ends, in the first week in June. Fig. 13(c) shows the prestressing of the top of the shaft, i.e., only the tensioning of the last 40 tendons, while Fig. 14(a) shows the strains at the base of the shaft and therefore the tensioning of both sets of tendons.

During the interval from June 1980 till deck mating at the end of March 1981 no significant loads were applied to the structure. The installation of the structure took place in August 1981 at which time the water pressure on the structure increased.

4.4 Comparison of curves

Fig. 14(a) shows a generally good correspondance between the observed and the calculated strains. The tensioning of the first prestressing tendons was chosen as a clearly defined starting point for the calculated curve since effects such as increase in shaft weight, curing temperature, etc., complicate the calculations for the initial part of the curve. It appears that the instant elastic deformation in the first part of the curve (tensioning of tendons) is somewhat underestimated although an increasing E-modulus was used. The development of creep and shrinkage strain with time show a very good agreement with the measured values. After approximately five years the measured strain appears to approach a limiting value of about 700 microstrain which is the same value calculated for the strain at infinite time, ε_∞.

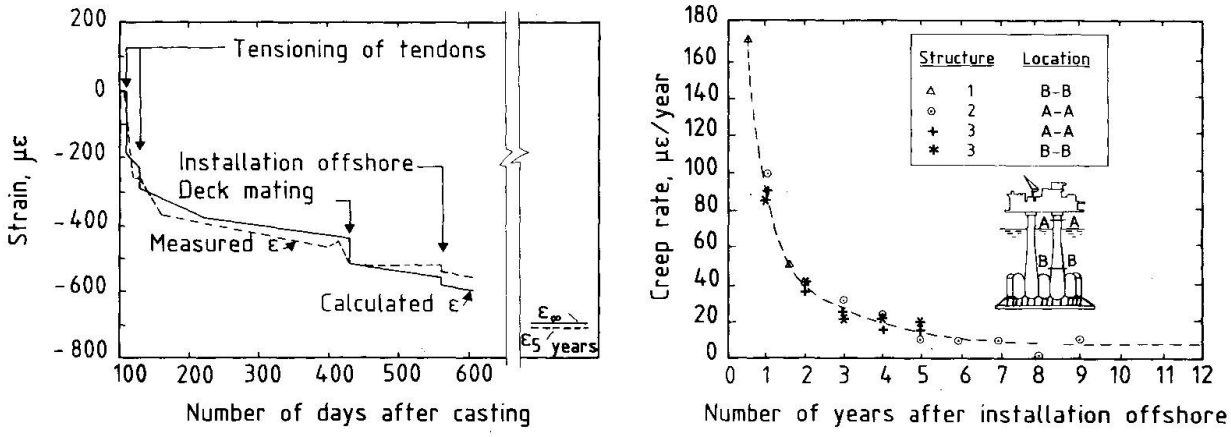

a/ COMPARISON OF MEASURED AND CALCULATED STRAIN

b/ MEASURED LONG TERM CREEP FOR THREE STRUCTURES

Fig. 14 Strain and creep data from the shafts of Condeep structures

A comparison of the observed creep rate for three Condeep platforms is shown in Fig. 14(b). The data represents long-term creep data for structures that have been subjected to cyclic loading for several years, one structure for more than nine years. The three rates are almost identical. This is perhaps to be expected since the structures are similar in concept, designed in the same manner, and subjected to the same type of loading.

5. CLOSING REMARKS

The vibrating-wire reinforcement strain gauge has proven to be a very useful and versatile instrument for monitoring strains in large concrete structures. With the good performance record of the gauge and with continually new problems facing the structural engineer, e.g. fjord crossings, oil platforms at deep water sites, new bridge designs, etc., the gauge should continue to play an important role in performance monitoring programs.

ACKNOWLEDGEMENTS

The authors gratefully acknowledge the help and support of their collegues, particularly Dr Elmo DiBiagio of the Norwegian Geotechnical Institute, who provided many of the ideas and much of the information contained in this paper.

REFERENCES

1. GREGERSEN O.S., AAS G., and DIBIAGIO E., (1973), Load tests on friction in piles loose sand. International Conference on Soil Mechanics and Foundation Engineering, 8. Moskow 1973. Proceedings, Vol. 2.1, pp. 109-117. Also publ. in: Norwegian Geotechnical Institute. Publication, 99.

2. KARLSRUD K., (1981), Performance and design of slurry walls in soft clay. ASCE Spring Convention, May 1981, Preprint 81-047. Also publ. in: Norwegian Geotechnical Institute, 149.

3. FERGESTAD S., LARSEN O.G., NÆSS K., (1987), Instrumentation and monitoring of Norddalsfjord bridge. Proceedings IABSE Colloquium, Bergamo, Italy, Oct 1987.

4. TJELTA T.I., GUTTORMSEN T.R., and HERMSTAD J., (1986). Large scale penetration test at a deep water site. Offshore Technology Conference, 18. Houston, Texas 1986. Proceedings, Vol 1, pp. 201-212.

5. DIBIAGIO E., MYRVOLL F. and BORG HANSEN S., (1976), Instrumentation of gravity platforms for perfomance observations. International Conference on the Behaviour of Off-shore Structures, 1. BOSS'76. Trondheim 1976. Proceedings, Vol. 1, pp. 516-527. Also publ. in: Norwegian Geotechnical Institute. Publication, 114.

6. SOCIETY FOR UNDERWATER TECHNOLOGY, (1980), Shell Brent 'B' Instrumentation Project. Seminar, London 1979. Proceedings, 116p.

Cross-Spectrum Technique for High-Sensitivity Remote Vibration Analysis by Optical Interferometry

Analyse vibratoire ultra-sensible à distance par interférometrie optique

Schwingunsanalyse mittels optische Interferenzmessungen

M. CORTI (*), S. MARAZZINI (**), A. MARTINELLI and A. DE AGOSTINI CISE S.p.A., Pob 12081, Segrate, Milano, Italy

(*) present address: Department of Electronics, University of Pavia, 7100 Pavia (Italy)
(**) present address: Aeritalia S.p.A. - 20014 Nerviano (MI) (Italy)

SUMMARY

An application of cross-correlation techniques aimed to the improvement of the sensitivity of laser interferometric vibration sensors is described. The interferometer operates remotely, up to 200 meters away, from a moving target without requiring retroreflecting tools. The overall sensitivity in oscillation amplitude measurements is of the order of 0.1 microns in a bandwidth 0,1-150 Hz, with normal atmospheric conditions. Cross-correlation of the output signals of two identical interferometric vibration sensors pointing to the same target from simmetrical remote positions, allows reduction of the air-turbulence background noise giving an ultimate sensitivity of the order of 0,01 microns. Examples of application of this technique for in situ measurements on an hydroelectric arch dam are presented.

RESUME

On décrit une application des techniques de corrélation croisée pour l'amélioration de la sensibilité des instruments de mesure dynamique pour interférometrie laser. L'interférometrie fonctionne à distance, éloigné jusqu'à 200 m du point mobile de mesure, et sans nécessiter des éléments réfléchissants.
Dans des conditions atmosphériques normales, la sensibilité globale pour la mesure d'amplitudes de vibration est de l'ordre de 0.1 microns dans une gamme de fréquences de 0.1 a 150 Hz. La corrélation croisée des signaux provenant de deux interféromètres dynamiques identiques, mirant la même point de mesure à partir de deux positions éloignées symmétriques, permet de réduire le bruit de fond dû à la turbolence atmospherique signe garantissant ainsi une sensibilité extrème de l'ordre de 0.01 microns. Comme exemple d'application de cette technique on présente des mesures in situ pour un barrage-voûte.

ZUSAMMENFASSUNG

Es wird eine Anwendung der Kreuzkorrelationstechnik für die Verbesserung von Laserinterferenzschwingungsmessgeräten behandelt. Der Interferenzmesser kann, ohne Zurückstrahlkörper zu benötigen, bis 200 m entfernt von dem schwingenden Zielpunkt verwendet werden.
Die Gesamtempfindlichkeit unter normalen atmosphärische Zuständen ist ungefähr gleich 0.1 Mikron in einer Frequenzenbreite von 0.1 - 150 Hz. Durch Kreuzkorrelation von zwei symmetrischen Interferenzmessungen eines gleichen Punktes kann man das atmosphärische Störungsgeräusch vermindern, und so eine Empfindlichkeit von ungefähr 0.01 Mikron erreichen Dieser Beitrag beschreibt eine Anwendung von dieser Technik für die Ortsmessungen an einem Gewölbstaudamm.

INTRODUCTION

In this paper we describe an application of cross-correlation techniques aimed to the improvement of the sensitivity of a laser intereferometric vibration sensor. The interferometer operates remotely from a moving target without requiring retro-reflective mirrors. It is a polarizing interferometer based on a Michelson scheme with a short internal reference path and a long external path which projects to the target through a telescope (Fig. 1). The same telescope collects the laser light scattered back from the target. Any surface is suitable: concrete, metals, bricks, etc. The surface roughness provides the scattered light which is used by the interferometer. The power of the projecting laser light (λ = 632.8 nm) is kept below 5mW for safety reasons.

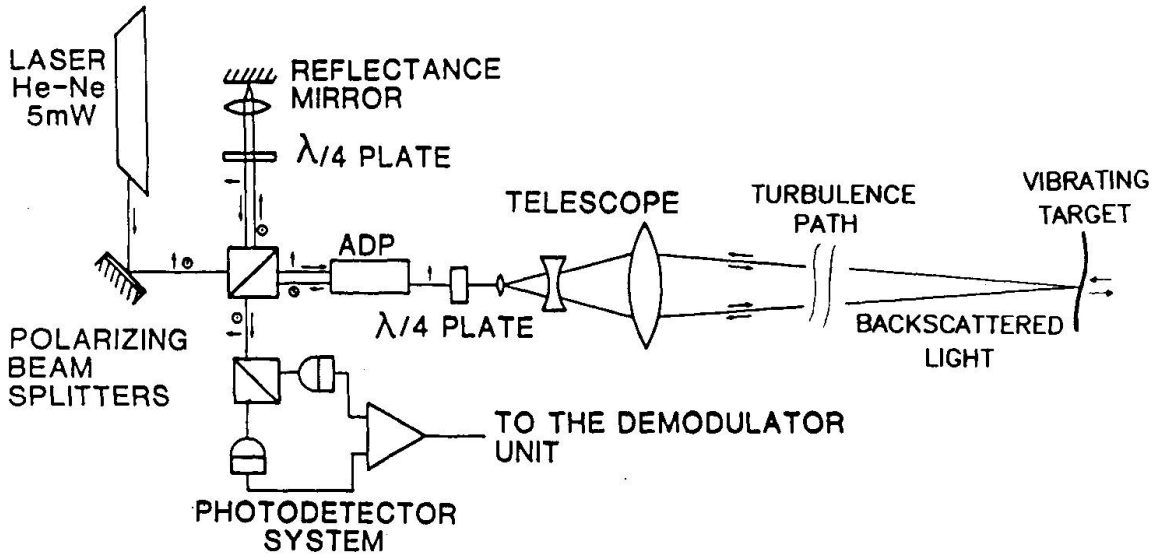

Fig. 1 - Optical set-up of the interferometer.

The interferometer operates up to 200 meters away from the target and is optimized for vibration measurement in the range 0.1-150 Hz which is suitable for tests of large civil structures. A detailed description of the interferometer and some examples of field applications are presented in Ref. 1 and 2. In Ref. 1 the sensitivity of the interferometer is discussed in terms of various sources of noise. The atmospheric turbulence gives the largest contribution since the random fluctuation of the refractive index along the propagation direction is detected by the instrument as target vibration. The effect of the beam wandering in the atmosphere due the turbulence, has been efficently reduced by an opto-electronic beam steering loop built in the interferometer. The overall average sensitivity in oscillation amplitude measurements performed at 100 meters away from the target is of the order of 0.1 microns. An example of the frequency domain behaviour of the turbulence effect in real environment is shown in Fig. 2. The data

are obtained by aiming the interferometer to a fixed point on a rock 150 meters away. The spectral behaviour is roughly of the type 1/f.

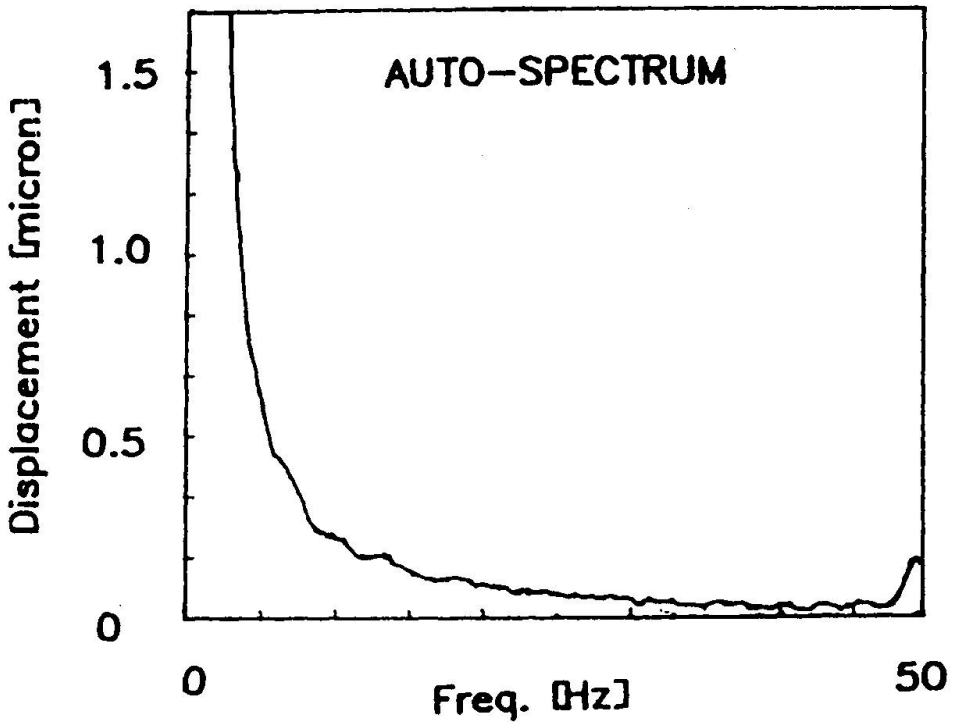

Fig. 2 - Typical noise frequency spectrum due to turbulence, measured by aiming the interferometer to a fixed point 150 meters away.

The idea described in this paper is to use two identical interferometric vibration sensors pointing to the same target from simmetrical remote positions and cross-correlate the two measured vibration signals. This configuration was experimentally tested in the laboratory on a simulation system and then used in field measurments. The obtained results show a good reduction of the turbulence background noise allowing an ultimate sensitivity of the order of 0.01 microns.

2. THEORETICAL BACKGROUND

Cross-correlation techniques are a powerfull tool to reduce uncorrelated informations among signals (Ref. 3). In our case, the vibration signal detected by the optical interferometric system (OIS) contain informations of the measurement path due to turbulence. When we use two OISs pointing to the same target, we obtain two vibration signals containing the same target vibration information (identical, except eventually for a constant multiplicative factor, which depends on the geometry) and two different noise contributions that can be considered a priori uncorrelated because the optical paths of the two intereferometric sensors are different. Therefore by averaging some suitable products of the two signals it is possible to obtain a spectral information of the vibrating status of the target without the turbolence noise. Let us consider the cross-spectrum C_{xy} of the two signals

delivered by the interferometers. The cross-spectrum gives, in the frequency domain, the same information of the cross-correlation function in time domain. We call C^N_{xy} the cross-spectrum between the two signals X and Y averaged N times, that is the aritmetical average of N determinations of C_{xy} each of which lasts for a time mainly determined by the frequency resolution required in the cross-spectrum measurement. For instance, for a commune Fourier Analyzer, like the HP 3582 A, a frequency resolution of 0.2 Hz at a frequency span of 25 Hz requires a time of 10 sec for each determination. At a span of 1 KHz with a frequency resolution of 8 Hz the time reduces to 0.25 sec. If we denote by * complex conjugation, C_{xy} is defined by

$$C^N_{xy} = 1/N \left[\sum_i^N X_i^* Y_i\right] \tag{1}$$

where

$$\begin{aligned} X &= Ae^{j\vartheta_A} + N_A e^{j\vartheta_{NA}} \\ Y &= Be^{j\vartheta_B} + N_B e^{j\vartheta_{NA}} \end{aligned} \tag{2}$$

are the frequency spectra of the two signals. A, B, ϑ_A and ϑ_B represent amplitudes and phases of the deterministic part of the two spectra and N_A, N_B, ϑ_{NA}, ϑ_{NB}, the corresponding noise contributions. In absence of the deterministic part of the signal (that is with turbulence noise only) the cross-spectrum goes to zero for large values of N. In fact combining equations (1) and (2)

$$C^N_{xy} = 1/N \left[\sum_i^N N_A N_B e^{j(\vartheta_{NB} - \vartheta_{NA})}\right]$$

the mean square modulus of the cross-spectrum becomes

$$\overline{|C_{xy}|^2} = \overline{(N_A N_B)^2}/N \tag{3}$$

With the assumption of random phase distribution among the noise signals. In presence of the deterministic signals (that is with target vibration signal mixed with turbolence noise) the mean square modulus of the cross-spectrum becomes

$$\overline{|C_{xy}|^2} = \overline{(AB)^2} + \overline{(AN_B)^2}/N + \overline{(N_A B)^2}/N + \overline{(N_A N_B)^2}/N \tag{4}$$

We see that increasing the number of averages the terms containinig noise reduce with respect to the derministic part of the signal and therefore the overall signal to noise is increased.
In order to give a qualitative understanding of cross-spectrum measurements on noise signals, in Fig. 3 we show the average noise level of the cross-spectrum measured in different conditions of frequency spans and number of averages N of the Fourier Analyzer for two independent white noise input signals of fixed amplitudes.For white input noise the cross-spectrum is flat with frequency. Therefore only its average value on all frequencies is reported in Fig. 3. We see that the noise cross-spectrum is reduced either by reducing the bandwidth (smaller frequency span) or by increasing the number of averages N.

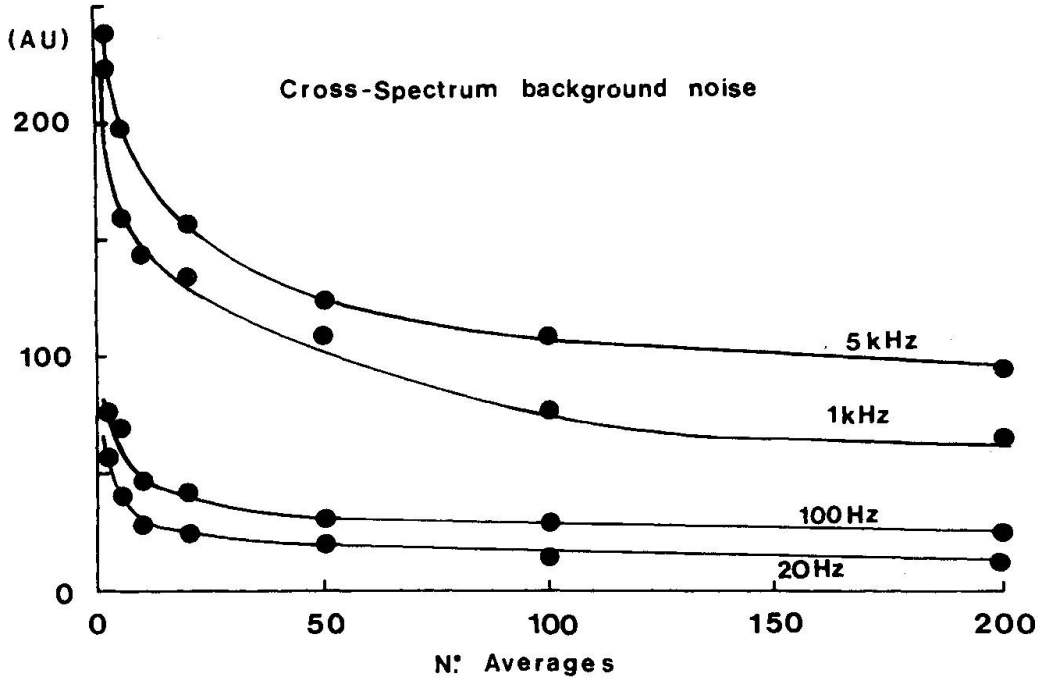

Fig. 3 - Average cross-spectrum of two uncorrelated white noise signals reported as a function of the frequency span of the spectrum analyzer and the number of averages.

Again the use of two white noise signals of fixed amplitudes N_A and N_B allowed us to check equation (3). We measured the mean square modulus of the cross-spectrum for a fixed frequency span of the Fourier Analyzer (100 Hz) for increasing N's. The data are reported as a function of N in a log-log plot. They follow a straight line with a minus one slope. The straight line is the prediction of equation (3) with the values N_A and N_B given by the white noise generators. In order to increase the accuracy of the test, each data

point corresponds to the aritmetic mean of repeated measurements (the number of which is indicated above the dots in Fig. 4) in the same experimental conditions.

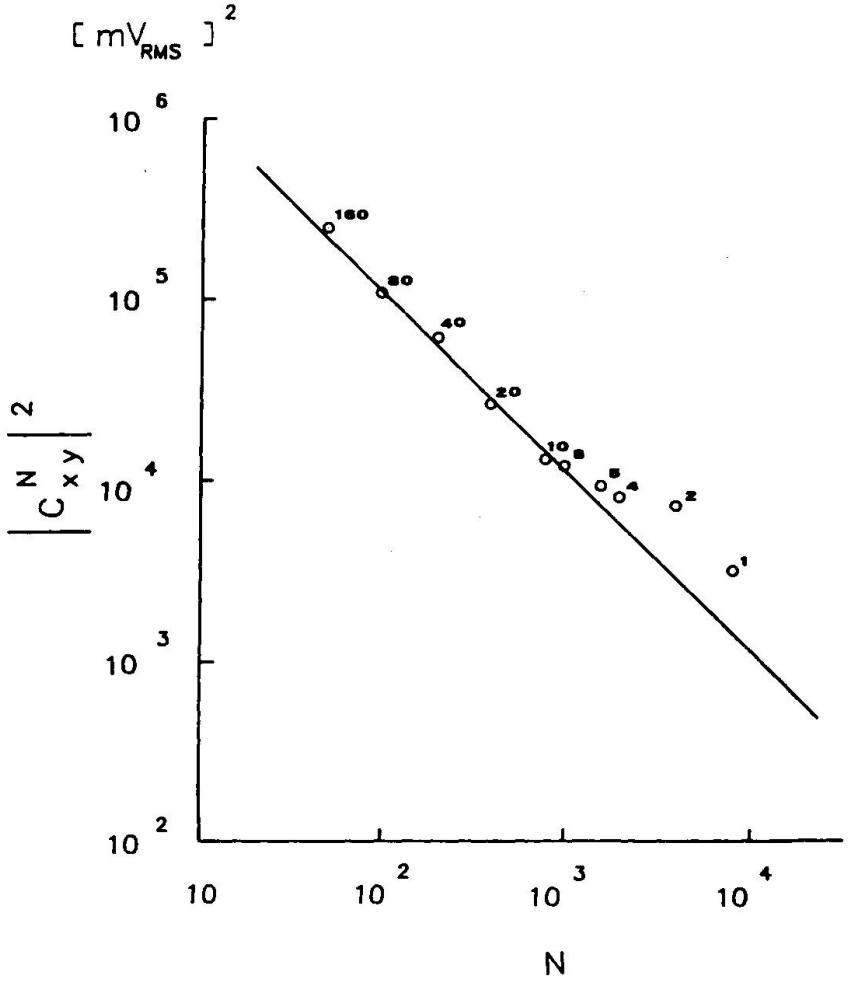

Fig. 4 - Log-log plot of the average square modulus of the cross-spectrum as a function of the number of averages for two uncorrelated white noise signals of known amplitudes. The straight line is the prediction of eq. (3).

3. LABORATORY SIMULATION

The cross-spectrum technique has been tested in the laboratory with a simulation of the turbulence noise. The experimental set-up is sketched in Fig. 5. The laser vibrometers are placed on a stable granite table. They are directed to a piezoelettrically driven target along simmetrical paths. A turbulence simulator is inserted on the trajectory of both laser beams. The simulator introduces a random optical path modulation with the same spectral characteristics of real atmospheric turbulence measured in the field (see Fig. 2).

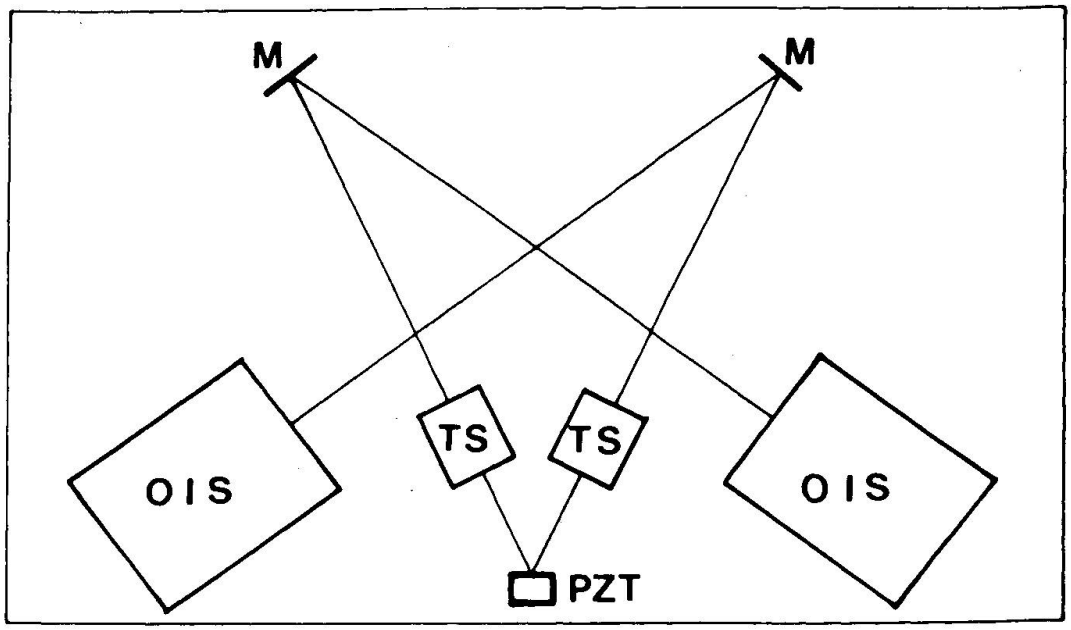

Fig. 5 - Experimental set-up for simulation of the turbulence noise.

Fig. 6 shows the operating principle of the simulator. Two glass plates are mounted on the shaft of two galvanometers which are driven by an electrical signal of opposite polarity. The plate rotation introduces the desired optical path modulation and an undesiderable beam displacement. This is compensated by the antiphase rotation of the other plate. The simulator are driven by random noise signals produced by two independent noise generators which have a 1/f spectral distributions (obtained via amplification and filtration of a diode junction noise).

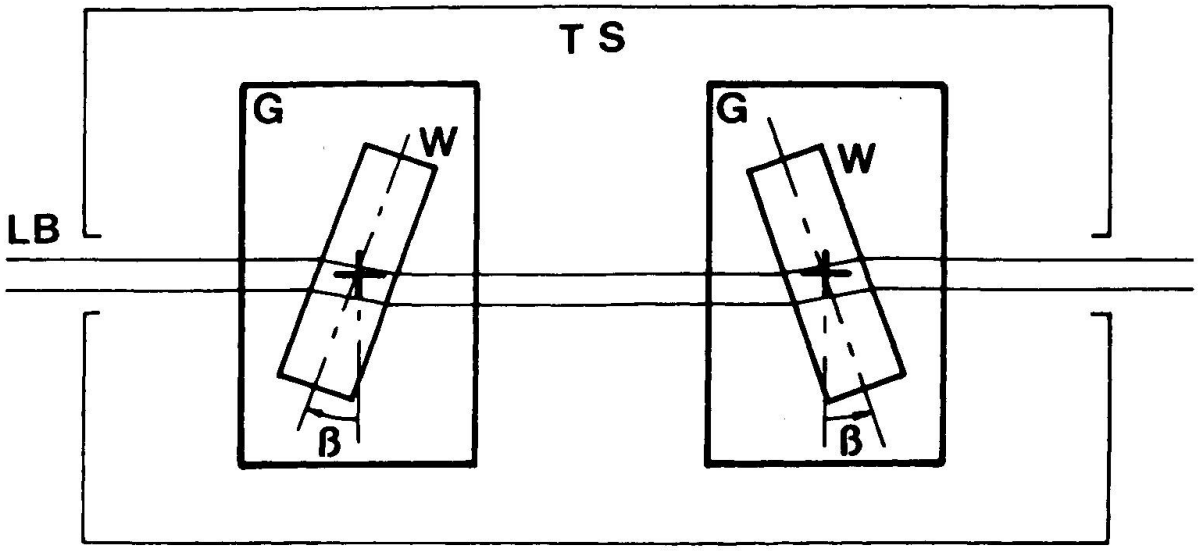

Fig. 6 - Operating principle of the optical turbulence simulator.

The vibrometer signals are analized by an HP 3582 A Fourier Analyzer connected to an HP 85 desktop computer. Figg. 7a) and 7b) show the performance of the cross-spectrum technique applied to the simulation signals. Fig. 7a) reports the individual spectra of the two vibrometer signals with both noise and deterministic parts. The target vibrates at 5 Hz with an amplitude of about 0.34 microns. The cross- spectrum of the same signals, analyzed in the same conditions (100 averages) as for Fig. 7a), is shown in Fig. 7b). The increase of sensitivity is quite noticeable.

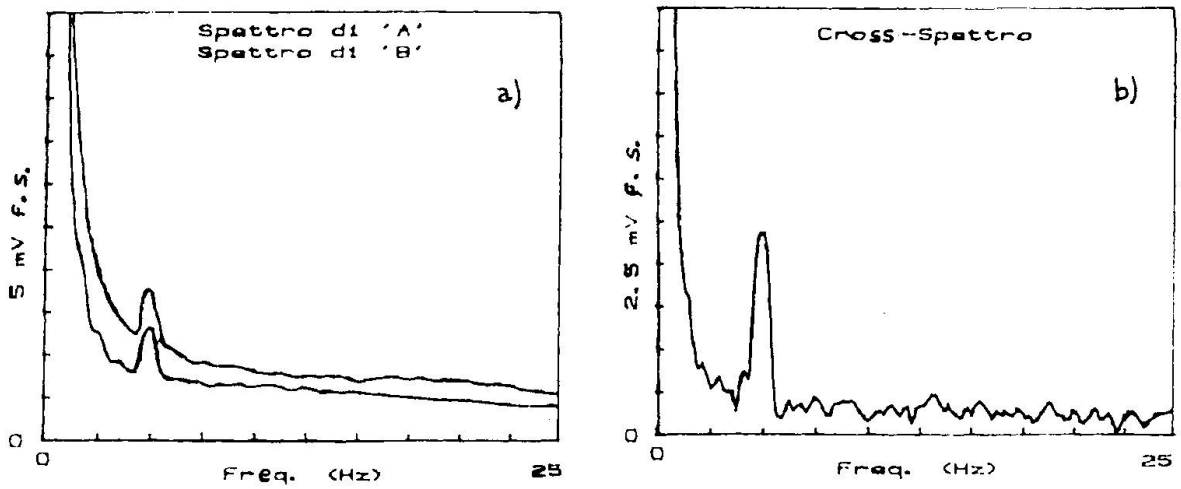

Fig. 7 - a) Spectra and b) Cross-spectrum of signals from the simulation system.

4. - FIELD MEASUREMENTS

The cross-spectrum technique has been tested in situ on an hydroelectric arch dam placed in the Eastern Italian Alps, 150 meters large and 100 meters high. The work was aimed to access the maximum sensitivity of the laser interferometric vibration sensor in field measurements.
The dam vibration was excited by the random noise produced by a waterfall (approximately 10 tons of water per second falling into the lake, 50 meters away from the dam from a height of 10 meters). The two laser vibrometers were placed about 150 meters away from the dam, one at each side of the valley below the dam. The distance between the two interferometers was about 200 meters. The optical paths of the two laser beams are completely different so that the turbolence noise is uncorrelated in the two signals. Fig. 8a) shows the frequency spectrum of the signals given by the two laser vibrometers pointing to two different points of the dam. The peaks, which correspond to the resonance frequencies of the dam, are barely detectable untop of a turbolence noise background. The cross-spectrum of the two signals, after 64 averages, is shown below in Fig. 8b).

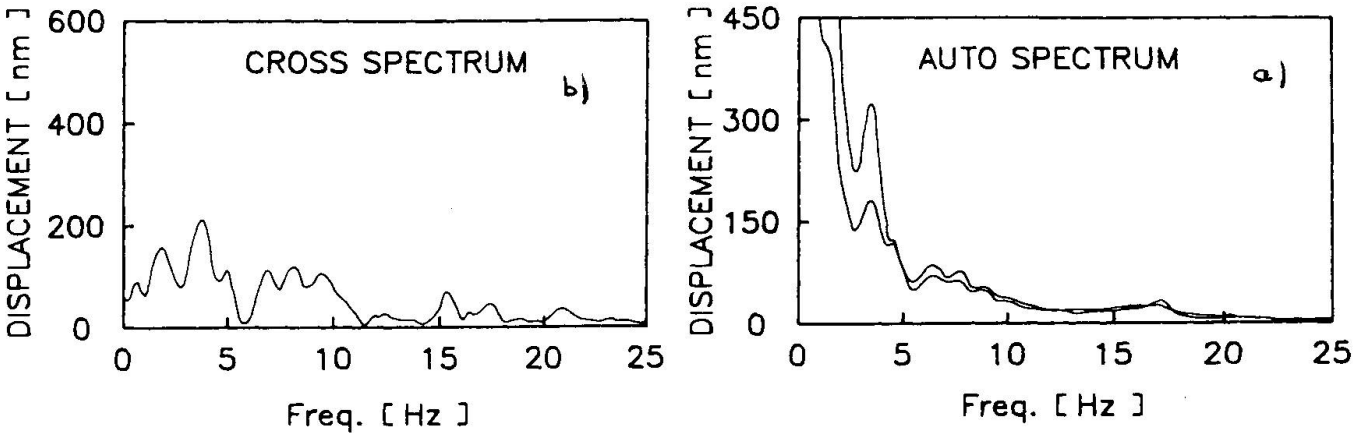

Fig. 8 - a) Spectra and b) Cross-spectrum of signals obtained in situ, measuring the natural vibration of an arch dam.

The noise contribution is strongly reduced and the structure resonance of the dam is evident. Figg. 9 and 10 show two examples of measurements of the dynamical responce of the dam with random excitation (noise from the waterfall).

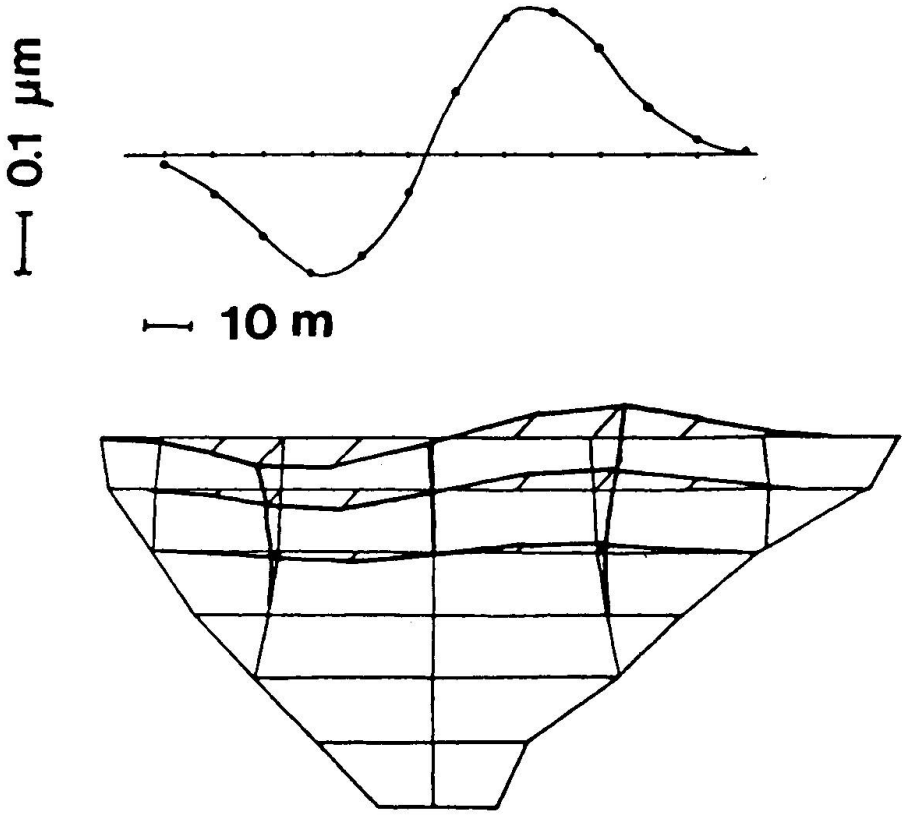

Fig. 9 - First antisimmetrical mode at 3.8 Hz measured by the interferometric vibrometers compared with a finite-element calculation.

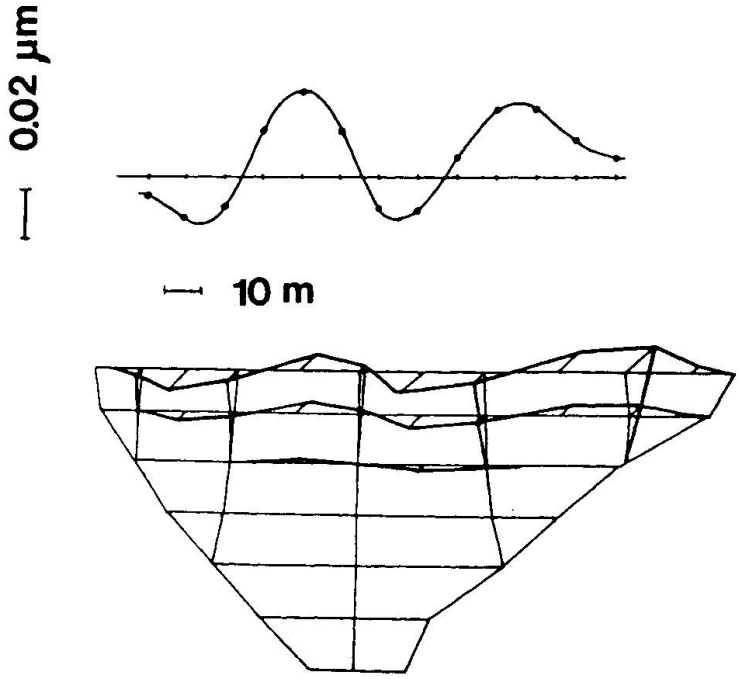

Fig. 10 - The same as Fig. 9 for the first simmetrical mode at 7.6 Hz.

One vibrometer is aimed to a fixed point of the dam. The other one is scanned and data are recorded. For each resonance frequency it is possible to draw the vibration pattern along the line of scanning. Normalization of the amplitude of the fixed vibrometer accounts for the fluctuations in the random excitation force (Ref. 4). The upper parts of Figg. 9 and 10 correspond to the measured vibration patterns at 3.8 and 7.6 Hz measured with this technique along the upper horizontal line of the dam. The lower parts of the figures give the dinamical responce of the dam predicted with a "Finite Element" model calculation (Ref. 5) for that frequencies. The agreement between calculated and measured pattern is good. The sensitivity of the technique is remarcable because it allows measurements of vibration amplitudes which are well below the rubulence noise level (compare Fig. 2 with Fig. 9 and 10).
Work performed in CISE, supported by ENEL CRIS Contract LADIR.

BIBLIOGRAPHY

1. CORTI M., PARMIGIANI F., BOTCHERBY S.C.L., Description of a Coherent Light Technique to Detect the Tangential and Radial Vibrations of an Arc Dam. Journal of Sound and Vibration (1982), 84 (1), 35-45.

2. CORTI M., PARMIGIANI F., DE AGOSTINI A., Measurement on the Dynamical Behaviour of a Naturally Excited Chimney by a Laser Technique. Journal of Sound and Vibration (1983), 88 (1).

3. BENDAT J.S. and PIERSOL A.G., (1971). Random Data, Analysis and Measurement Procedures. New-York: Wiley-Interscience.

4. CORTI M., PARMIGIANI F., Apparatus for Detecting the Displacements of Points of Excited Structures. U.S. Patent n. 4.526.465 Jul. 2, 1985.

5. FANELLI M.A., GIUSEPPETTI G., The Italian Approach to Seismic Engineering. Water Power and Dam Construction, November 1985, pag. 15.

Leere Seite
Blank page
Page vide

Structural Monitoring of Cancano Dam with an Automatic System

Système de contrôle du barrage de Cancano au moyen d'un systeme automatique

Struktüberwachung des Cancano Damm mit einem automatischen System

Francesco ANESA
ISMES-Bergamo Italy

Born 1941. Head instrumentation and Systems Dept.

Alberto MASERA
ISMES-Bergamo Italy

Born 1959, got his Civil Engineering Degree at the Politechnic of Milan. He is involved in numerical analysis of dam behaviour.

Giovanni RUGGERI
ISMES-Bergamo Italy

Born 1955, got his Civil Engineering Degree at the Politechnic of Milan. He is involved in numerical analysis of structural behaviour.

Vincenzo CROCE
AEM-Milano Italy

Born 1953, got his Civil Engineering Degree at the University of Pavia. Supervisor of the Civil Dept of Structural Design.

Sergio DE CAMPO
AEM-Grosio Italy

Born 1952, got his Civil Engineering Degree at the Politechnic of Milan. Supervisor of the AEM Hydroelectric plants.

SUMMARY

This article describes the activity carried out for on-line checking of the behaviour of the hydroelectric power plant structures during their operation. All the measurements are gathered and checked by an automatic monitoring system located on each dam and collected together in a local processing center using a teletrasmission network.

RESUME

L'article explique l'activité conduite pour vérifier le comportement des structures des installations pendant leur fonctionnement. Les mesures sont réunies et contrôlées par un système automatique de contrôle installé sur chaque barrage. Une centre local rassemble toutes les mesures par un réseau de transmission.

ZUSAMMENFASSUNG

Der Artikel beschreibt die Aktivitäten zur Kontrolle des Verhaltens der Bauwerke in den AEM Anlagen während des Betriebes. Ein Ueberwachungssystem für die Dämme sammelt und prüft die Messdaten, welche durch ein Datenübertragungsnetz in ein lokales Verarbeitungszentrum übermittelt werden.

1. DESCRIPTION OF THE DAM

The Cancano dam, located in the higher part of Valtellina Valley (province of Sondrio) is situated in the complex of the Azienda Energetica Municipale (AEM) plants for water resources exploitation of the Valtellina area.

The whole complex (Fig.1) involves a catchment area of about 990 Kmq and is comprised of three dams (S. Giacomo, Cancano, Fusino), two fluvial transverses (Le Prese, Sernio), 26 water plugs and 6 idroelectric power plants.

The Cancano dam has the biggest basin in the area (basin capacity: 123 Mmc) and feeds into the cascade to the other following plants.
The basin takes water from the down-flowing, taken by the water plugs, and collected by gutter system with longitudinal development of about 70 Km.
The dam, constructed during 1953-56, is a single-curve arch gravity dam, pratically symmetrical with respect to the main section, with a pulvino foundation along the excavated profile; the height of the dam is 136 m and the development of the crest is 381 m. The main features of the dam are reported in Fig. 2

2. SURVEILLANCE NETWORK

Since the time of construction, the surveillance of the dam behaviour has been manually performed recording the following quantities: environmental data, temperature inside the dam body, horizontal and vertical displacements, deformation inside the concrete, joint opening, seepages through the dam body and through the rock foundation.

The schedule of the installed instruments, which comprise the surveillance network, is reported in Table 1 ; it also reports the average frequency of measurements taken by AEM. All measurement data collected are recorded on bulletins stored in the AEM archives and periodically they are manually plotted and visually checked for cronological trend in congruency and homogeneity.

3. BEHAVIOUR INTERPRETATION ANALYSIS

In 1980 ISMES has been requested by AEM to perform in depth investigative studies for interpreting the dam behaviour (2). A computerized database is created in which all the collected data are stored starting from the beginning of the construction.

A 3D finite element mesh of the dam was made to calculate the theoretical response of the dam to the operating loads (water level and temperature). In this way the real behaviour is analyzed by comparing it with the theoretical reference behaviour. In Figs. 3 and 4 the 3D mesh is reported showing comparison between the theoretical and the measured data. An in-depth analysis, using computer methods, have shown repetition of dam behaviour, specifically noticeble movements of the dam with a daily cycle. Also from the analysis a more in depth characterization of the foundation behaviour is required which can be further used to define a better calibration of the interpretative model parameters.

4. AUTOMATIC MONITORING SYSTEM

From the results of interpretative analysis and following the program of AEM towards a completed automated monitoring system that collects, stores and processes the data, in 1986 an automatic monitoring system was realized, for Cancano dam, by automating the readings of some instruments and by installing new automatic sensors. That would enable a better description of the rock foundation deformation and the thermal condition of the dam body. The system operates daily, in a complete automatic manner, by collecting and processing the data from different sensors.

A connection between the dam monitoring system and a local center for storage and processing the data is made. The local center is able to store and process the data through the computer center of ISMES, via telecomunication, where the computerized measurement database is located.

4.1. Description of the automatic monitoring system

The Cancano monitoring system is a "distributed"

one (3). It is composed of two Peripheral Measurement Units (PMU) placed in the dam tunnel and connected through a single optical fibre digital data transmission line to a Central Control Unit (CCU) placed in the warden house. The advantages of a "distributed" system are: higher precision and reliability of the measurements, reduction of the costs for the electric cables and for their setting up.

Fig. 5 shows a simplified block diagram of the monitoring system where the main "hardware" components of the system are pointed out:
Measurement sensors, Peripheral and Local Measurement Units, (PMU,LMU); Central Control Unit (CCU); Power Supply Unit (PSU); interconnecting lines.

The main features of each component are described hereunder.

4.1.1. Measurement sensors

Fig.6 shows the location of the measurement instrumentation. The already existing instrumentation network, has been enlarged adding no. 28 thermoresistors into the concrete, no. 1 communication vessel level meter, no. 10 rockmeters, no. 1 telecoordinometer and no. 1 meteorological station. Dam and foundation water leakage measurement have been automated. Three telecoordinometers and one water level meter already automated, have been connected to the acquisition system.

- Water level meter

The level meter is made of a Ryttmeyer precision balance (1 cm resolution), with pneumatic pressure transmission, completed with display and 14 bit GRAY code decoder.

- Plumbline telecoordinometer

On plumbline systems - two direct and one reverse- already working on the dam , have been installed 4 automated telecoordinometers. These are the ISMES mod. TEL 140 D optoelectomecanical unit with digital signal output on serial line. They allow to measure the two displacement coordinates with a 0.03 mm precision range.

- Communicating-vessel level meter

A communicating-vessel level meter ISMES LCM-3 has been installed in the radial tunnel at the base of the central section of the dam. The level meter vessels have a +/- 50 mm measurement range and a 0.04 mm precision within a temperature variation ranging around 10 C.

- Dam and foundation leakage measurement

The automation of the dam leakage measurement is carried out by means of two proximity sensors on the teetering tank (60 l.) placed downstream the catch water.

The foundation leakage measurement which come together in the short-plumbline well , is carried out calculating the functioning time of a pump that at maximum level, drains out water from the well. Besides a water drill meter has been installed , as to provide the water leakage measure even when these are extremely reduced.

- Rockmeter

N. 4 multibase rockmeters have been installed; N.2 rockmeters double base on the main section, with a 10 degrees inclination on the vertical (upstream-downstream) N. 1 rockmeter with 3 bases on the right edge , with 25 degrees inclination on the horizontal; N.1, as the previous one, but on the left edge. The wide base rockmeters have been automated by means of a water/air tight displacement transducer with plastic conductive resistor, 50 mm stroke and 0.1% linearity.

- Dam core concrete temperature

As to measure the dam core concrete temperature no. 28 armored thermal drills with two platinum thermic resistors housed in stainless steel sheaths, have been placed.

- Meteorological station

This consists of an instrument shelter with a sensor for the air temperature measurements and a rain gage cabin for the rainfall measurements. The temperature sensor is made of a platinum thermal resistor with +/- 0.3 C precision and provided with an

electric fan device. The rain gage has teetering tank with a 1000 cmq calibrated vent 0.2 mm resolution and provided with a oil electric heater as to melt ice and snow.

4.1.2. Local and peripheral measurement units

The signal coming from different sensors installed on the dam are headed to the two peripheral measurement units, configured for 24 and 36 channels.

Whereas the water level meter and meterological sensor signals, are headed to the local measurement unit, installed in the same rack containing the control unit in the warden house.

4.1.3. Central control unit

The central control unit is made of the following components :

- computer, provided with memory modules; operating system on ROM, output/input interfaces towards peripherals;
- command and display unit made of a video-display and multifunctional keyboard;
- multifunctions interface unit, provided with local measurement unit for the meterological data acquisition and water level meter acquisition.
- printing unit
- recording unit on magnetic tape
- Interface unit towards the teletransmission device (modem)

4.1.4. Uninterruptable power supply unit

As to allow the system functioning also during short power black-out, the entire monitoring system is supplied through an uninterruptable group made of supplier, batteries, and one direct/alternating voltage inverter.

4.2. System main functions

The main functions performed by the system are summarized hereunder.

- Continous monitoring

This is the normal system function. The continous monitoring has an acquisition and control cycles with 10 min. intervals and is used for every sensor, except those which have to be read less frequently, because, being exposed to prolonged stress, are more liable to wear and tear.

- Periodic acquisition

A complete acquisition cycle is performed at fixed intervals including also those instruments which were not acquired during the continuous monitoring phase. During this phase structural checks are also triggered, by comparing the acquired data and its speed with relevant threshold levels.

- Accelerated acquisition

If required the system can be set up to activate acquisition cycle at closer intervals. This is done to have a greater quantity of data at one's disposal and to have effective check right after a particular event,as for example: earthquakes, landslides, floods or after sudden variation of certain significant quantities or measurement values.

- Required acquisition

A complete acquisition cycle (including printing and recording of the measurements) can be performed at any moment, if the user requires it.
This can be useful when carring out maintainance operation or in case of anomalyies, and also when a comparison between measurement data of sensors connected to the automated system with other measures of manually read instruments.

- Display, Local printing, teletransmission

The system is able to supply summarized printouts of measurements and checks on the system video monitor or on hardcopy printout. Such printouts can be automatically produced by the system at fixed intervals and when particular events occur. The

printout content can be delivered to the Grosotto local center through an interfacing unit to the teletransmission.

- Data storage

Data can be stored on magnetic tape automatically at prefixed intervals or at the request of the local qualified user. Each record contains the ensamble of all measured values with identification numbers, time reference (date,time) and validation code.

4.3. Interconnection with the local and remote center

The Cancano dam monitoring system is integrated in the data teletransmission network, heading to the Grosio and Grosotto control centers.
Fig.7 shows the complete scheme of the data teletransmission network in the Valtellina area, when all monitoring systems will be installed on AEM dams and all network linking activated.

The dedicated "point-to-point" network has its two control centers in Grosio and Grosotto.
The teleoperation center is located in Grosio and it's responsable for all plants telecontrol; also the anomalyies teletransmission network connected to the monitoring system is headed here. By means of this network,information of both, structural and instrument breakdowns or anomalyies are sent in real time to the center which is supervised 24 hours a day.

The office responsable of the dam structural control is in Grosotto; the structural data teletransmission network connected to different monitoring system is headed he Thanks to this network the center receives daily updated measurement which are automatically read on the different monitoring system together with possible signalling of structural or instrument anomalyies. The local center is connected to ISMES through a telephonic line. By means of a PC the acquired data are transferred in a database to be processed. The PC terminal operates with the MIDAS database and through this PC it is possible to interrogate the database and to process locally the data, producing plots and tables by the centre itself.

5. FUTURE DEVELOPMENTS

AEM in cooperation with ISMES are so projecting a complete programm for the progressive automated system for checking the behaviour of the different plants using automated monitoring system and data teletransmission towards a local processing center (Fig. 7).

All the collected data will be stored in the relevant databases located in the computer center of I-SMES for further elaboration.
The realization and the use on-line of theoretical behaviour models will allow the continuous automatic check of the structure behaviours during their operation.

REFERENCE

1. "The Valtellina Development" - Water Power 1961

2. Bonaldi, Lionetti, Peano, Riccioni, "Thermal craking due to periodic temperature variation on the downstream face" - 2nd Int. Conference on numerical methods in thermal problems, Venice July 1981.

3. Anesa, Bonaldi, Giuseppetti, Ruggeri, Torri Tarelli "On-line monitoring of dams during their operation: Italian experience" - 2nd Int. Conference on On-line Surveillance and Monitoring, Venice May 1896

MONITORING NETWORK

MEASURED QUANTITIES	SENSOR	NUMBER	FREQUENCY	
Water level	hydrost. balance	1	daily	AUT
	levelling staff	1	daily	
Air temperature	max-min therm.	1	daily	
	electric therm.	1		AUT
Rain fall	rain gauge	1	daily	AUT
Snow	levelling staff	1	daily	
Ice thickness	levelling staff	1	daily	
Water temperature				
- surface	immersion therm.	1	daily	
- 5 m below surface	immersion therm.	1	daily	
Horizontal displac.				
- crest collimation	optical collimator	3	weekly	
- 3 direct plumbline	coordinometer	6	weekly	
	telecoordinometer	4		AUT
- 1 short plumbline	coordinometer	1	weekly	
- 1 inverted plumbl.	telecoordinometer	1		AUT
Vertical displac.				
- levelling network	topographic level.	38	semiannual	
Deformation				
- casting restart	extensometer	21	fortnightly	
- dam body	rosetta ext.	10	semiannual	
- cracks	movable ext.	64	semiannual	
	extensometer	26	semiannual	
- in rock foundation	long base extens.	10		AUT
Movement of joints	teledilatometer	26	semiannual	
Rotation	fixed clinometer	1	fortnightly	
	hydrostatic level.	1		AUT
Temperature				
- inside dam body	electric therm.	60	fortnightly	
- on the surface	electric therm.	28		AUT
Seepage	weirs	4	daily	
	volumetric meas.	1		AUT
	timer pump	1		AUT

AUT = automatic acquisition sensors

Table n. 1

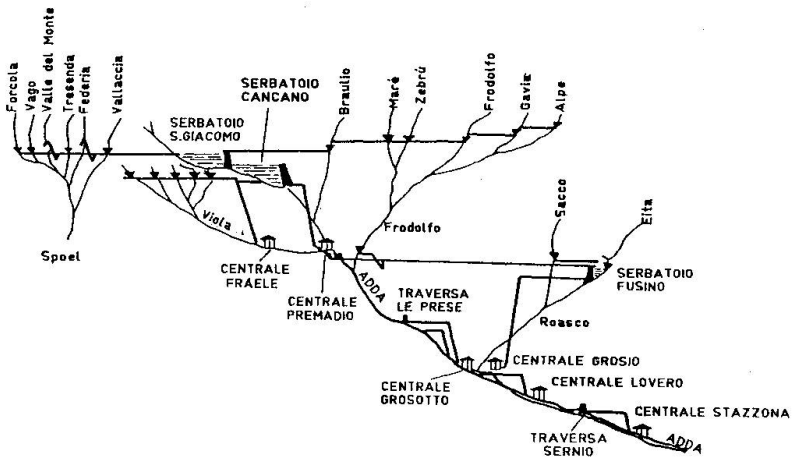

Fig. 1: AEM Plants - Altimetric scheme

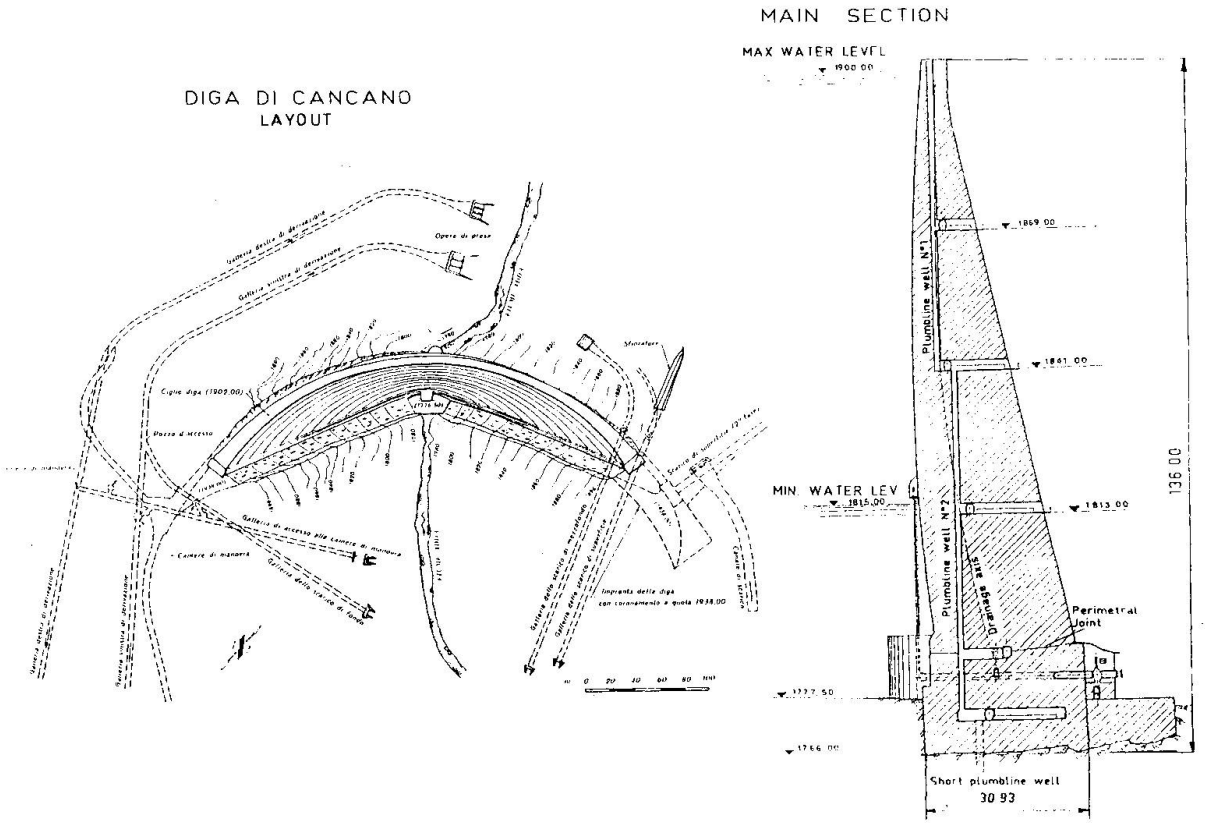

Fig. 2: Dam features

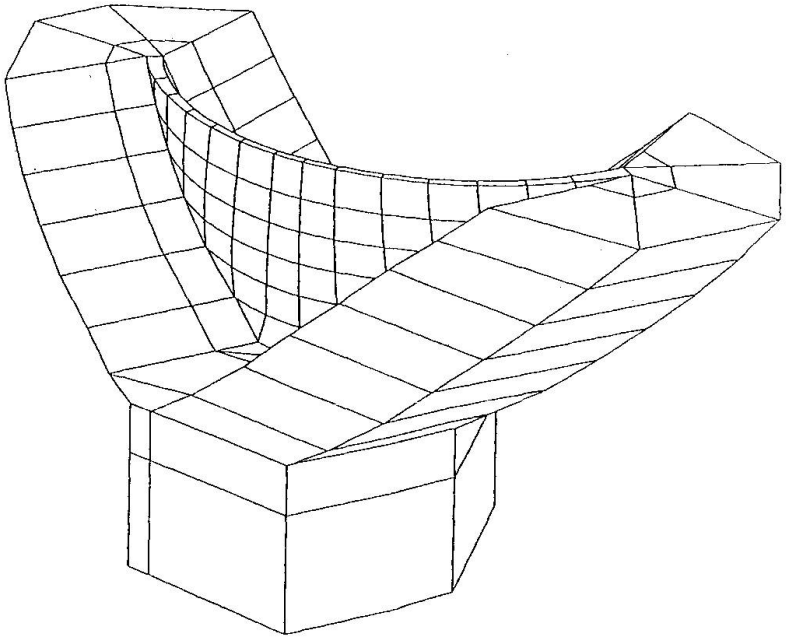

Fig. 3: 3D mesh of the dam and the foundation

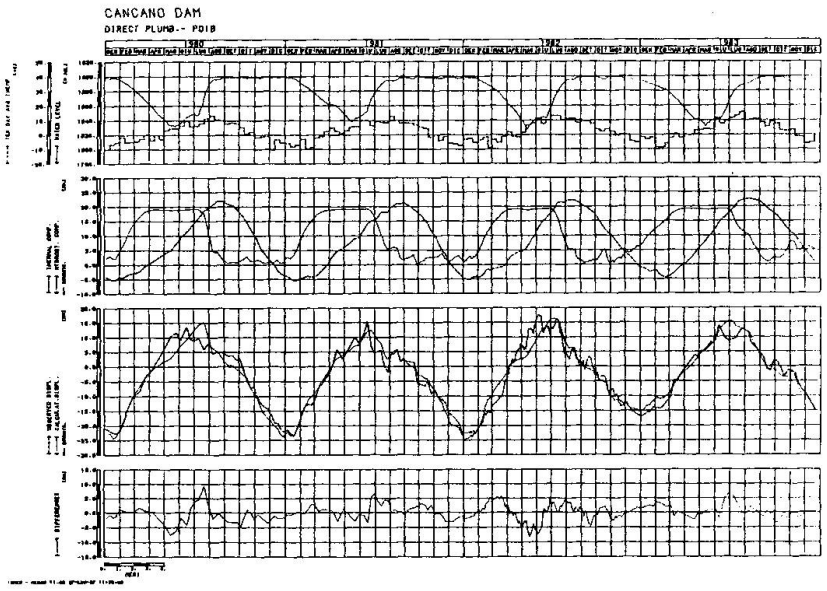

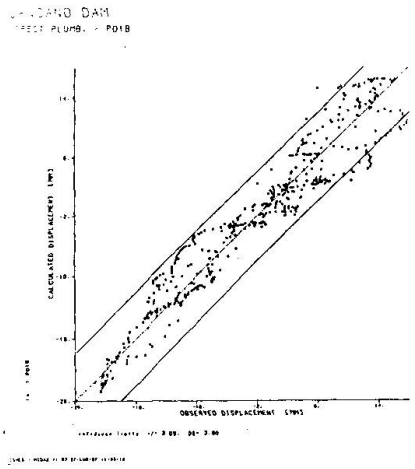

Fig 4: Comparison between measured and theoretical displacement

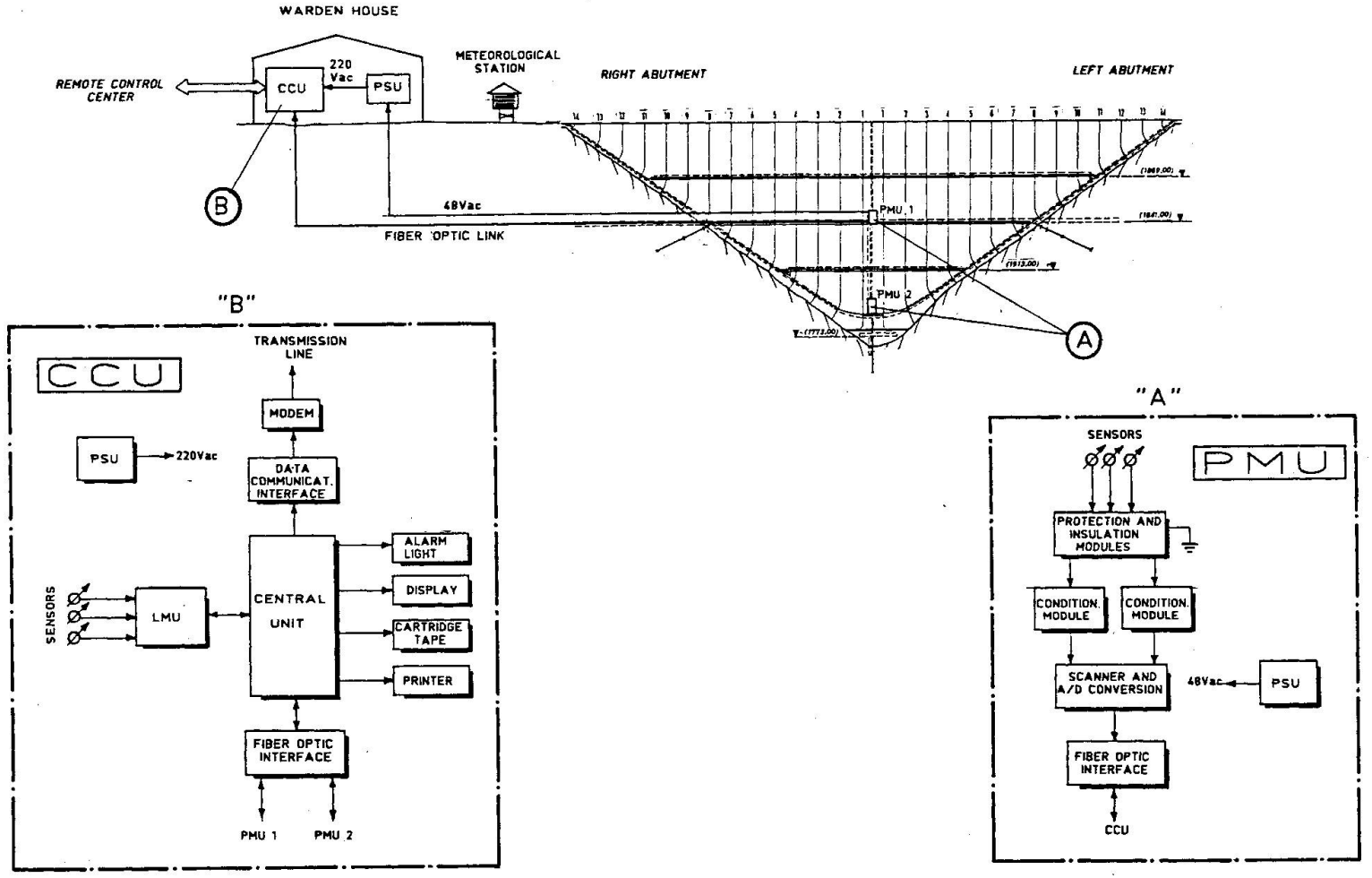

Fig. 5 - CANCANO DAM : MONITORING SYSTEM BLOCK DIAGRAM

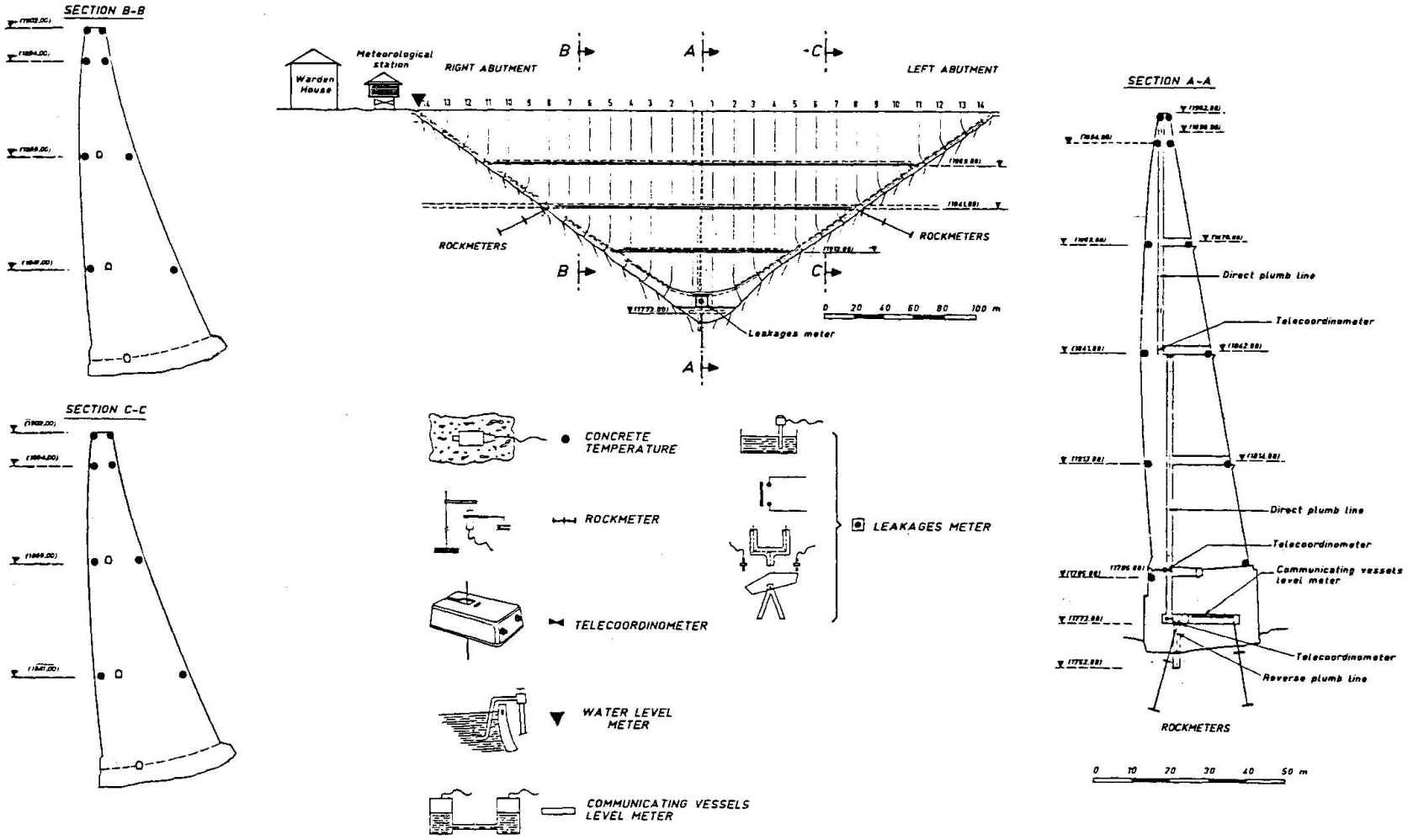

Fig. 6 - CANCANO DAM : LOCATION OF THE SENSORS WITH AUTOMATIC READING

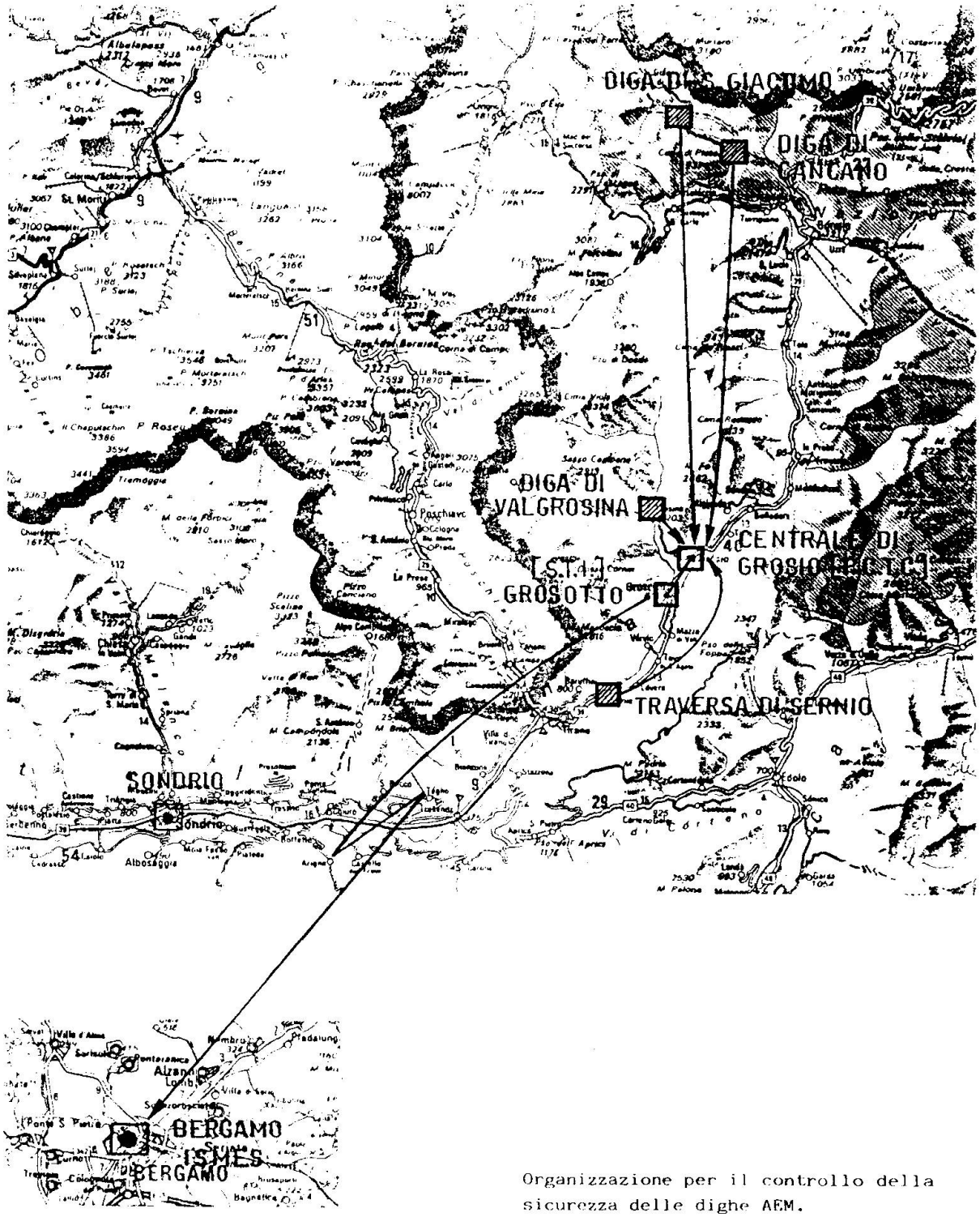

Organizzazione per il controllo della sicurezza delle dighe AEM.
Ubicazione degli sbarramenti e dei centri di controllo.

Fig. 7: Data teletransmission network in the Valtellina Area

Leere Seite
Blank page
Page vide